Old Wine in New Bottles: Active Tectonics and Active landscapes in an Ancient Orogen

Guidebook Editors:

Kevin Stewart

Rick Wooten

Trip Leaders:

Andy Bobyarchick (University of North Carolina - Charlotte)

Ellen Cowan (Appalachian State University)

Andy Heckert (Appalachian State University)

Jesse Hill (University of North Carolina - Chapel Hill)

Keith Seramur (Appalachian State University)

Kevin Stewart (University of North Carolina - Chapel Hill)

Anne Witt (Virginia Department of Mines, Minerals and Energy)

Rick Wooten (North Carolina Geological Survey)

Logistical Support: Tyler Clark

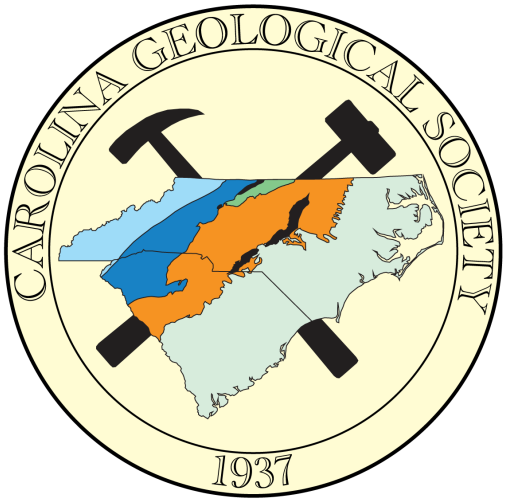

Carolina Geological Society

79th Annual Meeting, October 5-7, 2018

Boone, NC

Carolina Geological Society

http://carolinageologicalsociety.org/

2018 BOARD OF DIRECTORS

President
Lee Phillips UNC - Greensboro
Vice President
Arthur Merschat USGS
Secretary Treasurer
Timothy W. (Tyler) Clark Raleigh, NC carogeoscoc@me.com
Past President
Brenda Hockensmith SC DNR
Board Members
Heather Hanna UNC - Chapel Hill
Craig Kennedy Applied Science and Engineering
Robby Morrow SC Geological Survey

SPONSORS

CONTENTS

Foreword

The theme of this field trip is integrating basic and applied research, and the need for one to build upon the other. On this trip we will see how the geologic disciplines of structural geology and tectonics, geomorphology, slope stability, and hydrogeology, all underpinned by basic geologic mapping, can be brought to bear on answering questions and solving problems.

The one-and-a-half-day field trip will focus on the relationships between tectonic history, landscape evolution, and landslide processes and deposits, by examining faults, lineaments, rock slides, debris flows and debris fans. We will also see how these processes and features have affected the human history of Watauga County, and the implications they may have for the future.

Storms with intense rainfall are the primary triggers (inciting factors) for landslides like debris flows and debris slides in the Southern Blue Ridge. The underlying geology, however, is the chief cause (predisposing factor) for slope instability. Here we will examine the effects of Cenozoic uplift and faulting that overprint Paleozoic thrusts faults resulting in bedrock structural controls on landslides, and as processes that drive the landscape's influence on weather patterns like the orographic forcing of rainfall along the Blue Ridge Escarpment. Much more work is needed on these younger brittle structures and related fractures that have direct applications to the kinematic and hydrogeologic aspects of slope stability at the site, mountainside and larger scales.

We will learn about the devastating effects of August 13-14, 1940 tropical cyclone that triggered over 2,000 landslides in Watauga County, and will see some of the scars and deposits that remain from that event. Quaternary and older(?) debris fan deposits make up a significant part of the Watauga landscape. As we will see these deposits are important in understanding hillslope hydrogeology and contaminant transport. Debris fans are also fertile ground for future research, as they hold answers on the spatial and temporal aspects of uplift and erosion; linkages between climate change and the recurrence intervals of catastrophic storms; and, what areas could be affected by future debris flow events.

Several of the stops on this year's trip are focused on the bedrock geology including the recent discovery of the Neogene Boone fault. The abundance of landslides in the area near Boone and Deep Gap, NC is related in part to the intense fracturing of the bedrock associated with motion on the Boone fault and the development of a series of parallel topographic lineaments that correspond to fracture zones or brittle fault zones. These zones of brittle deformation likely accommodated Neogene uplift of crustal blocks in this area, which is part of a recognized regional uplift event affecting the southern Appalachians, beginning in the Miocene.

As challenging as it has been to reach the current level of geologic understanding for this area after more than 50 years of research, a bigger, perhaps more important challenge lies ahead. How can we engage the public and policy makers to make them appreciate the importance of earth science in addressing societies' needs for sustainable resources, and reducing the losses from geologic hazards? Much development has occurred in areas impacted by the 1940 storm. Storms of the magnitude of the August 1940 storm will eventually affect the Southern Blue Ridge again. What lessons can be learned from the 1940 storm that can be used to make communities more resilient, and protect people and property during future heavy rainfall events? How can we convey scientific information on geologic hazards like landslides so that it is not perceived as a threat to property rights, to property values, and lead to regulations and expense? Delivering the message in ways that capture the human sides of stories put into historical context may help bridge the gap between science and public awareness.

Geologic mapping of the Grandfather Mountain Window and vicinity by Bruce Bryant and John Reed, U.S. Geological Survey, has formed the foundation for much of the research presented here. More recent mapping by Jesse Hill has allowed us to refine our understanding of both the bedrock geology in this area as well as the interaction between recent motion on the Boone fault and the response of the landscape to this motion. Research by Gerry Wieczorek (deceased) on debris flows in the Southern Appalachians, and particularly those in the Deep Gap area, provided the impetus to undertake landslide hazard mapping in Watauga County. We gained many insights from Hugh Mills' research on debris fan deposits, especially those on Snake and Rich Mountains. His consultation and participation in field reviews of landslide hazard maps are much appreciated. The dedicated work of Jennifer Bauer, Tommy Douglas, Stephen Fuemmeler, Ken Gillon, Rebecca Latham, and Anne Witt of the NCGS landslide mapping team from 2005 to 2011 resulted in landslide hazard maps for Macon, Watauga, Buncombe and Henderson Counties.

Geohazards studies by the NCGS starting in 2003

were in cooperation with the N.C. Division of Emergency Management with funding from the Federal Emergency Management Agency.

The NCGS would like to acknowledge the U.S. Department of Interior – National Park Service for their funding contribution to the geologic inventory of the Blue Ridge Parkway in North Carolina. Appropriations by N.C. General Assembly from 2005-2011 providing funding for landslide hazard mapping by the NCGS. Kevin Stewart and Jesse Hill acknowledge funding from the USGS EDMAP program as well as funding from the Butler and Martin funds, Department of Geological Sciences at UNC-Chapel Hill.

Rick Wooten, Asheville, NC
Kevin Stewart, Chapel Hill, NC

FIELD TRIP DAY 1

SATURDAY, OCTOBER 6, 2018

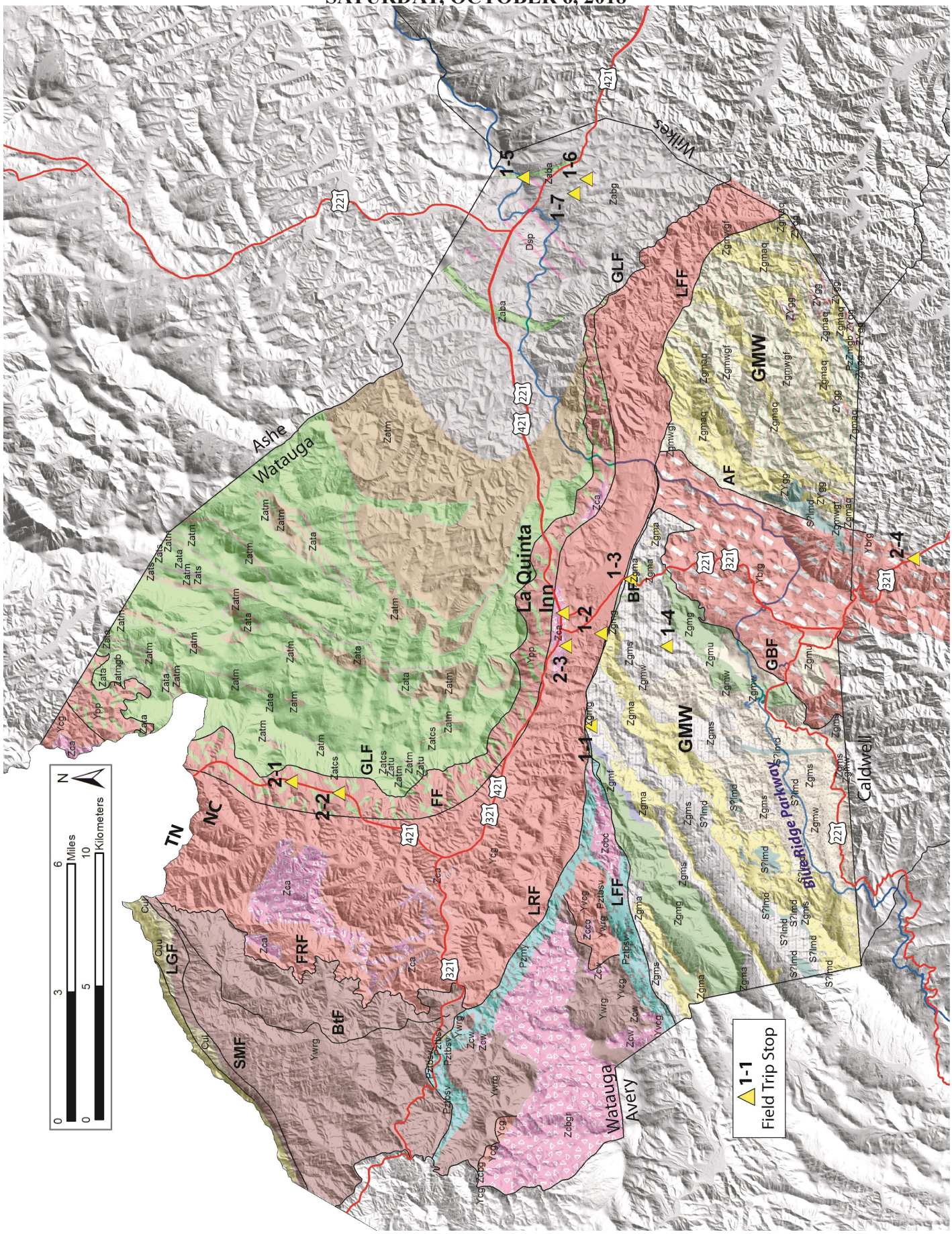

Stop 1-1: Brittle fracturing and faulting associated with the Boone fault, Vulcan Boone quarry

Location: 36.2043°N, 81.7140°W

Stop leaders: Kevin Stewart, Jesse Hill.

This stop is an active quarry and requires hard hats. We will also get a short safety lecture before we enter the quarry. Warning: You must stay far back from the quarry walls. Rocks, large and small, can and do fall off the active quarry faces.

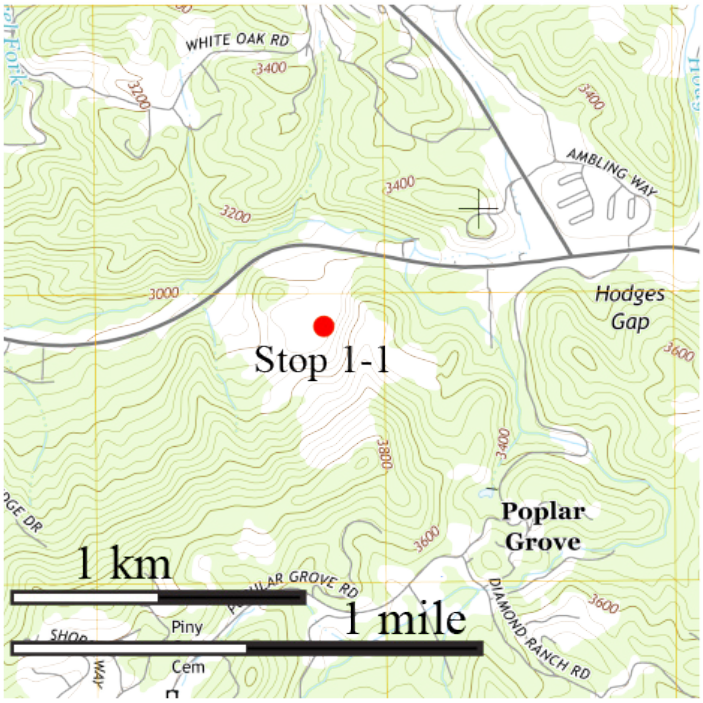

The purpose of this stop is to see the bedrock that underlies a large part of the field trip area as well as intense brittle fracturing in this area that is associated with Neogene uplift and motion on the Boone fault. The rocks exposed in the Boone quarry are within the northernmost part of the Grandfather Mountain window and consist of metamorphosed sandstone and siltstone. The northern half of the quarry is within a quartz-rich metasandstone that Bryant and Reed (1970) interpreted to be a slice of early Cambrian Chilhowee Formation, which was incorporated into the Late Paleozoic Linville Falls thrust (Figure 1). Due to the absence of unequivocal evidence that the sandstones are Chilhowee, Hill (2018) mapped both facies as Late Proterozoic Grandfather Mountain formation. Bedding in the metasandstone is not well developed but is locally well preserved in the metasiltstone. Both rocks have a pervasive greenschist-facies

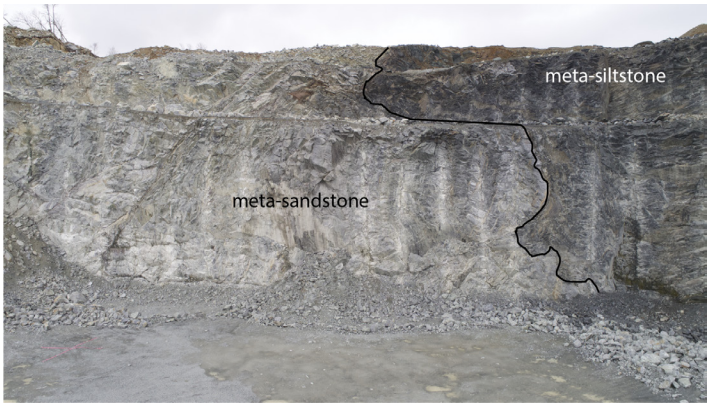

Figure 1. Exposure of meta-sandstone and meta-siltstone in the eastern wall of the Boone quarry. Contact has been interpreted by Bryant and Reed (1970) as a splay of the Linville Falls fault.

overprint, most likely associated with burial during the Alleghanian orogeny, and there is ductile deformation (cleavage and folding) present within the metasiltstone that is likely associated with Alleghanian deformation, including motion on the Linville Falls fault.

All of the rocks in the quarry show evidence of brittle deformation (Figure 2), both fracturing and faulting. Gillon et al. (2009) measured abundant fracture surfaces and dip-slip brittle faults within the quarry and Hill (2018) measured fractures and minor faults in rocks outside the quarry (Figure 3). Hill and Stewart (this volume) present a paleostress analysis that shows that the minor faults and fractures in these rocks are likely associated with motion on the Boone fault. The calculated maximum and minimum compressive stress directions are not consistent with Alleghanian shortening nor Mesozoic rifting but instead indicate that the motion on the Boone fault was primarily vertical with the rocks to the south of the fault moving up.

As we will see at later field trip stops, the area near Boone and Watauga County has been especially

Figure 2. Fractures and faults within the meta-sandstone. We interpret these structures to be associated with Neogene motion on the Boone fault.

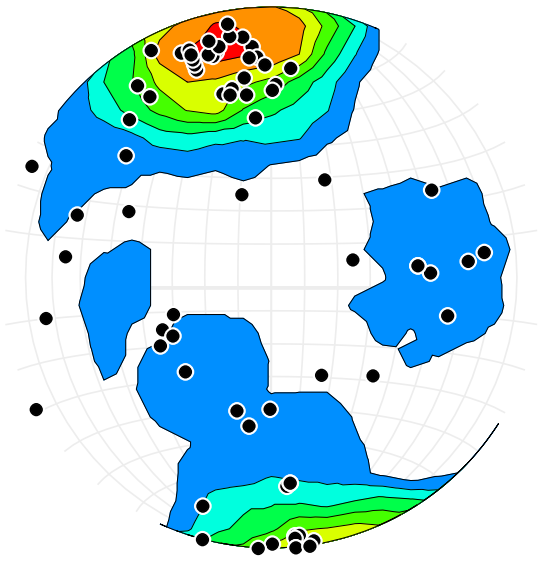

Figure 3. Equal-area plot of poles to fractures and minor faults exposed in a roadcut through the meta-sandstone body along NC-105 near Boone quarry entrance. Measured by Jesse Hill.

prone to landslides. The Boone fault, as well as other post-orogenic fracture zones have created a series of topographic lineaments, easily seen on DEMs of this area (Figure 4). Other lineaments within this swarm may also be faults but slip has not yet been documented on these features. Post-orogenic lineaments south of the Grandfather Mountain window have been shown to correspond to fracture zones with no detectable slip (Stewart and Dennison, 2006).

The abundance of fractured rock associated with the Boone fault and associated lineaments likely had a profound effect on the susceptibility of this area to landsliding. The Deep Gap reentrant of the Blue Ridge escarpment (Figure 4) is the location of abundant landslides (Wooten and Witt, this volume) and marks where the lineament swarm intersects the escarpment.

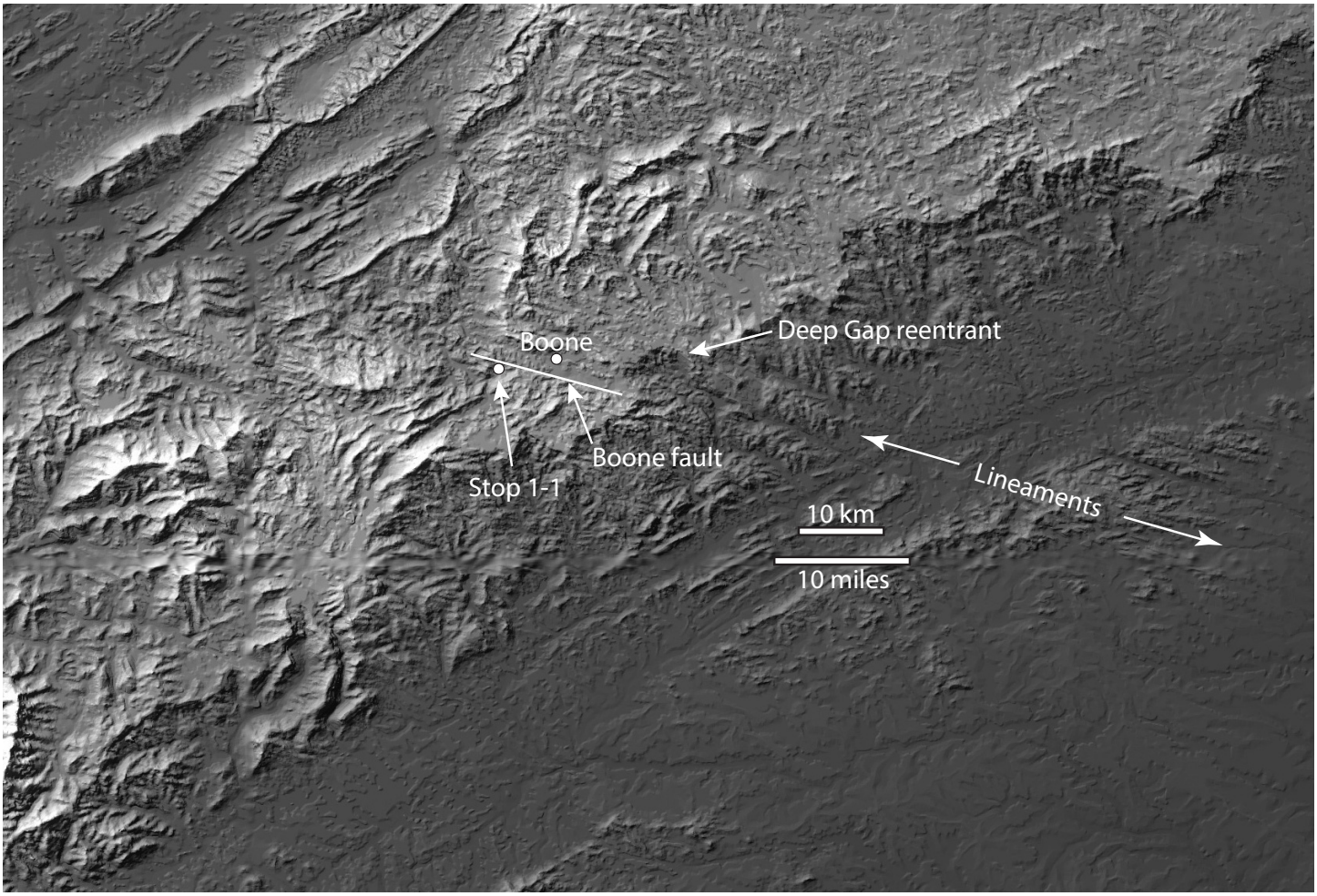

Figure 4. DEM hillshade showing location of the Boone fault and associated topographic lineaments. Note the deep reentrant where the lineaments cross the Blue Ridge escarpment. Intense fracturing of the bedrock has made the area more susceptible to landsliding.

REFERENCES

Bryant, B., and Reed, J.C., Jr., 1970, Geology of the Grandfather Mountain window and vicinity, North Carolina and Tennessee: U.S. Geological Survey Professional Paper 615, 190p.

Gillon, K.A., Wooten, R.M., Latham, R.L., Witt, A.W., Douglas, T.J., Bauer, J.B., and Fuemmeler, S.J., 2009, Integrating GIS-based geologic mapping, LiDAR-based lineament analysis and site specific rock slope data to delineate a zone of existing and potential rock slope instability located along the Grandfather Mountain Window-Linville Falls shear zone contact, Southern Appalachian Mountains, Watauga County, North Carolina, In: Proceedings of the 43rd US Rock Mechanics Symposium and 4th U.S.-Canada Rock Mechanics Symposium, Asheville, North Carolina, June 28th – July 1,2009; American Rock Mechanics Association ARMA 09-181, 13p.

Hill, J.S, 2018, Post-orogenic uplift, young faults, and mantle reorganization in the Appalachians, PhD Dissertation, University of N.C. Chapel Hill, 139p.

Stewart, K. G., and Dennison, J. M., 2006, Tertiary-to-recent arching and the age and origin of fracture-controlled lineaments in the southern Appalachians: Geological Society of America Abstracts with Programs, v. 38. no. 3., p. 27.

Stop 1-2 Rock slide on NC-105 Boone, North Carolina

Location: 81.6758°W 36.2023°N

Stop leaders: Rick Wooten, Keith Seramur, Ellen Cowan

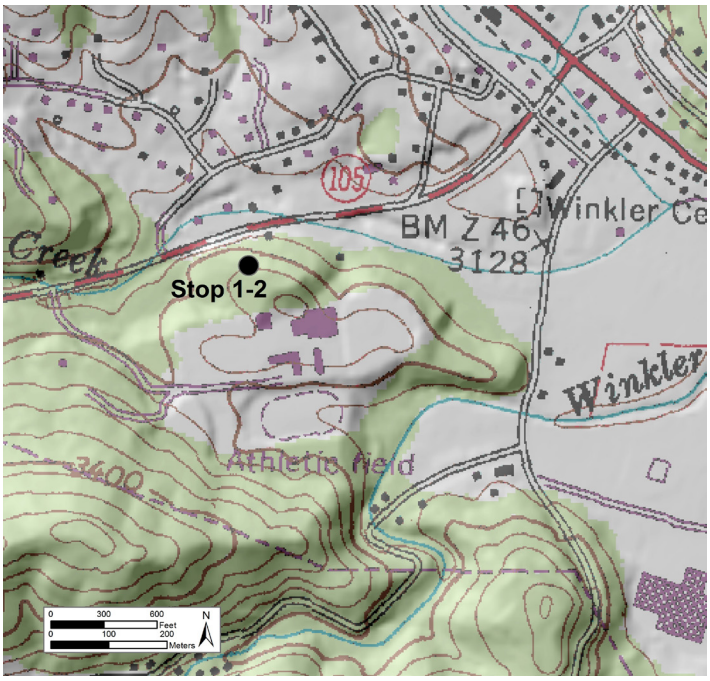

Figure 1. Stop location shown on an excerpt of the Boone 7.5-minute quadrangle map superimposed onto a shaded relief map derived from a 6m pixel resolution LiDAR DEM. Note the locations of the former buildings of Watauga High School.

Stop Description

At this stop we will examine an active slide in weathered rock. Buses will park in the Appalachian State University parking lot near the former Watauga County High School, now demolished. We will walk in shifts to the rock slide located on the hill north of the parking area. Field trip leaders will be on hand at several locations to point out and discuss features related to the slide. Figures 1-4 show the location of the slide, and Figure 5 is a geologic cross section though the slide.

During landslide hazard mapping in Watauga County, the NCGS made a reconnaissance investigation of the rock slide after it was brought to their attention by Loren Raymond (personal communication). Like the Boone Quarry at Stop 1-1, this site is within the Zone of Existing and Potential Rock Slope Instability (ZEPRSI) delineated on the Watauga County slope movement hazard maps (Wooten et al., 2008).

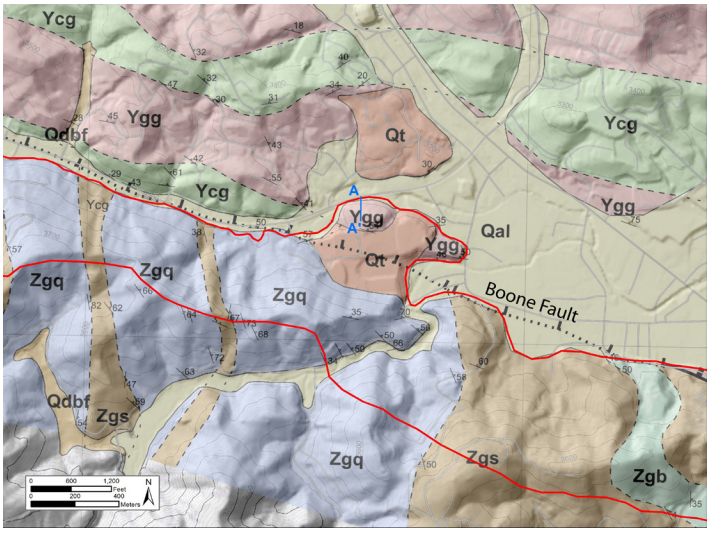

Figure 2. Excerpt of the geologic map from Hill (2018) and mapped extent of the Zone of Existing and Potential Rock Slope Instability (ZEPRSI = red outline) from Wooten et al. (2018) in the vicinity. A-A' shows the location of the geologic cross section through the rock slide (Fig. 5). Quaternary Deposits: Qal = alluvium; Qt = terrace; Qdbf = debris fan. Grandfather Mtn. Formation: Zgb = metabasalt; Zgs = metasiltsone; Zgq = metasandstone. Basement Rocks: Ycg = chlorite feldspar gneiss; Ygg = granitic gneiss.

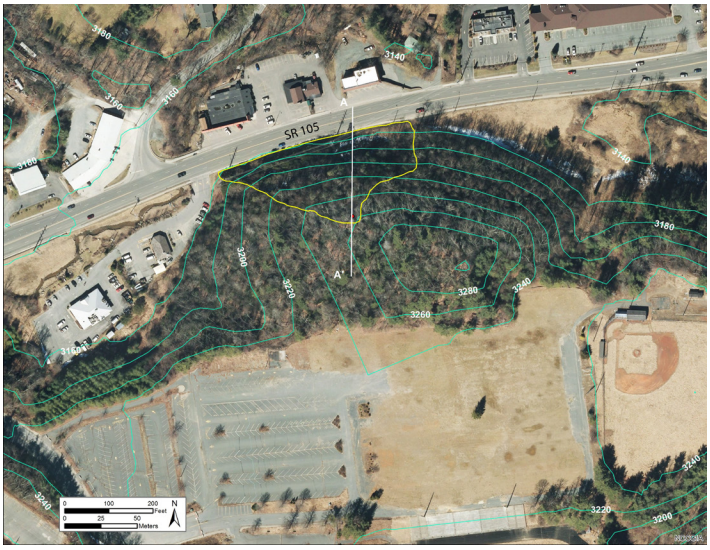

Figure 3. Map view of the rock slide at Stop 1-2 (yellow outline). Base map is 2015 ortho-photography with topographic contours (20ft contour interval) derived from a 6m pixel resolution LiDAR DEM. A-A' shows the location of the geologic cross section through the rock slide (Fig. 5). Red dot = point location for the slide in the NCGS landslide geodatabase.

Figure 2 shows the mapped extent of the ZEPRSI in the area of this stop. The methods used to investigate and delineate the ZEPRSI are summarized in Wooten and Witt (this volume), and in more detail in Gillon et al., (2009).

Rocks at this location are Mesoproterozoic base-

ment gneisses designated as the Cranberry Gneiss (Ycg) by Bryant and Reed (1970), and later described here as granitic gneiss (Ygg) a subdivision of Ycg (Hill, 2018) (Fig. 2). At this locale, a mylonitic, chlorite-sericite-quartzo-feldspathic gneiss is exposed in the main scarp of the slide. Structurally the rocks are within the Fork Ridge thrust sheet (Hatcher et al., 2006), and in the hanging wall of the Linville Falls fault, and the Boone fault (Hill, 2018). All other known rock slides within the ZEPRSI are in the Neoproterozoic rocks of the Grandfather Mountain Formation within the Grandfather Mountain Window, and located in the footwall of the Linville Falls fault, and the foot wall of the Boone fault. In both settings, brittle fabrics related to the Boone fault (e.g., fractures, faults) overprint earlier ductile fabrics of the Linville Falls shear zone (e.g., foliation, mylonitic foliation) which increases the potential for rock slides on excavated, north-facing slopes in the ZEPRSI.

Mylonitic foliation associated with the Linville

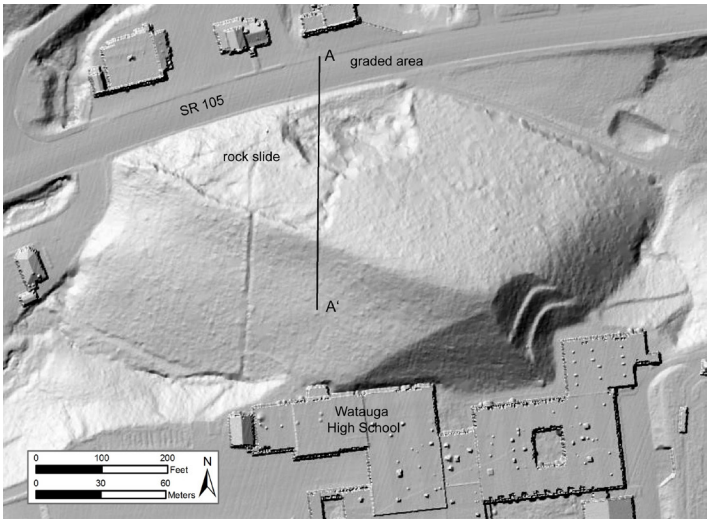

Figure 4. LANSat image of the slide area reprinted with permission from Casale (2016). LANSat image courtesy of the Department of Geography and Planning, Appalachian State University.

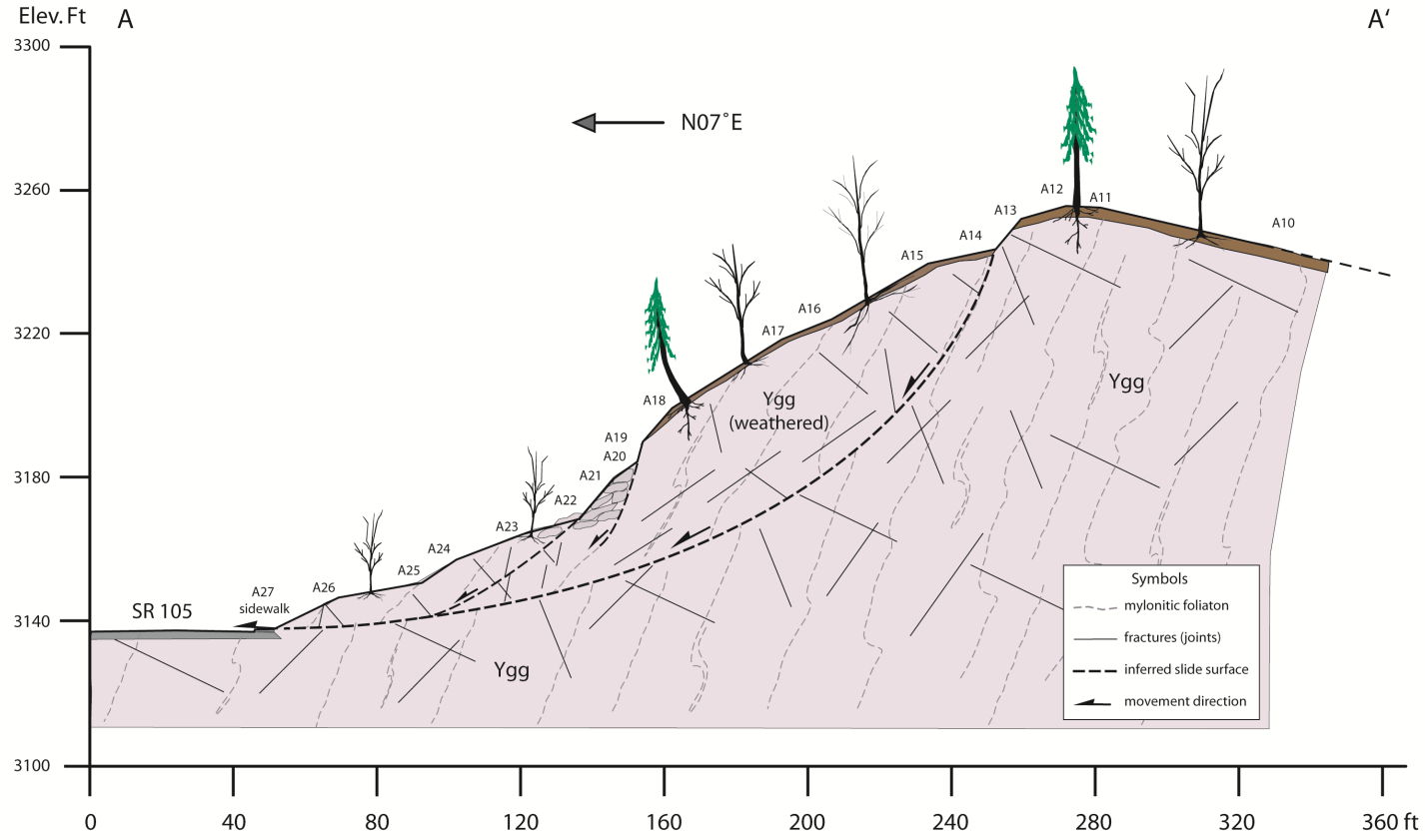

Figure 5. Field-developed geologic cross section and conceptual model of the rock slide. Line of section shown in Figures 2-4. Ygg = granitic gneiss of Hill (2018), exposed here is a mylonitic, chlorite-sericite-quartzo-feldspathic gneiss (Figs. 6,7). Survey: 2018/07/05 cloth tape, Brunton compass, clinometer by R. Wooten, B. Cattanach, S. Isard, NCGS. Station locations are numbered. Drafted: 2018/08 S. Isard, R. Wooten. Orientations of mylonitic foliation and fractures (joints) are based on measurements in the vicinity; however, locations of these features portrayed on the cross section are schematic.

Figure 6. Outcrop of folded, fractured mylonitic chlorite-sericite-quartzo-feldspathic gneiss (Ygg) exposed in the main scarp of the slide. The mylonitic foliation dips out of the slope toward the north. View looking south. 2018_05_17 NCGS photo.

Figure 7. Close-up view of the folded mylonitic foliation exposed on a fracture face in the outcrop in Figure 6. Mylonitic foliation consists of mm-scale, alternating quartzo-feldspathic, and sericite-chlorite layers. 2018_07_05 NCGS photo.

Figure 8. Photograph of curved and leaning trees on the rock slide. Slide movement is downhill toward the left (north). 2018_07_05 NCGS photo.

Falls shear zone exposed in the main scarp and vicinity dips moderately to steeply toward the NNW to NNE (Figs. 6, 7). Sliding surfaces at depth are interpreted to take advantage of mylonitic foliation planes. Fracture planes act as lateral release surfaces allowing slide blocks to detach from the slope and disarticulate within the displaced mass. Abrupt slope breaks indicate scarps within the displaced mass. Other features indicative of slide movement include leaning and curved trees (Fig. 8), uneven topography, displaced rock blocks, and bulging of the slide debris and its advance over the sidewalk at the slide toe (Fig. 9).

Movement History

Dendrochronology studies by Appalachian State University student Emma Idol under the direction of Dr. Gabriele Casale and reported in Casale (2016) identified tilting events in trees that indicate slide movement dating back to the mid-18th century. The tree ring analysis points to a period of more recent movement beginning in the mid-1990's, consistent with a 2008 NCDOT report describing movement in response to grading for commercial construction sev-

Figure 9. Photograph of the rocky debris at the slide toe impinging on the sidewalk along SR 105. View looking west. 2018_07_05 NCGS photo.

eral years prior to 2008 (Fig. 4). Ground disturbance is visible in 1993 and 1998 orthophotography in the area interpreted to be where the grading occurred. Bulging of the slide toe, buckling of the sidewalk, and rocky slide debris advancing over the side walk observed by the NCGS in 2008 and in July 2018 indicate that the slide remains active, with average rates of movement over that timeframe estimated to be on the order of cm (in)/year.

Slide Impacts

Impacts of the slide on infrastructure appear to be mitigated by routine removal of slide debris at the toe and repairs to the sidewalk. To date slide movement does not appear to have adversely impacted SR 105 or the buried gas line, which may be because the rupture surface of the slide exits (daylights) at the toe of the slope and does not extend to depths that would affect the pipeline or road. Any future slope modifications of the active slide area, especially excavation of the toe area, could result in increased rates of movement. Our recommendation would be that any alterations to the slope should be done under the guidance of a qualified geologist or engineer.

Steep Slope Development in the Town of Boone

Development continues in this setting on the Linville Falls fault zone, especially along NC-105. Fortunately, the Town of Boone has steep slope development regulations. These regulations require that the development plans for parcels of land with a slope greater than 30% have a licensed geologist or engineer sign and seal a slope stability report. The steep slope regulations require that these studies address four points that include:

- pre-existing landslide deposits
- thick soils
- daylighting fractures, and
- localized oversteepened slopes

All of these factors are associated with previous landslide events.

Watauga County had the old high school property on the market for several years. Investors were interested in leveling the property and building a large mutli-use commercial/residential development. The investors were advised that the area along the slope should not be disturbed, which reduced the footprint available for buildings and parking. This reduction limited the value of the planned development and the investors walked away from the project. Appalachian State University acquired the property through a land exchange and promised future financial settlement. The university is using the property for student parking and plans to build a new track and field facility.

The accelerated movement along the slope failure is a result of undercutting the toe slope. This type of slope failure is of prime concern when performing slope stability assessments along the NC-105 corridor.

REFERENCES

Bryant, B., and Reed, J.C., Jr., 1970, Geology of the Grandfather Mountain window and vicinity, North Carolina and Tennessee: U.S. Geological Survey Professional Paper 615, 190p.

Casale, G., 2016, Dendrochronology study of the active slide - Hwy 105 at the old Watauga High School, Stop 4, in Wilson, C.G., ed., Evolution of the Linville Falls fault zone and its influence on topographic relief and slope stability today, Carolina AEG Fall 2016 meeting and field trip guidebook, Aug. 26-27, 2016, Boone, NC, 51p.

Gillon, K.A., Wooten, R.M., Latham, R.L., Witt, A.W., Douglas, T.J., Bauer, J.B., and Fuemmeler, S.J., 2009, Integrating GIS-based geologic mapping, LiDAR-based lineament analysis and site specific rock slope data to delineate a zone of existing and potential rock slope instability located along the Grandfather Mountain Window-Linville Falls shear zone contact, Southern Appalachian Mountains, Watauga County, North Carolina, In: Proceedings of the 43rd US Rock Mechanics Symposium and 4th U.S.-Canada Rock Mechanics Symposium, Asheville, North Carolina, June 28th – July 1,2009; American Rock Mechanics Association ARMA 09-181, 13p.

Hatcher, R.D., Jr., Merschat, A.J., and Raymond, L.A., 2006, Geotraverse: Geology of north-eastern Tennessee and the Grandfather Mountain region, in Labotka, T.L., and Hatcher, R.D., Jr., eds., Geological Society of America 2006 Section meeting Field Trip Guidebook: Knoxville, University of

Tennessee, p. 129-184.
Hill, J.S, 2018, Post-orogenic uplift, young faults, and mantle reorganization in the Appalachians, PhD Dissertation, University of N.C. Chapel Hill, 139p.
Wooten R.M., Witt A.C., Gillon K.A., Douglas T.J., Latham R.S., Fuemmeler S.J., and Bauer J.B., 2008, Slope movement hazard maps of Watauga County, North Carolina: North Carolina Geological Survey Geologic Hazards Map Series 3, 4 sheets, scale 1:36,000, and Digital Data Series GHMS-3 (DDS-GHMS-3).

Stop 1-3: Southern, upthrown block of the Boone fault zone

Location: 36.1933°N, 81.6528° W

Stop leader: Jesse Hill

PLEASE BE CAREFUL! This stop is on a busy highway with fast moving vehicles; please stay off of the shoulder of the road.

Figure 1. Exposure of foliated Grandfather Mountain formation meta-siltstone cut by steeply dipping brittle faults and fractures associated with motion on the Boone fault.

We previously saw the Boone fault zone at the Vulcan Quarry, but were unable to get a close look at the rocks. This stop is located in the southern, upthrown block of the Boone fault zone where the Grandfather Mountain formation is in fault contact with the Cranberry Gneiss formation to the north. The

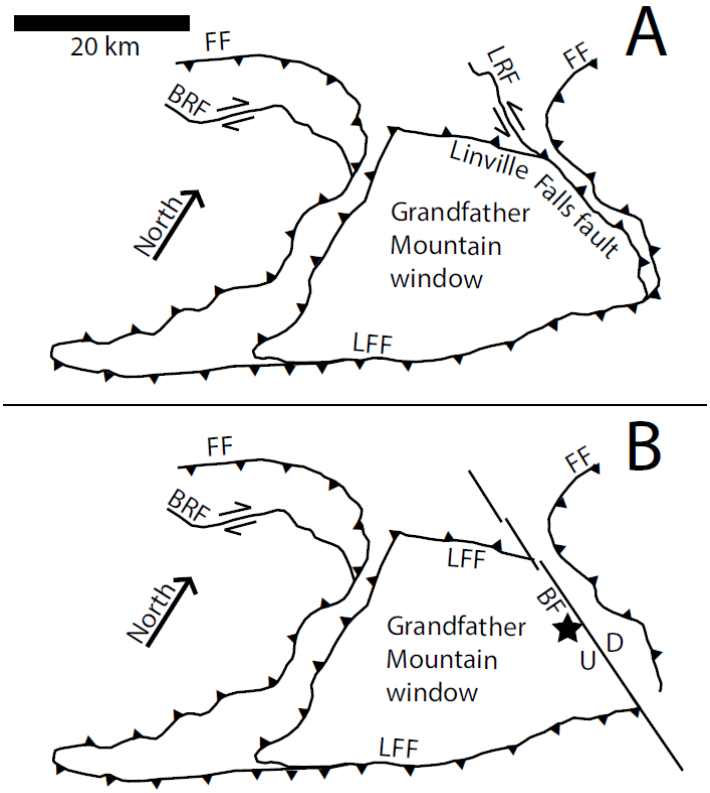

Figure 2: (A) Map of the Grandfather Mountain window and bounding faults (BRF = Burnsville fault, FF = Fries fault, LFF = Linville Falls fault, LRF = Long Ridge fault) (Modified from: Bryant and Reed, 1970; Hibbard et al., 2006). (B) Map of the window where the Boone fault (BF) replaces a section of the Linville Falls fault. Black star indicates approximate location of this field stop.

purpose of this stop is to view the Boone fault at the outcrop-scale (Figure 1) and to discuss how to interpret fault slickenlines as indicators of past motion. We will also view a potential future slope-failure-detachment surface along the fault and discuss the implications of the Boone fault on modern slope-failure hazards.

This stop is along the northeastern edge of the Grandfather Mountain window, along a fault that Bryant and Reed (1970) mapped as part of the Linville Falls thrust fault, which they showed as bounding the entire window. The rock is a silvery-grey metamorphosed siltstone of the Grandfather Mountain formation with a mylonitic texture including stretched feldspar and quartz clasts. The foliation at this stop dips to the NE at ~45° into the outcrop and strikes towards 315° (Figure 1). It formed during Paleozoic NW-directed motion along the Linville Falls thrust fault and was tilted by subsequent duplexing of the window (e.g. Bryant and Reed, 1970; Adams and Su, 1996; Stewart et al., 1997). This metamorphic layering is crosscut by high-angle brittle fault surfaces with

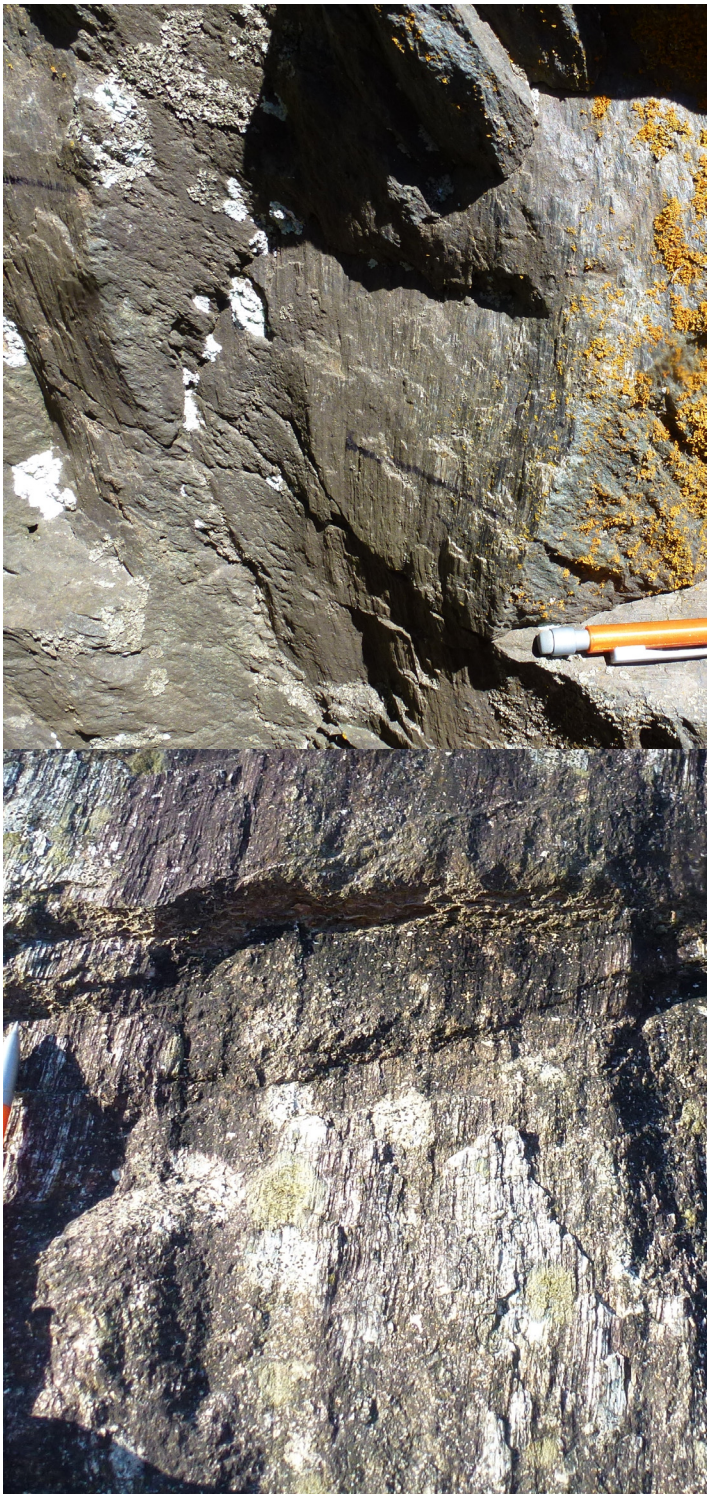

Figure 3: Steeply plunging slickenlines on minor fault surfaces.

slickenlines, or deformation grooves carved into the fault surface during the last motion (Figure 3). This high-angle fault zone contains near-vertical surfaces that dip both north and south and strike towards ~285°.

Slickenlines are important tools for interpreting fault histories because they form in the slip direction and record the maximum shear stress along the failure surface (Twiss and Moores, 2007). The orientation

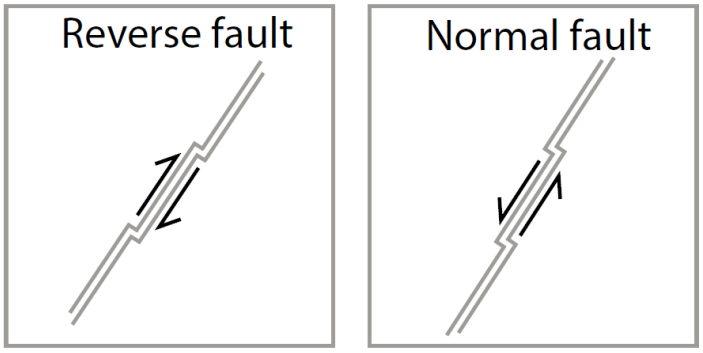

Figure 4: Example slickenline with steps. Fault surface is coming out of image and grey lines indicate steps along the plane.

of the slickenline can be described with the strike and dip of the fault plane, and the pitch, or angle between strike line and the slickenline. These three measurements give the orientation of the line but provide no information about the sense of motion. The mm-scale steps on the fault plane can be used to determine the direction of motion by assuming that each fault block moved in the direction needed to preserve the steps (Figure 4). For example, the hanging wall block in a normal fault moves down the steps of the footwall.

A population of minor faults with slickenlines can be used to determine the stresses driving fault forma-

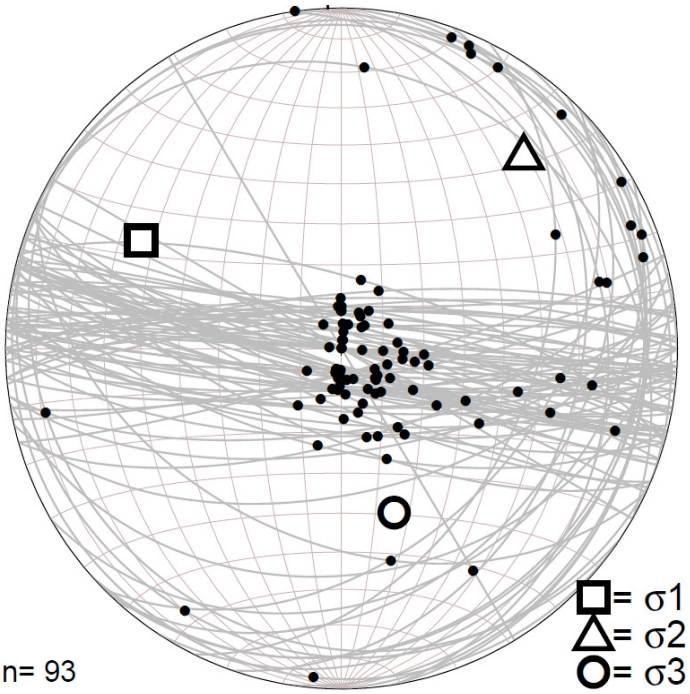

Figure 5: Lower-hemisphere plot of faults (grey lines) with slickenlines (black dots). Arrows on normal faults point towards center and on reverse faults they point away. Large square, triangle, and circle icons are the least, intermediate, and most compressional stress directions calculated with the paleostress inversion. Note: we are using the engineering convention so that the maximum compressive stress corresponds to σ_3.

Figure 6: Potential rock-slide detachment surface (visible from bottom-left corner to top-right corner of image) created by intersection of foliation and fractures.

tion, assuming: 1) the faults have not been reoriented since the time of motion; 2) all of the faults formed due to the same stress system; and 3) the slickenlines formed in the maximum shear stress direction. To simplify this cause-and-effect analysis, we performed a paleostress inversion with software called WinTensor (Delvaux and Sperner, 2003) to solve for the best-fit principal stresses, which describe the state of stress with only normal and no shear stresses. We compare the resultant stresses to principal stresses known to have caused shortening and rifting events in the study area to test if the Boone fault can be explained by known tectonic events, such as the Paleozoic collision or Mesozoic break-up of Pangea.

The faults with slickenlines at this stop (n = 93) occur in a WNW-striking, steeply-dipping set and a gently-dipping set with variable strike directions (Figure 5). These two sets of faults also exist at a nearby outcrop beside the Meadowview apartments, where the Boone fault is also well-exposed. The high-angle faults show evidence of dip-slip motion along N-dipping normal and S-dipping reverse faults, most often with the south block moving upwards.

The stress inversion of the faults at this site yields south-plunging maximum compressional directions, which are inconsistent with the stresses that drove NW-directed Paleozoic shortening or Mesozoic E-W rifting. However, the results are consistent with south-side-up motion of the Grandfather Mountain window along the steeply-dipping, WNW-striking Boone fault zone. A detailed discussion of these faults can be found in Hill (2018).

The two sets of brittle faults combine with the metamorphic foliation to produce large blocks that can detach from the outcrop, eventually leading to slope-failure. There is a detachment surface at this site that can be traced continuously for tens of meters and bounds a large block that may be a potential hazard (Figure 6). Gillon et al. (2009) described how a combination of fractures and foliation may have led to an increased risk of slope failure and instability in Watauga County.

REFERENCES

Adams, M. G. and Su, Q., 1996, The nature and timing of deformation in the Beech Mountain thrust sheet between the Grandfather Mountain and Mountain City windows in the Blue Ridge of Northwestern North Carolina, The Journal of Geology, v. 104, p. 197-213.

Bryant, B., and Reed, J.C., Jr., 1970, Geology of the Grandfather Mountain window and vicinity, North Carolina and Tennessee: U.S. Geological Survey Professional Paper 615, 190p.

Delvaux, D. and Sperner, B., 2003, New aspects of tectonic stress inversion with reference to the TENSOR program. In: New Insights into Structural Interpretation and Modelling (D. Nieuwland Ed.). Geological Society, London, Special Publications, 212: 75-100.

Gillon, K. A., Wooten, R. M., Latham R. L, Witt A. W. Douglas, T. J., Bauer, J. B., and Fuemmeler, S. J, 2009, Integrating GIS-Based Geologic Mapping, LiDAR-Based Lineament Analysis and Site Specific Rock Slope Data to Delineate a Zone of Existing and Potential Rock Slope Instability Located Along the Grandfather Mountain Window-Linville Falls Shear Zone Contact, Southern Appalachian Mountains, Watauga County, North Carolina, American Rock Mechanics Association ARMA 09-181.

Hibbard, J. P., van Staal, C.R., Rankin, D.W., and Williams, H., 2006, Lithotectonic map of the Appalachian Orogen, Canada-United States of America, Geological Survey of Canada, Map 2096A, scale 1:500,000.

Hill, J. S., 2018, Post-orogenic uplift, young faults, and mantle reorganization in the Appalachians, PhD Dissertation, University of N.C. Chapel Hill, 139 p.

Stewart, K. G., Adams, M. G., and Trupe, C. H., 1997, Paleozoic structure, metamorphism, and tectonics of the Blue Ridge of western North Carolina, Carolina Geological Society, 1997 Field Trip Guidebook, p. 16-17.

Twiss, R. J. and Moores, E., M., 2007, Structural Geology, second edition; W. H. Freeman and Company, New York.

STOP 1-4 Sky Valley: Stream Morphology, Debris Slide Scar and Bedrock Walking Tours

Lat 36.1837° Long 81.6821°

Leaders: Ellen A. Cowan, Keith C. Seramur, and Richard M. Wooten

Stop description

Sky Valley is a northeast–southwest trending valley between Deck Hill and Pine Ridge, located between Boone and Blowing Rock, NC. The valley and surrounding hillsides were purchased as a 150-acre parcel in 1946 by Jack B. Sharp, of Greensboro, NC. A summer camp, named Camp Sky Ranch was opened in 1948 for children with physical disabilities. It was operated by the Sharp family for 61 years until 2008. The lumber for the buildings was cut from blighted chestnut trees on the property and dressed at a neighboring sawmill. Native rocks were used for foundations, chimneys and fireplaces. Approximately 115 boys and girls attended each two-week long session between June and mid-August, where they participated in traditional camp activities including horseback riding, tennis, nature study, boating, archery and swimming (Fig. 1).

A one-acre lake was constructed by building a 90 ft-long concrete dam across the bedrock narrows of Flannery Fork at one end of the valley. An engineering study estimated that a million gallons of stream water per day ran through the lake. The lake was last dredged 20 years ago, however the weir can be opened to allow the lake to drain in the winter (Fig. 2). Drinking water for the camp was obtained from springs and a reservoir on the mountainside and piped 600 feet to the valley floor. Cabins, a dining hall, a chapel, a swimming pool, as well as the foundation of the tennis courts still remain on the valley floor. Although the valley usually appears as a peaceful paradise, floods of Flannery Fork have covered much of the valley floor (Fig. 2)

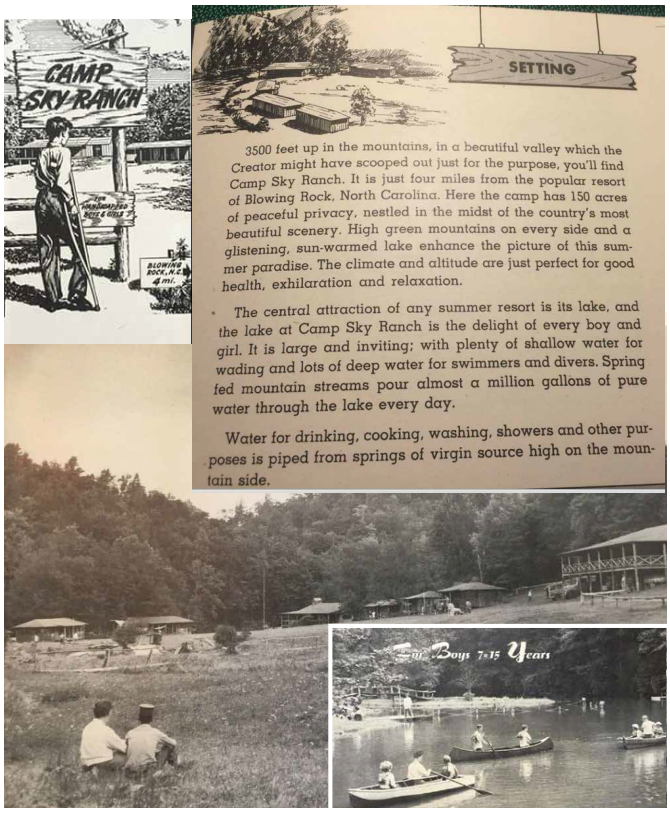

Figure 1. Photographs from Camp Sky Ranch ~1948 and a passage from the camp brochure describing the setting.

Today, Sky Valley Zip Tours, LLC is operated on the property by Jack L. Sharp, the grandson of the original owner. The guided tour zig-zags on 10 different zip lines through the forest canopy and across Sky Valley. The longest zip line referred to as "Big Momma" is 1600 ft long and 300 ft above the valley floor. In addition, two features of the tour utilize unique elements of the landscape; a 45 ft high rope-assisted cliff jump from an overhanging quartzite outcrop and 120 ft-long swinging bridge that crosses 50 ft above cascading waterfall of Flannery Fork. The zip line course begins to the south of the open valley and is accessed by ATVs on a steep gravel road. The facilities are also used for meetings, social gatherings, and weddings as Camp Sky Ranch Events.

Walking tours of Sky Valley

The buses will approach Sky Valley on Winkler's Creek Road from the South. This is the lunch stop as well as the opportunity to participate in walking tours to see exposures of the bedrock geology, stream morphology, and the scar of the 1940 landslide scar. The bedrock geology tour will follow the road to the

south of the open valley, include a stream crossing (on boulders) and a hike up a steep set of stairs to a 45 ft exposure of quartzite (Fig. 3). The steam tour will follow the same road to a steep path down to the cascades of Flannery Fork, then follow the stream traverse through the open valley until reaching the dam at the furthest northern end of Sky Valley (Fig. 3). The slope stability tour will require a short hike to the slope after crossing the stream using boulders (Fig. 3).

Figure 2. Historical photographs from Camp Sky Ranch. Upper shows the drained lake bottom in winter. Middle shows the spring house that supplied water to the camp. Lower shows Flannery Fork flooding in 1977.

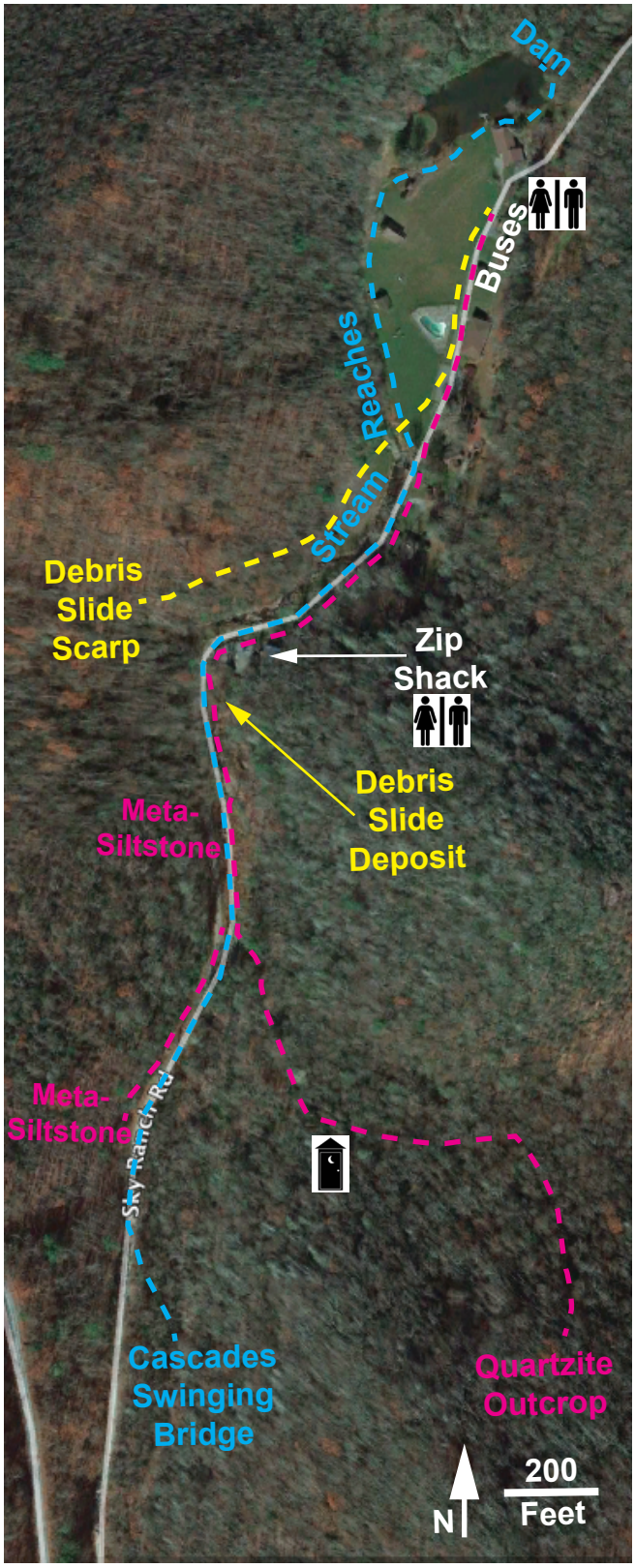

Figure 3. Topographic map of Sky Valley showing location of 3 walking tours: bedrock geology (magenta), mountain stream channel morphology (blue), and debris slide scar (yellow).

Bedrock Geology – No Rock Hammers Please

Sky Valley is located within the Grandfather Mountain window and has exposures of the Grandfather Mountain Formation including meta-siltstone, phyllite and meta-sandstone (quartzite) (Bryant and Reed, 1970) (Fig. 4). Examples of these rock types can be seen as meter-sized boulders and outcrops within the creek bed of Flannery Fork or in discontinuous, partly covered outcrops along the northwest side of the road between the entrance off of Winkler's Creek Road and the Zip Shack (meta-siltstone) or along the eastern valley wall behind the cabins (quartz-rich meta-sandstone). The valley floor separates outcrops of phyllite and meta-siltstone to the west from quartz-rich meta-sandstone to the east and it appears that the contact between these rock types is covered beneath sediment of the valley floor.

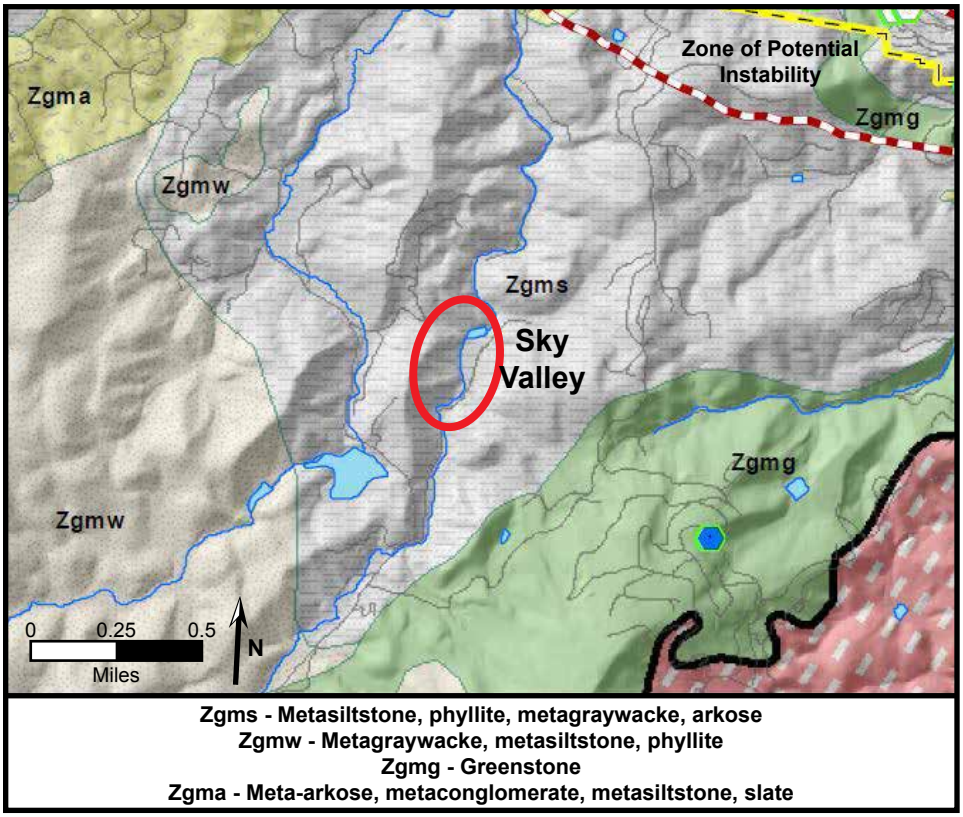

Figure 4. Generalized bedrock geology map showing the location of Sky Valley within the Grandfather Mountain Formation (Zgms). Map from NCGS Geologic Hazards Map Series 3, 2008 (Wooten et al., 2008).

Bedrock Walking tour

Exposures of meta-siltstone and phyllite occur along the west side of road to the south of the Zip Shack. Follow the road, passing the exposure of slide-deposited diamicton in the stream cut adjacent to the bridge (Fig. 5). This deposit is a matrix-supported yellowish red (5YR 4/6) sandy clay loam with many angular, tabular phyllitic clasts ranging from pebbles to boulders. This deposit with large "floating" clasts in sandy clay loam was deposited as debris originating from a slide on the west side of the valley in August 1940.

The meta-siltstone outcrops show a well-developed foliation with local open folds (Fig. 6). The rocks are metamorphosed to chlorite grade phyllite and have a silky luster or sheen formed by muscovite. Bedding is preserved locally. Few bedrock fractures or joints are present within the outcrops.

Figure 5. Exposure of diamicton with pebble to boulder size clasts originating from the western valley wall. It was deposited in August 1940 by a debris flow that began as a slide and became a flow as it blocked Flannery Fork (as shown on Figure 21).

Figure 6. Examples of meta-siltstone outcrop on the west side of Sky Ranch Road and phyllite from the creek bed. Note the gentle to open fold in the sample in the lower picture.

Follow the first road that intersects to the left and crosses the stream. A stream crossing can be accessed by following the foot path on the right side of the road. Cross Flannery Fork using boulders in the stream and follow the path back to the road. As you walk up the steep gravel road you will pass the Whistle Pig Kids Park on the right. Continue along the road until you come to the wooden steps to the right Take these steps up to the Cliff Jump. When arriving at the top, take the steps to the right down to the location of the black and white wooden landing zone (Fig.7).

The outcrops in front of you are light gray, porphyroclastic, foliated quartzite (Fig. 8). A thin section of a piece of boulder float collected nearby shows that this rock type is mostly quartz with small amounts of muscovite defining a weak foliation (Fig. 8E). Pseudo-ripple marks can be observed on the dip slope to your right as you face the cliff jump (Fig. 8E). They are formed by two intersecting fracture sets (Fig. 8B). When these fractures weather along an oblique surface they produce a ripple-like pattern on the outcrop surface. In vertical exposures, sheared foliation planes give the appearance of cross bedding (Fig. C & D). The original bedding is probably represented as faint color bands on the vertical outcrop face.

Figure 7. View from the top of the stairs of the quartzite outcrop that forms the Cliff Jump. The black and white landing pad is the target for guests on the Zip line tour as they make a controlled rope descent from the top.

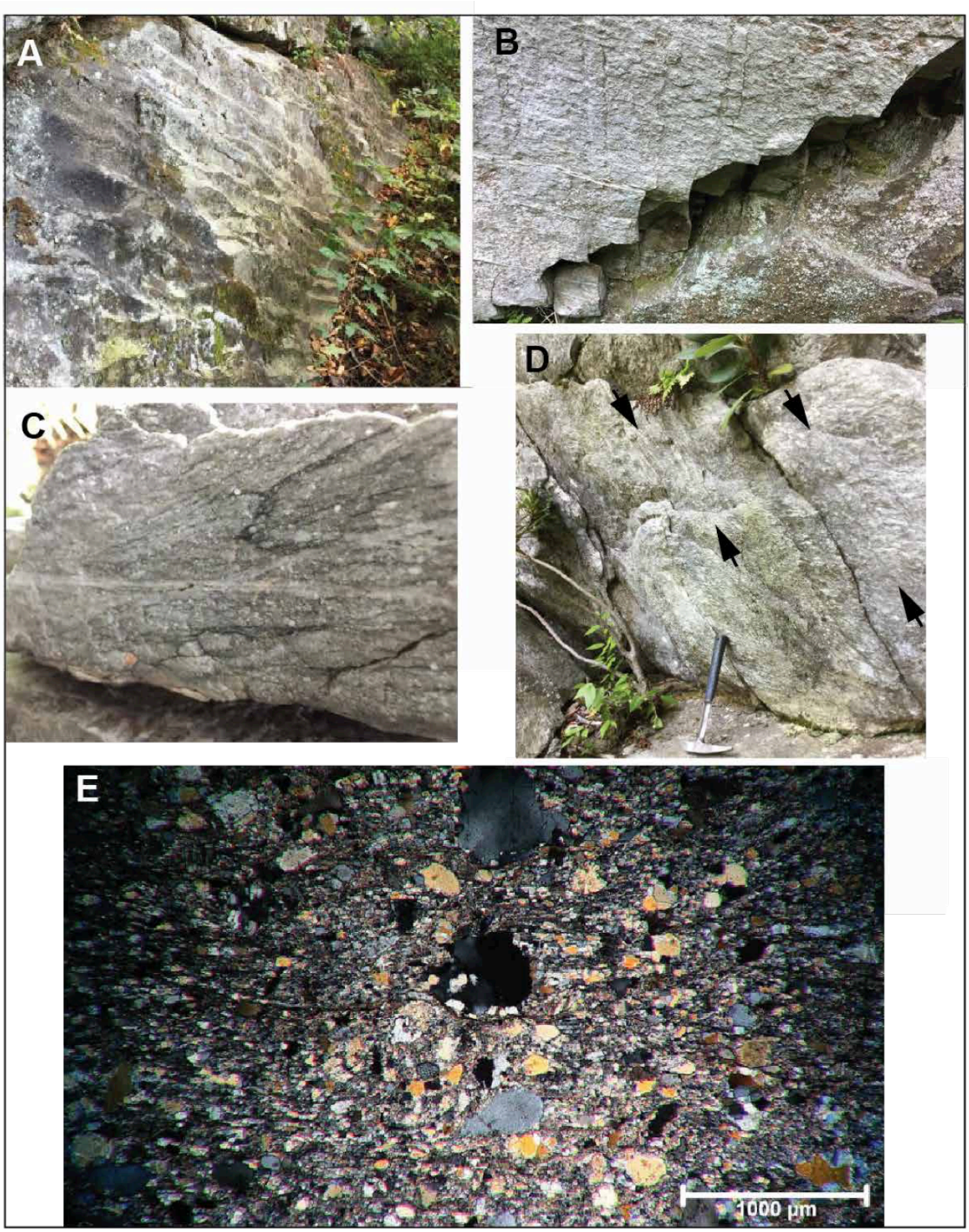

Figure 8. Exposures of quartzite from the Cliff Jump outcrops showing A) pseudo-ripple marks, B) intersecting fracture sets C and D) pseudo-crossbedding, and E) quartzite thin section.

Stereonets

Stereonets of the bedrock foliation and fracture or joint sets were plotted along with the slopes on the east and west sides of Sky Valley (Fig. 9). The fracture and foliation orientations were collected in the field with a Brunton compass and the strike and dip of the fractures in each set were averaged and plotted on stereonets (Fig. 9). The sets of fractures with a similar orientation were grouped together. The slope of the west valley wall was determined at the location of the 1940 landslide by measuring from the crest of the ridge to the toe of the slope. The slope of the east valley wall was determined at the gravel road that leads up to the quartzite (Cliff Jump) outcrop.

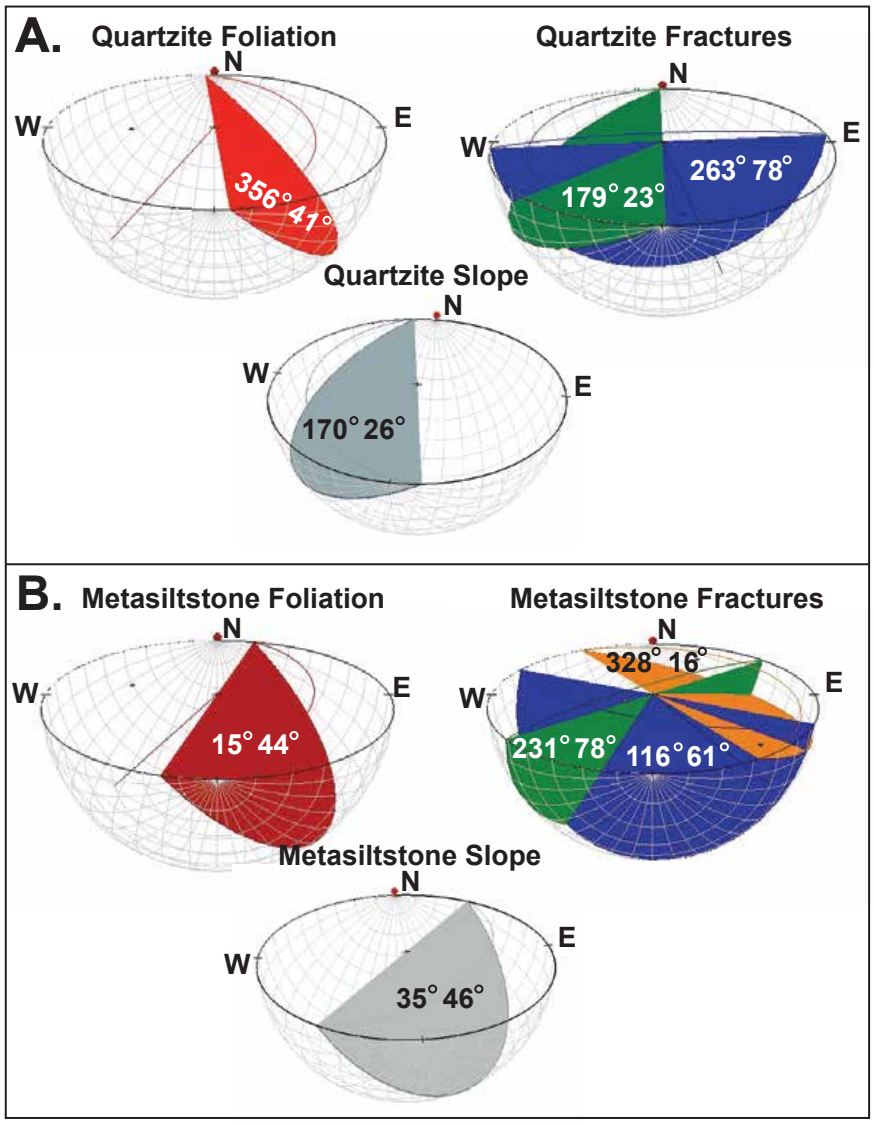

Figure 9. Stereonets showing orientation of structural features measured in quartzite (A) and meta-siltstone (B) outcrops.

The foliation in the quartzite and meta-siltstone dips 41º to 44º to the east. The east side of the valley is underlain by quartzite or quartz-rich rocks. Two prominent bedrock fracture sets were recorded at the quartzite outcrop. One fracture set (179º 23º) has an orientation and dip similar to the slope of the east valley wall (170º 26º) (green fracture set on Fig 9A). These rough open joints that trend parallel to the slope are most likely sheeting joints, which result in curved surfaces common in quartz-rich rocks within the Grandfather Mountain window (Hack, 1966).

Three fracture orientations were measured in the meta-siltstone outcrops. Two of the measured fracture orientations are perpendicular or opposite of the slope (blue and green fracture sets on Fig. 9B). One fracture measurement (328º 16º) has a line of dip that is 47º north of the slope (orange fracture on Fig 9B). The infrequency of this fracture in outcrop and the oblique angle of the line of dip indicate that it was most likely not a significant contributing factor to the 1940 landslides.

The foliation (15º 44º) in the phyllite has an orientation and dip similar to the slope of the west valley wall (35º 46º) (Fig 9B). This west wall is a dip slope and the dip of the foliation is considered a significant contributing factor to the 1940 landslides.

Flannery Fork: Headwaters of the New River Drainage Basin

Flannery Fork flows through Sky Valley and offers an opportunity to observe several types of channel-reach morphologies over a walkable distance. Channels in mountainous drainage basins have mixed bedrock-colluvial to alluvial reach morphologies that result from local variations in sediment delivery, accumulation or storage. Flannery Fork is a second order stream originating 2.5 miles (4 km) to the south of Sky Valley as tributaries draining Flat Top Mountain and an unnamed mountainside into Trout Lake (Fig.10). Flannery Fork joins with Winkler Creek north of Sky Valley and then meets the South Fork New River at Clawson-Burnley Park near the National Guard Armory in Boone. Therefore, Flannery Fork is a headwaters contributor to the New River Watershed, part of the National Wild and Scenic Rivers System.

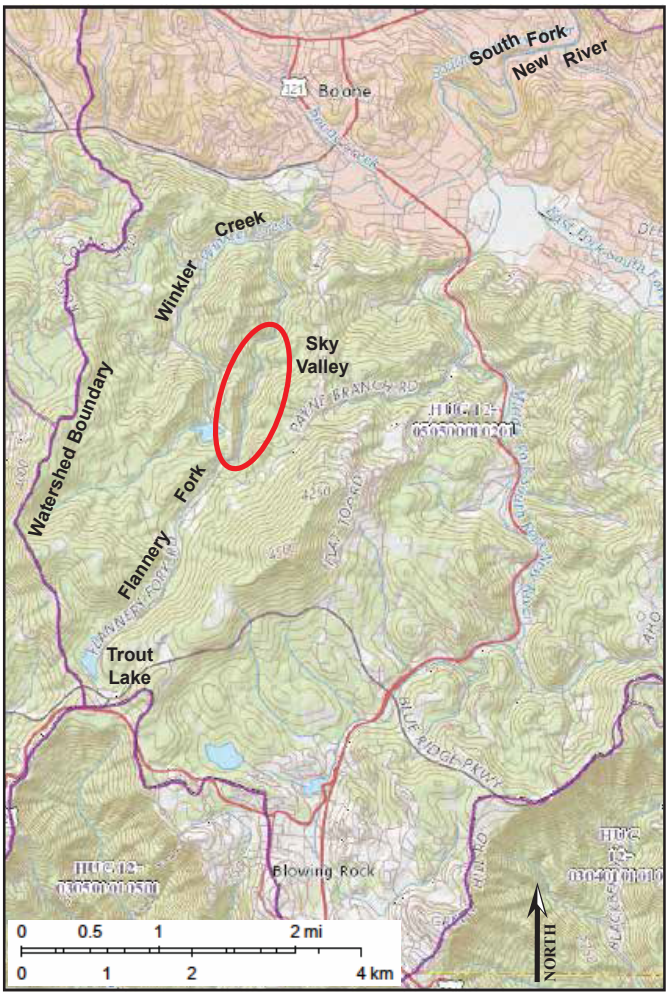

Figure 10. Topographic map showing the location of Sky Valley with respect to Flannery Fork, which flows through it. The watershed boundary is shown in purple.

Stream morphology walking tour

The most upstream reach of Flannery Fork can be observed by walking south on Sky Ranch Road ~0.1 miles past the Zip Shack. Follow the path to the left just past the 10 mile/hr speed sign down to the channel. This short steep trail leads to the Cascades beneath the swinging bridge. This steep channel reach is scoured to bedrock with large boulders protruding through the flow creating a disorganized bed (Fig. 11). The stream's transport capacity exceeds the limited sediment supply due to the steep slope and stable well vegetated slopes. Native vegetation is dense, growing into the clearing at the channel edge.

Hike up the trail and follow the road north back toward the open valley. Between the road on your right and the bridge you will pass an overgrown stream reach with a flattened gradient. This area was flooded in 1940 when debris originating from the valley wall to the west temporally blocked the flow of Flannery Fork. The impounded water appears in this area on the aerial photograph dated 10-21-1940 (see Fig. 21).

Flannery Fork follows along the west side of the ~0.28 mile-long (450 m) valley. The furthest upstream reach, for ~ the first 0.1 mile is characterized by step-pool morphology (Figs.12 and 13). The steps are formed by accumulations of large boulders that span the width of the channel and between them are deeper pools that contain somewhat finer grained sediment (Fig. 14). Through this section the overall gradient is 4% (2.3°), however the elevation drop is accounted for by the steps below each pool (Fig.15). Steps form where large clasts accumulate across the channel in zones with local high flow resistance (Bierman and Montgomery, 2014). Steps grow by trapping additional clasts during flood events. Step-pool morphology occurs where Flannery Fork crosses the 1940 debris flow deposit.

It is notable that the largest boulder diameter is reduced in the downstream direction, suggesting that the largest clasts in the stream originated as colluvium from this source. Further downstream, the largest diameter clasts are smaller, gravel and sand bars form and the gradient is 2% (1.2°) (Figs. 12 and 15).

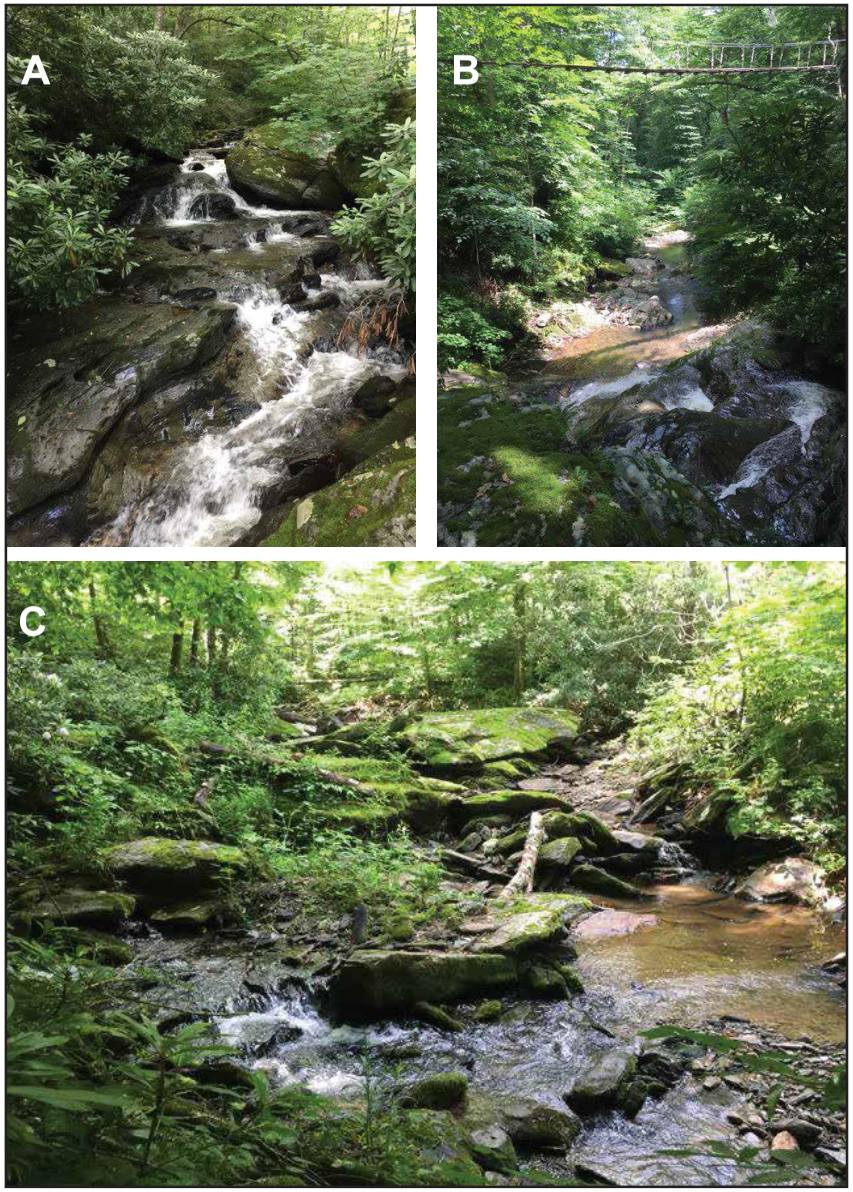

Figure 11. Upstream channel morphology of Flannery Fork. A) view upstream of the Cascades, B) downstream view with the swinging bridge above C) large boulders in the channel reach with native vegetation.

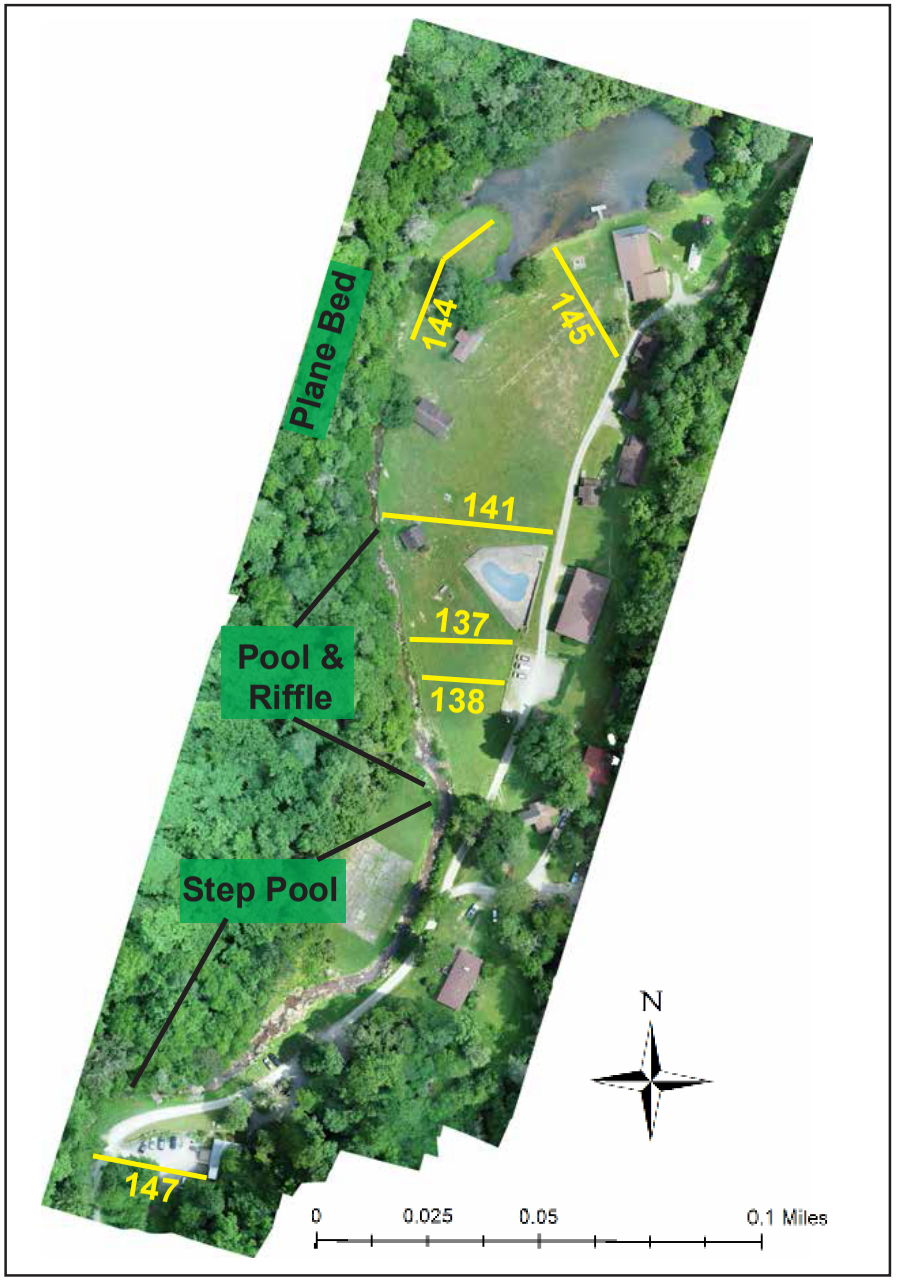

Figure 12. Overview of Sky Valley from 250 ft collected on a drone flight survey. Stream morphology is labeled and the locations of GPR profiles are shown. The drone was piloted by Brian Zimmer from the Department of Geological and Environmental Sciences, Appalachian State University.

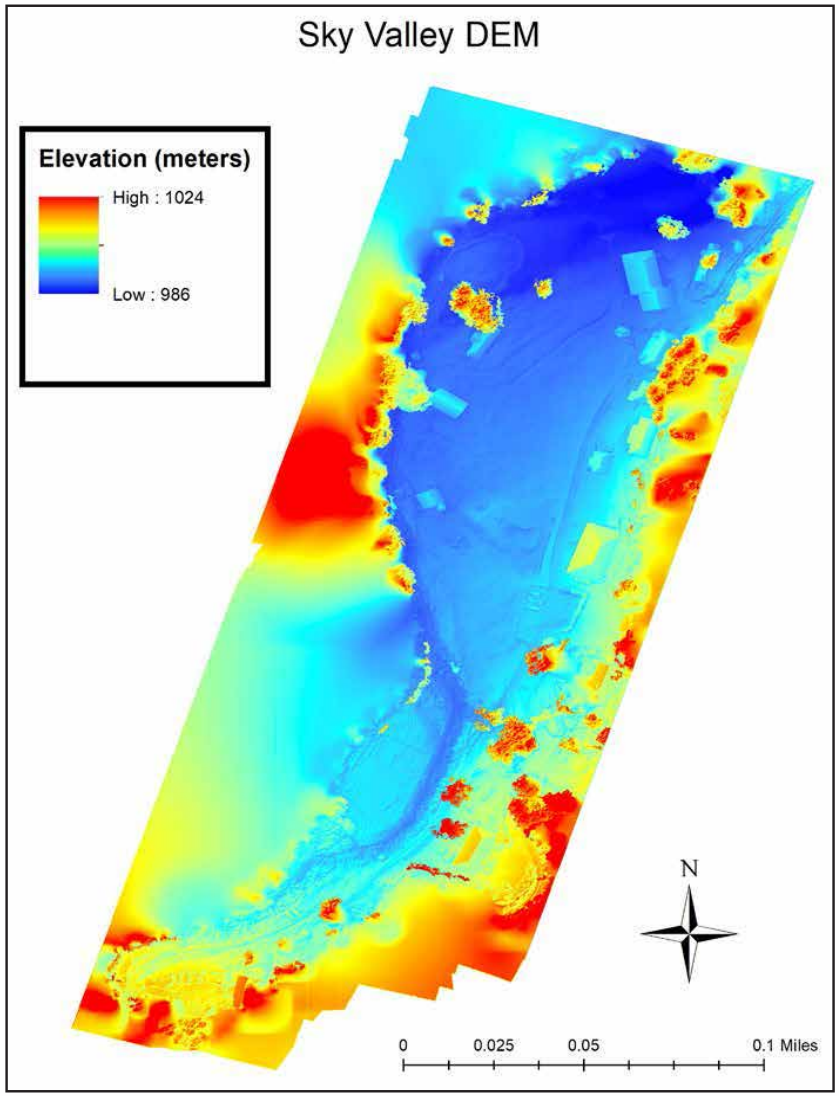

Figure 13. Digital Elevation Model of Sky Valley. Data collected on the drone flight.

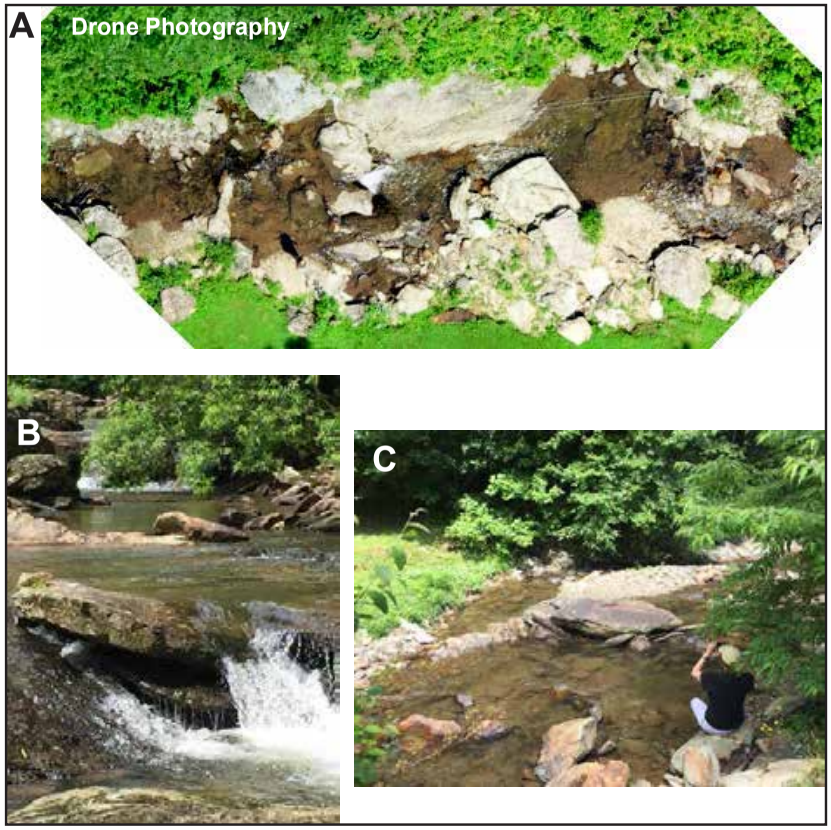

Figure 14. Step-pool channel morphology. A) aerial view showing pools separated by accumulations of large boulders, B and C) photos from within the channel.

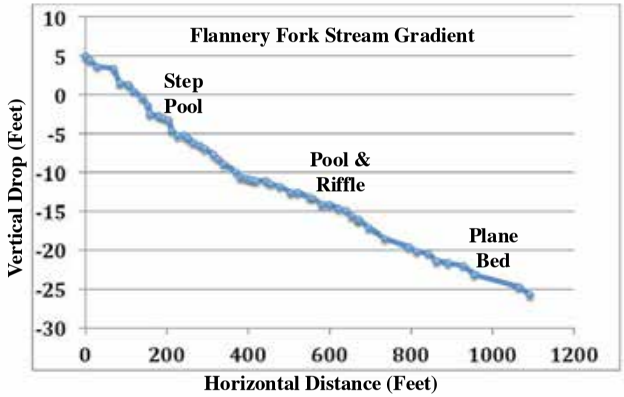

Figure 15. Flannery Fork stream gradient with types of stream channel morphology indicated.

A pool and riffle sequence forms indicating additional sediment supply and a reach that is limited by the ability of the stream to transport this load (Fig. 16) (Bierman and Montgomery, 2014). Recent large discharge events have caused undercutting of the bank along this reach.

Figure 16. Pool and riffle channel morphology. Aerial view and channel view shown.

Further downstream, the gradient is about the same, however the streambed becomes flat and uniform (Figs.12 &17). A featureless cobble bed is characteristic of plane bed morphology (Bierman and Montgomery, 2014). Compared with the upstream reaches, clasts are smaller relative to the depth of flow. This reach is beneath the tree canopy but lacks accumulations of large woody debris that would develop pool and riffle morphology. A 90-foot long concrete dam across the bedrock narrows forms a lake at the north end of Sky Valley (Figs.12 &18).

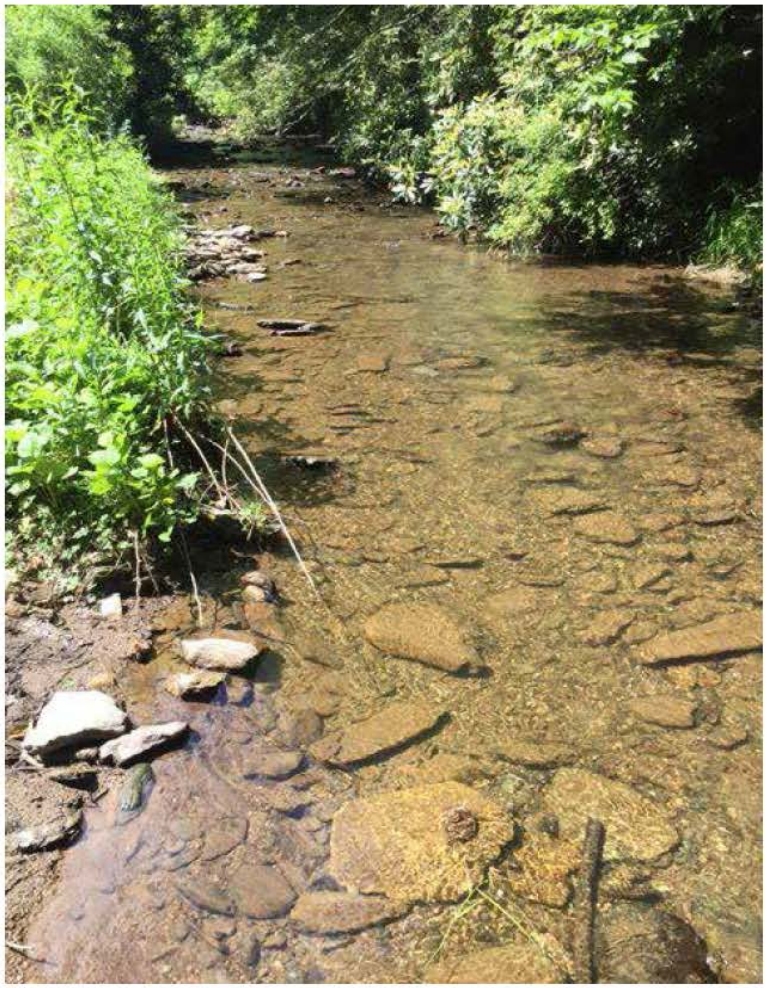

Figure 17. Plane bed stream morphology.

Figure 18. Ninety foot-long concrete dam anchored on bedrock at the north end of Sky Valley.

Ground Penetrating Radar (GPR) Survey

A ground penetrating radar (GPR) survey of the valley floor was completed using a GSSI 250 mHz antenna and a SIR-3000 single channel data acquisition system with a calibrated survey wheel. Thirteen transects were collected each running from the east to west across the valley. The GPR data was downloaded and processed using Radan® software. GPR data processing including adjusting time zero, completing a background removal and adjusting the time variable gain to enhance deeper reflections. Radargrams or GPR profiles of each transect line were produced to show a cross-section of the subsurface.

The radar pulse appears to have penetrated to a depth of 17.5 feet and the radargrams show clear and distinct reflections to the base of the profile. Six transects of radar data are shown and discussed here (Figs.19 and 20).

Three GPR transects, 137, 138 and 141 were collected along the southern portion of the valley (Fig. 19). Transects 137 and 138 show an infilled stream channel. Previously, Flannery Fork had a bifurcated channel in this area but it was filled with soil graded during construction of the tennis courts. Transect 141 shows a high amplitude continuous reflection at a depth of 7 to 10 feet on the east side of the transect (red dashed line on Fig. 19). A similar reflection is observed at a depth of 5 to 7 deep on the west side of Transect 141. These high amplitude continuous reflectors are likely the contact between coarse alluvium and bedrock.

Transect 144 was collected across the center of an island that is located on the sourthern end of the lake (Fig. 12). A filled depression occurs on the west end of the profile (blue dash line on Fig, 20). A low area on the island was reportedly filled with dredge spoils from the lake. The island was connected to the T1 terrace with fill material. This fill is represented by medium amplitude, discontinuous, horizontal reflections (yellow dashed line). The adjacent alluvium is also represented by medium amplitude, horizontal reflections, but they are continuous.

Transect 145 was collected across the northern end of the valley floor. A high amplitude discontinuous reflection on the west side of the transect dips down toward the enter of the valley (red dashed lined on Fig. 20). This reflector could represent an older coarse-grained deposit (colluvium) or perhaps bedrock. A second, relatively high amplitude, discontinuous, sub-horizontal reflection is observed on the east side of the profile (dashed blue line). This reflector is likely a bed of coarse-grained alluvium separating older and younger deposits of fine-grained overbank sediment. Two high-amplitude, shallow reflectors (~2.5 feet) are interpreted to be buried infrastructure related to the septic drainfield used by Camp Sky Ranch (green ovals on Fig. 20).

Transect 147 was collected on a topographically high area across from the 1940 debris slide scar (Figs.12 and 13). The surface was graded level for construction of the building that houses the Zip Shack, The debris flow deposit is shown on the radargram as medium to high amplitude discontinuous to chaotic reflections (Fig. 20). This radar facies shows a distinct contrast with the horizontal reflections that represent the alluvial deposits on the T1 terrace.

Mass Movement on western Sky Valley slopes

Historically the western slopes, underlain by phyllite and meta-siltstone have been unstable while the slopes to the east underlain by quartz-rich rock have been stable. Most recently, debris flows were initiated during the “1940 Flood” described in detail elsewhere in the guidebook. An aerial photograph from October 21, 1940 show fresh debris flow tracks and a slide scar originating along the western slopes (Fig. 21). It is evident from this photograph that debris formed a temporary dam across Flannery Fork, impounding the flow behind it. Today, Sky Ranch Road passes through this area next to the parking lot and Zip Shack located on the higher elevation landform (Fig.12 &13). The diamicton exposed along the stream bank is evidence that this landform originated from the debris slide (Fig 5).

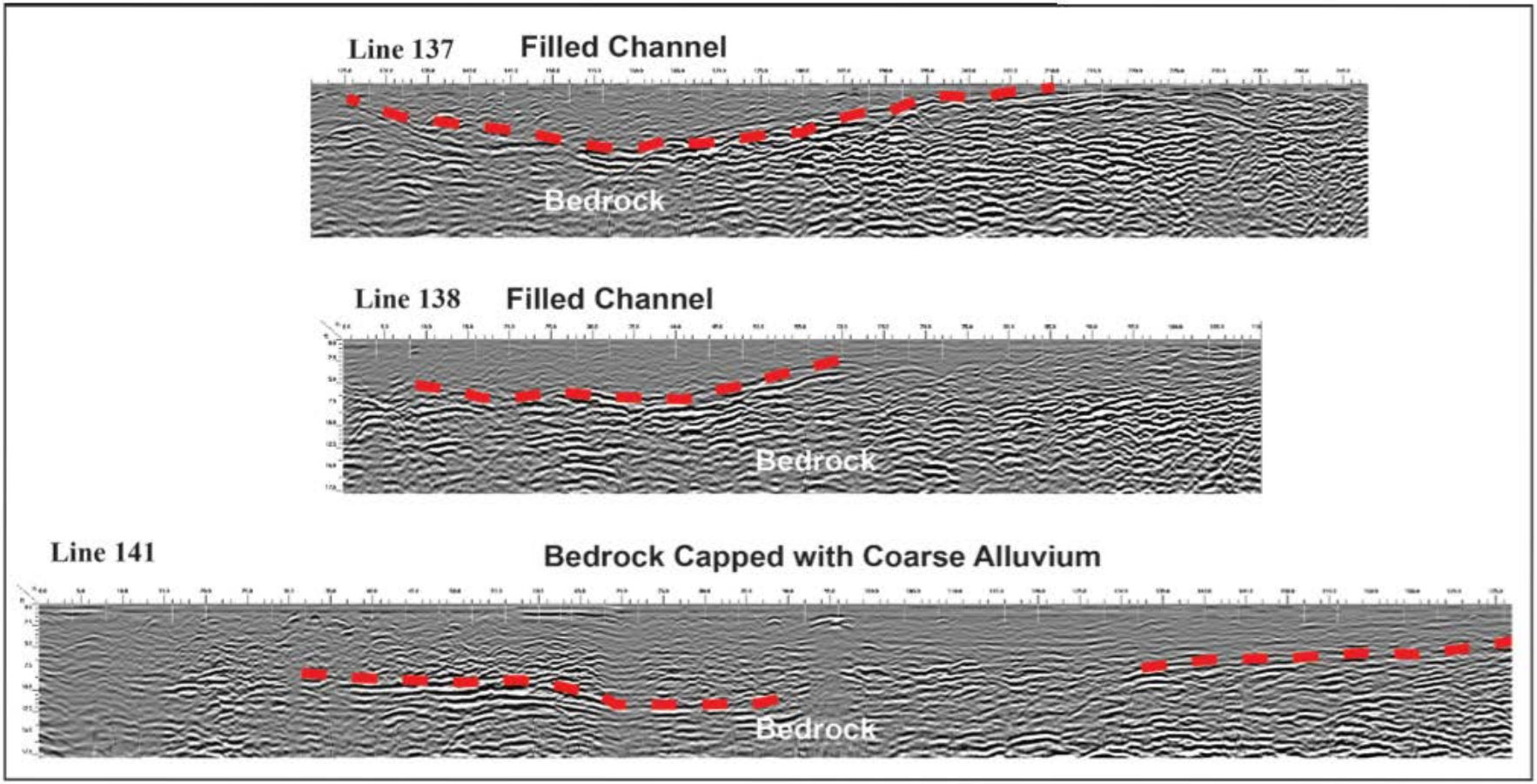

Figure 19. Radargram of GPR transects across valley floor. Scale is in feet.

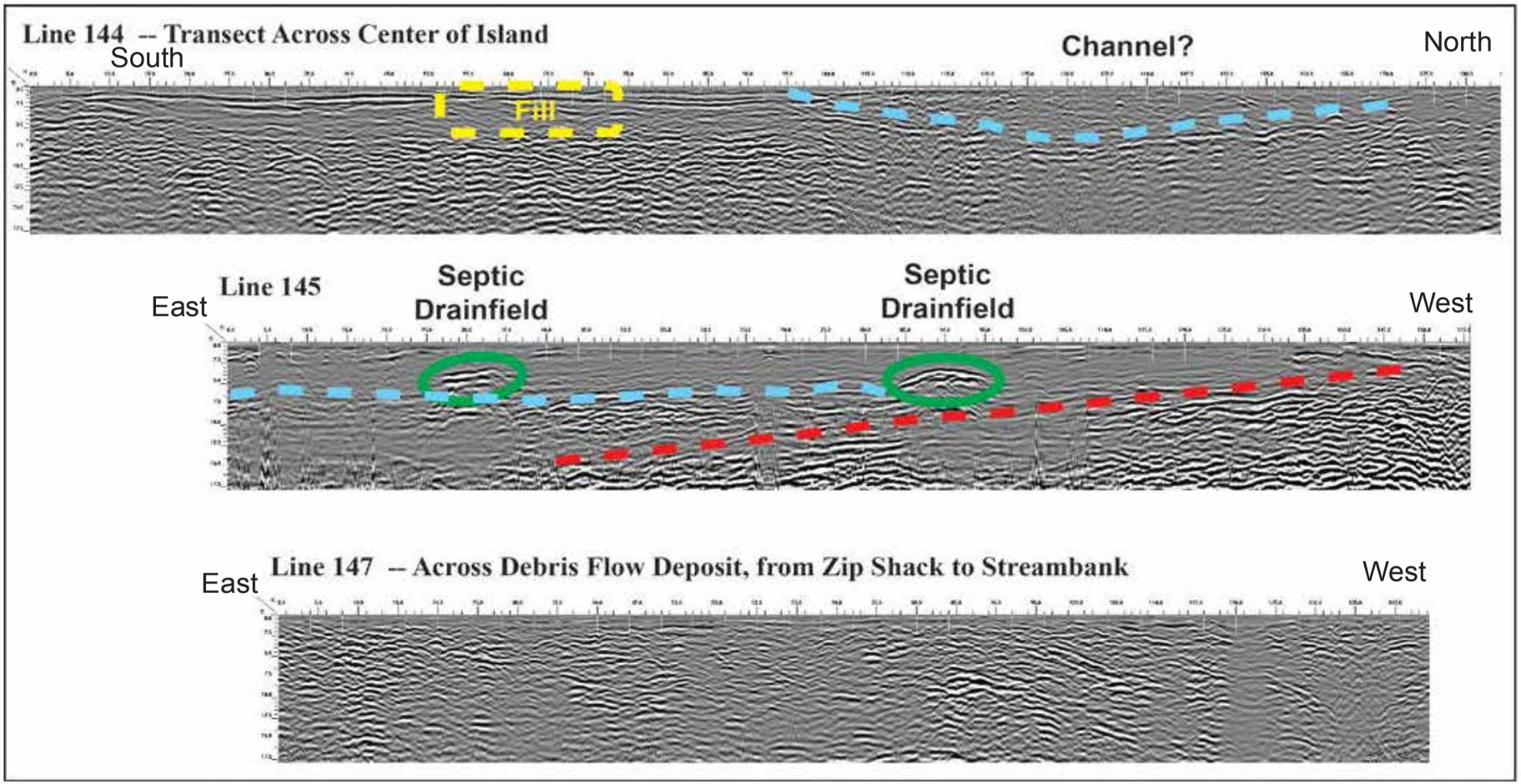

Figure 20. Radargram of GPR transects across valley floor and debis slide-flow deposit. Scale is in feet.

Figure 21. Aerial photograph taken on October 21, 1940. Scars from debris flows and a slide that occurred in August 13-14, 1940 can be clearly seen. Flannery Fork was blocked by debris that flowed across the valley.

In Fall 2017, the Geomorphology class at Appalachian State University spent several lab periods investigating the Sky Valley landscape. Evidence of slope instability was identified in 4 specific areas along the western slope (Fig. 22). The edges of these areas were mapped during a traverse using a hand-held GPS. The slide areas near the top of the slope were identified by steep scarps that exposed boulders and bare roots (Fig. 23). Occasionally, phyllitic bedrock was exposed with the foliation parallel to the slope direction. Edges of the debris transport zone were identified by subtle changes in topography or vegetation (Fig. 23). Trees within the initiation zone were smaller (younger) than those on the surrounding stable slopes. Trees with bent trunks were also identified in unstable areas on the western slope (Fig. 24). The areas of slope instability outlined by the geomorphology students generally correspond with scars shown on the 1940 aerial photograph (Fig. 21) and identified by the NCGS during their landslide mapping program in Watauga County (Fig. 25). However, Track 2 shown on Fig. 22 appears to incorporate the slope above and adjacent to the 1940 scar.

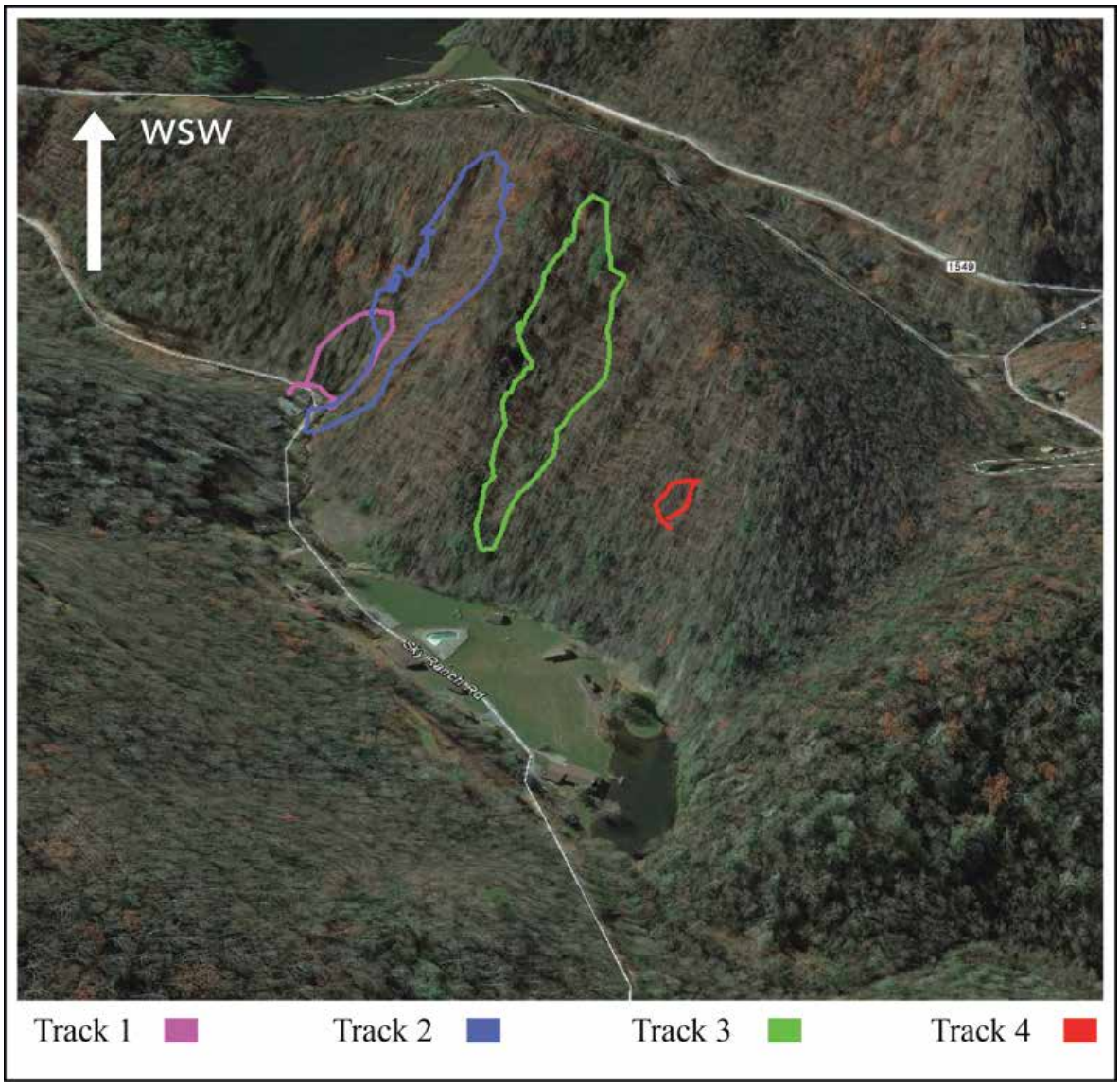

Figure 22. Boundaries of slope disturbance recorded by walking the slope with a hand held GPS during fall 2017. Track 1 outlines the boundary of the 1940 debris slide.

Figure 23. Views of the 1940 debris slide scar. The vertical scarp is present at the top of the scar. Smaller trees occur within the scar and scattered exposures of bedrock can be observed.

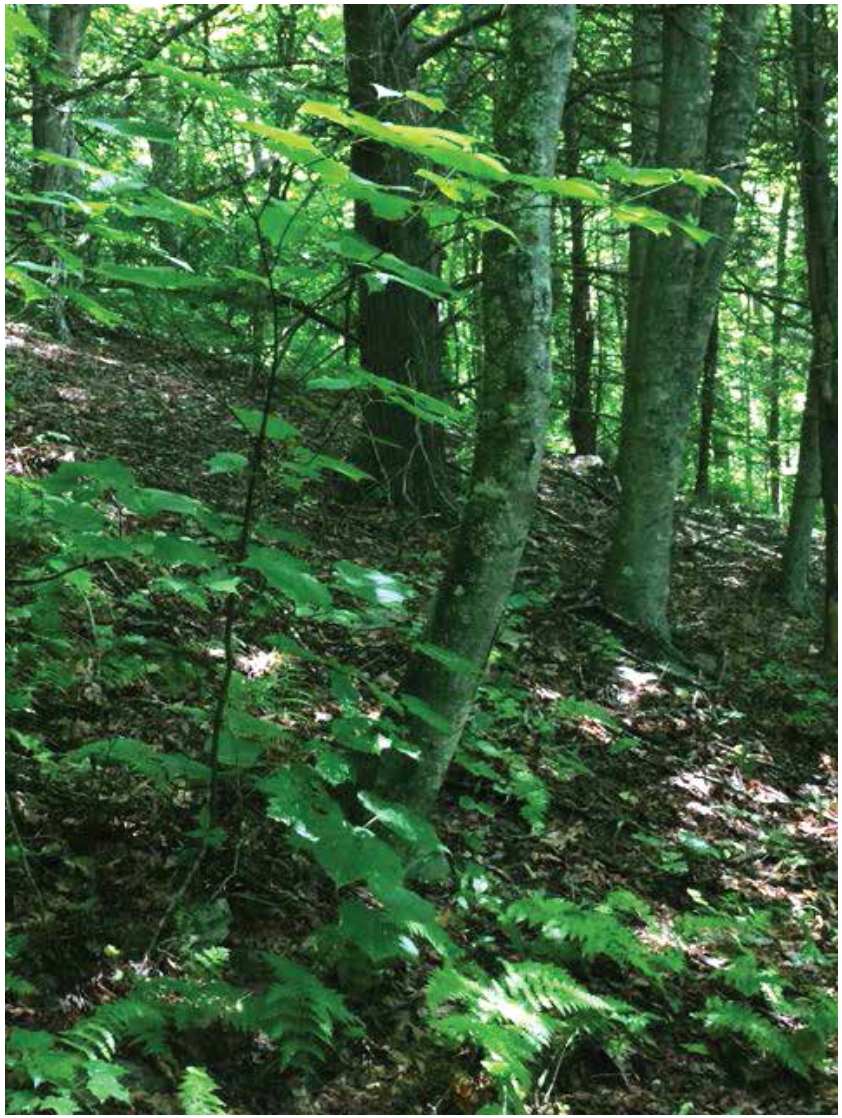

Figure 24. Bent trunks are an indication of continuing soil creep on the steep western slope.

Figure 25. Location of debris slide scar and tracks. Study site 3005 is also shown.

Detailed Site Investigation - August 13-14, 1940 Debris Flow Initiation Zone ID 3005

The NCGS investigated in detail six debris flow initiation sites in Watauga County, and similar studies were done in Macon, Buncombe, Henderson, Transylvania and Jackson Counties as part of the landslide hazard mapping process (Wooten and Witt, this guidebook). These investigations aimed to characterize the geologic and geotechnical aspects of locations where debris flows originate, and to constrain the physical parameters of soil used in the flow susceptibility modeling (e.g., soil depth, soil unit weight, shear strength, and hydraulic conductivity).

At this location (Fig. 25), as in the others, hand auger borings and test pits augmented observations of surface exposures. Hand-driven Shelby tubes were used to sample for quality and consolidated undrained triaxial shear strength testing conducted by the NCDOT Materials and Test Unit. An Amoozemeter™ constant head permeameter was used for in situ measurement of saturated hydraulic conductivity (Ksat). This site is within the Grandfather Mountain Formation metasedimentary unit Zgms (Fig. 4) included in calibration unit 7 used in the Stability Index Map (SINMAP) modeling of debris flow susceptibility (Wooten et al., 2008).

The source area for this debris flow is a colluvial hollow at the head of an intermittent tributary stream to Flannery Fork, typical of the steep, topographically convergent slopes at debris flow initiation zones. Figure 26 portrays the field developed geologic cross section measured through the hollow, with locations of hand auger borings and test intervals, and the test results. Geologic units at the site consist of post-1940 colluvium and older colluvium overlying residual soil that grades into weathered calcareous phyllite and phyllonite. The overall ground slope is 35° and coincides with the dip slope of the foliation which is inclined 35° to 42° to the southeast and east respectively. Of the 6 Watauga County study sites, two coincide with the dip slope of the foliation; whereas the other 4 sites are on slopes oblique to the foliation (where the angle between the foliation strike and the cross section bearing is within 35°). The 1940 rupture surface is interpreted to involve the upper zone of the residuum; however, it is possible that some part the rupture surface may have coincided with contact between the colluvium and residuum.

The high value of 284 lb/ft^2 (1.97 lb/in^2; 13.6 KPa) for effective cohesion (Ceff) measured here is interpreted to be the result of relict mineral grain bonding in the residuum derived from the calcareous phyllite (Figs. 26, 27). In fact, this value for Ceff is the highest measured for the 15 debris flow sites, and 6 potential debris flow sites investigated in Buncombe, Macon, Henderson, Transylvania, Jackson and Watauga Counties (Wooten et al., 2012) as part of the NCGS landslide hazard program. This high value for cohesion suggests that any residual soil involved in the rupture surface had lower cohesion. The effective friction angle (ϕeff) of 29° is approximately 1 standard deviation (3.6°) from the mean value of (ϕeff) 32.7° for the Watauga dataset. The order of magnitude of the Ksat value of 1.45E-04 cm/sec measured in the residual soil (Figs. 26, 28) falls within the E-03 and E-05 order of magnitude range for the Watauga County dataset. Measurements of shear strength and hydraulic conductivity the colluvial unit, not done in this study, would be useful to determine if a there is a shear strength and hydraulic conductivity contrast between the colluvium and residuum here.

Walking tour to 1940 debris slide scar

Cross Flannery Fork on the boulder crossing and scramble up the slope into the woods following the flagging tape. We will hike up the steep slope and then approach the slide scar from the north by following along contour through the forest. This will allow an appreciation of the steepness of the slope and the surface, and vegetation changes that indicate soil creep. When you reach the top or side of the slide scar you will be able to visualize the amount of debris missing from the slope as well as the run out direction into the creek below (Fig 23). If you venture up slope you will see the continued effects of soil creep in the region of Track 2 (Fig. 22). The former scarp of Track 2 is distinguished by subtle topographic changes across the slope.

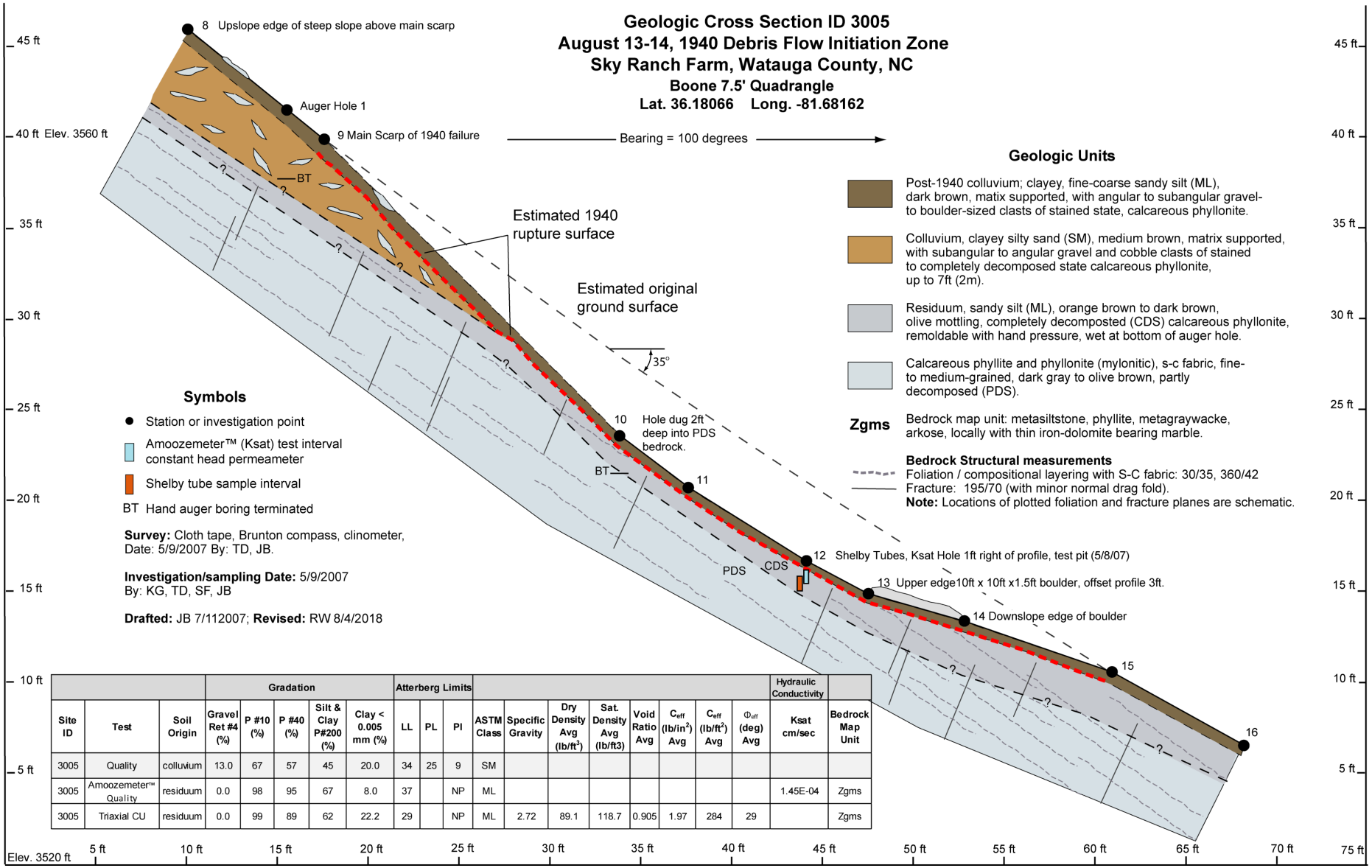

			Gradation					Atterberg Limits											Hydraulic Conductivity	
Site ID	Test	Soil Origin	Gravel Ret #4 (%)	P #10 (%)	P #40 (%)	Silt & Clay P#200 (%)	Clay < 0.005 mm (%)	LL	PL	PI	ASTM Class	Specific Gravity	Dry Density Avg (lb/ft^3)	Sat. Density Avg (lb/ft3)	Void Ratio Avg	C_{eff} (lb/in^2) Avg	C_{eff} (lb/ft^2) Avg	Φ_{eff} (deg) Avg	Ksat cm/sec	Bedrock Map Unit
3005	Quality	colluvium	13.0	67	57	45	20.0	34	25	9	SM									
3005	Amoozemeter™ Quality	residuum	0.0	98	95	67	8.0	37		NP	ML								1.45E-04	Zgms
3005	Triaxial CU	residuum	0.0	99	89	62	22.2	29		NP	ML	2.72	89.1	118.7	0.905	1.97	284	29		Zgms

Figure 26. Field developed geologic cross section for the August 13-14, 1940 debris flow initiation zone – Site ID 3005.

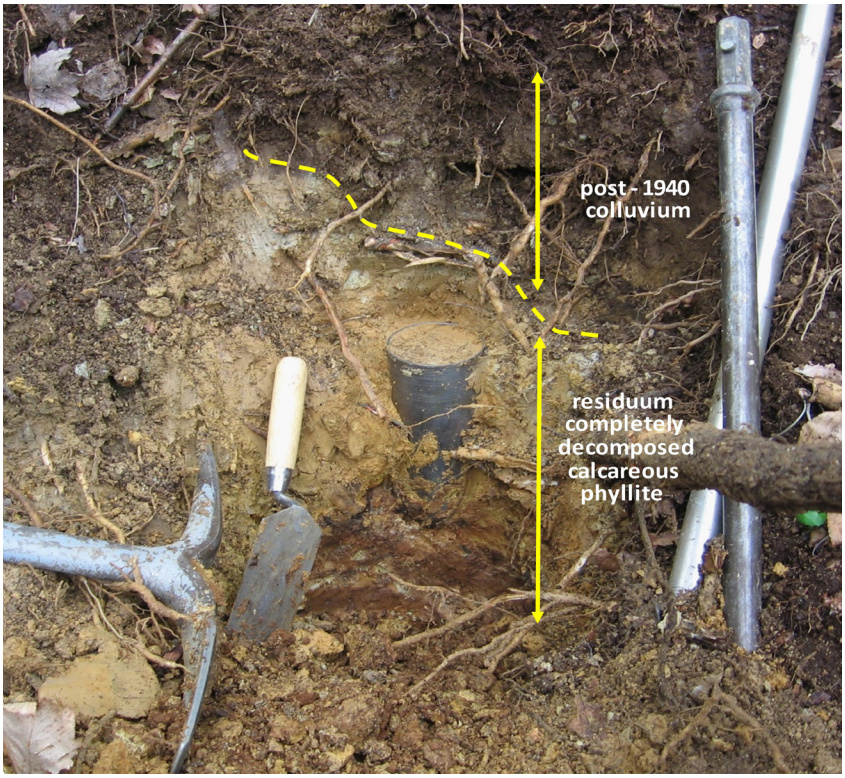

Figure 27. Photograph of the test pit used to excavate the Shelby tube sampler in the debris flow initiation zone. Dark brown post-1940 colluvium directly overlies residual soil derived from completely decomposed calcareous phyllite and phyllonite. May 9, 2007 photograph.

Figure 28. Geologists Stephen Fuemmeler and Jennifer Bauer (now with Appalachian Landslide Consultants, PLLC) prepare the Shelby tube sampler and record data from the Amoozemeter™ constant head permeameter in the debris flow initiation zone. May 9, 2007 NCGS photograph.

ACKNOWLEDGEMENTS

We wish to thank the landowner, Jack L. Sharp for access to his property on many occasions. He provided the historical context as well as access to early camp photographs. Brian Zimmer and Anthony Love provided technical support for the drone flight and thin section preparation, respectively. We wish to thank Arthur Merschat for making a field visit to examine the bedrock and review the field trip entry. This study began as a class project in Fall 2017 Geomorphology Class. The entire class is acknowledged for their contributions to data collection.

REFERENCES

Bierman, P.R. and Montgomery, D.R., 2014. Key Concepts in Geomorphology: W.H. Freeman and Company Publishers, New York, NY, 494 p.

Bryant, B. and Reed, J.C., Jr., 1970. Geology of the Grandfather Mountain Window and Vicinity, North Carolina and Tennessee: United States Geological Survey Professional Paper 615, 190 p.

Hack, J.T., 1966. Circular patterns and exfoliation in crystalline terrane, Grandfather Mountain Area, North Carolina: Geological Society of America Bulletin, v. 77, p.975-986.

Wooten R.M., Witt A.C., Gillon K.A., Douglas T.J., Latham R.S., Fuemmeler S.J., and Bauer J.B., 2008, Slope movement hazard maps of Watauga County, North Carolina: North Carolina Geological Survey Geologic Hazards Map Series 3, 4 sheets, scale 1:36,000, and Digital Data Series GHMS-3 (DDS-GHMS-3).

Wooten, R.M., Douglas, T.J., Bauer, J.B., Fuemmeler, S.J., Gillon, K.G., Witt, A.C, Latham, R.S., 2012, Geologic, Geomorphic and Geotechnical Aspects of Debris Flow Initiation Sites in the Blue Ridge Mountains of Western North Carolina at Study Locations in Buncombe, Haywood, Henderson, Jackson, Macon, Transylvania and Watauga Counties [abs]: Geol. Soc. of Amer. Abstracts with Programs, p.147.

Stop 1-5 Blue Ridge Parkway Overlook of Stony Fork/Deep Gap: An Introduction to the debris flow history of the August 13-14, 1940 Storm Event in Watauga County

Location: 36.2328°N, 81.4865 °W

Stop leaders: Rick Wooten and Anne Witt

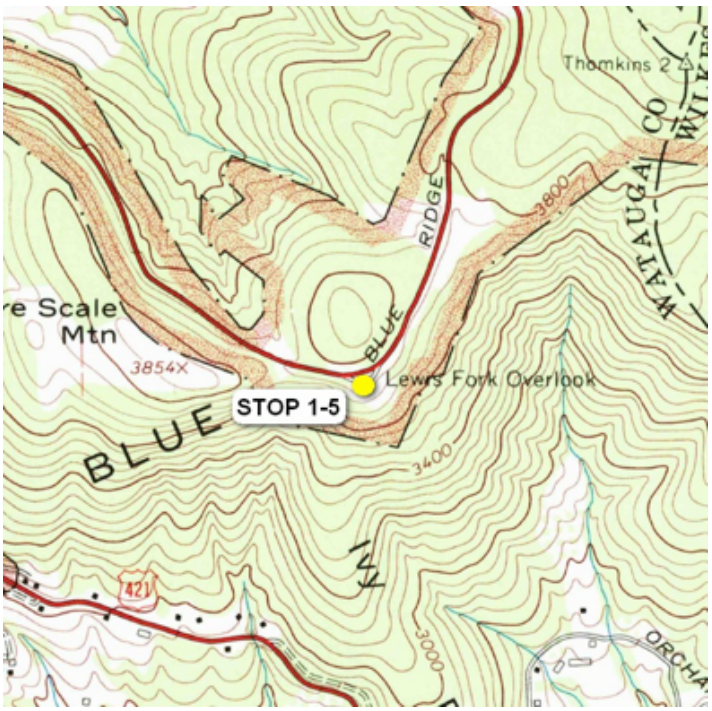

Location Map: From the Maple Springs 7.5' Quadrangle

Stop Description

As you look into the tranquil valley below, keep in mind that over 75 years ago, hundreds of debris flows ravaged this area. This vantage point overlooks the community of Stony Fork, south of U.S. 421, just to the east of the Blue Ridge escarpment (Figure 1). A hurricane made landfall on August 11, 1940, slightly north of Savannah, GA. Eventually, it slowly tracked north and west, turning easterly on August 13. Over the week of August 10-17, 1940, this area of Watauga County accumulated nearly 14 inches of rain. During the highest intensity rainfall, on the evening of August 13-14, 1940, over 2000 landslides, mostly debris flows, were triggered in Watauga County (for a detailed discussion of the storm, see the article in the earlier section of the guidebook). At this stop, we will discuss the history of landslides in western North Carolina (WNC) as well as the mid-August 1940 storm that killed 14 people in Watauga County. Debris flow producing storms of this magnitude tend to occur about every 25 years in western North Carolina. Looking back to the southwest you can see the scar of a February 12, 2018 rockslide on the Blue Ridge Parkway. Coincidentally, the rock slide is located in the path of a 1940 debris flow about 280 ft (85 m) below where the debris flow initiated prior to construction of the section of the Parkway south of U.S. 421. What would be the impact on this community if another storm of this magnitude were to happen again? How can we build more resilient mountain communities that are aware of, and take precautions for, these inevitable events?

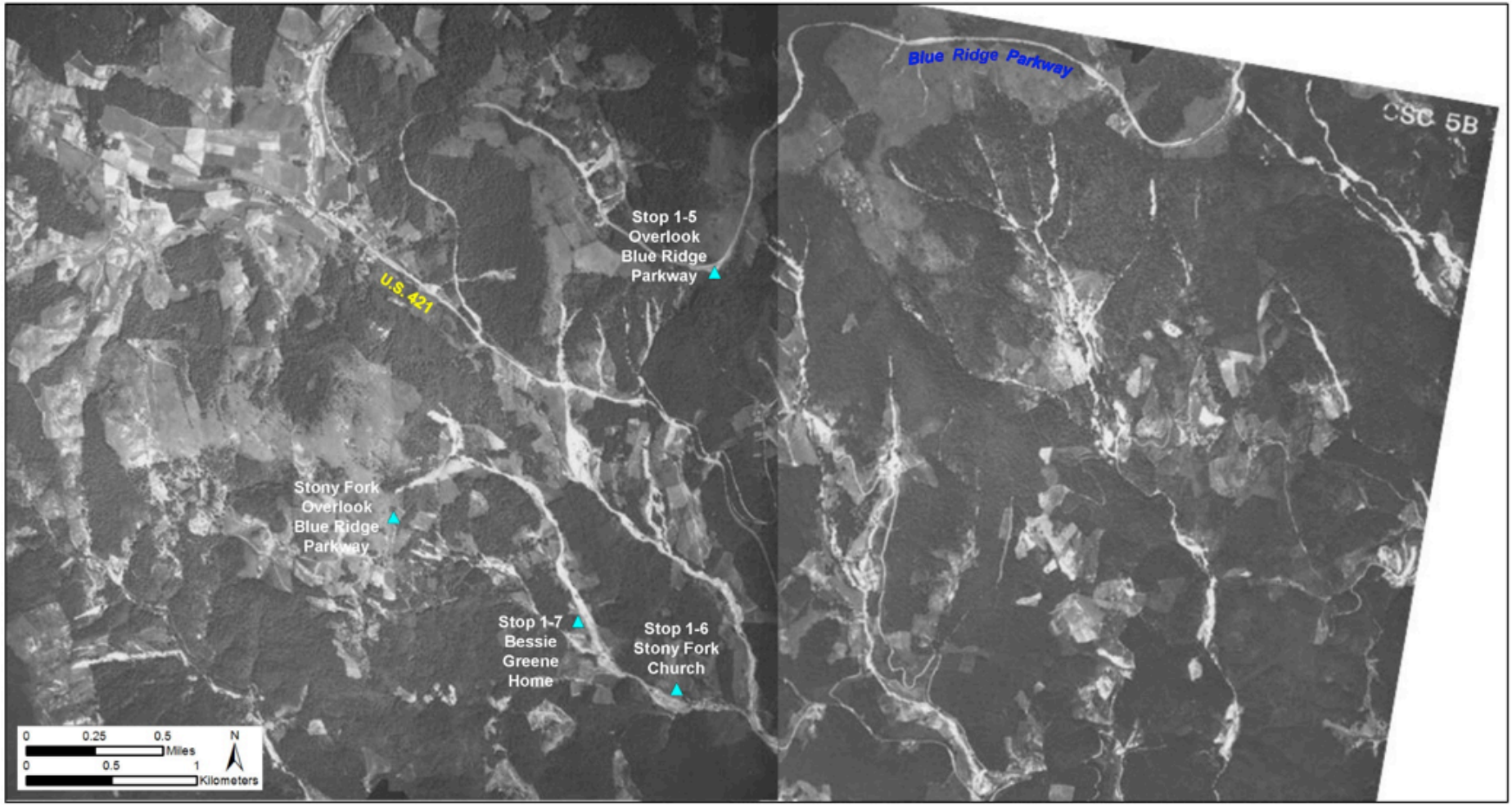

Figure 1: Mosaic of 9_29_1940 (left) and 9_27_1940 (right) aerial photographs showing field trip stop locations in the Deep Gap and Stony Fork area. The approximate location of the present day Stony Fork overlook on the Blue Ridge Parkway is shown prior to its construction south of U.S. 421. Scale is approximate.

Stop 1-6 Stony Fork Baptist Church: The Greene Family and the Debris Flows in Stony Fork

Location: 36.2117°N, 81.4863°W

Stop leaders: Anne Witt and Rick Wooten

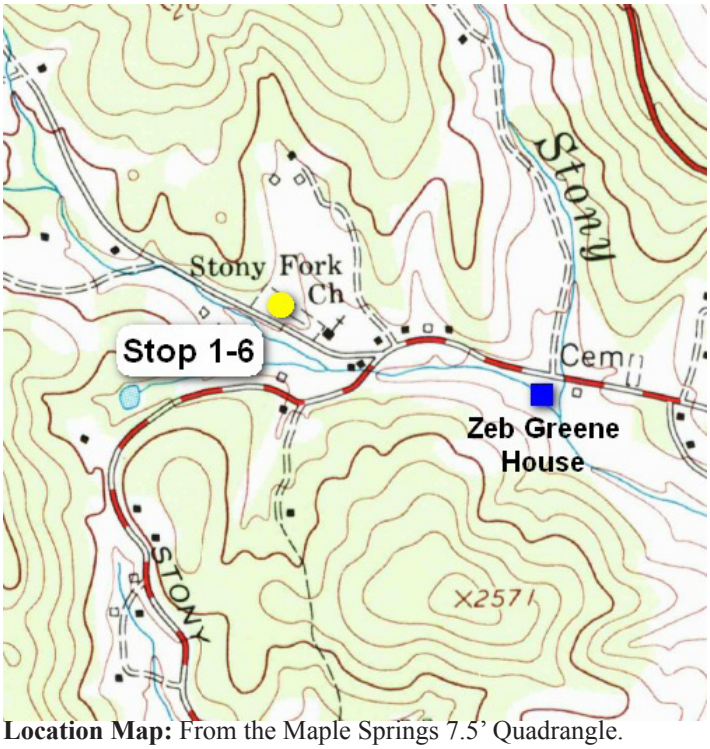

Location Map: From the Maple Springs 7.5' Quadrangle.

Note: We have the kind permission of the pastor of Stony Fork Church to stop here and walk up the hill to the cemetery. Please be respectful of the place and the property.

Stop Description

The Stony Fork Baptist Church was the heart of the community, and emergency response and relief operations, during the mid-August 1940 storm. Many of the local residents who lived further up valley were killed in debris flows on the night of August 13 and are buried in the church cemetery. You will notice among the headstones that there are a number of Greenes, Cooks, and Watsons. The Greene family has lived in Stony Fork for generations. Here we will visit the grave of Andrew Greene (46) and his three daughters: Creola (16), Velma Lea (14) and Vernita (12). All were killed by a debris flow that travelled down the western branch of Stony Fork, destroying their house and those of several of their relatives (see Figure 1 for an example of these debris flows). Andrew Greene's wife, Eliza, and his two sons, Hooper (19) and B.L. (7) both survived the debris flow. His oldest son Earl (20) was not home at the time. Andrew Greene's brother Millard, who lived farther up valley, close to the head scarps of the main debris flow, also saw his house destroyed. Andrew's older brother Lawrence's house survived the debris flow, as it was on a knoll several feet above the stream valley.

On our way to Stony Fork Church, we drove past the home of Zeb Greene (see location map). This house was built in the 1800's and is one of the oldest residential structures in Watauga County (Figure 2). On the night of August 13, Worth Greene, his wife Lucy, baby daughter Betty and their cousin 15-year old Nina Todd were up the valley visiting Lucy's mother, Bessie Greene (Optional Stop 1-7). As they tried to make their way home, they were stopped by floodwaters that had washed out the bridge over Stony Fork Road. With no way to make their way home, they took shelter at the home of Zeb Greene (no direct relation). At some point during the evening, Zeb, Worth and Nina stepped out onto the porch to watch the rising floodwaters. At that same moment, a tree caught in a massive debris flow that had originated far upslope along the Blue Ridge Parkway (Stop 1-5), swept Zeb and Nina from the porch. Worth managed to save himself by grabbing onto a cedar tree next to the porch (Figure 2). Sadly, Zeb and Nina's bodies were found days later several miles downstream. After the flood, Zeb's brother Elster cleaned up the property and moved into the home. The house remains in the Greene family to this day.

After the flood, much of the bouldery debris was removed or regraded so that little of the original debris flow material remains in place today. A member of the Greene family, who is current church member, remembers that large boulders from the 1940 debris flows were hauled by tractors up from the valley and placed in the garden area at the top of the hill in the Stony Fork Church cemetery.

Figure 1: Image of a debris flow that occurred in Stony Fork on the night of 13 August 1940. The debris flow originated upslope (top right) and traveled between a barn and a cabin (owners unknown). Notice the side failure into the main debris flow track near the center of the picture. (Source: Paul Weston, "Landslide with House and Barn, August 1940," Digital Watauga, accessed August 16, 2018, https://digitalwatauga.org/items/show/6332.)

Figure 2: Photograph of the home of Zeb Greene taken soon after the 1940 flood. The cedar tree on the left is probably the tree that saved Worth Greene's life that night, based on the direction of flow. Also, notice the prominent mud line on the front of the building and porch posts, indicating the height of the debris flow as it surged past the house. (Source: Paul Weston, "Zeb Greene House, Stony Fork, August 1940," Digital Watauga, accessed August 16, 2018, https://digitalwatauga.org/items/show/6368.)

Stop 1-7 The House that Moved (Optional)

Location: 36.2157°N, 81.4927°W

Stop leaders: Anne Witt and Rick Wooten

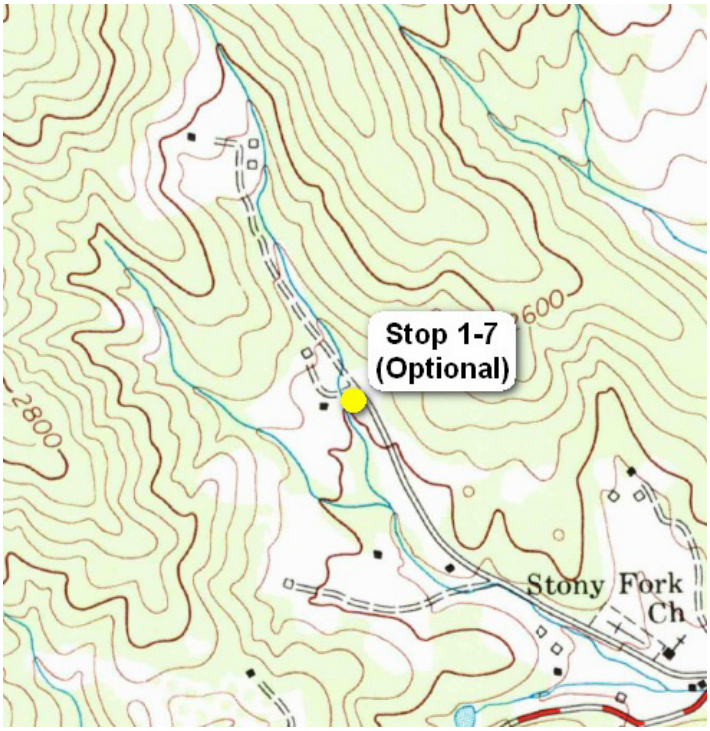

Location Map: From the Maple Springs 7.5' Quadrangle

Stop Description

At the end of Lawrence Greene Road is the former home of Bessie Greene. A widower, she lived in this home with her five children, built by the members of the Stony Fork Church, after her husband died. On the night of August 13, 1940, a debris flow came through this valley, and moved the house into its current position. A large sugar maple stopped the downstream movement of the structure and probably saved the home from disintegrating completely. Even though the chimney had collapsed and the porch was missing, the Greenes decided to repair the home. The Lucas family resides there today. Mr. Lucas commented that although he suspects the house was built before the framing square was invented, he reckons that the sturdy chestnut sill timbers used in it were part of the reason it survived the trip down the debris flow. Figure 1 shows a comparison between the house photographed immediately after the flood in August 1940 and a recent photograph from May 2018.

August 1940

May 2018

Figure 1: The Bessie Greene home immediately after the August 1940 flood (left) and a recent photograph from May 2018 (right). (Source: Paul Weston, "Bessie Greene House, Moved Off Foundation by Flood #4, August 1940," Digital Watauga, accessed August 16, 2018, https://digitalwatauga.org/items/show/6365).

FIELD TRIP DAY 2

SUNDAY, OCTOBER 7, 2018

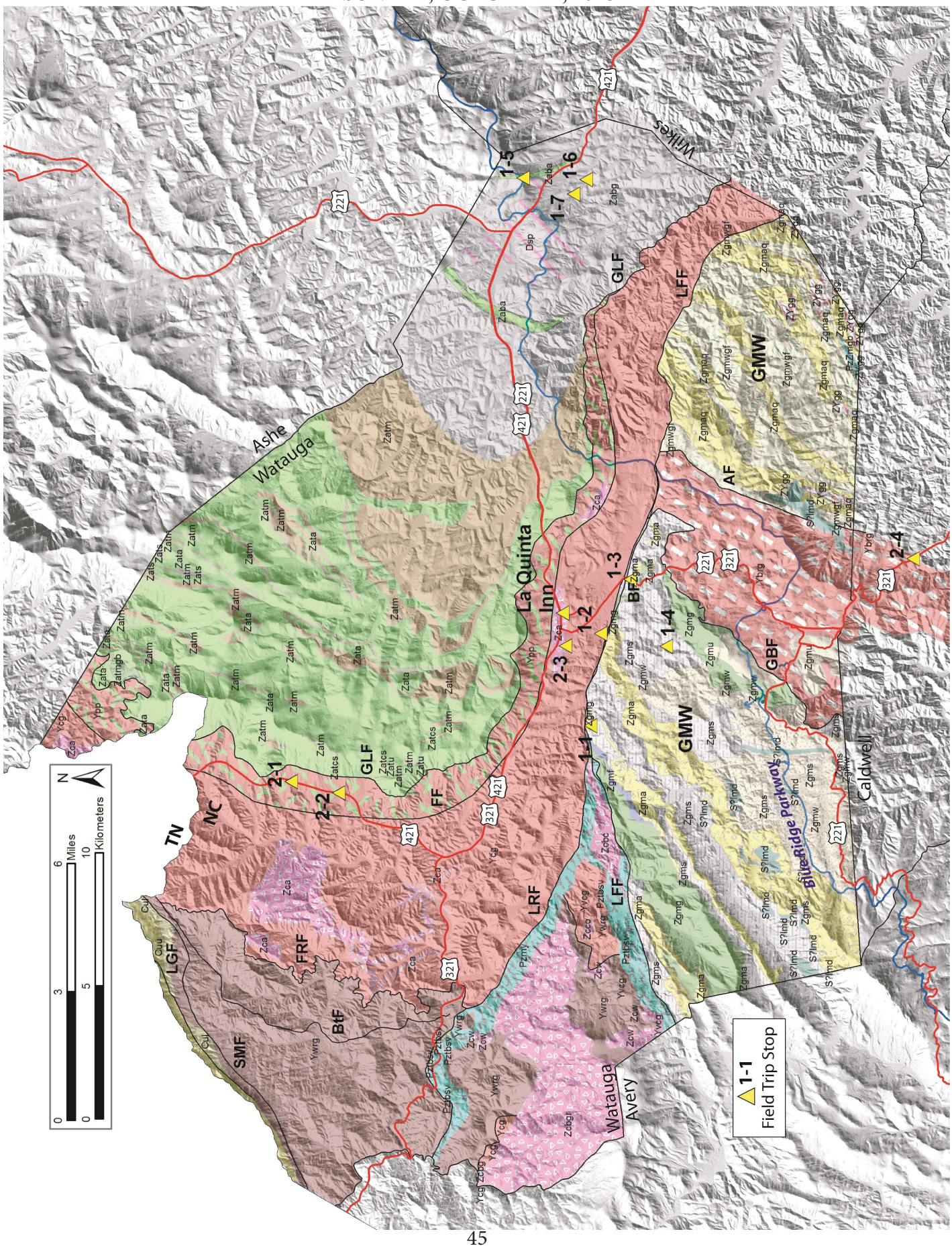

Stop 2-1: Surficial Deposits and Landforms on the West Piedmont Slopes of Rich and Snake Mountains between Silverstone, North Carolina, and Trade, Tennessee: A Field Guide

Hugh H. Mills
Department of Earth Sciences, Tennessee Technological University, Cookeville, TN 38505

Stop Leaders: Keith Seramur and Ellen Cowan

This article was originally published in the 1998 Southeastern Friends of the Pleistocene Field Trip Guidebook compiled by Dr. Hugh Mills. Some figures were re-drafted to improve resolution or to add locations. Reprinted here with permission.

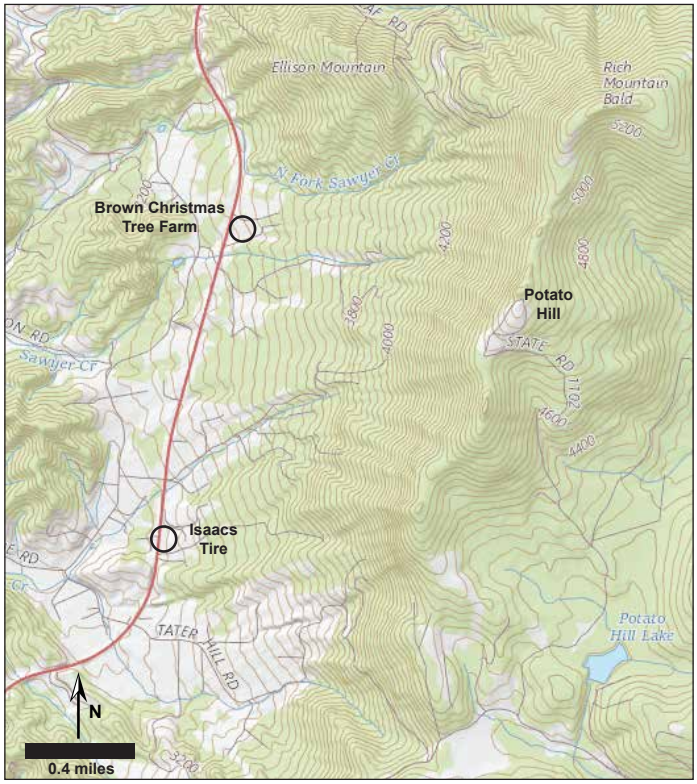

Figure 1. Topographic map of study area, from west part of Zionville and east part of Sherwood 7.5-minute quadrangles. Contour interval is 40ft (12.2m). Circles show field trip stops in the area.

INTRODUCTION

Accumulations of coarse-grained deposits on mountain piedmont slopes have long attracted the interest of geomorphologists. By far the greater part of research in this environment has taken place in tectonically active areas, particularly those in dry regions. Humid areas with low tectonic rates where piedmont slopes are smaller and less prominent, such as the Appalachians, have received much less attention. Previous work on Appalachian fans has been carried out by Mills (1982a, 1982b, 1983, 1986), Mills and Allison (1995), Gryta and Bartholomew (1983), Kochel and Johnson (1984), Kochel (1990, 1992), Whittecar and Ryter (1992), and Whittecar and Duffy (1992).

A dichotomy is often made between piedmont slopes dominated by deposition (i.e., alluvial fans and bajadas) and those dominated by erosion (i.e., pediments). However, as Denny (1967) pointed out, many piedmont slopes show a complicated picture of both erosion and deposition, with actively accumulating fans interspersed with older, relict fan surfaces now undergoing erosion and with pediment surfaces. Foot slopes in the Blue Ridge appear to conform with Denny's view. Detailed mapping in the central and southern Blue Ridge has showed that many foot slopes portrayed on earlier geologic maps uniformly in yellow (i.e., Quaternary alluvium or colluvium) are actually complexes composed of fan surfaces of different ages interspersed with ridges and knobs of saprolite. Blue Ridge fans have been referred to as fan pediments (Mills, 1983) because they have features of both fans and pediments. In that they are crudely fan shaped and composed of debris-flow and upper-flow-regime deposits, they are fans. In that they are relatively thin (exceeding 30 m in thickness in some places, but in many places only a few meters thick) and are underlain by truncated saprolite, they are pediments (in the sense of Rich (1935) and Schumm (1977, p. 286-288)). However, for brevity, herein fan pediments will be referred to simply as fans.

The present study addresses piedmont-slope evolution in the Appalachian region by presenting the results of fan mapping in an area where relative-age dating can be done with unusual precision owing to an abundance of clasts with well defined weathering rinds. An eight kilometer- long section of U.S. Highway 421 between Silverstone, North Carolina, and Trade, Tennessee, which lies along the western foot slopes of Rich and Snake Mountains, provides excellent examples of fan-pediments probably typical of many other areas in the southern Blue Ridge Mountains. More details can be obtained in Mills and Allison, 1995.

My attention was first called to this area by Gryta

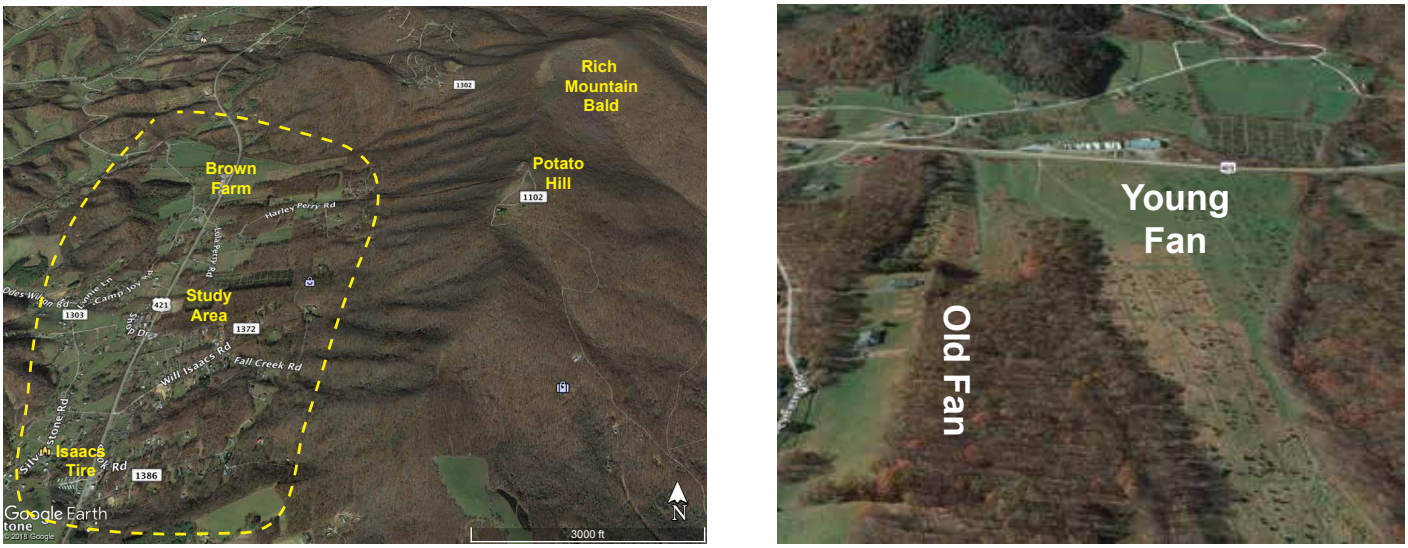

Figure 2. Looking north across study area from Potato Hill to Rich Mountain Bald (altitude 5372 ft or 1638m) (a). Downslope view of debris flow fans at Brown's Christmas Tree Farm (b).

and Bartholomew (1983), who studied small fans in the Sherwood quadrangle immediately west of the present study area. These authors were kind enough to show me their field area, where I noticed large number of amphibolite and amphibolite-gneiss clasts with well developed weathering rinds. In addition, Bartholomew and Wilson's (1985) geologic map of the Zionville quadrangle showed large areas of fan deposits on the west slopes of Rich and Snake Mountains, inviting a detailed study. Later, an abstract by Haselton and Acker (1989) on fans and periglacial features on Snake Mountain further stimulated my interest, and Lewis Acker subsequently showed me some fascinating exposures of fan sediments. Without this earlier work, I never would have undertaken research in this area.

PHYSICAL SETTING

The study area lies near the northwestern corner of North Carolina. Elevation ranges from a high of 1638m to a low of 844m, with a relief of 794 m. The basic topography is that of a long ridge oriented approximately N 15° E, with a small offset to the east north of Rich Mountain Bald (Figs. 1 and 2). Rich Mountain Gap (elevation 1348 m) separates Rich Mountain to the south from Snake Mountain to the north. The piedmont slopes studied in this paper lie on the west side of this ridge, occupying a north-south belt roughly 8 km long and 1.5 km wide, extending from Trade, Tennessee, to Silverstone, North Carolina. U.S. Route 421 cuts through many fans along this belt. The nearest weather station is located at Banner Elk, North Carolina, at an elevation of 1143 m (corresponding approximately to the top of the foot slopes in the study area), approximately 20 km to the southwest. At this station the mean annual temperature is 9. 7° C and the mean annual precipitation is 1285 mm (Owenby and Ezell 1992).

According to mapping by Bartholomew and Wilson (1985), the mountain slopes and upper ends of the foot slopes are underlain mainly by the Ashe amphibolite, with small areas of Ashe gneiss and schist, while the foot slopes proper are underlain mainly by the Cranberry Gneiss. The Ashe amphibolite consists of dark-gray to black fine- to medium-grained amphibolite and amphibolite gneiss, chiefly of staurolite grade. The amphibolite consists of 70 percent or more black hornblende and 20 percent or less feldspar, and 10 percent or less garnet, quartz, magnetite, and sphene. The amphibolite gneiss consists of about 40 to 50 percent black hornblende, 40 to 50 percent feldspar and garnet, and 10 percent or less quartz, magnetite, and sphene. Alteration minerals consist of actinolite, chlorite, biotite, and quartz.

The foot slopes in the study area are largely covered by relatively unsorted and unstratified gravels. Although most deposits are diamictons, on distal foot slopes these deposits also suggest fluvial influence, as shown by the presence of subrounded clasts and a clast-supported structure. Deposition from hyperconcentrated flows seems likely. Maximum clast sizes rarely exceeded 50 cm, relatively small for Blue Ridge fan deposits. Slope angles on fans range from 3% to 21% (2° to 12°), but generally fall between 9% and 16% (5° and 9°). Many exposures show a thickness of only 1-3 m of gravels overlying saprolite, although gravel thickness appears to be much thicker in some places. Water-well logs in this area were not useful in determining gravel thicknesses. The deposits are

Table 1. Characteristics of profile-description sites

Site No.	Altitude (m ASL)	Slope (%)	Aspect (deg.)	Location (UTM Coord., Zone 17)		Mean rind thickness
154	1116	11	315	434820	4022390	9.2
155	1000	8	285	433610	4022630	6.7
156	982	11	290	433070	4018310	0.1
157	1311	27	270	435730	4020150	0.1
158	927	14	280	433060	4016150	1.6
159	982	7	280	434060	4020580	10.7
161	1055	18	275	433650	401795	0.1

rich in amphibolite and amphibolite-gneiss clasts, the weathering rinds of which allow excellent measurements of relative age.

No modern Soil Surveys are published for either Watauga County, North Carolina, or Johnson County, Tennessee, but both counties are currently being mapped. According to preliminary field sheets and data supplied by Roy Mathis of the Soil Conservation Service (personal communication, 1993), young fan surfaces are mapped as Cullasaja series (classified as loamy skeletal, mixed, mesic, Typic Haplumbrept) or Tusquitee series (coarse-loamy, mixed, mesic Umbric Dystrochrept) or sometimes Saunook series (fine-loamy, mixed, mesic, Humic Hapludult). Intermediate surfaces are usually mapped as Saunook, but old surfaces, although occasionally mapped as Saunook, typically are mapped as residual soils to include the series Chestnut (coarse-loamy, mixed, mesic, Typic Dystrochrept), Edneyville (same classification as Chestnut), Evard (fine-loamy, oxidic, mesic, Typic Hapludult), and Cowee (fine-loamy, mixed, mesic, Typic Hapludult). The practice of mapping the higher fan surfaces as residual soils, if geomorphologically misleading, is not unreasonable. First, the intensely weathered nature of these gravels produces soils similar in many ways to soils on saprolite. Second, as the gravels on these surfaces are thin, erosion has exposed saprolite at the surface in many places. Hence, from a soil management point of view, such mapping is appropriate.

WEATHERING RINDS AND SOILS

Rind thickness was measured on clasts ranging in composition from amphibolite to amphibolite gneiss. The procedure used was to measure the rind thickness on the side of the clast where the rind was thickest (excluding comers) to the nearest 0.5 mm. Slightly weathered clasts with surface stains but with indiscernible rind thicknesses were assigned a nominal thickness of 0.1 mm to differentiate them from completely unweathered clasts. Ten rind thicknesses were measured at each of 118 sites.

Soil profiles were described at seven excavations (Tables 1 and 2). Sites 154, 155, and 159 are on old fan surfaces and show mean rind thicknesses ranging from 6.7 to 10.7 mm. Two have reddest hues of 5YR and one has 2.5YR. Argillic horizon (Bt) thicknesses range from 58 to 105 cm. Only one profile on an intermediate fan surface, site 158, was described. The mean rind thickness of 1.6 mm is compatible with the fan's level, as is the reddest hue (7 .5 YR) and the Bt thickness (47 cm). Sites 156, 157, and 161 are on young surfaces, each having a mean rind thickness of 0.l mm. The soil profiles of 157 and 161, with no argillic horizons and reddest hues of 7.5 YR, seem appropriate for young surfaces. However, site 156 has a reddest hue of 5 YR and a Bt thickness of 60 cm, seemingly too "old" for a young surface. This profile suggests that development of weathering rinds may start more slowly that does that of weathering profiles.

MAPPING

The fan surficial geology map is shown in Figure 3. Fan surfaces were first mapped on the basis of

Note for Table 2: Coarse fragments were counted only if they were intact; decomposed "ghosts" were not considered to be clasts. The parameter vc/t is the ratio of very coarse sand to total sand. This parameter was included as an aid to detecting lithologic discontinuities, the rational being that sand is less likely to be affected by pedogenic effects than is silt and clay, so that abrupt changes in the particle-size distribution of sand may indicate a change in the parent material. The vc/t ratio serves as a single-value index of this distribution. The percent coarse fragments also serves to help detect lithologic breaks. Percent iron was determined using citrate-dithionite extraction.

Table 2. Soil Profiles

Site	Horizon	Thickness (cm)	Color (moist)	Snd (%)	Slt (%)	Cly (%)	pH	Stucture	Consist. (moist)	Coarse frag. (%)	vc/t	Fe (%)
Site 154	A1	0-6	10YR3/3	62	30	8	5.9	2mgr	fri	-	0.12	
	A2		10YR3/4	39	46	15	6	2mfsbk	fri	3	0.13	
	Bt1	28-61	7.5YR4/6	25	44	31	5.4	2mfsbk	fri	8	0.09	2.0
	Bt2	61-110	7.5YR4/8	26	39	35	5.5	2fmsbk	fri	4	0.11	3.1
	Bt3	110-131	5YR5/8	28	22	50	5	3cmsbk	firm	3	0.11	4.7
	CB	131-200	Multicol.	37	23	39	4.7	massive	fri	45	0.11	
Site 155	A1	0-5	7.5YR4/4	33	45	22	5.2	2mfgr	fri	3	0.18	
	A2		7.5YR4/4	45	36	19	5.4	2mfgr	fri	3	0.16	
	Bt1	17-45	2.4YR3/8	25	23	52	4.7	3msbk	fri	5	0.07	5.4
	Bt2	45-75	2.5YR4/8	33	25	42	4.8	2msbk	fri	10	0.08	4.6
	BC	75-101	5YR5/8	62	19	19	4.8	1msbk	v. fri	35	0.14	
	C	101-200	2.5YR	74	20	6	5.1	massive	ex. firm	55	0.07	
Site 156	Ap	0-28	7.5YR3/2	36	42	22	5.9	3cabk	firm	11	0.06	
	Bt	28-86	5YR4/4	40	22	38	5.9	3mfabk	firm	42	0.1	2.1
	BC	86-143	7.5YR4/8	58	23	19	6	2mabk	fri	62	0.07	1.9
	C	143-200	7.5YR5/6	58	20	22	5.9	massive	fri	70	0.05	
Site 157	A1	0-10	2.5Y2/0	77	17	6	5.7	1fcr	v. fri	20	0.15	1.3
	A2		2.5Y2/0	74	17	9	5	2msbk	fri	6	0.08	1.7
	Bw	28-80	7.5YR5/6	73	19	8	5.3	2csbk	fri	20	0.05	1.4
	C	80-140	10YR6/6	81	17	2	5.7	massive	v. fri	42	0.07	
	2Bw	140-195	8.75YR4/8	86	13	1	5.7	2msbk	fri	30	0.06	1.4
	2Bc	195-240	10YR5/6	77	19	4	5.6	3csbk	fri	32	0.07	
	3Bw	240-270	7.5YR5/8	79	19	2	5.7	2mcsbk	fri	50	0.04	2.0
Site 158	A	0-15	10YR2/1	38	45	17	5.5	2fsbk	fri	5	0.09	
	E	15-27	10YR3/2	42	44	14	4.9	2fmsbk	fri	5	0.14	
	Bt	27-48	7.5YR4/8	53	23	24	5.6	3mfsbk	firm	13	0.19	3.3
	2Bt	48-74	7.5YR5/8	40	21	39	5.8	3mfsbk	firm	1	0.09	3.8
	2BC	74-112	7.5YR5/8	61	31	8	5.6	2csbk	firm	27	0.08	
	2C1	112-175	7.5YR5/8	57	27	16	6.3	massive	ex. firm	50	0.08	
	2C2	175-200	7.5YR5/8	61	32	7	6.2	massive	ex. firm	65	0.08	
Site 159	A1	0-5	10YR2/1	61	28	11	6.1	1mgr	v. fri	5	0.07	
	A2		10YR3/2	43	43	14	5.4	2msbk	fri	5	0.06	
	Bt1	18-56	7.5YR4/6	30	34	36	5.5	3mfabk	firm	3	0.08	2.2
	Bt2	56-104	5YR5/6	17	25	58	5.6	3mfabk	firm	1	0.10	3
	Bt3	104-123	7.5YR5/8	21	13	66	5.6	3mfabk	firm	3	0.22	3.9
	C1	123-171	multicol.	41	14	45	5.7	massive	ex. firm	20	0.12	
	C2	171-200	multicol.	76	14	10	5.6	massive	ex. firm	75	0.15	
Site 161	A1	0-35	10YR2/2	68		3	7.3	1cm/2fsbk	v. fri	40	0.12	
	A2	35-77	10YR2/2	69		3	7.9	2msbk	fri	50	0.06	
	Bw	77-100+	7.5YR2/4	70		9	7.3	2fsbk	fri	80	0.15	1.7

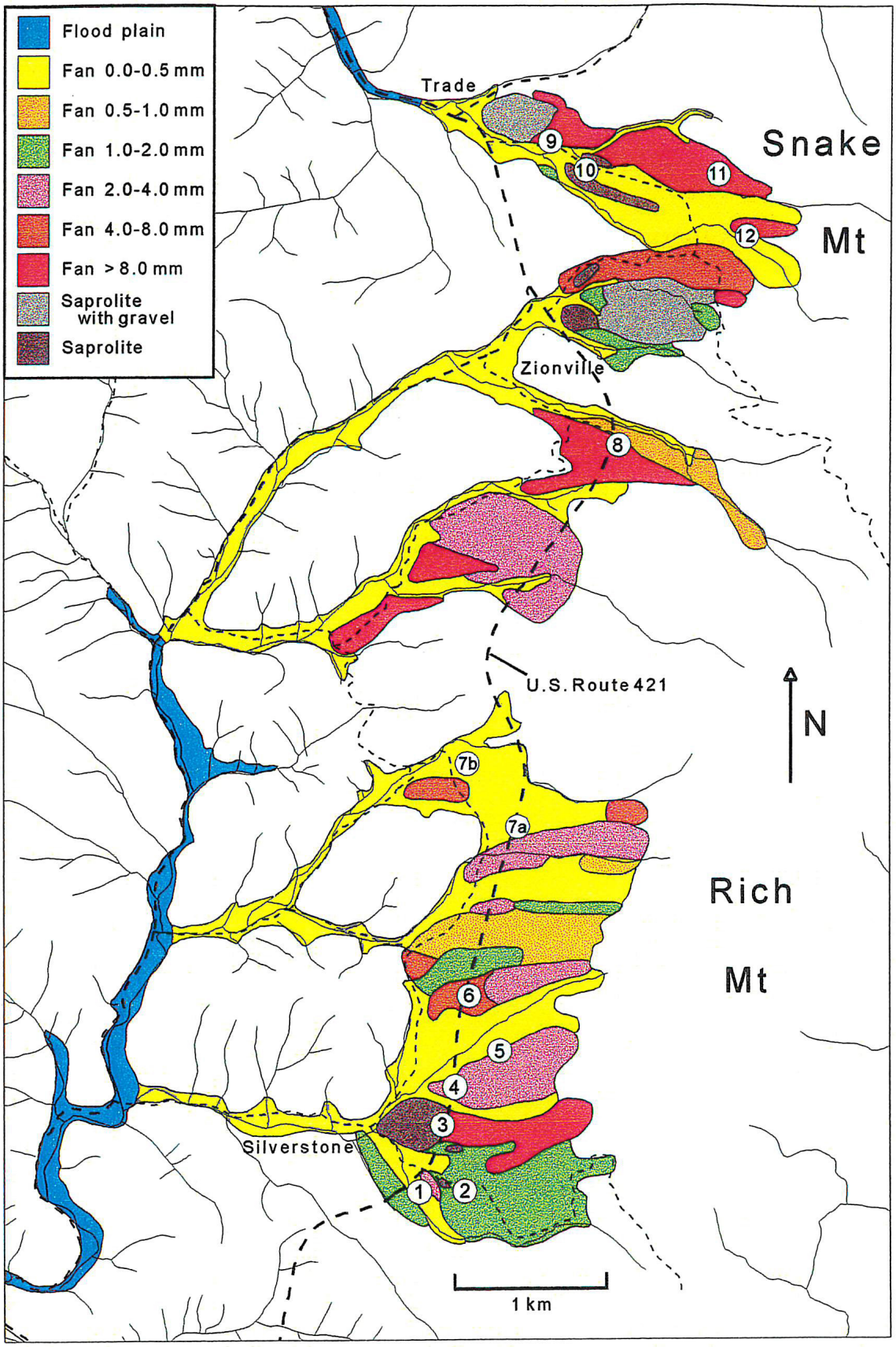

Figure 3. Surficial geology map of study area. Mapping procedure is discussed in text. Young deposits along drainage ways less than 30 m wide are not shown. Saprolite is shown only where surrounded by fan deposits. Dashed lines show roads, fine solid lines show streams. (Numbers indicate stops from a field trip previously led by Hugh Mills.) We will stop at 7a Brown's Farm and 4 Isaacs Tire on this trip.

topography using 1:24,000-scale stereo aerial photographs. Relative ages were then assigned to individual surfaces on the basis of weathering data gathered in the field, particularly Munsell hue and clay content of the B-horizon, and amphibolite-rind thickness. The final classification, however, was based strictly on rind thickness, which proved to be the most consistent weathering property. For mapping purposes, surfaces were classified into one of six rind-thickness age classes:

Age Category	Mean rind thickness (mm)
1	<0.5
2	0.5 - 1.0
3	1.0 - 2.0
4	2.0 - 4.0
5	4.0 – 8.0
6	8.0 – 16.0

In addition, one unique fan remnant fell into a 32.0-64.0 mm class. Two other map categories were 7, saprolite with scattered gravel, and 8, saprolite (mapped only where surrounded by fan surfaces).

The 118 rind-thickness counts were not the sole criteria used in classifying surfaces, for in the process of field mapping the thickness of 2-3 rinds were inspected at hundreds of additional locations, and this information also was used in assigning ages. Thus, the class assigned to a surface does not necessarily correspond to the class indicated by the mean of the rind-thickness counts made on that surface, but in fact it never differs by more than one class.

Generally the rind thicknesses were consistent over each geomorphic surface as mapped on the aerial photographs, but in several cases what originally appeared to be one surface was found in the field to show areal changes in rind thickness, and was therefore subdivided. In several cases contiguous surfaces, which had been distinguished on the basis of topography, were found not to differ with respect to rind thickness, and therefore were collapsed into one surface. One problem in mapping was where to place the downstream boundary of the youngest fan surfaces. As Figure 3 shows, we chose to extend these surfaces some distance down the small valleys draining the piedmont. One might object that these are stream floodplains, not fans. However, in most cases there was no break in surface along these valleys, and the deposits in the lower ends of the valleys appeared very similar to those in the upper ends.

In plan form, individual surfaces tend to be elongate, with long axes normal to the mountain front. The surfaces parallel one another and may either increase or decrease in width downslope; on average, the surfaces remain about the same width downslope. In the cross-piedmont direction, the sequence of surface ages suggests a relatively random arrangement.

There is some tendency for the oldest surfaces to be more irregular than the younger ones, indicating that they have undergone more dissection.

PALEOMAGNETISM MEASUREMENTS

Although no absolute dates were obtained, a minimum age for one fan deposit was obtained by paleomagnetic dating. Most fan deposits are too stony to allow such dating. An almost unique exception is a unit of massive fines sandwiched between two diamicton units exposed in a cut along U.S. Route 421 near Silverstone (Stop 3 on Figure 3). This unit is of uncertain origin and is intensely weathered. It occurs at the lower end of a fan with mean rinds 8-16 mm thick. At this site the overlying diamicton unit has a mean amphibolite rind thickness of 15.1 mm and the underlying diamicton unit has a rind thickness of 8.7 mm, so that the deposit represents one of the older ones in the study area. Four paleomagnetic samples were taken from the fine unit and analyzed by the late Victor Schmidt of the University of Pittsburgh. After extraction from the outcrop in plastic cubes, the samples were transported to the laboratory and processed. As discussed elsewhere (Mills and Allison, 1995), all four samples showed reversed magnetism, indicating a minimum age for the sediment of 780,000 ka. Moreover, other considerations suggest that the coherent reversed magnetization resides in hematite of secondary origin. The hematite content appears to be very high; the hue of the fine unit is 2.5YR, and the free iron content (as measured by citrate dithionite extraction) is 4.4%. To develop this amount of secondary hematite probably took 100,000 yr or more, so that the unit and fan probably have a minimum age on the order of 1 Ma.

THE TRANSVERSE PROFILE AS A FUNCTION OF SURFACE RELATIVE AGE

Figure 4 shows examples of transverse profiles across fan surfaces of different ages. Most upland streams flow along the contacts between two surfaces rather than across an individual surface. Commonly these streams are incising or undermining saprolite or weathered bedrock. Profiles 148 and 152 show typical height differences between older surfaces and the youngest surfaces. Where the oldest surfaces are involved, these differences can reach 30 m. However,

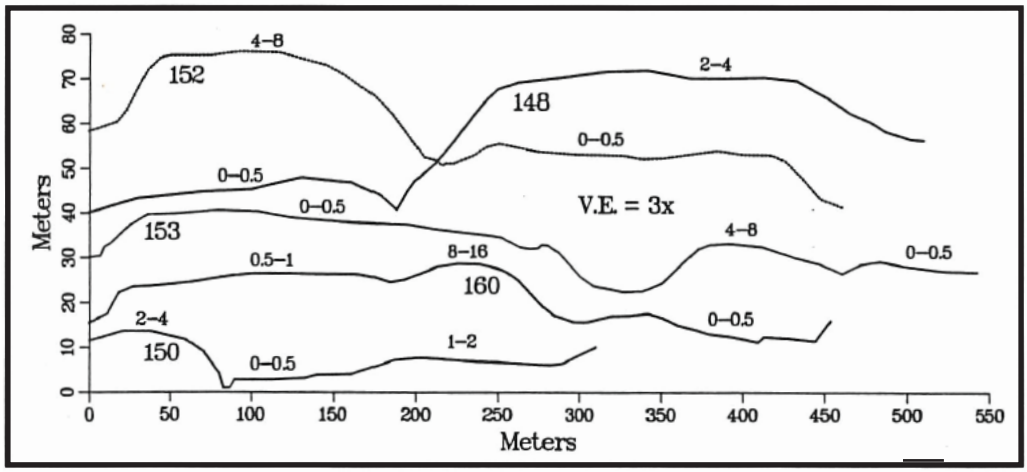

Figure 4. Selected transverse topographic profiles across fan surfaces showing the relative heights of older and younger fan surfaces. Numbers in larger font show profile numbers; those in smaller font show weathering-rind class (in millimeters) for each surface.

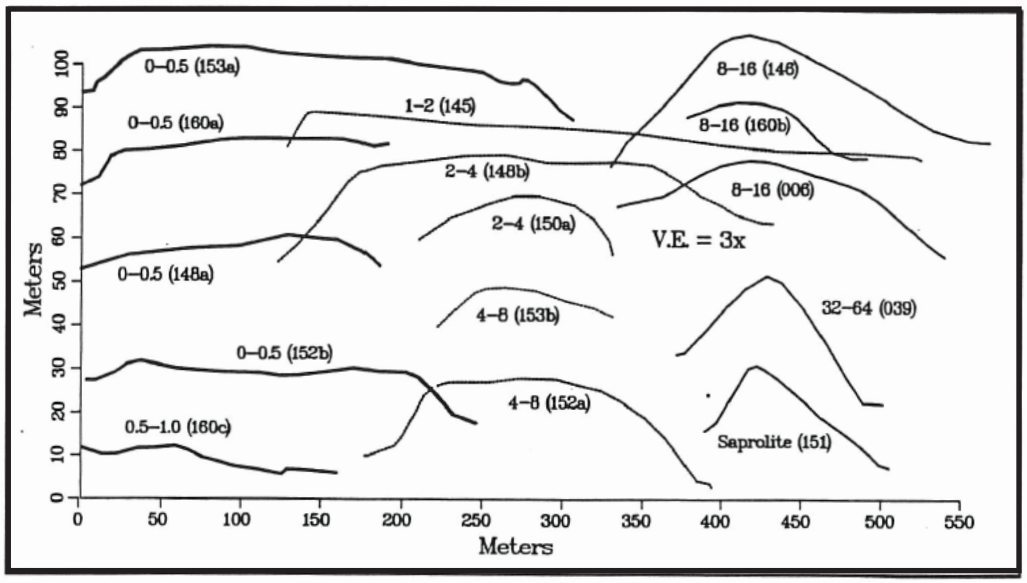

Figure 5. Transverse topographic profiles across individual fan surfaces arranged in order of relative age as indicated by weathering-rind class (shown in millimeters). Profile numbers are in parentheses.

as profiles 150, 153, and 160 show, height differences between older and younger surfaces may be much less, and can even approach zero (e.g., profile 153). Thus, assigning ages to surfaces based on relative heights as seen, for example, on stereo aerial photos may be misleading. Profile 153 also illustrates that surfaces in the youngest weathering-rind class may be as much as 10m above adjacent drainage ways. This observation may provide more proof that substantial time is required for the initiation of weathering rinds, as suggested earlier, or it may simply indicate that substantial incision of streams adjacent to fans can occur quite rapidly, as suggested by Gryta and Bartholomew (1983).

Although these profiles show that relative height is only an approximate index of relative age of the surfaces (as measured by weathering-rind thickness), they also suggest that the older surfaces may differ from the younger surfaces in another way: their transverse profiles are more convex. To examine this relationship more systematically, in Figure 5 transverse profiles of 15 individual surfaces have been arranged in order of increasing age as defined by rind-thickness class. The ends of the profiles are located at boundaries with surfaces of different age or with saprolite/bedrock ridges. Typically streams or at least unchanneled drainage ways occur along these boundaries. The transverse profiles of younger surfaces (0-2 mm mean rind thickness) generally show only a slight convexity, although as noted already, even surfaces with mean rind thicknesses in the 0.0-0.5 mm class can have streams incised as much as 10 m along one or both margins. Profiles of intermediate-age surfaces (2-8 mm rinds) may show somewhat deeper incision, up to 20m. In addition, note that the fan shoulders have become somewhat more rounded, presumably owing to the action of hill slope processes that promote convexity, such as creep and (Pleistocene) solifluction (Carson and Kirkby 1972, p. 297-300).

Transverse profiles of old surfaces (>8 mm rinds) can show marginal incision as much as 30m, although it may be much less. These profiles show a

pronounced convexity: fan surfaces have been transformed into noses. In most cases gravel deposits are confined to the crests of these noses, with the lower flanks exposing saprolite or weathered bedrock. Profiles 039 and 151 in Figure 5 (lower right) provide a clue to the ultimate fate of fan remnants. Site 039 has uniquely thick weathering rinds (mean of 53 mm), and so presumably is quite ancient, perhaps several million years in age. It is flanked on either side by young fan surfaces, and stream erosion along the margins of these fans apparently has reduced this fan remnant to a steep-sided, narrow ridge. More common in the study area are steep-sided saprolite ridges devoid of gravel, exemplified by site 151. Given its position, also between two young fan surfaces, a reasonable interpretation is that this was also once a gravel-capped ridge, the gravels having been completely stripped away by retreating flanks, exposing the saprolite beneath.

Extrapolating this sequence one step further, the ridge would finally be removed by a combination of lowering by hill slope processes and lateral erosion by streams. Expansion of young fan surfaces at the expense of older remnants is facilitated by the lack of gravel mantles on the lower flanks of the remnants, for the saprolite generally is more susceptible to erosion than is gravel. In this manner, old fans are eventually replaced by younger.

DISCUSSION

The use of weathering rinds allows fan surfaces to be subdivided by relative age on a finer scale than possible by most other means. This allows the distribution and area of fan surfaces of different ages to be ascertained in detail, and also allows the forms of fan transverse profiles to be investigated as a function of relative age.

The map patterns shown in Figure 3, particularly those on Rich Mountain, differ significantly from those reported previously in the Appalachians. Although they show a more or less random arrangement of surface ages in a cross-piedmont direction, as do previously studied areas, they show little tendency for older surfaces to occur farther downslope than younger surfaces. In addition, surfaces tend to be elongate downslope with roughly parallel lateral contacts. Most variation in surface age occurs in a cross-slope, rather than in an along-slope, direction. There seems to be little capture of upland streams by piedmont streams. To be sure, upland streams shift about on the piedmont, but it is a continuous lateral shifting as streams move away from young bouldery deposits (in drainage ways and on young fan surfaces) and toward more easily eroded saprolite on the flanks of old fans.

The map patterns, the locations of streams, and the transverse profiles of fan surfaces suggest a developmental sequence for the piedmont different from those previously proposed. A young fan widens by lateral corrosion of flanking older fans or saprolite ridges. Because deepening accompanies the lateral erosion, however, eventually the central part of the young fan stands sufficiently higher than its margins that it no longer receives deposition even during the largest floods. (It is recognized that aggradation can ·occasionally cover older fan surfaces and build up the fan surface, but that the long-term trend on the piedmont is erosion.) At this time it becomes a relict surface, and the long process of fan destruction begins. Marginal incision continues at the same time that hill slope erosional processes round the scarps at the fan margins. By the time the fan remnant is on the order of perhaps a million years old, it has become a nose with a pronounced convex-up transverse profile. Fan deposits may be preserved only along the crest of the nose, with the flanks exposing saprolite, which is vulnerable to lateral erosion by streams flowing along the margins of younger fans. Within several million years, the remnant is totally removed.

The applicability of the findings of this study to other parts of the Blue Ridge province is not known. There are several peculiarities of this area that might lead to a sequence of geomorphic development different from piedmonts elsewhere. The first is the small size of boulders in the deposits. This may allow hill slope processes such as creep and solifluction to operate more effectively than in places where boulders are much larger. The second is the thinness of the deposits (which may be due in part to the paucity of large boulders, which makes surface erosion of deposits easier). This results in more abundant outcrops of saprolite than on most other piedmonts, which might also affect landform development. Another factor, on the west flank of Rich Mountain, is the small size of the contributing area relative to the area of the fans. Unlike other fans in the Appalachians (e.g., Kochel 1992), the contributing area is actually less than the fan area. A possible consequence of this situation is thinner fan deposits.

REFERENCES

Bartholomew, M. J., and Wilson, J. R., 1985, Geologic map and mineral resources summary of the Zionville Quadrangle, N.C.: North Carolina Geological Survey, GM 213-SW and MRS 213-SW.

Carson, M.A., and Kirkby, M. J., 1972, Hillslope Form and Process: London, Cambridge University Press, 475 p.
Denny, C. S., 1967, Fans and pediments: American Journal of Science, v. 265, p. 81-105.
Gryta, J. J., and Bartholomew, M. J., 1983, Debris-avalanche type features in Watauga County, North Carolina, in Lewis, S. E., Geologic investigations in the Blue Ridge of northwestern North Carolina: Carolina Geological Society, Field Trip Guidebook, October 21-23, 1983, 22 p.
Haselton, G. M., and Acker, L., 1989, Pleistocene/Holocene geomorphic landforms, northern Watauga County, North Carolina: Geological Society of America Abstracts with Programs, v. 21, p. 20.
Kochel, R. C., 1990, Humid fans of the Appalachian Mountains, in Rachocki, A. H., and Church, M., eds., Alluvial fans: a field approach: New York, Wiley, p. 109-129.
Kochel, R. C., 1992, Geomorphology of alluvial fans in west-central Virginia, in Whittecar, G. R. (ed.), Alluvial fans and boulder streams of the Blue Ridge Mountains, west-central Virginia: Southeastern Friends of the Pleistocene 1992 Field Trip Guidebook, p. 4 7-60.
Kochel, R. C., and Johnson, R. A., 1984, Geomorphology and sedimentology of humid temperate alluvial fans in central Virginia, in Koster, E., and Steel, R., eds., Memoir on gravels and conglomerates: Canadian Society of Petroleum Geologists, p. 109-122.
Mills, H. H., 1982a, Long-term episodic deposition on mountain foot slopes in the Blue Ridge province of North Carolina: Evidence from relative-age dating: Southeastern Geology, v. 23, p. 123-128.
Mills, H. H., 1982b,. Piedmont-cove deposits of the Dellwood Quadrangle, Great Smoky Mountains, U.S.A.: Zeitschrift fur Geomorphologie, v. 26, p. 163-178.
Mills, H. H., 1983, Pediment evolution at Roan Mountain, North Carolina, USA: Geografiska
Annaler, v. 65A, p. 111-126.
Mills, H. H., 1986, Piedmont-cove deposits of the Dellwood quadrangle, Great Smoky Mountains, North Carolina, U.S.A.: Some aspects of sedimentology and weathering: Biuletyn Peryglacjalny, v. 30, p. 91-109.
Mills, H. H., and Allison, J. B., 1995, Weathering rinds and the evolution of piedmont slopes in the southern Blue Ridge Mountains: Journal of Geology, v. 103, p. 379-394.
Owenby, J. R., and Ezell, D. S., 1992, Monthly station normals of temperature, precipitation, and heating and cooling degree days, 1961-1990: North Carolina: NOAA, Climatography of the United States, no. 81 , 29 p.
Rich, J. L., 1935, Origin and evolution of rock fans and pediments: Geological Society of America, v. 46, p. 999-1024.
Schumm, S. A., 1977, The fluvial system: New York, Wiley, 338 p.
Whittecar, G. R., and Ryter, D. W., 1992, Boulder streams, debris fans and Pleistocene climatic change in the Blue Ridge Mountains of central Virginia: Journal of Geology, v. 100, p. 487-494.
Whittecar, G. R., and Duffy, D. L. , 1992, Geomorphology and stratigraphy of late Cenozoic alluvial fans, Augusta County, Virginia, in Whittecar, G. R., ed., Alluvial fans and boulder streams of the Blue Ridge Mountains, west- central Virginia: Southeastern Friends of the Pleistocene field trip guide, p. 79-112.

Field Trip Stop 2-2: Groundwater contaminant plume at Isaacs Tire

Location: 36.2897°N, 81.7457°W

Stop leaders: Keith Seramur and Ellen Cowan

INTRODUCTION

Environmental assessments conducted on the Piedmont and in the Blue Ridge Mountains commonly model groundwater flow through saprolite, fractured bedrock and alluvium. The typical model of groundwater flow for these areas consists of recharge in the uplands, groundwater flow through an unconfined aquifer consisting of saprolite and fractured bedrock, and discharge to springs and streams (Heath, 1980). However, landforms such as fans consisting of debris flow deposits can have a strong influence on the local hydrogeology. These deposits, dominantly diamicton, form a unique hydrostratigraphic unit that should be considered when modeling groundwater flow in the Blue Ridge Mountains. This study evaluates the hydraulic properties of diamicton and saprolite and their influence on groundwater flow and contaminant migration on the foot slopes of Rich Mountain, northwestern North Carolina (Figure 1).

Cashion Oil Company operated five underground storage tanks (USTs) at Isaacs Tire from the mid-1970s until 1995. Petroleum was discovered in a spring box fed by the North Spring down gradient of the USTs in 1983 (Figure 2). The local pastor, his wife and several other neighbors used this spring as a drinking water source. The pastor's wife reportedly had been having stomach problems for an extended period of time. One day when they turned on their faucet, free product (gasoline) filled their sink. The layer of free product had accumulated in the spring box until it reached the water line leading to the pastor's house. A water supply well was drilled for the houses that were using the spring. The neighbors blew up the spring box with dynamite so that no one else would ever drink from that spring.

The USTs were reportedly repaired in 1983, but the tanks continued to leak posing a significant health threat to local residents. Free product seeped out of the road embankment and into a mobile home park on the west side of Highway 421. Many residents in the mobile homes were renting through a HUD rental assistance program. High concentrations of petroleum vapors accumulated around the trailers near the road embankment. The local residents burned the petroleum seeps in the summer time in an effort to reduce the petroleum vapor concentrations.

Geonetics Corporation conducted an environmental assessment at the site to determine the extent of soil and groundwater contamination and to develop a conceptual of model contaminant migration. Contaminated groundwater was mapped from the location of the former USTs to springs that discharged down gradient on either side of a fan-shaped debris flow deposit (Figure 2). Groundwater flow and contaminant migration occurs through two hydrostratigraphic units, diamicton and saprolite, each having different hydraulic conductivities and preferential flow paths that interact to produce unique hydrogeologic conditions.

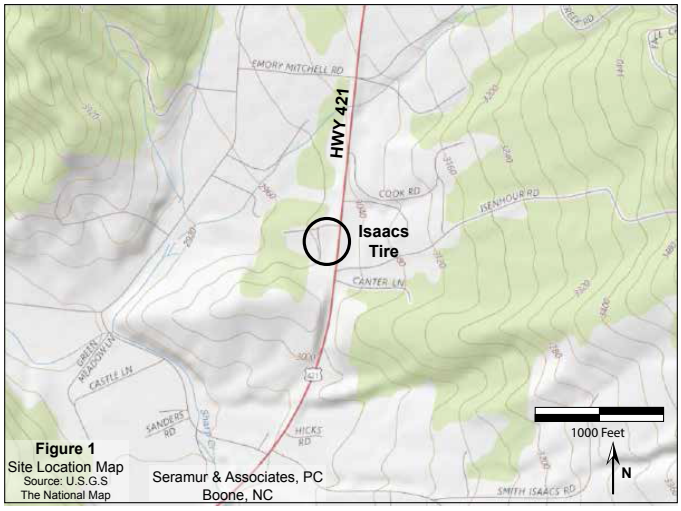

Figure 1. Topographic map of study area.

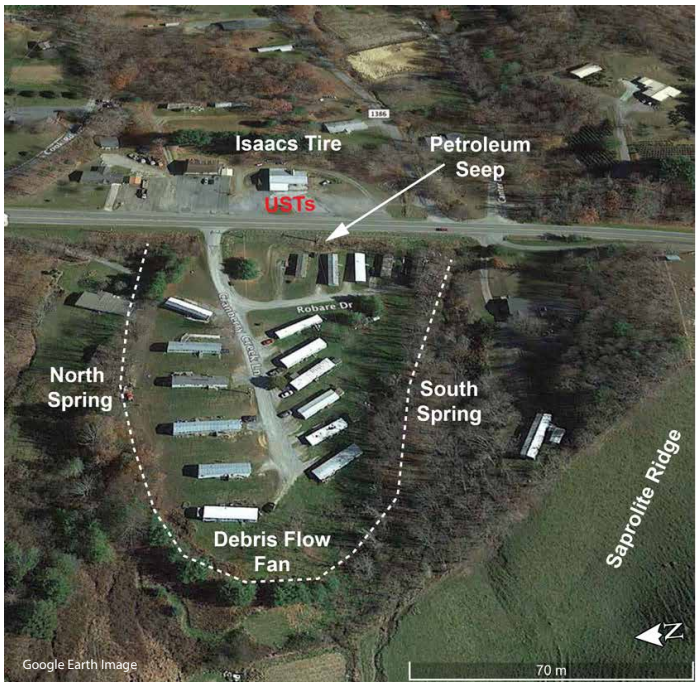

Figure 2. Google Earth aerial photograph of Isaacs Tire and the mobile home park located down gradient.

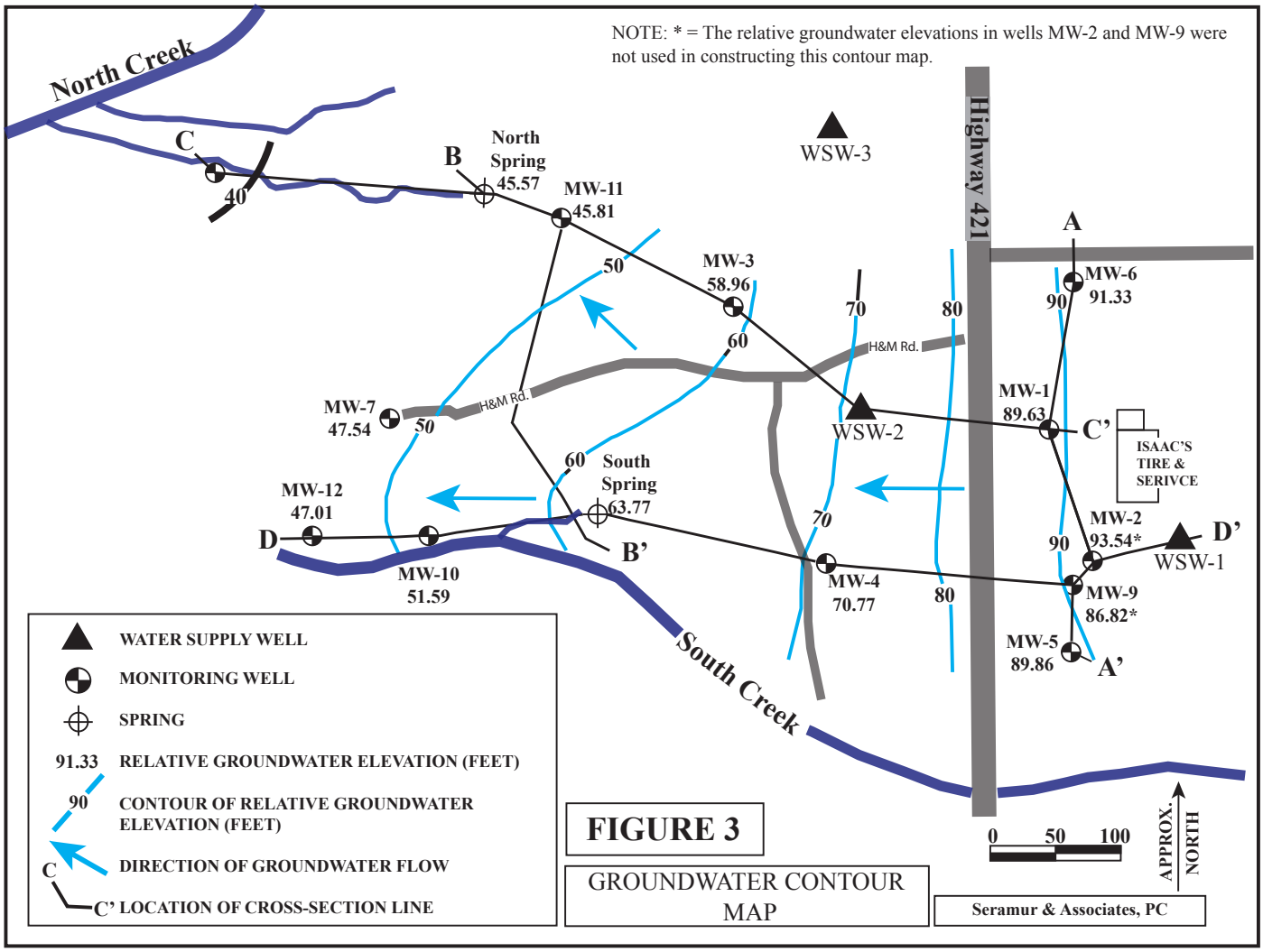

Figure 3. 1996 Groundwater Contour Map for Isaacs Tire.

In this study, nine soil borings and eleven monitoring wells were drilled with solid stem augers (Figure 3). Soil descriptions were based on auger cuttings and soil samples collected at specified depths. One deep aquifer well (MW-9) was drilled with an air rotary drill rig capable of drilling through competent bedrock. Soil samples were also collected from backhoe excavations during closure of the USTs and from four shallow test pits excavated with a hand shovel.

Cashion Oil Company went out of business within a few years of the discovery of this release. The monitoring and remediation of this incident is being completed by the NCDEQ State-Lead Program.

SITE GEOLOGY

The service station is located in the Zionville community of Watauga County, North Carolina. The site is on the western slope of Rich Mountain within the Blue Ridge Geologic Belt of northwestern North Carolina. Bedrock in the vicinity of the site consists of amphibolite of the Ashe Metamorphic Suite along the steep slopes and upper footslopes of Rich Mountain and Cranberry Gneiss along the footslopes and further to the west (Rankin et al., 1972). Bedrock below the site appears to be Cranberry Gneiss. However, a thick mantle of saprolite (51 feet to 58 feet) overlies the competent bedrock, which was not encountered during this project.

The surficial deposits above the saprolite include overlapping lobes of diamicton of different ages (debris flow deposits) with alluvial sand and gravel in the ravines. The lower foot slopes of Rich Mountain consist of fan surfaces interspersed with residual saprolite ridges and knobs (Mills and Allison, 1995).

The locations of the cross-sections discussed below are shown on the Groundwater Contour Map (Figure 3). Profile A-A', east of Highway 421, shows that the fan thickens from about 10 feet at well MW-6 to 20 feet thick at well MW-9 (Figure 4). This profile does not show the original surface morphology of the fan because the area was graded during construction of the highway, which probably removed the younger

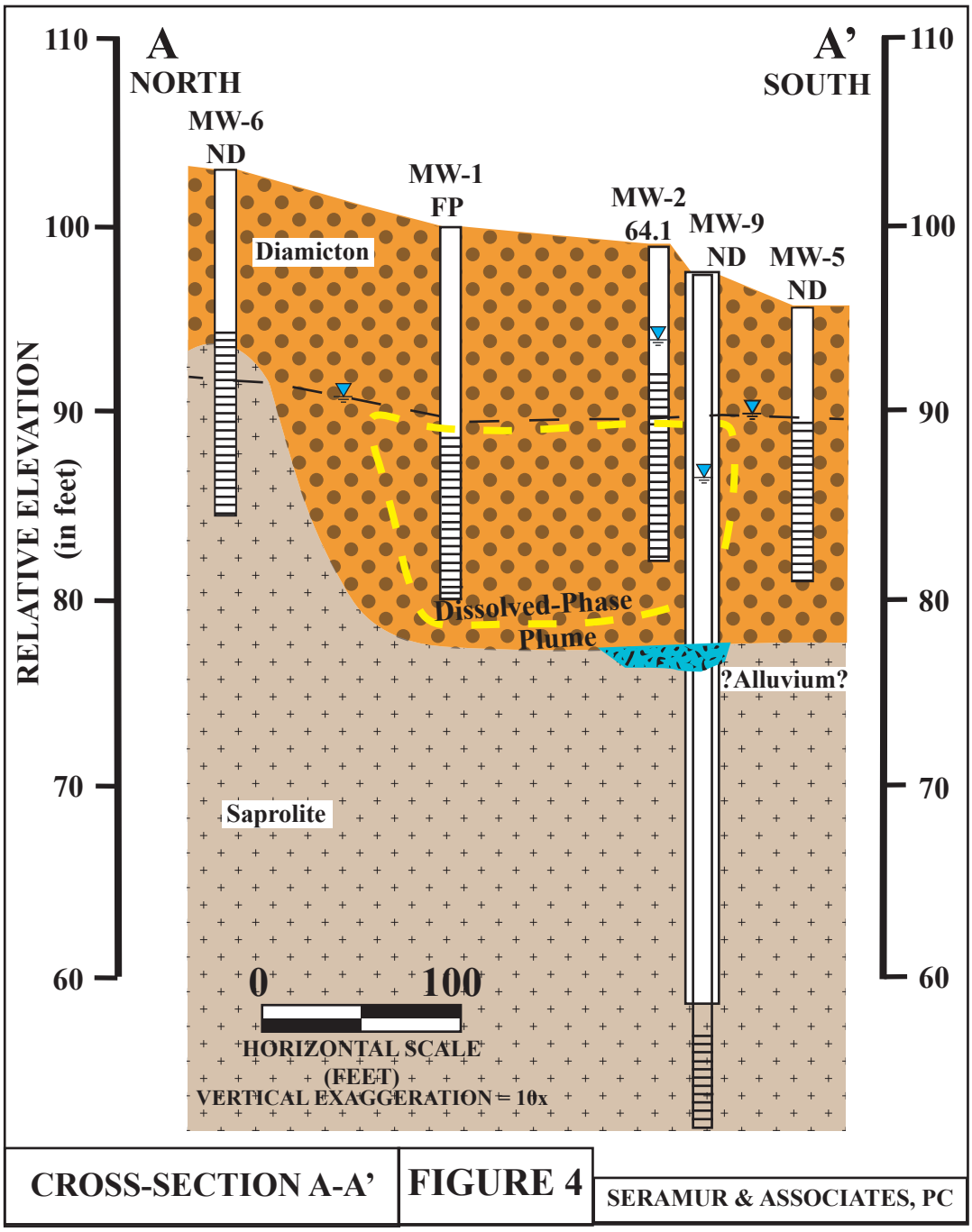

Figure 4. Cross-Section A-A' showing the diamicton thickness, water table and contaminant plume on the east side of Hwy 421.

diamicton. To the west of Highway 421, the younger diamicton is 3-5 feet thick and overlies the older diamicton, which attains a thickness of about 10 feet (Figure 5). The saprolite below the diamicton, slopes upward to the south, leveling off near the south spring (Figure 5) and eventually rising up to form a residual saprolite ridge to the south of the fan (Figure 2). The fan morphology shown on Profile B-B' between the North and South Springs has a convex surface with streams on each side (Figure 5). Mills and Allison (1995) suggest that these streams continue to erode the edges of the fans increasing convexity with age. The northern edge of the fan is steeper than the southern edge, possibly because less erosion has occurred where the fan abuts the residual saprolite ridge to the south.

The diamictons consist of a silty sand to sandy-silt matrix with granular- to boulder-sized clasts of amphibolite and quartz. An older diamicton is matrix supported and has a slightly indurated matrix consisting of a clayey, silty sand with amphibolite clasts that are completely weathered. Over-excavation of contaminated soil was completed during the UST closure. The scoops of diamicton in the trackhoe bucket had a

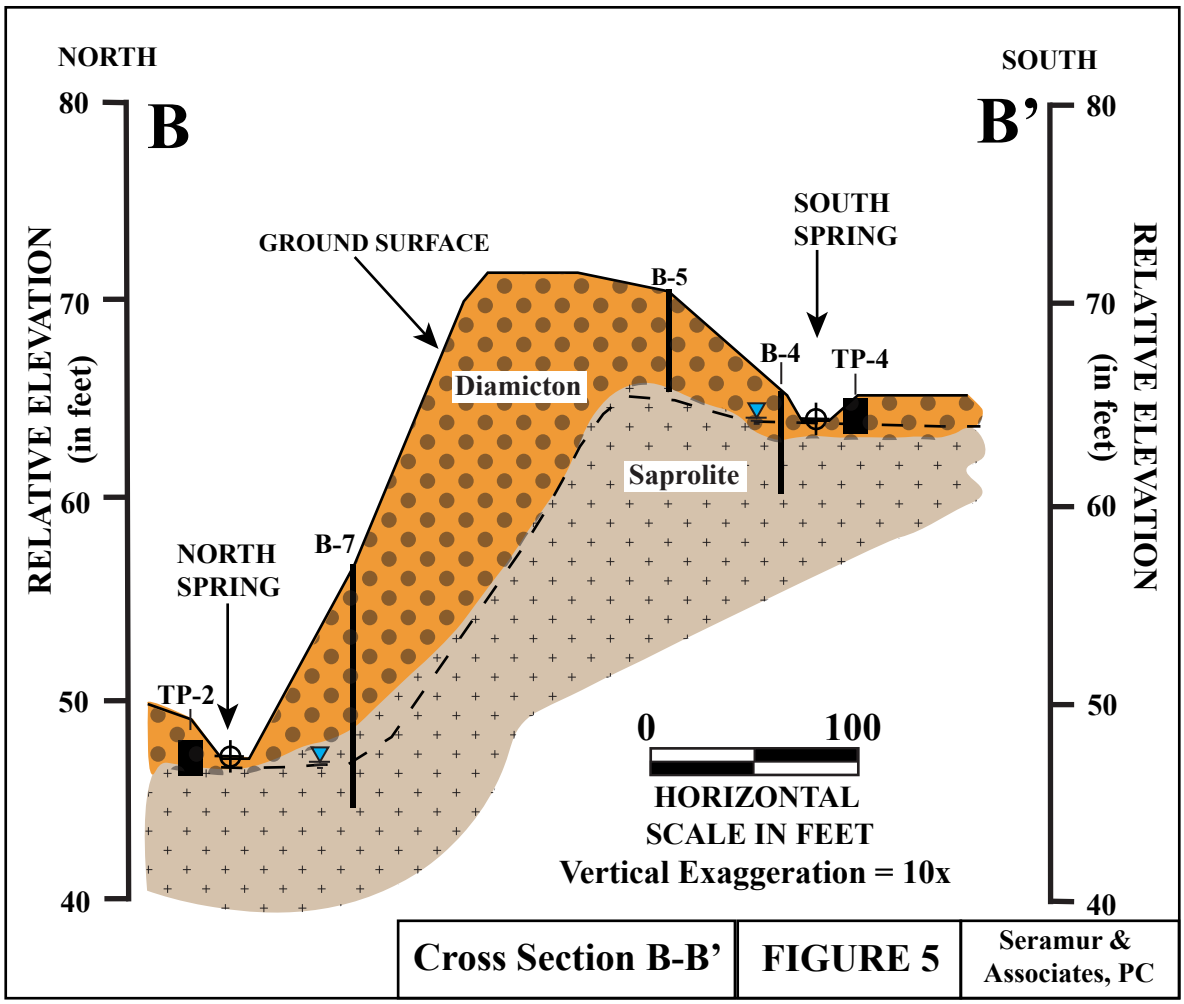

Figure 5. Cross-Section B-B' across the debris flow fan from the South Spring to the North Spring.

"leopard skin" appearance with the spots produced by the black, saprolitized amphibolite clasts in the older diamicton. The younger diamicton is clast supported and has a matrix consisting of loose silty sand with amphibolite clasts that have weathering rinds 2 to 6 mm in thickness.

These diamictons were deposited by debris flows from the upper slopes of Rich Mountain. Debris flows moved down ravines to the foot slopes burying the former land surface with their deposits. As a result, deposits from former stream channels can be found beneath the diamictons. An example of this was observed in a road cut about 1 mile north of the site where diamicton overlies saprolite. Along the contact between the saprolite and diamicton was a channel-shaped alluvial sand and gravel deposit that had apparently been buried during a debris flow event.

The saprolite consists primarily of a silty sand to a sandy silt with granules occurring along quartz veins and remnant quartz-rich foliations. Variations in grain size within the saprolite were observed at a road cut approximately 750 feet south of the site. In this outcrop, the changes in mineralogy within the foliation resulted in differences in weathering and thus variations in grain size.

The older diamicton and saprolite can readily be distinguished in an outcrop or trench. The matrix of the older diamicton is poorly sorted and appears to have a higher clay content than the saprolite. Furthermore, the saprolite can be excavated with the point of a pick, but the slightly indurated diamicton is stiff and resistant to the pick.

SITE HYDROGEOLOGY

The general movement of groundwater across the site is from east to west and is shown on the groundwater contour map (Figure 3). The aquifer underlying the gas station and the adjacent properties can be divided into three hydrostratigraphic units: diamicton, saprolite, and fractured bedrock.

The diamictons are a heterogeneous, isotropic hydrostratigraphic unit with groundwater flow through the sandy-silt to silty-sand matrix, gravel lenses, and possibly through fractures in the slightly indurated

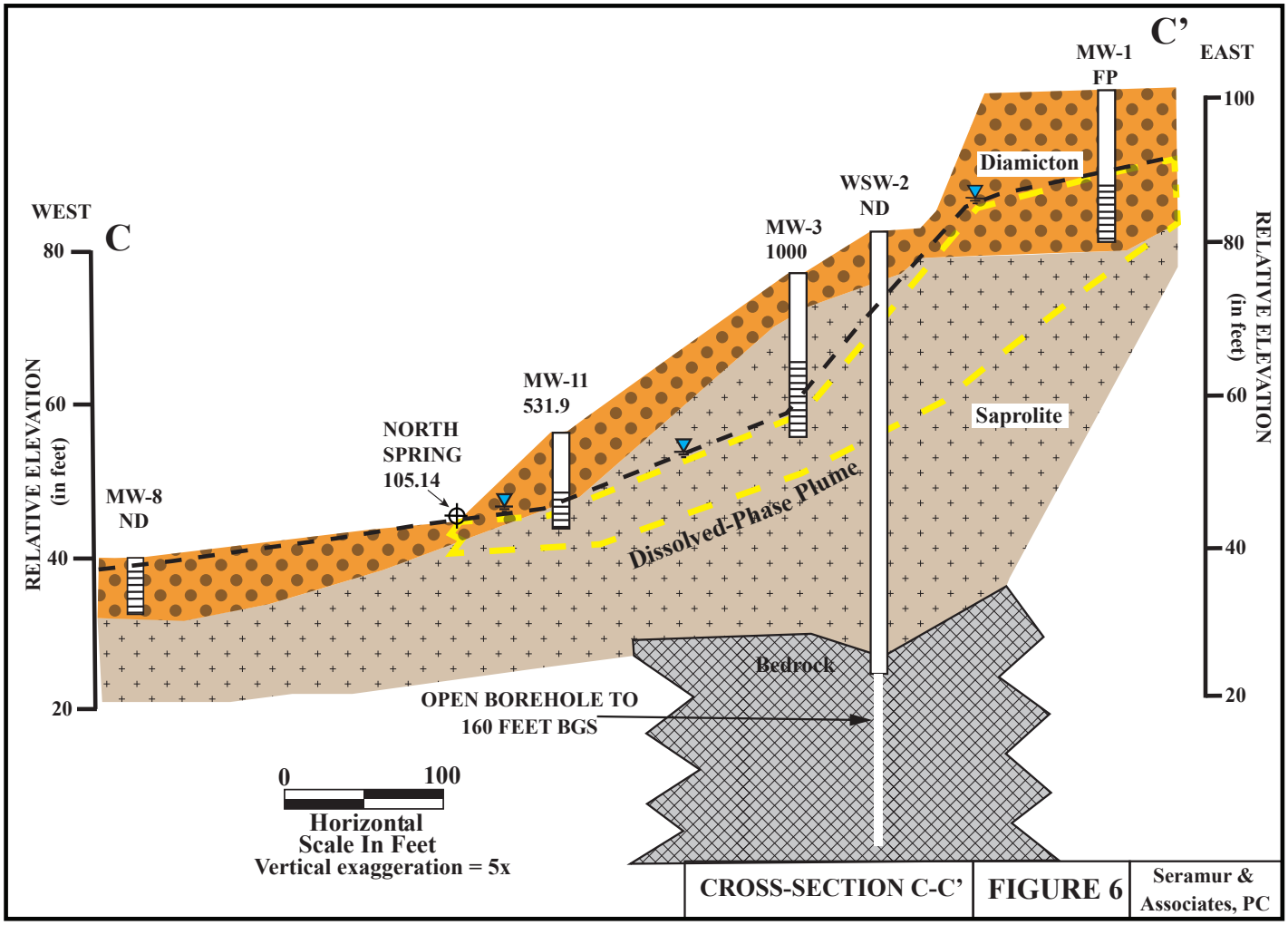

Figure 6. Cross-Section C-C' extending from the source area to the North Spring.

units.

The saprolite is considered a heterogeneous, anisotropic hydrostratigraphic unit composed primarily of a sandy silt with higher concentrations of sand and granules along quartz veins and quartz-rich remnant foliation.

Fractured bedrock is the lower most hydrostratigraphic unit at the site. This unit is tapped by wells as a source of drinking water for the residents and businesses in the area. Groundwater flow is primarily along fracture planes in the Cranberry Gneiss bedrock below the site.

In the vicinity of the former USTs the water table is within the diamicton and groundwater flows west through the diamicton and into saprolite, west of Highway 421 (Figures 6 and 7). Within the saprolite, groundwater flows west to the South Spring and a component of groundwater flow diverges north, to the North Spring (Figure 3). At both springs, groundwater flows from the saprolite and through younger diamicton prior to discharging at the surface (Figures 6 and 7). In the eastern half of the site, groundwater contours form nearly straight lines (perpendicular to the slope of the land surface) where groundwater flow is through the isotropic diamicton. The groundwater contours diverge west of Hwy 421, possibly following preferential pathways through the anisotropic saprolite (Figure 3).

The horizontal gradient across the site was measured at 0.07 feet per foot. The vertical gradient in the vicinity of well MW-9 is estimated to be a downward gradient of 0.09 feet per foot. This downward gradient indicates that the shallow groundwater in the diamicton and saprolite could be recharging the fractured bedrock aquifer below.

Slug tests were conducted in wells MW-2, MW-5, and MW-9 to assess the relative conductivity of the diamicton and saprolite. The hydraulic conductivities were calculated using the Bouwer and Rice Slug Test (Bouwer, 1989).

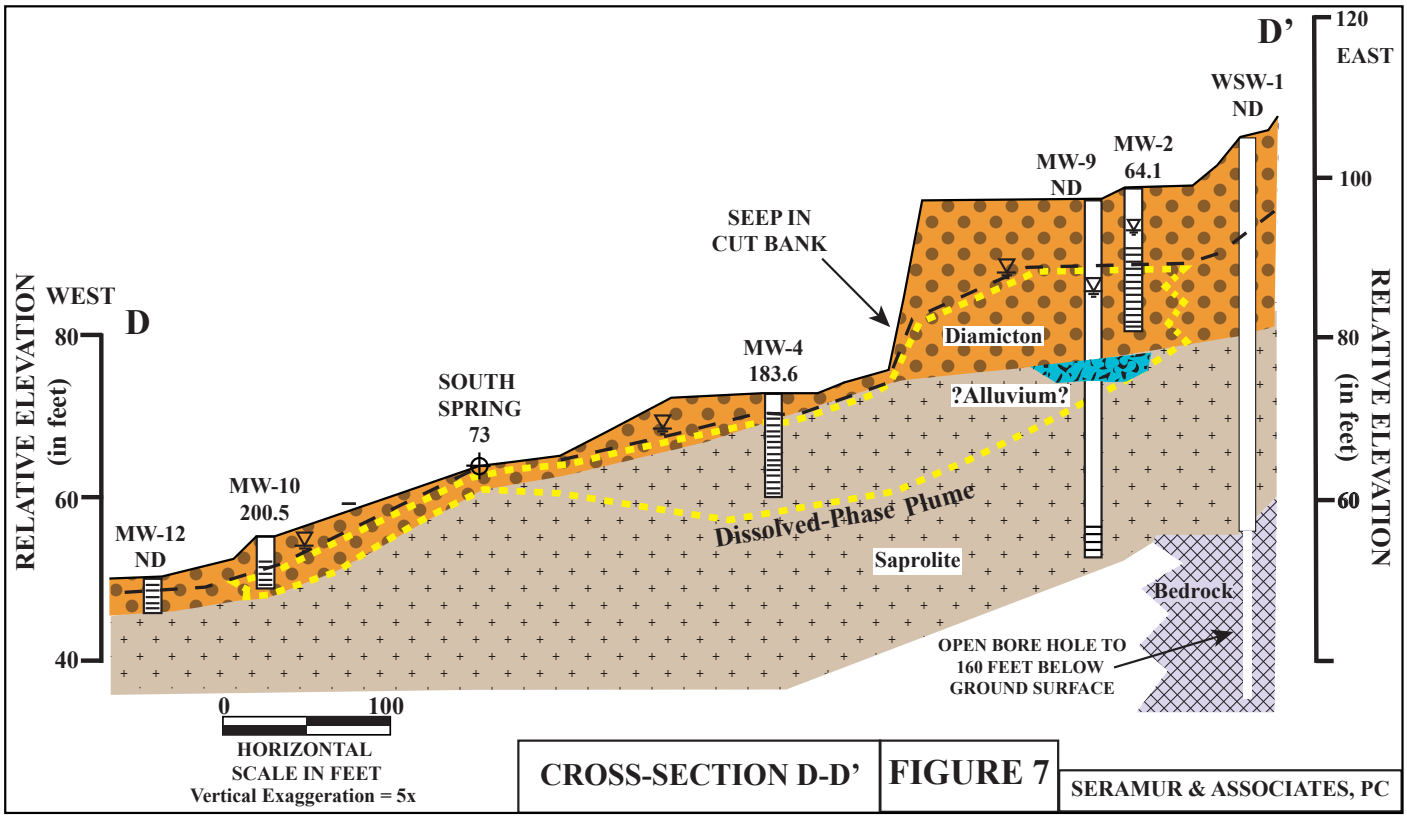

Figure 7. Cross-Section D-D' extending from the source area to the South Spring.

Hydrostratigraphic Unit	Well Number	Hydraulic Conductivity
Diamicton	MW-2	7.8 x 10-4 ft/sec
Diamicton	MW-5	6.3 x 10-5ft/sec
Saprolite	MW-9	3.8 x 10-4ft/sec

An artesian condition was noted when deep aquifer (Type III) monitoring well MW-9 was installed. A 6-inch steel casing was set to a depth of 42.6 feet and tremie grouted in place. The following morning, water was observed discharging from around the outside of the steel casing. This water continued to discharge for a period of 2 days.

Initially we suspected this discharge water could be from a septic system or some other type of shallow, perched water. A second boring was drilled to a depth of about 8 feet adjacent to well MW-9 to determine if this apparent artesian condition was from a shallow source. This 8-foot boring was dry after 24 hours. The artesian condition does not exist in the saprolite aquifer at well MW-9 that is screened at a depth of 40.6 to 45.6 feet (Figure 4).

The screen for well MW-2 was set from 7 to 17 feet to intercept the predicted unconfined water table at this location. The water level in well MW-2 rose to 5.6 feet, above the screened interval. The 8-foot boring drilled between wells MW-9 and MW-2 was dry even though it was 2.4 feet deeper than the potentiometric surface measured in well MW-2 (Figure 4). The higher than expected water level in well MW-2 is also attributed to the artesian condition.

The artesian condition or confined aquifer zone is interpreted to have originated along the contact between the saprolite and the diamicton at a depth of about 20 feet. We propose two hypotheses for the artesian condition at well MW-9. The first is that the older diamicton forms a confining bed above the saprolite aquifer. Relative groundwater elevations in wells MW-1 and MW-5 range from 89.63 to 89.86 feet (Figure 3). The groundwater elevation in the deep saprolite aquifer well MW-9 is 86.82 feet, which indicates a downward vertical gradient between the diamicton and the underlying saprolite. This groundwater elevation data indicates that this first hypothesis is not valid.

The second hypothesis is that an alluvial deposit or buried stream bed exists along the contact between the diamicton and saprolite (Figure 4). This alluvium would have a much higher hydraulic conductivity and the overlying diamicton would act as a confining layer. If this lens or bed of alluvial sand and gravel extended up slope along this contact, then it would have a hy-

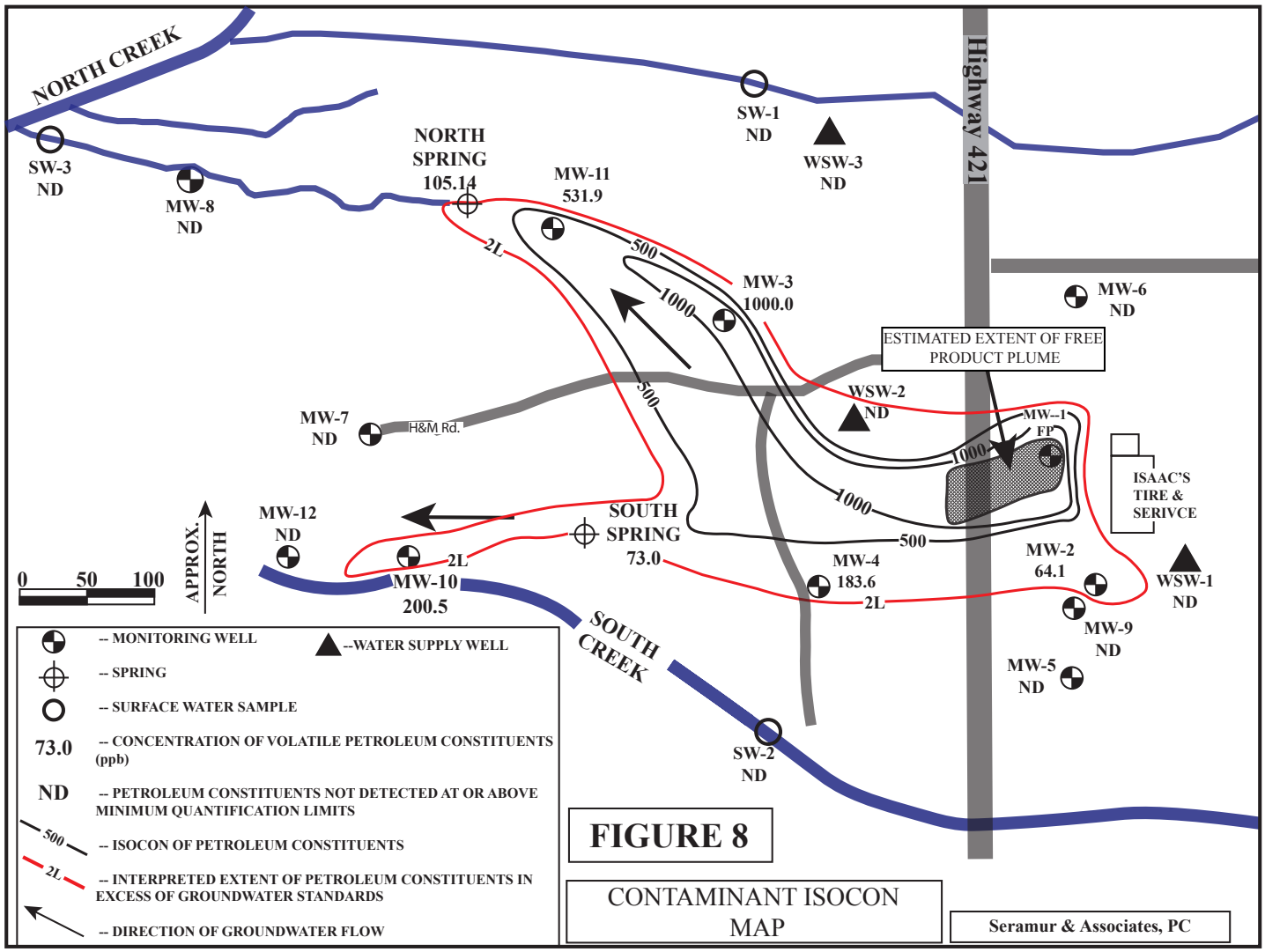

Figure 8. Contaminant Isoconcentration Map showing the extent of free product. Note how the dissolved-phase plume splits on the west side of Hwy 421.

draulic head capable of producing the artesian condition observed around the casing of well MW-9.

CONTAMINATION MIGRATION

Soil contamination at the site occurs in the unsaturated zone near the former USTs and along the capillary fringe where free product has migrated from the service station to the North and South Springs. In the vicinity of the former USTs, soil contamination occurs within the diamicton down to the water table. Down gradient of the source, soil contamination occurs primarily in the saprolite except at the springs where groundwater discharges to the surface through the younger diamicton.

When this assessment was completed in 1996, source area well MW-1 contained 0.16 feet of free product or light non-aqueous phase liquid (gasoline) floating on the water table. The free product plume originally extended from the service station to both the North and South Springs. A spring house used for drinking water at the North Spring reportedly had a thick accumulation of gasoline. Both the South Spring and a seep in the cut bank west of Highway 421 were reportedly set on fire on several occasions to burn off the fuel. During the initial assessment, free product was not observed at either of these springs, but a film of gasoline was observed seeping from the road bank west of Highway 421. This seep formed when the road bank was cut back to accommodate additional mobile homes and the road cut intercepted the shallow water table. The extent of the free product plume and dissolved-phase plume is shown on the 1996 Contaminant Isocon Map (Figure 8). The vertical extent of contamination is shown on Cross-Sections A-A', C-C', and D-D' (Figures 4, 6, and 7).

Initially, contaminant migration is west, from the source area toward the South Spring. However, the direction of contaminant migration developed a com-

ponent of flow to the north, toward the North Spring (Figure 4). This change in direction is in part related to site topography, as the North Spring (relative elevation 45.57 feet) is lower in elevation than the South Spring (relative elevation 63.77 feet). However, this change in the direction of contaminant migration did not occur until the water table dropped below the diamicton into the saprolite where preferential flow pathways also influence the direction of contaminant migration.

The downward vertical gradient calculated for well MW-9 indicates that it is possible for the contaminant plume to migrate down to the bedrock aquifer that supplies water to local wells. However, the drinking water wells nearest the contaminant plume (wells WSW-I, WSW-2, and WSW-3 shown on Figure 3) were sampled and petroleum constituents were not detected in any of these wells until 2017 (S&ME, 2017).

DISCUSSION

An interceptor trench was installed in the road bank below Hwy 421. This reduced the health threat posed by gasoline seeping into the trailer park. The effluent from this infiltration trench is being treated before being discharged into a stream. The interceptor trench clogged with mud about a year ago. Gasoline reportedly began to seep out of the bank again and gasoline was also observed discharging from the north spring. The residents reported negative health effects including skin rashes. The interceptor trench was repaired and is once again collecting effluent at a reported rate of around 300/gallons per day.

Fan morphology and stream erosion along the edges of the fan influence the direction of groundwater flow, particularly near the edge of the fans where groundwater discharges to adjacent streams. The diamicton at this site produces a confined aquifer zone with a relatively high hydraulic head along the contact with underlying alluvial deposits and saprolite.

This confined aquifer zone might prevent the contaminant plume from migrating downward into the fractured bedrock. Petroleum constituents were not detected in the drinking water wells until 2017 (S&ME, 2017). Sampling events in 2017 detected some 6200B constituents in water samples from the trailer park well that could be related to the release. These were detected at concentrations below the drinking water standards.

The diamicton behaved as an isotropic medium directing the initial contaminant migration down slope, east to west toward the South Spring. The contaminant plume split into two lobes in the saprolite aquifer and discharged at the North and South Springs. This change in direction of contaminant migration is attributed to preferential pathways through remnant foliation within the saprolite as well as topography.

Hydrogeologic investigations on debris flow fans in the Blue Ridge Mountains and Piedmont of western North Carolina require thorough understanding of the geomorphology and geology in order to model groundwater flow and contaminant migration. The presence of a diamicton stratigraphic unit within debris flow fans introduces a complexity not recognized in the typical groundwater flow models for this region. This is particularly important when there are potential threats to the public health and safety.

REFERENCES

Bouwer, H., 1989, The Bouwer and Rice Slug Test- An Update, Groundwater, v. 27, pp. 304-309.

Heath, R.C., 1980, Basic Elements of Ground-Water Hydrology With Reference to Conditions in North Carolina, U.S. Geol. Surv., Water Res. Inv., Open File Rept. 80-44. 86 pp.

Mills, H. H., and Allison, J.B., 1995. Weathering Rinds and the Evolution of Piedmont Slopes in the Southern Blue Ridge Mountains, Journal of Geology, vol. 130, p. 379-394.

Rankin, D.W., Espenshade, G.H., and Neuman, R.B., 1972, Geologic Map of the West Half of the Winston-Salem Quadrangle, North Carolina, Virginia, and Tennessee. Misc. Geol. Invest. Map I-709-A Dept. of the Interior, U.S. Geol. Surv., Washington D.C., 1 Map.

S&ME, 2017, State-Lead Monitoring Report Isaac's Tire, Incident No. 13526, UST No. WS-4059 Zionville, Watauga County, North Carolina S&ME Project No. 4305-17-094B. From NCDEQ online database.

Stop 2-3 The Fred Webb Jr Outdoor Geology Laboratory at Appalachian State University

Location: 36.2145°N, 81.6815°W

Stop leader: A.B. Heckert

The Fred Webb Jr Outdoor Geology Laboratory, or "rock garden" at Appalachian State University is a unique campus resource consisting of 50 oversized specimens (mostly boulders) from six states and at least 10 geological provinces (Fig. 1). The garden was dedicated in 2007 and honors its namesake, Dr. Fred Webb Jr, who arrived on campus in 1968 as one of the first professors of geology and served as the inaugural chair of the Department of Geology from 1976—1994. Fred loved taking students in the field, and taught a variety of field-based geology courses on two continents so, on the occasion of his retirement in 2004, the department set out to honor him by constructing the rock garden and thus helping bring "the field" to more students and others on campus. Since 2007 we have continued to expand the exhibit area and it now one of the most striking features on campus (Fig. 2).

Specimens in the rock garden come from North Carolina (28), Virginia (10), Tennessee (5), Ohio (2), South Carolina (1) and Georgia (1), as well as two benches made of surplus landscaping granite that may be from Ontario and two pieces of "marble" of unknown origin. Rock garden specimens include representatives of common igneous, sedimentary, and metamorphic rocks and range in age from late Mesoproterozoic (Pumpkin Patch Metamorphic Suite) to latest Triassic/early Jurassic (basalt and gabbro from Manassas, Virginia). Geological provinces include the stable interior (Ordovician limestone from Ohio), Cumberland Plateau (2), Valley and Ridge (8), eastern (10) and western (4) Blue Ridge, inner Piedmont (2), Charlotte Belt (5), Kings Mountain Belt (1), outer Piedmont/Carolina Slate Belt (1), as well as Triassic rift basins (3) and associated Central Atlantic Magmatic Province (CAMP) intrusions (2). These specimens document at least five major tectonic events (Grenville, Taconic, Acadian, and Alleghenian orogenies as well as Triassic rifting/CAMP magmatism).

The rock garden is a fabulous educational resource both formally and informally. Not only do the specimens represent a geologically and geographically diverse suite, but their large size allows students to observe numerous features not easily seen in traditional hand samples, including sedimentary structures, fossils (body and trace), folds, intrusions, veins, slickensides, xenoliths, and more. Their bulk also means that multiple students can be examining the same specimen simultaneously.

Hundreds of Appalachian students use the rock garden as part of their formal course work each year. Subsets of the specimens form the basis of exercises in classes at all levels with the department, including physical, historical, and environmental geology, evolution of the earth, mineralogy, petrology, structural geology, and geomorphology (Table 1). Several First Year Seminar (FYS) courses arrange visits of the rock garden, and, many other classes and groups outside

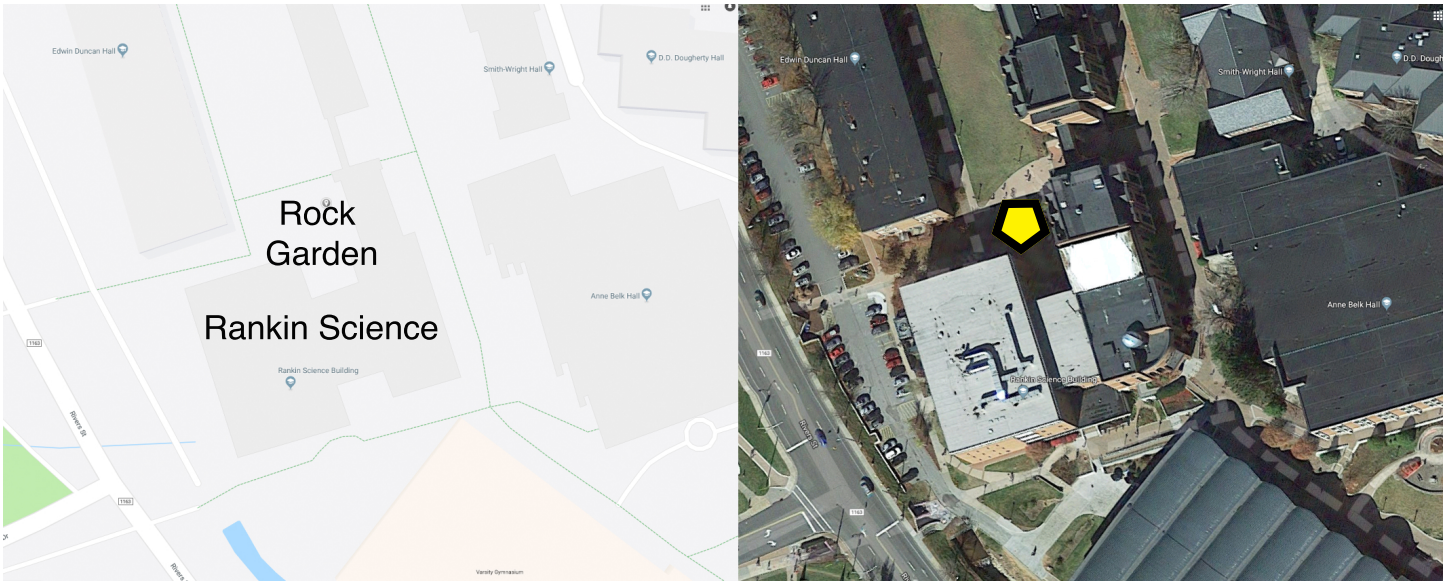

Figure 1. Google Maps® map (left) and satellite image (right) of the vicinity of the Rankin Science complex of Appalachian State University in Boone, NC. The Fred Webb Jr Outdoor Geology Laboratory is located at the pentagon on the campus image.

Figure 2. Montage of photographs of the Fred Webb Jr Outdoor Geological Laboratory ("rock garden") at Appalachian State University. A) Nameplate and entrance to the main body of the rock garden. B) In the opposite direction from the middle of the garden. C) View toward the rock garden from the "triangle" expansion of 2018. D) The "triangle" expansion from overhead. E) Main body of the rock garden from overhead. Photographs D-E captured with a drone operated by Brian Zimmer.

Table 1. Geology Courses that use the "Rock Garden" for one or more lab activities

Number	Course Name	Exercise(s)
GLY 1101	Physical Geology	Rock identification & formation
GLY 1102	Historical Geology	Rock identification & formation, provenance comparisons
GLY 1103	Environmental Geology	Rock identification & formation
GLY 2250	Evolution of the Earth	Rock & mineral identification, rock formation, provenance comparisons
GLY 2745	Preparation of Geologic Reports	Measuring features
GLY 3150	Structural geology	Measuring features
GLY 3333	Geomorphology	Weathering comparisons
GLY 3715	Petrology	Thin-section work

the department also use the rock garden as an informal meeting place.

Presently each rock is labeled with some data, but not identified. Provided information includes formation name (e.g., Knobs Fm, Ashe Metamorphic Suite), locality, numerical and relative age estimates, geologic province and, if appropriate, donor. Traditionally we have not included rock names/identifications because we use the specimens in class exercises. To facilitate rock and mineral identification and to preserve the softer specimens we provide a "key to destructive tests" with information on hardness and susceptibility to acid. We have a library of thin sections and SEM stubs of most specimens for use by upper-level classes as well.

Perhaps the rock garden's biggest contribution is to the department's outreach. The rock garden and the F. Kenneth and Marjory J. McKinney Geology Teaching Museum inside the department host dozens of classes from the greater "high country" region. Thus, every year hundreds of children ranging in age from pre-K to 12th grade visit the rock garden and museum. Weather permitting, the rock garden serves as an excellent place for these school groups to meet up with Appalachian faculty and students and dissipate a little of the energy that built up during their bus ride to campus. We have multiple activities at various grade levels (principally 1st, 4th, and 6th grades, following current NC educational standards) that we use to provide hands-on experience with rock identification and to learn a little about their economic use.

During our most recent expansion we took over additional space on the quadrangle and turned this into the home for nine rocks that will have more signage and interpretation than the others. We envision both introductory labs and school groups starting with these specimens (three each igneous, sedimentary, and metamorphic) and using them as a guide to interpreting the others by providing examples of common textures and compositions.

The rock garden space remains dynamic in other ways. Our acquisition of Triassic rift basin specimens is part of an effort with a studio art class to build, bronze, and install a life-sized model of the Triassic fossil reptile and North Carolina native *Gorgetosuchus pekinensis*. Thus, the southeast corner is envisioned as an "aetosaur habitat" with a variety of ferns and other "age-appropriate" vegetation in addition to several boulders from the Sanford sub-basin of the Deep River basin.

Recently one of the faculty members, Brian Zimmer, has overseen creation of digital models of many of the rock garden specimens by students. These 3D renderings are scalable and will be made available on the web, augmenting existing materials and enabling "virtual visits" of the rock garden beyond what we currently offer (see https://mckinneymuseum.appstate.edu/rock-garden).

Construction of the rock garden resulted in a variety of unforeseen activities, most of which are beneficial to the department. In 2014 an earth science education major and dance minor choreographed a piece that was performed in the rock garden that fall. We also adopted an art piece after it was orphaned when the university tore down its home in 2016. Thus, "Bernini: After the rape of Persephone" is a 2-part marble sculpture by Be Gardiner (and the 1989 winner of the Rosen Sculpture Contest on campus) that provides a further link between the sciences and the arts. We are aware of at least one successful marriage proposal in the rock garden, and it is also, apparently, a hotspot of Pokemón activity. We often see photography students using the rock garden for their subjects, and the campus day care facility often brings toddlers to the rock

garden. Finally we (and other departments) often host a variety of social activities (picnics, etc.) here.

LOGISTICS

This resource is open 24 hours a day, 7 days a week, 365 days a year, although we do recommend visiting during daylight hours for the best viewing of specimens. For the most part the rocks themselves require little to no maintenance, but we do pressure wash some to combat oxidation, lichen, and other weathering processes. Vandalism has been minimal, but much of the garden is now under automated camera surveillance. My criterion for inclusion in the rock garden has traditionally been that I had to believe that three inebriated, testosterone-laden students could not move the specimen, and those guidelines have served us well, even if not empirically tested.

PROSPECTUS

We remain on the lookout for additional specimens. Generally speaking the single greatest logistical hurdle is hauling the specimens from the donor location to Appalachian. We would love to expand our offerings to include the Castle Hayne Limestone (one of the few Coastal Plain specimens that could be sufficiently lithified to include in the garden), the Murphy Marble, Day Book Dunite, and others. If you have an idea for a specimen that we should add, we are certainly interested, especially if you have access to transportation.

ACKNOWLEDGMENTS

The rock garden could never have come to fruition without the generosity of numerous donors, the single most important sponsor being Vulcan Materials Company. Not only have they donated at least 13 specimens from facilities in three states, but they transported those specimens and several others to Appalachian. They have also provided additional landscaping material and are very active supporters of the department's outreach programming. Other donors include North Carolina Granite Corporation, Feldspar Corporation, Forterra Brick, Maymead, Patterson Exploration, and others. Donations by Appalachian alumni and faculty as well as the equipment and hauling of the first ~14 specimens by Brian Elliston '04 were also essential, as was support from Academic Affairs. We have forged an excellent working relationship with our physical plant, especially Landscape Services, and they have invested considerable effort in plants, mulch, and upkeep to make the rock garden an even more visually appealing facility than it already was. Numerous faculty, staff, and students have provided ideas, innovations, and service to the rock garden. Key among these have been Marta Toran (outreach ideas and materials), Brian Zimmer and his student workers (3D models, drone photography), Anthony Love (sampling, thin sections, sign installation, student supervision, maintenance), Ashley "Bart" Bartholomew (original website), Annie Klyce (latest database) and numerous student workers that have helped lead hundreds of tours. Lauren Waterworth and Travis Donovan are the brainchild and sculptor behind the planned aetosaur bronze, and the garden itself was conceived before my arrival at Appalachian by faculty Ellen Cowan and Steve Hageman.

Stop 2-4. Blowing Rock Gneiss near Bailey Camp, NC on US-321.

Location: 36.0992°N, 81.6420°W

Stop leader: Andy R. Bobyarchick

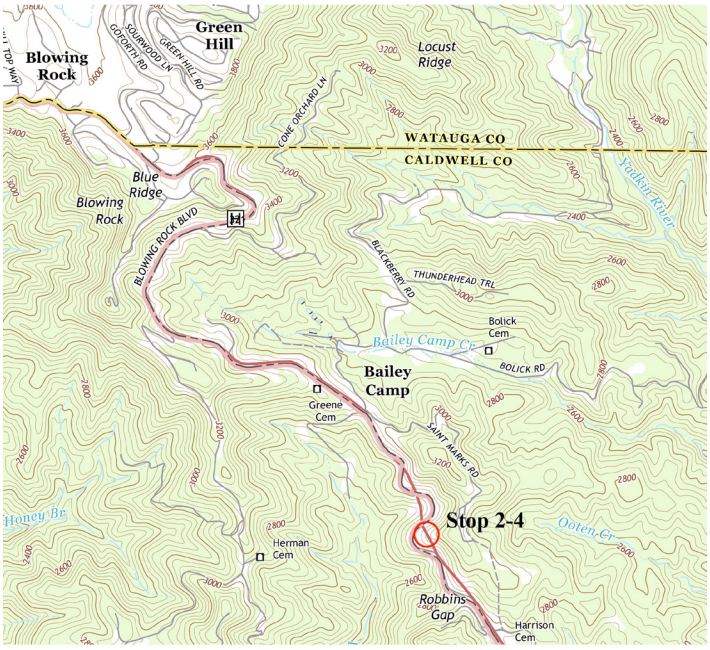

Figure 1. Location of Bailey Camp section. Base from U.S. Geological Survey Globe 7.5' topographic quadrangle. Red circle indicates Stop 2-4.

Park in the NC DOT gravel lot at the north end of the main exposure (Figure 1). Stay inside the barrier fence to walk along the outcrop. Some sections of the exposure are unstable; hard hats are recommended. Please do not destroy any exemplary in situ parts of the outcrop and remain aware of other participants if you use a rock hammer. Many good samples of most exposures can be collected from colluvium at the base of the exposure.

STOP DESCRIPTION

This Bailey Camp section on US-321 (Figure 1) is a remarkable exposure of highly deformed Blowing Rock Gneiss, metamorphosed mafic dikes intruding the gneiss, ductile shear zones, many forms of vorticity and shear sense indicators, and the contact between Blowing Rock Gneiss and Wilson Creek Gneiss (Figure 2).

The regional geology for the Bailey Camp section and details of porphyroclast development and measurement are described in Bobyarchick (2018, this guidebook). A very detailed description of the petrography and mineralogy of Blowing Rock Gneiss is in Hoff (1982). Bryant and Reed (1970) is the classic reference for regional geology of the Grandfather Mountain window. Bryant (1966) evaluated metamorphic reactions involved in producing phyllonitic ductile shear zones, some of which are exposed here.

Figure 2. Bailey Camp section. Gravel parking lot indicated by red circle.

Features noted in this text are arranged roughly from north to south, starting in the gravel parking area. Some specific features, such as mafic dikes, occur throughout the exposure.

Several bodies of greenschist – metamorphosed mafic dikes – are present in coarse Blowing Rock augen gneiss adjacent to the gravel lot (Figure 3). Several irregular bodies of coarse-grained granitic gneiss are in contact with both augen gneiss and greenschist layers. McDermitt and Bobyarchick (2011) examined these relationships soon after the exposure was created and decided that there was insufficient evidence to prove that the dikes that are now greenschists were substantially folded during or after peak metamorphism. Subsequent detailed investigations now suggest that the greenschist layers are tightly folded by nearly reclined, south-plunging folds such as can be demonstrated at this part of the outcrop. These folds are not as obvious along the main length of the Bailey Camp section because the orientations of the fold hinge lines are close to parallel to the trend of the exposure.

Bryant and Reed (1970) described these meta-mafic rocks as "inclusions" in Blowing Rock Gneiss and did not explicitly call them dikes or place them on their geologic map. This may be the result of inadequate exposure and the mapping scale used.

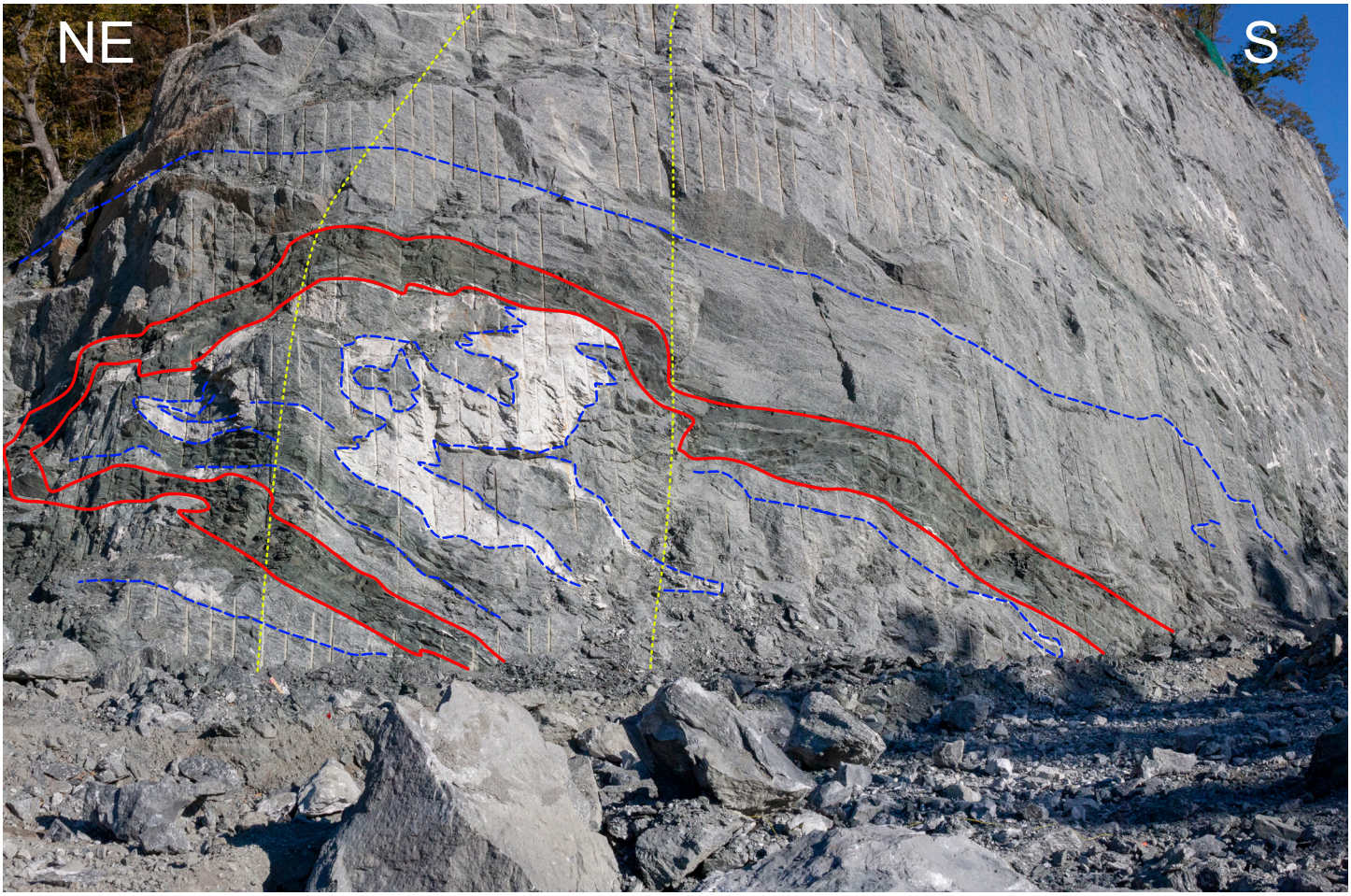

Figure 3. Panoramic image of north end of Bailey Camp section main outcrop. Dotted yellow lines are bends in outcrop surface with opening angles toward southeast. Left bend is ~90°; right bend is ~30°. Red solid lines approximately trace irregular greenschist margins. Dashed blue lines are form lines on foliation or compositional boundaries. The northeastern fold closure is problematic but smaller folds in the overturned antiformal hinge zone have similar geometries. View is toward southeast.

The antiform in Figure 3 includes similarly folded leucocratic veins in its hinge region. In places, very thin quartzose veins internal to greenschist are tightly to isoclinally folded (Figure 4). (Fold asymmetries in such veins may depend on pre-folding geometry of the veins and should be used with care.) Shorter wavelength folds of layering are common in the northern part of the section, especially near greenschist layers and quartzofeldspathic veins. Tight and complex folding dominates in the layered parts of Wilson Creek Gneiss at the far south end of the section.

The primary schistosity in the area of the antiform is axial planar to this large fold and to most smaller folds (Figure 1). In augen gneiss, the schistosity is a shape fabric defined by flattened augen (Bobyarchick, 2018, this guidebook) and in greenschists the schistosity is defined by aligned phyllosilicate minerals and sometimes a faint compositional layering. On the lower limb of the antiform, careful examination of the augen shape fabric near the contact between gneiss and schist shows that the contact geometrically truncates that shape fabric (Figure 5). This is the result of finite strain acting in all rock types and does not necessarily indicate an intrusive truncation of original igneous layering or fabric.

Figure 4. Tight and isoclinal folds in veinlets in greenschist at boundary with augen gneiss. View is toward southeast. Outcrop at north end of section.

Figure 5. Contact between greenstone and augen gneiss. Note the obliquity between the shape fabric (porphyroclast dimensions) and contact. Primary schistosity within the greenstone is, however, approximately parallel to the augen gneiss foliation. At hammer head there is a ghost fold made from a disarticulated vein.

In many places, Blowing Rock Gneiss contains pre-major folding leucocratic veins. As noted, some of these veins are granitic and pegmatitic, but others are medium- or fine-grained granite gneiss or aplites. Both kinds of veins are tightly to isoclinally folded, with the former ranging between still continuous to disarticulated to segmented pseudo-augen in "ghost folds" (Bobyarchick, 2018, this guidebook) (Figure 5).

In places, greenschist layers show a fairly strong crenulation with possible crenulation cleavage and/or a crenulation lineation. These crenulations are not present everywhere but they are late in the folding history, possibly a superimposed folding event on an earlier, more intense event. Chlorite coated slickensides are present near many greenschist layer boundaries, some striated. These structures like the crenulations appear to be later, but not the latest tectonic features in the section.

Ductile shear zones appear at several places throughout the Blowing Rock Gneiss in the Bailey Camp section. One of the best and most enigmatic is in the topographic notch on the north side of the gravel lot. These exposures pre-date the exposures created by excavations to straighten Highway 321 and are thus more covered and weathered. Figure 6 illustrates these rocks and their variations in strain intensity. These tectonites range between augen-bearing mylonite gneiss and flaser-structured mylonite. The rocks are considerably more recrystallized than "normal" Blowing Rock augen gneiss. In addition, domino porphyroclasts (see Bobyarchick, 2018, this guidebook), some of which are also sigma or delta porphyroclasts, are common but there are some small zones where the shear sense

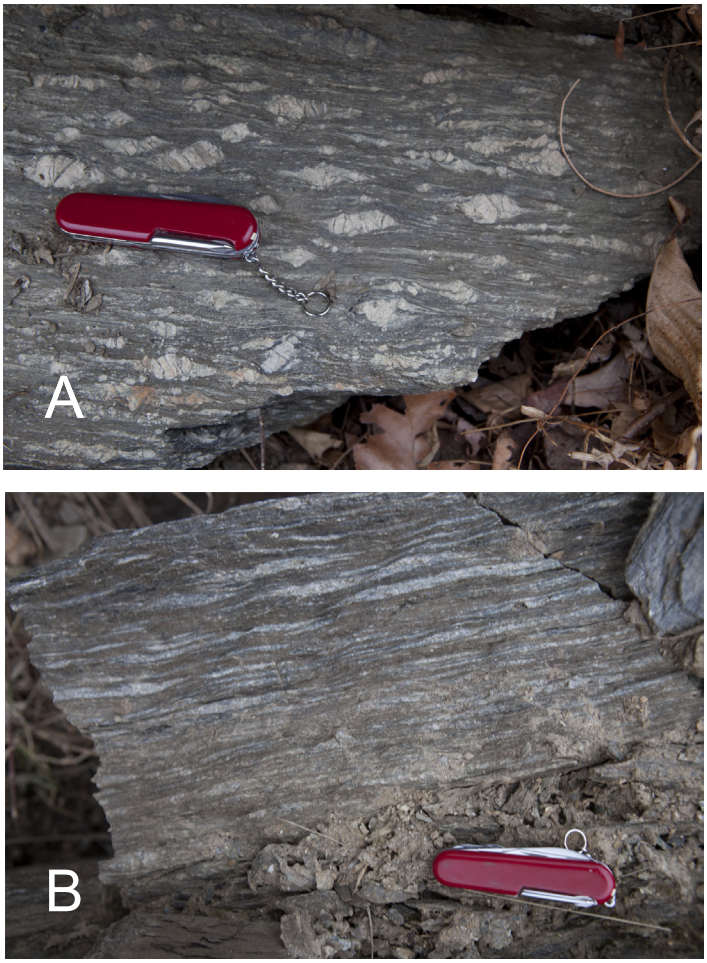

Figure 6. Progressive deformation from mylonitic augen gneiss to flaser laminated mylonite. Outcrop in topographic notch near gravel parking area. A – Porphyroclastic augen gneiss with domino porphyroclasts. Cleavage fragment rotation for most clasts indicates sinistral shear but some clasts like those near knife top are equivocal. If treated as sigma porphyroclasts, some asymmetric tails would suggest dextral shear, but these may be an artifact of rigid rotation counterclockwise of the clast bodies, making these particles more like delta porphyroclasts. B – Felsic lenses are sheared augen and vein fragments. Mylonite foliation is wavy, possibly because of incipient shear band formation.

indicated by individual augen are opposite the common sinistral, top-to-north shear sense. There may be late stage folds disrupting some of these porphyroclasts. It's possible that this shear zone is associated with measurable regional offset; the next roadcut exposure to the north is still Blowing Rock Gneiss, but there the overall appearance is less deformed than the main part of the Bailey Camp section.

Several good ductile shear zones are within Blowing Rock Gneiss south of the large antiform described above (Figure 7). The most intense of these are phyllonitic and mylonitic gneisses or schists. The gradient from coarse augen gneiss to mylonite is typically continuous but fairly sharp. Ductile deformation zones

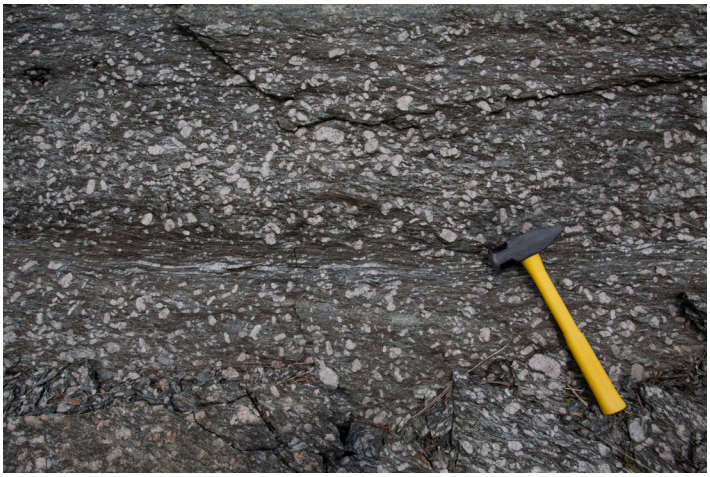

Figure 7. Small ductile deformation zone in augen gneiss. Outcrop is south of antiform near gravel lot. Overall this rock is mylonitic but only the clasts in the middle of the shear zone near the hammer head are as highly strained as those in Figure 6. There is considerable white mica in this outcrop. The soup of augen has a few domino porphyroclast but most are not fractured and some retain cleavage outlines. Note that a large number of clasts are aligned at large angles to the mylonite foliation, suggesting a comparatively lower accumulated strain than more strongly sheared parts of the section or back rotation because of a strong flattening component.

Figure 8. Pyrite or sulfide cluster in augen gneiss. Most pyrite is present as single cubes or clots of a few, but rarely sulfides appear with quartz or calcite tails or as here with a long pyrite tail.

range in thickness between several centimeters to several tens of centimeters. The micaceous mylonites are bright green because of the increased abundance of chlorite and white mica and possibly quartz. Throughout the section there are zones of apparent greenschist facies retrogression and they are usually associated with ductile shear zones, but there are also patches of saussuritization in feldspar grains and clasts that are not directly in ductile shear zones.

Sulfide minerals are present throughout Blowing

Figure 9. Coarse calcite/dolomite in mixed quartz/carbonate vein. Host rock is mylonitic augen gneiss. The light colored vein beneath hammer head has multiple internal veins that terminate at boundary with matrix. Pink carbonate crystals to right of hammer head. Vein segment beneath hammer and the segment at the top of the image appear to have been continuous at one time, perhaps as joined limbs of an isoclinal fold now broken.

Rock Gneiss in the section. The most common are visible cubes of pyrite as much as two centimeters in diameter. The most abundant sulfide mineralization is in greenschists, but micaceous parts of augen gneiss also carry these minerals. In greenschists, pyrite crystals sometimes have quartz or calcite pressure shadows, usually asymmetric within schistosity. Pyrite crystals are rarely deformed, but clusters have been sighted with what appear to be tails into the surrounding foliation (Figure 8). Visible sulfide mineral crystals have not yet been observed to be very common in ductile shear zones.

Carbonate minerals, mainly calcite and dolomite, are common in veins and in the matrix in Blowing Rock Gneiss. Calcite can be distinguished from coarse quartz by the former's strong cleavage (Figure 9). The source for abundant carbonate mineralization is not determined. There are calc-silicate rocks in the Wilson Creek Gneiss in the Bailey Creek section that are limited to discrete layers (Figure 10). Rocks in the Grandfather Mountain window have been transported westward over early Paleozoic sedimentary Laurentian margin sequences during the Alleghanian orogeny and may have interacted with that same sequence during a mid-Paleozoic event as well. Decarbonation of, for example, Early Cambrian Shady Dolomite, at depth during emplacement of Blue Ridge thrust sheets could have contributed to calcite recrystallization higher in the structural sequence. Reed (1964) described Shady Dolomite in the Tablerock thrust sheet as "silicified to a fine-grained white sugary or porcelaneous rock

Figure 10. Layered sequence in Wilson Creek Gneiss near Linville metadiabase dike. From left: strongly laminated and layered biotite gneiss generally not showing intense folding seen elsewhere in Wilson Creek Gneiss in this section; non-layered green chlorite-epidote(?) gneiss with calcite or quartz-calcite veins parallel to layering; boudinaged carbonate and/or calc-silicate layer at pencil; massive gray-green weakly layered gneiss. These rocks have not yet been analyzed in detail. The green layer does not have all of the characteristics of greenschists in the north part of the section. It does, however, appear similar to greenschist facies metasedimentary rocks in the Grandfather Mountain Formation to the north.

Figure 11. Linville metadiabase(?) at contact between Blowing Rock Gneiss (several meters to the left) and layered phase of Wilson Creek Gneiss. The dike is the dark brown, blocky weathering unit on the left. Below and above the dike is strongly foliated felsic gneiss with concordant leucocratic veins. The overlying dark green layer is a greenschist. Light colored, bulbous layer above greenschist is an orthogneiss(?) in Wilson Creek Gneiss.

resembling quartzite". These rocks are presently structurally higher than rocks in the Bailey Creek section.

Calcareous rocks are also present in the Grandfather Mountain Formation where the carbonates are matrix minerals and in marble (Bryant and Reed, 1970). These rocks are presently stratigraphically and structurally higher than Blowing Rock Gneiss. Calc-silicate lenses occur in the Bailey Camp section as boudinaged concordant layers in Wilson Creek Gneiss or the transition between the Wilson Creek and Blowing Rock gneisses (Figure 10).

Calcite of some source is integral to the matrix of Blowing Rock Gneiss and is precipitated in deformed veins within the gneiss. (Calcite also coats some fracture and slickenside surfaces.) It's possible that some vein-forming carbonates are remobilized locally. Should the carbonate sources for matrix calcite in Blowing Rock be exotic, the timing of their derivation from overthrusted sequences are critical to interpretation of tectonics in the Bailey Camp section. The traditional view of Alleghanian metamorphism in the Blue Ridge is that it was greenschist facies or lower. Casale et al. (2017), however, have suggested that early Alleghanian metamorphism in the eastern Blue Ridge in north Georgia may have reached amphibolite facies. If those conditions approximately applied here, the predominant foliation (though possibly not the oldest foliation) could be early Alleghanian.

Purple fluorite is rarely present in the Bailey Camp section. It occurs in late fractures and veins. Fluorite is also reported from similar settings in the Grandfather Mountain Formation elsewhere in the Grandfather Mountain window. Please do not destroy the outcrop trying to remove tiny purple crystals.

To the south and about halfway along the main outcrop of the Bailey Camp section, the contact or transition zone between Blowing Rock Gneiss and Wilson Creek Gneiss is marked by what Bryant and Reed (1970) called Linville Metadiabase. Keith (1903) originated that nomenclature. Bryant and Reed (1970) showed this unit to intrude the contact between Blowing Rock Gneiss and Wilson Creek Gneiss near Bailey Camp and to extend for several miles in both directions along strike. We will refer to this body as a dike based on that interpretation.

This dike is easily recognized (Figure 11). It is very fine-grained, hard, and much more densely jointed than surrounding rocks. The larger outcrop is often wet around the dike because of groundwater seepage through the fracture network and consequently this part of the section is covered by surficial mineral deposits. Daylighting of some fractures contributes to very local rock falls and slides. The edges of rock fragments are very sharp, so avoid falling on them.

Bryant and Reed (1970) described Linville Metadiabase as mafic rocks (diabase or diorite) metamorphosed to greenschist facies. The Bailey Camp dike

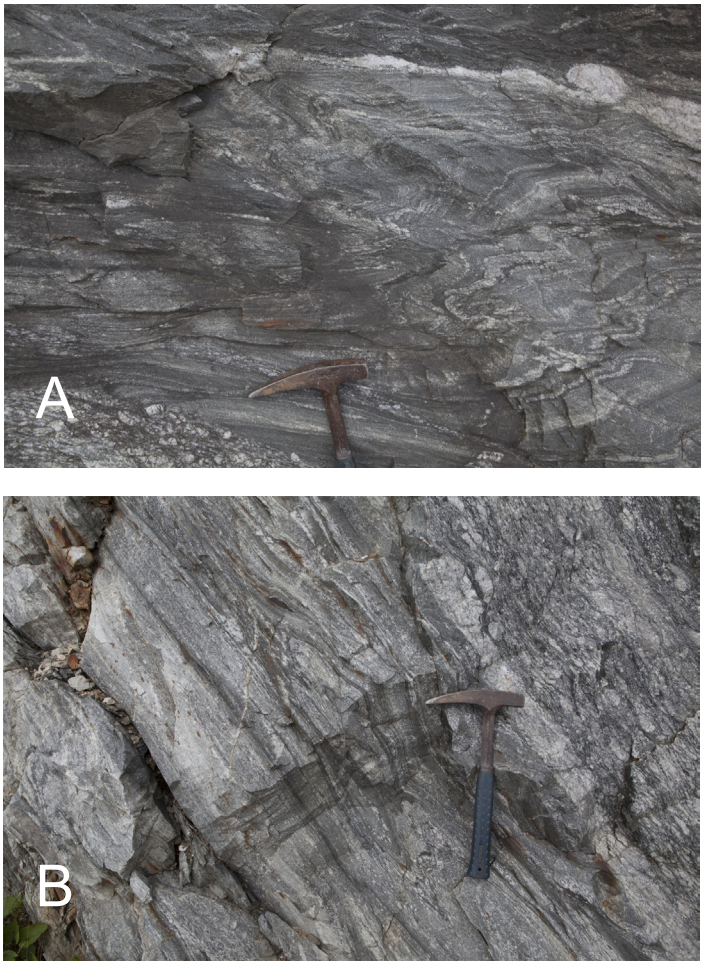

Figure 12. Folds in Wilson Creek Gneiss. Both images are viewed facing southeast, oblique to most fold profiles. A – Fold sets in layered biotite gneiss. The folds deform a schistosity parallel to layering and there is an axial planar cleavage to them. It is not known how either foliation relates to the principal schistosity north of the contact between Wilson Creek Gneiss and Blowing Rock Gneiss. B – Orthogonal views through folds in A. The hammer handle is resting on the main cut face of the road cut, and the hammer's pick point is above a cut and broken face on the cut so that the two views are normal. These folds are isoclines that are highly attenuated but the closure patterns do suggest they have curved hinge lines, so they are minimally non-cylindrical. If inferred to be sheath-like folds, this geometry would suggest shear toward northwest or southeast depending on the convexity of the hinges.

does not fit most of their descriptions. This rock is extremely fine-grained, dark green or gray, non-layered, and contains abundant epidote and chlorite. Many minerals are difficult to determine petrographically; we do not yet have chemical analyses for comparison. In thin section, the rock contains a few quartz or plagioclase grains that appear euhedral or subhedral. A foliation is present but as far as can be seen optically most mineral grain boundaries are reasonably equilibrated.

The covered or obscured area around the dike is also the contact between Blowing Rock augen gneiss and strongly tectonized layered Wilson Creek Gneiss. As noted by Bryant and Reed (1970), the contact between these two units is by no means simple or even uniform. Bryant (1962) described Wilson Creek Gneiss as a metamorphosed plutonic complex, but significant parts of areas mapped as this unit are layered gneiss and schist, much of it mylonitic. From the north and to several meters before the dike, the Blowing Rock Gneiss is a fairly homogeneous augen gneiss hosting multiple (or several folded) mafic dikes and quartz-feldspar masses as blobs or discontinuous lenses. Near the dike and partly covered there are layered gneisses and a coarse-grained, deformed granitic rock. The latter more closely compares with plutonic phases of the Wilson Creek Gneiss to the south than to Blowing Rock Gneiss. The granitic rock is much more quartzose than Blowing Rock Gneiss; it is foliated but not a characteristic augen gneiss.

South of the dike, the Wilson Creek Gneiss is best described as a metamorphic complex of ortho- and para-gneisses. Layered gneiss and schist are pervasively deformed by tight to isoclinal folds of layering (Figure 12); refolding is visible locally. Quartz-feldspar stringers – folded and non-folded – are common. Extremely deformed calc-silicate layers fall within this sequence and some layers may be calcareous gneiss (Figure 11). Some isoclinal folds in this area appear as sheath folds on outcrop surfaces and, given the deformation intensity, could have curved hinge lines (Figure 12). Because of the obliquity between fold axes and observation surfaces, however, what appear to be eye folds may be tangential sections of plunging isoclines.

We have not spent a lot of time in the Wilson Creek Gneiss part of the Bailey Camp section and so do not have a preferred interpretation of the origin of these rocks. Paragneiss sequences include lithologies that correlate with the finer grained parts of the Grandfather Mountain Formation. Some of the coarser units in the transition zone approximate arkose, also possibly correlate with similar units in the Grandfather Mountain Formation. Granitic orthogneiss such as is exposed at the southern end of this section, however, appears to be intrusive into paragneiss. Should Wilson Creek Gneiss here be part of the Late Proterozoic cover sequence, its contact with Blowing Rock Gneiss could be an unconformity. Without better age or lithostratigraphic control, it is also possible that, as historically assumed, Wilson Creek Gneiss is a completely separate package of rocks. What is visible of Wilson

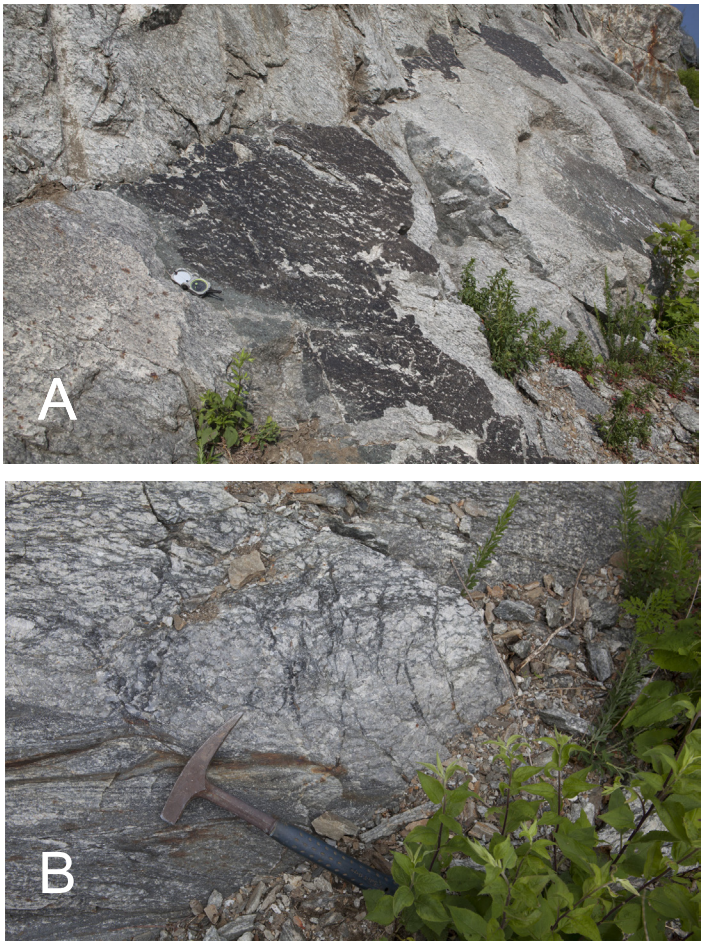

Figure 13. Late, discrete moderately dipping faults and associated structures. These structures are in the Wilson Creek Gneiss part of the Bailey Camp section. A – Planar slip surfaces decorated with chlorite and calcite. These surfaces, interpreted as faults, dip southwest about 45°. Striations and steps on some surfaces indicate oblique thrusting toward southeast. Slickenlines are mainly displayed by chlorite films. Striations in some patches of calcite may have been created during excavation and construction of the road cut. B – Nearly vertical networks of chlorite-filled fractures and microfaults in granite gneiss in close proximity to faults in A. Some of these may be conjugate fractures as a couple were measured with dip vectors of 89°, 140° and 88°, 315°. Slip is minimal but where visible is north side down.

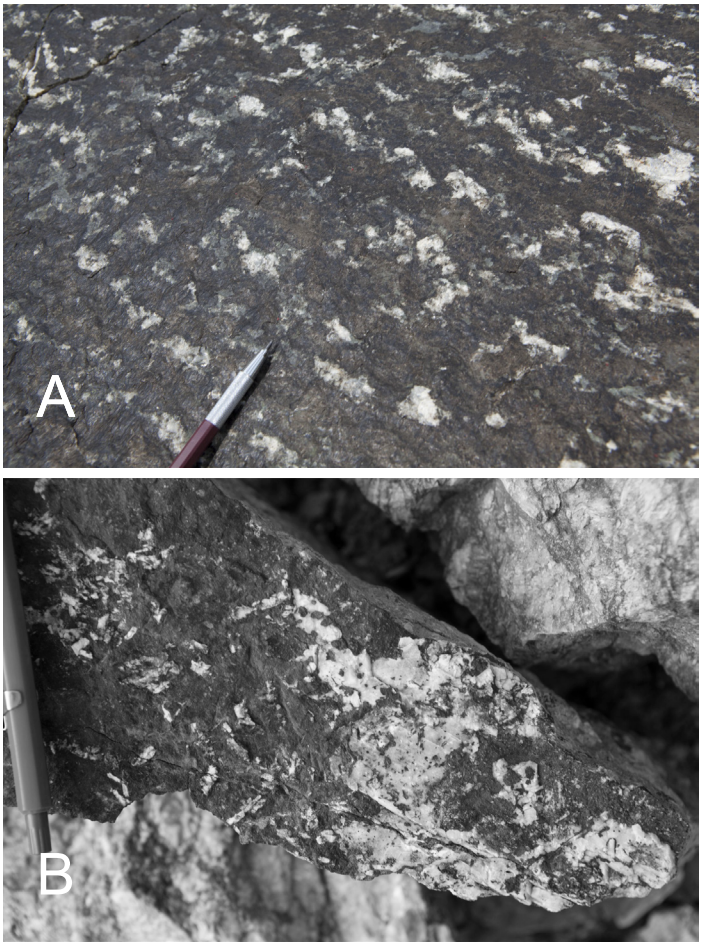

Figure 14. Chlorite and calcite on fault surfaces. A – Chlorite film with striations (parallel to pencil) and apparent calcite skips and steps. B – Similar surface on colluvial block. Distinct cleavage traces in calcite suggest some of these faults may have followed pre-existing veins or that calcite crystallized post-movement.

Creek Gneiss at Bailey Camp is representative of the metamorphic group southeast to the Linville Falls fault and Brevard fault zone.

An additional thought regarding the dike is to consider if it marks a fault zone. In some settings, a very fine-grained rock coincident with a major geologic boundary can be a recrystallized mylonite. On the map of the Grandfather Mountain window area (Bryant and Reed, 1970), the dike does not follow the nearest Blowing Rock Gneiss/Wilson Creek Gneiss contact. The projection of the dike does, however, lie directly on strike with a contact and thrust fault between the two formations. None of the original or derivative works compiled by Bryant and Reed continued this unnamed thrust fault or another to the east also at the same contact to the north. Wilson et al. (2008), however, did speculate that the main body of Blowing Rock Gneiss is isolated as a thrust slice between these two faults that ultimately merge with the Linville Falls fault. Parts of the deformation sequence Wilson et al. (2008) described in the Goldmine Branch fault zone and also in the "Tweetsie outcrop" of Blowing Rock Gneiss (Hatcher et al., 2006) correlate well with the Bailey Camp section but the Linville metadiabase dike(?) does not. A better comparison to Goldmine Branch and Tweetsie is the high strain zone that passes through the gravel lot for this stop.

A cursory examination of field and petrography samples of the dike did not reveal any features of prograde or retrograde mylonites and shear zones familiar to this author. If a fault zone rock, the fault must have

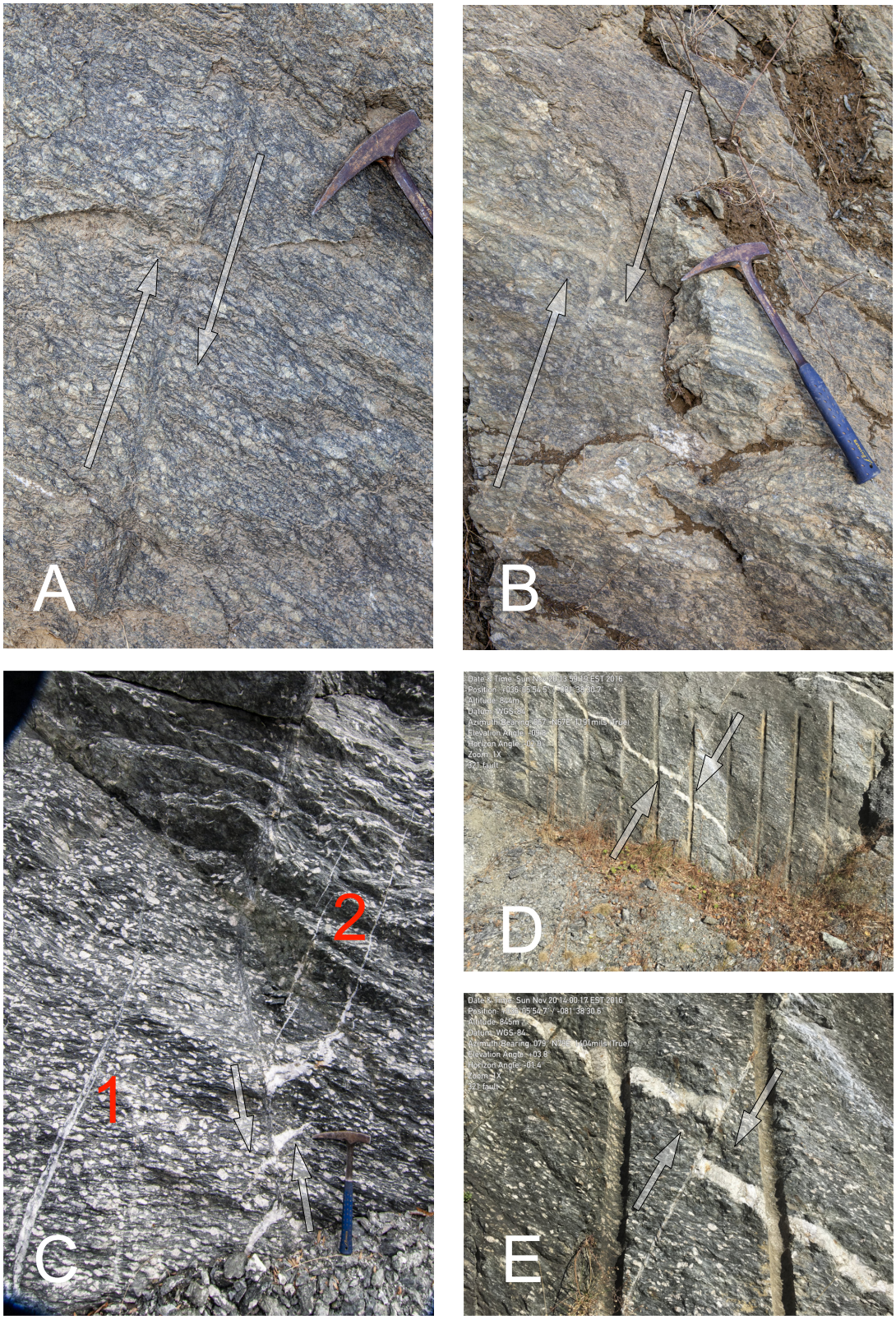

Figure 15. Array of late, high-angle faults. All views are toward southeast. A – Chloritic, micro-breccia reverse fault in Wilson Creek augen gneiss. Sectional shear sense deduced from rotated mylonite foliation and reorientation of porphyroclasts is top to southeast. B – Vein, possibly dilated fracture with sectional reverse offset in Wilson Creek Gneiss. Shear sense from displaced and folded vein and rotation of porphyroclasts. C – Chloritic micro-breccia gouge zone and fault of uncertain displacement. Sheared terminations of quartz veins suggest reverse motion with top toward northwest, but at the top of the image the foliation is clearly rotated in a dextral sense. The vein at 1 has a core of rock fragments and rims of quartz, clearly a dilational fracture. En echelon veins at 2 are closer in orientation to faults in A and B. Shear sense from these veins is sinistral on a steeply northwest-dipping plane, with top down to northwest. D and E – Dilational fault in Blowing Rock Gneiss with top to southeast.

pre-dated peak metamorphism. On the other hand, the map trace of the dike may be tracking a ductile shear zone that connects the Bailey Camp section with fault zones mapped by Bryant and Reed (1970) and Wilson et al. (2008).

Late, that is, discrete and younger relative to more pervasive structures, features at Bailey Camp include medium-dipping faults and slip surfaces and rare high angle semi-brittle faults and fault zones. Joints are more common in the southern half of the section. Large, daylighting fracture surfaces are also present. Late, moderately dipping faults with oblique reverse motion occur in several places along the length of the exposure but they are small in number (Figure 13).

Some chlorite and/or calcite coated faults dip moderately southwest and have striations raking north and calcite-filled steps indicating oblique reverse motion toward the northwest (Figure 14). These faults often are spatially associated with chloritic fracture webs possibly acting as accommodation structures (Figure 13). Moderately dipping large, planar outcrop fracture surfaces are inclined toward the highway and, with weathering, make the southern end of the Bailey Camp main section more prone to rock slides.

The few high-angle faults that have been found appear to be very late in the deformation sequence, although some do seem to be hosted in narrow, cohesive cataclastic fault zones (Figure 15). These faults dip 80°-90° northwest or southeast and appear to have both north side down and up displacements of a few centimeters. It's possible that the high-angle faults are also accommodation structures to the reverse faults noted above. Side fractures to one of the latter faults showed similar motions along near vertical chloritized fractures (Figure 13).

The Bailey Camp section could serve as a keystone to eastern Blue Ridge tectonics from Grenville to Alleghanian orogeny. These rocks present significant challenges to investigators interested in structure, metamorphism, and geochronology.

REFERENCES

Bryant, B., 1962, Geology of the Linville quadrangle, North Carolina-Tennessee; a preliminary report: Washington, D.C., U.S. Geological Survey, U.S. Geological Survey Bulletin 1121-D. https://pubs.er.usgs.gov/publication/b1121D

-, 1966, Formation of phyllonites in the Grandfather Mountain area, northwestern North Carolina: Washington, D.C., U.S. Geological Survey, Geological Survey Research 1966, D114-D150 p.

Bryant, B., and Reed, J. C., Jr., 1970, Geology of the Grandfather Mountain window and vicinity, North Carolina and Tennessee: Washington, D.C., U. S. Geological Survey Professional Paper 615, 190 p. https://ngmdb.usgs.gov/Prodesc/proddesc_4943.htm

Casale, G., Levine, J. S. F., Craig, T. D., and Stewart, C., 2017, Timing and deformation conditions of the Tallulah Falls dome, NE Georgia: Implications for the Alleghanian orogeny: Geological Society of America Bulletin, v. 129, no. 9-10, p. 1195-1208. 10.1130/B31595.1

Hatcher, R. D., Jr., Merschat, A. J., and Raymond, L. A., 2006, Geotraverse; geology of northeastern Tennessee and the Grandfather Mountain region, in Labotka, T. C., and Hatcher, R. D., eds., Geological Society of America 2006 Southeastern Section meeting field trip guidebook: Boulder, CO, Geological Society of America, p. 129-184. http://www.geoscienceworld.org/cgi/georef/georef;2006072751

Hoff, J. L., 1982, The petrography of the Blowing Rock Gneiss, Grandfather Mountain window, North Carolina [M.S. thesis]: Duke University, 196 p.

Keith, A., 1903, Description of the Cranberry quadrangle, North Carolina-Tennessee: Washington, D.C., U.S. Geological Survey Geologic Atlas, Folio 90, 9 p. https://pubs.er.usgs.gov/publication/gf90

McDermitt, H., and Bobyarchick, A. R., 2011, A comparison of the structural sequences between Blowing Rock Gneiss and late Proterozoic mafic intrusions in the Grandfather Mountain Window: Geological Society of America Abstracts with Programs, v. 43, no. 2, p. 10.

Reed, J. C., Jr., 1964, Geology of the Linville Falls quadrangle, North Carolina: Washington, D.D., U.S. Geological Survey, U.S. Geological Survey Bulletin 1161-B, 53 p. https://pubs.er.usgs.gov/publication/b1161B

Wilson, C. G., Raymond, L. A., and Love, A. B., 2008, Structures and deformation inside the Grandfather Mountain window: the northern Goldmine Branch fault: Geological Society of America Abstracts with Programs, v. 40, no. 4, p. 11.

Vorticity and Kinematic Indicators in the Blowing Rock Gneiss in the Grandfather Mountain window, North Carolina Blue Ridge

Andy R. Bobyarchick

Department of Geography and Earth Sciences, UNC Charlotte, 9201 University City Blvd., Charlotte, NC 28223

ABSTRACT

Blowing Rock gneiss in the eastern Blue Ridge of North Carolina and inside the Grandfather Mountain window is in part a megacrystic orthogneiss of quartz monzonite composition. It is commonly an augen gneiss, and where strongly deformed provides a remarkable array of vorticity and kinematic indicators. In addition to rotated rigid porphyroclasts, these rocks have shear bands, asymmetric layer boudinage, fold asymmetries, and stretching lineations that dictate a finite sinistral sense of vorticity, top to the north if the mylonitic schistosity is considered a flow plane approximately.

Kinematic analyses using porphyroclast shape factors and dimensional orientations give a kinematic vorticity number of ~0.8. This is consistent with sub-simple shearing where the deformation involved pure and simple shear components. Other kinematic structures are also compatible with this vorticity especially where strain is partitioned into ductile shear zones, shear bands, and rotated porphyroclasts with recrystallized mantles.

A complicating factor in the Bailey Creek section is that many of the porphyroclasts are domino types where the larger particles have segmented along mineral cleavage. In effect, when treated as a single clast, the dominoes produce aspect ratios that are very high. The domino effect also assists the porphyroclast in rotated to be nearly parallel to an enclosing schistosity. As dominoes evolve, their cleavage fragments spawn neoporphyroclasts that when grouped with progenitors could result in kinematic vorticity numbers lower than exist.

The ages of deformation to produce these augen gneisses is not well known. There are at least two periods of pervasive deformation and metamorphism, the latter focused on ductile shear zones of variable dimension.

INTRODUCTION

Shear sense and vorticity indicators are valuable tools in determining local regional flow in rock masses where standard displacement indicators are absent or equivocal. Kinematic structures imply at least a sense of displacement if not magnitude. These structures also may be imprecise in the analysis of finite displacement as they may be strongly influenced by late stage deformation and strain partitioning. Nonetheless, shear sense and vorticity indicators are tools commonly used by structural geologists.

Rotated rigid feldspar porphyroclasts and mantle asymmetries around semi-rigid porphyroclasts are commonly used vorticity gauges in deformed coarse-grained crystalline rocks such as augen gneiss. Few such tectonites involve pristine, textbook-quality rotated porphyroclasts. Often lesser or undeformed reference protoliths are not available for comparison. Some tectonites are the products of multiple, superposed deformations. In that case, vorticity estimates may be the cumulative result of unrelated flow regimes. Superposed deformations may be inhomogeneous, partitioned, and occur at different peak metamorphic conditions. Another phenomenon that subjugates established vorticity analyses is porphyroclast spawning (Bobyarchick, 2014a, b). This occurs when larger original feldspar porphyroclasts separate into cleavage fragments during the parent grain's rotation in a flow field. The neo-porphyroclasts reset grain rotation histories because their shape preferred orientations depart from that of the progenitor grain. Mixed populations of porphyroclasts in augen gneiss may therefore present overlapping rotation histories. The result, even though the clast population experienced the same vorticity field, can be an incorrect kinematic vorticity number.

This paper examines the geometry of feldspar porphyroclasts in augen gneiss of the Blowing Rock Gneiss within the Grandfather Mountain window in the Blue Ridge of North Carolina (Bobyarchick, 2006, 2012, 2014a, b). Augen gneiss in the study area is differentially mylonitic, ranging from augen gneiss to fine-grained, strongly foliated mylonite in ductile shear zones. Porphyroclasts in the gneiss range in character from euhedral or subhedral single crystals to strings of neo-porphyroclasts in mylonite gneiss to

flaser lenses in mylonite. In addition to porphyroclasts in these rocks, shear sense indicators include shear bands, asymmetric folds, and asymmetric foliation or layer boudinage (Bobyarchick, 2011). If it can be confirmed that there is a continuous (or periodic) evolution of porphyroclast spawning within the same flow regime that generated all of these indicators, then observations should agree with theory that vorticity (kinematic vorticity number) is in part locked to porphyroclast size fractions.

REGIONAL GEOLOGY

The study area will be referred to as "Bailey Camp" for a named intersection near the section (Fig. 1). The area is within the Grandfather Mountain window (GMW) in the eastern Blue Ridge Mountains of North Carolina. Bryant and Reed (1970) produced the seminal geological summary of the GMW area. Subsequent works refined relationships within and around the window (Adams and Su, 1996; Bobyarchick, 1983, 1984; Boyer, 1978; Boyer and Elliott, 1982; Boyer et al., 1982; Butler et al., 1987; Carrigan et al., 2003;

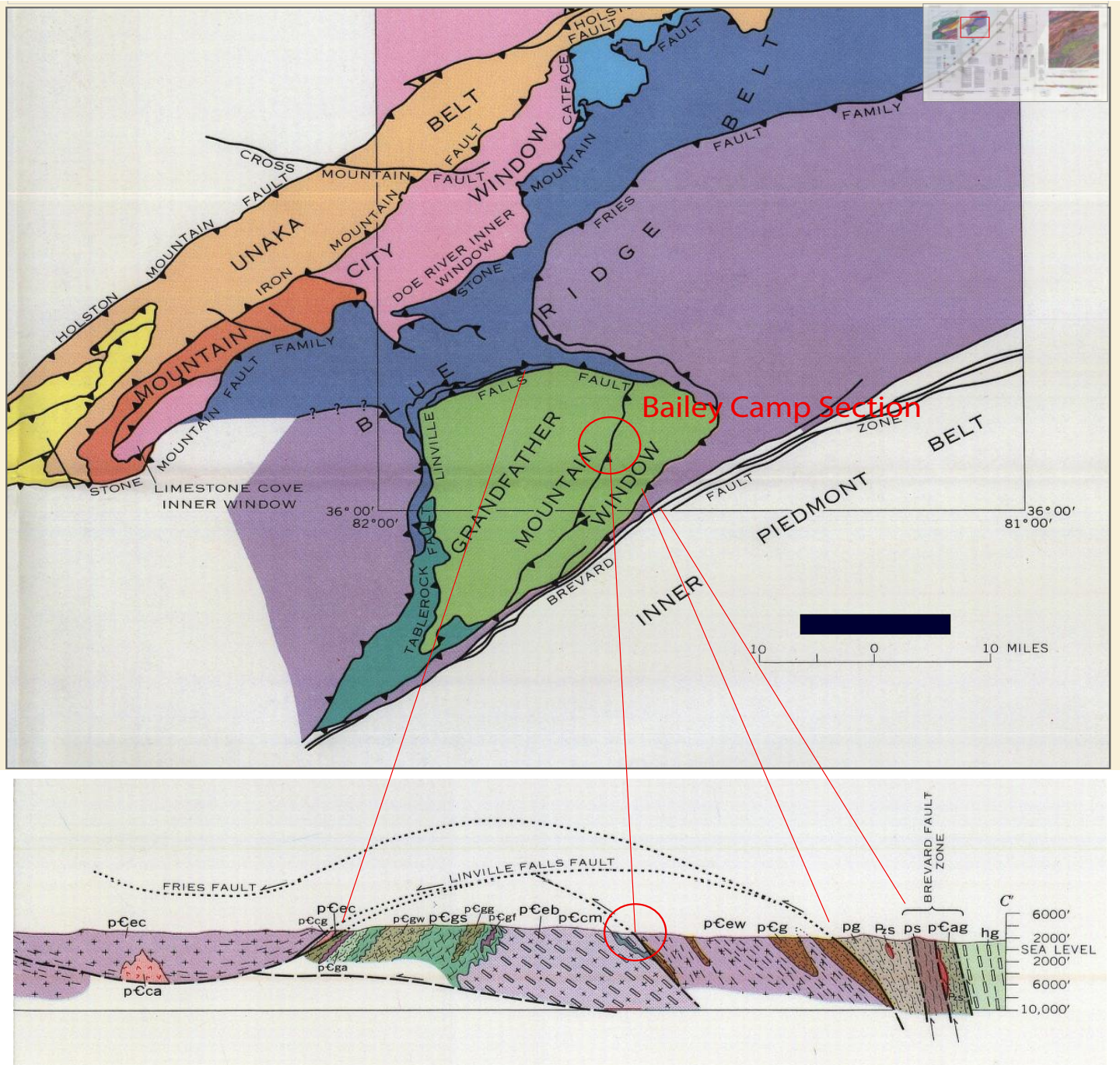

Figure 1. Location of Bailey Camp section on tectonic map and cross-section. Base figures from (Rankin et al., 1972).

Fetter and Goldberg, 1995; Goldberg and Dallmeyer, 1997; Hatcher Jr et al., 2006; Hatcher, 2001; Hatcher et al., 1988; Keith, 1903; McGill et al., 1980; Rankin, 1975; Rankin et al., 1973; Raymond and Abbott, 1997; Raymond and Love, 2006; Schwab, 1977; Stewart et al., 1997a; Szymanski and Christensen, 1993; Trupe et al., 2002; Trupe et al., 2004; Wagener and McHone, 1982) but the fundamental mapping and structural relationships established by Bryant and Reed are still reliable.

The bounding structure and roof thrust of the GMW is the Linville Falls fault (Fig. 1), one of a stack of Appalachian thrusts responsible for imbrication of the Alleghanian infrastructure in the central and Southern mountains. The Brevard fault zone, an orogen-parallel shear zone that extends from Virginia to Alabama, is either the root of or a splay from the Linville Falls fault (Bobyarchick, 1998, 1999; Hatcher, 2001). The latest contractional fault in the Brevard fault zone is the Rosman fault (Edelman et al., 1987; Hatcher et al., 2017; Horton and Butler, 1986), but the general style of deformation in the Rosman fault appears to be more consistent with faults in the western Blue Ridge and Valley and Ridge and possibly younger, discrete Alleghanian faults rarely exposed in the central and eastern Blue Ridge, and within the Piedmont to the east. Though sharply defined on maps, the Linville Falls fault actually lays within a thick shear zone in which cataclastic deformation is superposed on ductile mylonites (Boyer, 1976, 1978; Boyer and Elliott, 1982; Trupe, 1997; Trupe et al., 1990; Trupe et al., 2004). Although it is possible that bulk cataclastic deformation in such fault zones comes from older ductile shear zones acting as stress guides for systemically younger, higher level faulting, given general timing relationships in the Alleghanian orogeny it's more logical that the change in rheology results from surface-ward migration of active faults or an increase in strain rate, or both in a progressive orogenic event. In the central Appalachian foreland, sequences of deformation features suggest that the Alleghanian orogeny comprised a Pennsylvania Lackawanna Phase (the consequence of transpression) and a Permian Main Phase (the consequence of orogen normal convergence) (Geiser and Engelder, 1983).

In the GMW area Bryant and Reed in successive interpretations (Bryant and Reed, 1962, 1969; Bryant and Reed, 1970; Reed and Bryant, 1964; Reed et al., 1970) attempted to reconcile strike-slip motion in the Brevard fault zone (Reed and Bryant, 1964) with contemporaneous thrusting in the Blue Ridge by conceptual models that either required dextral strike slip in the Brevard fault zone to succeed thrusting in the Blue Ridge, or that involved sinistral transpression in the Brevard fault zone driving thrust sheets, including the Linville Falls fault, westward. Later kinematic studies in the Brevard fault zone in North and South Carolina determined that internal vorticity indicators suggest dextral sub-simple shearing in the pre-Rosman fault Alleghanian event (Bobyarchick, 1984; Edelman et al., 1987; Evans and Mosher, 1986; Goldstein et al., 1988; Liu, 1991; Ohlschlager et al., 2008; Tu et al., 2008) although Schwerdtner's (1998) kinematic analysis using tangential shear strain was somewhat equivocal.

Structural research and mapping in high grade terranes of the western Piedmont in North Carolina show that during Neoacadian orogeny (Late Devonian to Mississippian) flow paths (inferred from mineral stretching lineations, curvilinear fold axes, and other data) operated in a sub-simple vorticity field, but kinematic trajectories migrated from a more northwesterly orogen-normal path toward a southwesterly direction in the Brevard fault zone (Davis et al., 1989; Davis and Yanagihara, 1993; Merschat et al., 2005; Vauchez, 1987; Vauchez and Brunel, 1988). This pattern in the kinematics picture led to an interpretation of Neoacadian crustal flow with transport of the Inner Piedmont rocks to the southwest against a rigid buttress in the (Neoacadian) Brevard fault zone footwall (Merschat et al., 2005). Alternatively, spatial variations in kinematic vorticity and strain analysis suggest deformation more consistent with simple dextral transpression and strain partitioning is possible (Ohlschlager et al., 2008). It is implicit here that Alleghanian distributed deformation in the Brevard fault zone and subsequent displacement by the Rosman fault was insufficient to profoundly modify Neoacadian kinematic indicators. In the core of the Brevard fault zone where Alleghanian deformation and retrograde metamorphism are intense, kinematic fabrics are strongly dominated by shear bands, asymmetric boudinage, and stretching lineations that all indicate dextral sub-simple vorticity and that are consistent with dextral transpression (Bobyarchick, 1983, 1984, 2006, 2013; Edelman et al., 1987; Vauchez, 1987).

With reference to the Brevard fault zone, or at least to the Rosman fault, the present eastern Blue Ridge including the GMW are in the footwall of that fault zone. Bryant and Reed (1970) showed that systematic variations in mineral stretching lineations, which they treated more or less as transport directions, could be related to strain around the Linville Falls fault. Bryant

and Reed also pointed out the widespread overprinting tectonite fabrics within a thin sliver of the Blue Ridge thrust sheet and the Brevard fault zone and within Mesoproterozoic basement bodies in the GMW.

Considerable field research since the work of Bryant and Reed focused on the eastern Blue Ridge thrust sheets and their structural relationships to the western Blue Ridge and possible continuity along strike over the GMW (Adams, 2000; Adams and Trupe, 2004; Bartholomew, 1983; Boyer, 1992; Butler et al., 1993; Corrie and Kohn, 2007; Goldberg et al., 1992; Goldberg and Dallmeyer, 1997; Harris et al., 1981; Hatcher and Goldberg, 1991; Hatcher, 2001; Merschat et al., 2017; Miller et al., 2006; O'Hara, 1990; Raymond et al., 1989; Stewart et al., 1997b; Trupe, 1997; Trupe et al., 2004).

Trupe et al. (2004) designate five thrust sheets stacked above the GMW with mostly Alleghanian thrusts separating the sheets. From the top of the stack downward, these sheets are: (1) the composite Fries thrust sheet (Late Proterozoic cover with basement rocks only near the base in the Fork Ridge thrust sheet, and within and beneath the Devonian Burnsville-Gossan Lead fault west of the GMW; high-grade Taconic metamorphism), (2) the Sams Gap-Pigeonroost thrust sheet (Middle to Late Proterozoic mixed gneiss intruded by bodies of the Late Proterozoic mafic Bakersville Intrusive Suite; basal thrust splays from the Fries fault), (3) the Fork Ridge thrust sheet (hanging wall of the Linville Falls fault west of the GMW; Cranberry Mine basement gneiss intruded by Late Proterozoic Beech-Crossnore and Bakersville bodies), (4) the Linville Falls thrust sheet (roof thrust of the GMW; contains Mesoproterozoic Watauga gneiss and other metamorphic rocks invaded by Neoproterozoic granite and Bakersville intrusives), and (5) the Little Pond thrust sheet (Mesoproterozoic gneiss, intruded by Bakersville dikes, and unconformably overlain by Lower Cambrian Chilhowee Group sedimentary rocks; weakly affected by Paleozoic metamorphism and preserved Grenville and Neoproterozoic igneous textures). Generally, the Paleozoic metamorphic grade (and overprint on Grenville rocks) decreases down the structural section because of inversion in the thrust stack. Alleghanian basal thrusts on all thrust sheets are embedded in mylonite zones of variable thickness and characterized by greenschist metamorphism. All major faults northwest of the Burnsville fault are demonstrably no older than Alleghanian, whereas the Burnsville-Gossan Lead fault is a Devonian (Acadian) dextral strike-slip fault interpreted by Trupe et al. (2004) to have been transported in the Fries thrust sheet.

The Ashe Metamorphic Suite and other rocks now in the Fries thrust sheet and presumably parts of the Neoproterozoic to Early Ordovician Laurentian margin in upper parts of the thrust stack were metamorphosed to amphibolite or granulite facies during the Taconic orogeny. Trupe et al. (2004) note that the Burnsville fault was active under amphibolite facies conditions between 360 and 377 Ma. Dates of intrusions and structural sequences in the Blue Ridge thrust sheet support widespread effects of an Acadian or Neoacadian dynamothermal event in the eastern Blue Ridge (Corrie and Kohn, 2007; Hamil et al., 2009; Kunk et al., 2006; Miller et al., 2006) . It is compelling to draw comparisons between Neoacadian features in the eastern Blue Ridge and Inner Piedmont across the Brevard fault zone. Trupe et al. (2004) document retrogressive greenschist facies metamorphism in the bounding thrusts of the Blue Ridge that overprints Taconic (and where present Grenville) structures, and more pervasive greenschist metamorphic effects in the Fork Ridge and Linville Falls thrust sheets that they attribute to movement of the Fries thrust sheet over them. It also now appears that Alleghanian magmatic activity, pervasive ductile deformation, and metamorphism may have been more widely distributed than previously thought (Merschat et al., 2017; Miller et al., 2006).

SECTIONAL GEOLOGY

The Bailey Camp section (Fig. 1) is beneath the Linville Falls thrust fault and is therefore totally detached from rocks in the (upper) Blue Ridge thrust sheet. Boyer and Elliott (1982) combined along-strike orogen-normal seismic profiles (Cook et al., 1979; Cook et al., 1981; Harris and Bayer, 1979; Harris et al., 1981; Harris and Milici, 1977), down-plunge projections, cleavage and metamorphism relationships, and imagination to construct a cross-section, forward model, and palinspastic reconstruction for the GMW. They viewed the GMW as a folded duplex and connected it with the Mountain City window to the northwest to form the Windows duplex; these structures are above a floor thrust (the Pulaski fault according to seismic projections) that in turn rests on a hidden detachment along which the entire Blue Ridge along with Cambro-Ordovician shelf sequences were transported northwestward during the Alleghanian orogeny. Slices of the shelf, probably Chilhowee Group quartzites, appear as horses in the Linville Falls fault zone all around the GMW including the highly deformed

southeastern section of the window, and other possibly related rocks appear in the Brevard fault zone (Hatcher, 1971; Hatcher et al., 2017). Boyer and Elliott (1982) inferred that cleavage and amphibolite facies metamorphism were active in the southeastern part of the GMW during movement of the Linville Falls fault and, citing Conley (1978, p. 1122) suggested that the "principal" time of movement in the Brevard fault zone and of Blue Ridge thrusts rooted there was Late Devonian. In current conceptions, that would be the Neoacadian Brevard fault zone.

Boyer and Elliott (1982) did not much elaborate on the structural details of the interior of the GMW, except to note floor-to-roof splays in the southeastern half of the window along linear contacts where Bryant and Reed (1970, Plate 1) did not show faults. One of these faults is the Goldmine Branch fault (Wilson et al., 2008) that separates Neoproterozoic Grandfather Mountain Formation rocks from the Blowing Rock gneiss, one of the main Grenville basement rocks inside the GMW. Although it has been speculated that the contact along parts of the boundary could be nonconformable, structural studies show that at its northernmost extent, the boundary is indeed tectonic (Wilson et al., 2008). The second, unnamed thrust is southeast of and parallel to the Goldmine Branch fault so that a linear belt of Blowing Rock gneiss is confined between the two boundaries. The Bailey Camp section is along the unnamed thrust or fault zone. Here the boundary is between Blowing Rock gneiss on the north and another Mesoproterozoic formation to the south called the Wilson Creek gneiss (Bryant and Reed, 1970; Wagener, 1979).

Blowing Rock Gneiss

The Blowing Rock gneiss (Bryant and Reed, 1970; Keith, 1903) is megacrystic augen gneiss with large white or pink potassium feldspar in a matrix of biotite and quartz (Figs, 2, 3). Bryant and Reed (1970) determined that the gneiss is geochemically quartz monzonite with somewhat more felsic variations. They noted that the Blowing Rock gneiss is widely porphyroclastic and locally mylonitic or phyllonitic. Isotope ages for the Blowing Rock gneiss are 1,055 Ma (Davis et al., 1962), 1,027 Ma (Fullagar and Odom, 1973), and 1,080 Ma (Carrigan et al., 2003). Carrigan et al. (2003) collected ion microprobe U-Pb zircon analyses from several basement formations. (Samples from the eastern Blue Ridge included Toxaway, Wiley, and Sutton Creek gneisses.) Their data set included a magmatic pulse in the range 1,165-1,150 Ma, and most of those zircons had metamorphic rims dating to about 1,030 Ma. Blowing Rock gneiss samples did not have the metamorphic rims, but some of those samples had inherited zircon cores with a mean age of about 1,140 Ma. These are interesting results that have potential structural significance. If the Blowing Rock gneiss protolith were a syn-tectonic intrusion, the pre-Paleozoic deformational textures in the rock would be different, possibly simpler, from an early- or pre-tec-

Figure 2. Northern end of main Bailey Camp section. Dark layers are metadiabase dikes. Main rock mass is Blowing Rock augen gneiss. The dike's compositional boundaries truncate schistosity in gneiss at a low angle. These dikes are thought to be closely folded in the section.

Figure 3. Blowing Rock augen gneiss in Bailey Camp section. This is a moderately deformed part of the section and is an exposure of the VPP viewed toward East. Note that most porphyroclasts are dominoes with sinistral shear sense. (Between cleavage fragments the shear sense is antithetic.) Many sinistral sigma porphyroclasts are visible. The dark matrix is quartz-chlorite-sericite-biotite.

tonic Grenville basement rock. Various observers have noted how, for example inside the GMW, much less layered the Blowing Rock gneiss appears when compared to layered phases of the Wilson Creek gneiss. Carrigan et al. (2003) further observed that some of their eastern Blue Ridge zircon samples had 350 Ma metamorphic rims. That age is consistent with magmatic and metamorphic ages elsewhere in the eastern Blue Ridge.

Wilson Creek Gneiss

The second major basement unit in the section is Wilson Creek gneiss (Bryant and Reed, 1970). It is much more heterogeneous than Blowing Rock gneiss. Wilson Creek gneiss is mainly a massive, though strongly foliated metamorphosed quartz monzonite also containing granite and diorite. Bryant and Reed (1970) describe many parts of the Wilson Creek gneiss as having a cataclastic texture; this is because of porphyroclastic potassium feldspar grains and stretched quartz-feldspar-sericite folia. They also note that plagioclase enriched parts of the gneiss tend to be well foliated because of metamorphic alteration and recrystallization of this feldspar to albite, sericite, and epidote. A secondary phase of the Wilson Creek gneiss is layered. Most exposures of granular gneiss are porphyroclastic to some degree. Bryant and Reed (1970) describe numerous ductile shear zones containing mylonite and phyllonite. Some of these shear zones occur at contacts with Blowing Rock gneiss. Isotope ages for Wilson Creek gneiss are 640-1,000 Ma (Davis et al., 1962), and 1,135 Ma (Rb-Sr model age, Fullagar and Odom, 1973). Wagener (1979) thought that layered phases of the Wilson Creek gneiss are metamorphosed sedimentary and volcanic rocks correlative with the Grandfather Mountain Formation that are unconformable on the Grenville plutonic phase of Wilson Creek gneiss. He also thought that the Blowing Rock gneiss is a porphyroblastic meta-siltstone and a facies of Wilson Creek paragneiss.

Greenstone and Chlorite Schist

The third significant rock unit in the study area is a set of tabular greenstone bodies that are inferred to be metamorphosed diabase dikes (Fig. 2). These are part of the Linville Metadiabase (Bryant and Reed, 1970; Keith, 1903). Larger bodies of Linville Metadiabase are mostly in the Blowing Rock gneiss and Wilson Creek gneiss near contacts with the Grandfather Mountain Formation, but dikes also occur within the cover rocks. Recent road excavations farther down the Blue Ridge escarpment from the Bailey Camp area reveal several large bodies of metadiabase as well. Keith (1903) and Bryant and Reed (1970) both linked Linville Metadiabase to the basaltic Montezuma Member of the Grandfather Mountain Formation, possibly as feeder dikes. Depending on location, the metadiabase contains actinolite, biotite, chlorite, albitized plagioclase, and abundant sulfide minerals. Composition and relative age relationships suggest a comparison and correlation between the Linville Metadiabase inside the GMW with mafic rocks of the Bakersville Intrusive Suite in Blue Ridge rocks above the Linville Falls fault as part of the Neoproterozoic rifting event in Laurentia. One U-Pb determination, however, produced an Early Silurian age of about 422 Ma for Linville Metadiabase (Fetter and Goldberg, 1993) although Sm-Nd data for those rocks showed that they could have been derived from the same source region as Neoproterozoic mafic rocks in the area. Should that Silurian age be reliable, the Paleozoic metamorphic and deformation of basement rocks in the GMW would have to be Devonian or later.

Bailey Camp Area

The section is centered on a series of road cuts on Highway 321 about 4 km south of Blowing Rock, NC and then extending NE and SW to follow the contact between Blowing Rock gneiss and Wilson Creek gneiss (Fig. 1). A series of three long cuts is about 1 km long and one of the cuts is 100% exposure over about 0.5 km. The site is in the northeast corner of the USGS Globe 7.5' topographic quadrangle; along strike extension covers corners of the Buffalo Cove, Deep Gap, and Boone quadrangles. Bryant (1963) mapped this area as part of the Blowing Rock 15' sheet, and it later became part of the Bryant and Reed (1970) compilation. Wagener (Wagener, 1979; Wagener and McHone, 1982) conducted sampling traverses through the area on the old route of Highway 321 and elsewhere in the GMW area. Most work in the GMW has focused on specific topics: Blue Ridge thrust sheets above the Linville Falls fault, the Linville Falls fault as part of the Alleghanian imbrication of the Blue Ridge, sedimentology and stratigraphy of the Grandfather Mountain Formation, structure of the Brevard fault zone, mineral resources in the Spruce Pine district and elsewhere, formation of the Grandfather Mountain window, and geomorphology.

Bryant and Reed (1970) wrote detailed petrographic descriptions of the major rock types in the area. Efforts to investigate the Bailey Camp outcrops focus

on structural geology (Bobyarchick, 2011, 2012, 2013, 2014a, b; Bobyarchick and McDermitt, 2011; McDermitt and Bobyarchick, 2011).

The Blowing Rock gneiss at Bailey Camp is characteristic porphyroclastic augen gneiss though there are variations in strain intensity spatially. It is massive with little banding and maintains a remarkably uniform attitude dipping moderately to the southeast over most of the outcrop width. The main foliation is defined by biotite and flattened and stretched feldspar porphyroclasts. Some porphyroclasts are quartz-feldspar aggregates that are dismembered veins. Few folds of the foliation are visible, but felsic veins and granitic bodies in the gneiss are tightly or isoclinally folded with the main gneissic foliation being axial planar to these folds. In places the gneiss is chloritized, and this alteration increases near ductile shear zones (Bryant, 1966). Those shear zones feature extreme flattening of feldspar augen into flaser gneiss and those have a banded appearance in comparison with the rest of the Blowing Rock gneiss. Mylonites in these shear zones contain abundant sericite as well as chlorite and relict biotite. Shear zones and the general intensity of foliation increase to the south upon approaching the Wilson Creek contact. Blowing Rock gneiss is also transformed into phyllonite near contacts with some metadiabase dikes; some of the dike margins are also sheared. Potassium feldspar porphyroclasts display a range of structures. Many are nearly euhedral. Most have rims of quartz and sigma, delta, and domino porphyroclasts are widespread.

Trends of the road cuts are very close to parallel to a stretching lineation in the Blowing Rock gneiss. This is fortuitous because it provides a vorticity-parallel plane (VPP) for vorticity analysis, but on the other hand planar and linear structures on this viewing plane may appear deceptively simple. For example, many metadiabase dikes are concordant with or slightly discordant to schistosity in the augen gneiss. Along the roadcut, the dikes are parallel and seemingly undeformed, yet internally most dikes have slaty or phyllitic cleavage and often a crenulation cleavage. In sections of the exposure at high angles to the roadway, the dikes are much more irregular in orientation as are their contacts with Blowing Rock gneiss. This is an expected relationship given the orientation of the foliation plane and stretching lineation. A few of the dikes contain slim veins that are isoclinally folded into the cleavage. All of the Blowing Rock gneiss and metadiabase dikes here contain abundant metallic sulfide minerals. The gneiss contains two to four generations of foliated and non-foliated pegmatite, feldspar, quartz, and calcite veins. Close to the Wilson Creek gneiss contact, calc-silicate boudinaged layers are present, and so are larger calcitic veins. Carbonate minerals – calcite and dolomitized calcite – are common in Blowing Rock gneiss both in the matrix and as foliation-parallel veins.

The Wilson Creek gneiss in the southern end of these exposures is mostly a light colored medium to coarse grained, massive, strongly foliated granitic gneiss. A coarse-grained orthogneiss within the Wilson Creek gneiss is also present (Bryant and Reed, 1970).

Immediately at the contact with Blowing Rock gneiss the Wilson Creek gneiss is light colored, strongly banded and complexly folded. These gneisses contain much less biotite than Blowing Rock gneiss and do not have augen except where coarse pegmatite veins were deformed. There are also mafic dikes that intrude the Wilson Creek gneiss, but these dikes have less chlorite than those in the Blowing Rock gneiss to the north, and they are more crystalline. A very fine-grained meta-andesite occupies the contact between Blowing Rock and Wilson Creek gneisses.

VORTICITY AND KINEMATIC ANALYSIS

Field structural analysis is a form of backward modeling where the observer collects information to predict future history. In the case of vorticity, certain measurable finite structures allow one to look back along flow paths for local particle motions, and then to apply kinematic and rheological functions to recreate those structures. Vorticity analysis potentially recreates local particle flows, but most field studies have a higher goal to fit those local results into a bigger picture. Thus, stretching lineations become transport directions, and shear bands become transpression. Most vorticity measurement tools depend on one or more of the following conditions:

1. Asymmetry is desirable.

2. A material continuum is nice, but flow partitioning through rheological heterogeneity is helpful.

3. Incomplete recrystallization is better than full recovery.

4. Steady state flow dominates the flow history; run-up and –down strain rates (or their material effects) are negligible.

5. Much simple shear isn't, but the simple part still fits into the bigger picture.

A comprehensive review of vorticity analysis is by Xypolias (2010). All critical and foundational literature references are cited and discussed there and in related publications (Forte and Bailey, 2007; Fossen and Cavalcante, 2017; Gomez-Rivas et al., 2007; Grasemann et al., 2003; Holcombe and Little, 2001; Jessup et al., 2007; Johnson et al., 2009; Passchier, 1987a; Passchier and Urai, 1988; Piazolo et al., 2002; Simpson and DePaor, 1993; Stahr and Law, 2014; Tikoff and Fossen, 1995; Wallis, 1995). Ultimately, the objective of vorticity analysis is to gain a numerical expression for the degree of non-coaxiality in flow as dictated by the geometries of finite structures sensitive to flow paths in a deforming medium, or by physical changes in the deforming medium's rheology during flow. Rotating porphyroclasts, for example, express vorticity because of rigidity contrasts with a flowing matrix. Certain shear bands may reflect meso-scale strain partitioning of flow as a consequence of fluctuations in stress and temperature or changes in strain rate. Ordinal estimations of non-coaxiality denote shear sense. The degree of non-coaxiality can be expressed through decomposition of a velocity gradient tensor $\boldsymbol{L}$ into its symmetrical stretching tensor $\boldsymbol{D}$ and an asymmetric vorticity tensor $\boldsymbol{W}$:

$$\boldsymbol{L}=\boldsymbol{D}+\boldsymbol{W}$$

$\boldsymbol{W}$ is anchored to a local or material defined reference frame and is insensitive to external spin. In practical application, $\boldsymbol{W}$ is a vector w orthogonal to the instantaneous flow plane VPP (Robin and Cruden, 1994) or analysis plane. Flow may be monoclinic or triclinic depending on whether w parallels one of three instantaneous stretching axes or not. The kinematic vorticity number $\boldsymbol{W_k}$ (Means et al., 1980) is a scalar defined by the magnitudes of the three principal stretching rates in a stretching tensor where in monoclinic symmetry $W_k = 0$ is pure coaxial flow and $W_k = 1$ is simple shearing (DePaor, 1983). Values between 0 and 1 are sub-simple shearing, and those above 1 are super-simple shearing. Monoclinic flow simplifies to the sectional kinematic vorticity number $\boldsymbol{W_n}$ where:

$$W_n=w/2s_n$$

and $\boldsymbol{w}$ is vorticity vector magnitude, and $\boldsymbol{s_n}$ is the mean stretching rate.

Xypolias (2010) outlined the range of particle flow paths or streamlines that are induced by different vorticity regimes. In the VPP, the two dimensional shapes of streamline fields are dependent on vorticity number and area change (Passchier, 1987b), and can be of one of the following forms: hyperbolic, parallel, elliptical/circular, or radial. Hyperbolic flow fields ($W_k < 1$) are unique because flow lines converge on or diverge from one of two flow apophyses that in material space are lines of non-rotating particles. In shear zones, one of the irrotational apophyses is parallel to the shear zone boundary. In finite strain, the position gradient tensor $\boldsymbol{F}$ (t = time)

$$F=exp(L_t)$$

tracks particle positions in time and is therefore an expression of strain rate. $\boldsymbol{F}$ is thus a utility for vorticity analytical methods based on particle positions and rotations (Xypolias, 2010, p. 2077). These relationships are to a degree dependent on deformation in a steady-state environment. Vorticity spin-down especially in the declining period of a deformation event may modify the extrapolation of vorticity markers to finite strain.

Xypolias (2010) lists some cautionary information about applied vorticity analysis conducted in two dimensions on the VPP. First, shear zones that depart from monoclinic symmetry may not be accurately measured with these techniques because the VPP may not coincide with the flow plane. Second, non-plane strain shear zones may have slightly overestimated vorticity numbers (Tikoff and Fossen, 1995). Third, vorticity determinations in heterogeneously layered shear zones or shear zones where strain is otherwise partitioned will have variable kinematic vorticity numbers. This is a disadvantage if one is attempting to estimate the bulk shear of the zone, but if the objective is a determination of heterogeneity created by, for example, superposed non-distributed shear or the effect of post-vorticity indicator folding, then the range in vorticity numbers is a useful qualifying factor.

Kinematic Analysis in the Blowing Rock Gneiss

Numerous kinds of kinematic indicators and potential tools for vorticity analysis are in the Blowing Rock gneiss. General aspects of the augen gneiss and types of clasts are illustrated below (Figs. 3-10). Unless noted otherwise, all outcrop images in this proposal look along the normal to the VPP and to-

Figure 4. Sheared domino porphyroclasts in mylonitic augen gneiss. This outcrop is in a shear zone between the main Bailey Camp section exposure and a smaller northern section. It is one of the areas where shear sense is equivocal. Domino morphology suggests sinistral shear but tails on some porphyroclasts if they are interpreted as sigma porphyroclasts is dextral. The view is looking down the VPP normal direction.

Figure 6. Feldspar and quartz-feldspar porphyroclasts near a deformed quartz vein in Blowing Rock gneiss. Some porphyroclast margins are serrated by quartz-filled wedges along cleavage directions. This is an uncommon feature but it suggests that larger porphyroclasts may have a brittle-ductile (or elastic) internal boundary during deformation. View is looking down the VPP normal.

Figure 5. Internally deformed domino porphyroclasts in mylonitic ("cataclastic") section of Blowing Rock gneiss. Note the waviness of the schistosity as less viscous matrix was displaced by rigid clasts during flow. Some porphyroclasts are also crenulated and have split along wedge fractures filled in by quartz. It is possible that some of these structures are the results of interactions between rigid clasts. View is looking down the VPP normal.

Figure 7. Possible back-rotated porphyroclast. It is very uncommon to find the long axes of porphyroclasts at such a high angle to the flow plane/schistosity. In some shear zones, these orientations are supportive of the pure shear component of deformation. Here it is also possible that this grain is a remnant of a ghost fold (see text) or spawned from a larger porphyroclast, though none is visible in the image. View is looking down the VPP normal.

ward the northeast (Fig. 11). The stretching lineation is in the plane of the images, and foliation dips to the southeast. Shear sense from all kinematic indicators is consistently top to the northwest.

Shear Bands

Shear bands or inclined ductile deformation zones in S-C mylonites (Lister and Snoke, 1984) are present in the Bailey Camp section but care must be exercised in recognizing and measuring these structures. In the classic sense in a ductile shear zone, “S-planes” are finite foliation surfaces (schistosity, for example), “C-planes” are shear planes imposed on S-planes that are parallel to the shear zone, and “C’-planes” are spaced, discontinuous ductile deformation zones inclined at a low angle to C-planes. In practice, when working in pervasively mylonitized shear zones, the predominant foliation is often equivalent to C-planes and shear bands are the discrete planar ductile deformation zones inclined to the foliation. Shear bands

Figure 8. Highly deformed porphyroclasts in micaceous mylonite in Blowing Rock gneiss. Many porphyroclasts have white quartz mantles and are internally cloudy and altered. Few are dominoes. Shear bands in the lower part of the image indicate sinistral shear (top to the left/north) as do some sigma porphyroclasts. View is down the VPP normal.

Figure 9. Ghost fold in augen gneiss. Moderately deformed Blowing Rock gneiss near a granitic gneiss intrusion. Porphyroclast train above hammer head describes a fold in which the schistosity is axial planar. These porphyroclasts and many others in view are quartz-feldspar aggregates. View is down the VPP normal.

Figure 10. Asymmetric layer boudinage of felsic dike in Blowing Rock gneiss. Sharp, angular boundaries on the lateral margins of the boudins suggest a high viscosity contrast between the dike and enclosing augen gneiss at the time of separation. Shear sense is sinistral. Extensions of the dike are tightly to isoclinally folded. View is down the VPP normal.

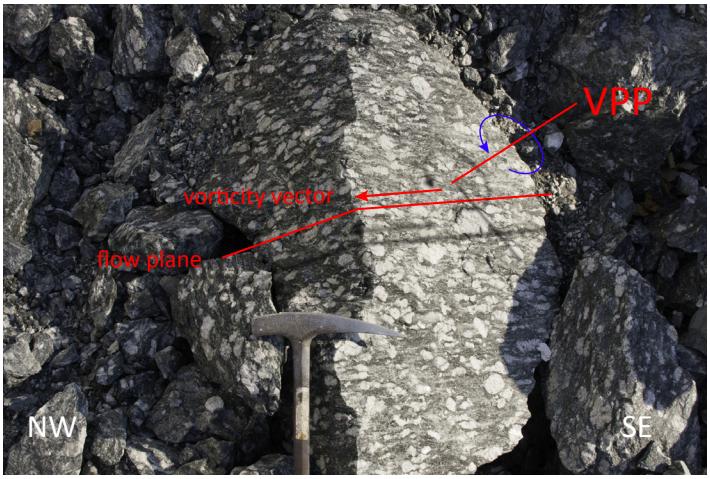

Figure 11. Illustration of vorticity components. VPP – vorticity-parallel plane. This is the surface on which kinematic indicators are observed (in monoclinic flow).

form in zones of sub-simple shearing where there was a component of flattening across the foliation. Geometrically, the down-dip directions of shear bands point in the direction of rotation or shear sense.

Shear bands give a mylonite a wavy appearance because of the displacements of foliation along the bands. In augen gneiss, the rock's schistosity may be wavy because of displacements around rigid porphyroclasts and no shear bands may be present. The tails of sigma porphyroclasts in parts of the Blowing Rock gneiss curve into shear bands defined by ductile deformation zones. There, the shear sense indicated by both structures is consistently sinistral, or top to the north.

In a way, shear bands are a form of asymmetric foliation boudinage (Arslan et al., 2008) where the asymmetries are qualitative indicators of vorticity. In the Bailey Camp section, some quartzofeldspathic or calc-silicate lenses show asymmetric boudinage as well, and those are sinistrally rotated.

Porphyroclasts

Although many feldspar porphyroclasts are tailless, most have complex internal structures and similarly complex mantles. Many porphyroclasts are "dominoes" extended into the mylonitic foliation with predominately sinistral rotations (Figs. 3-6). Some separate porphyroclasts clearly originated as cleavage

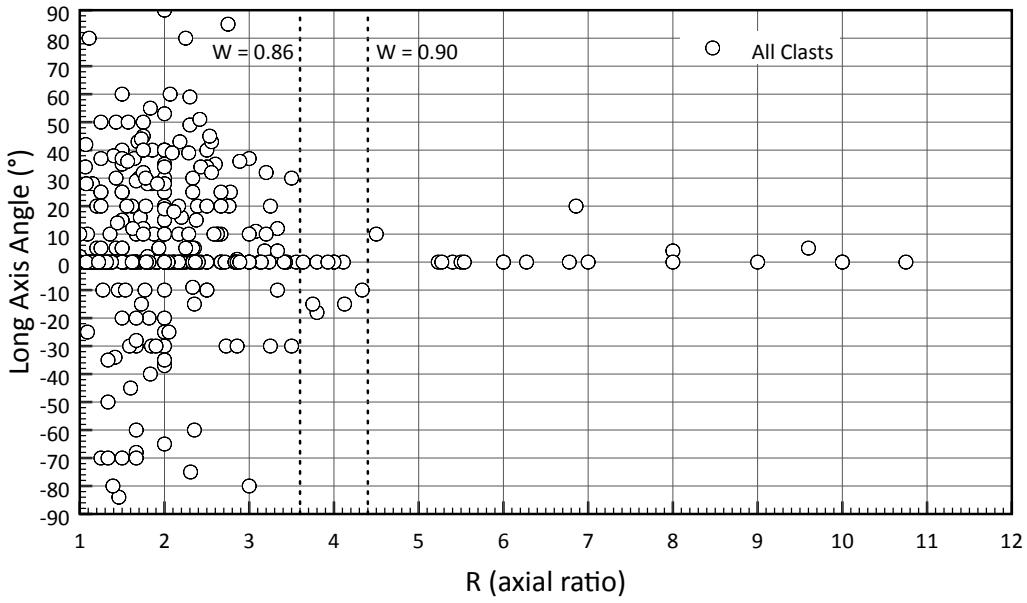

Figure 12. PAR plot of all clasts measured in the Bailey Camp section in Blowing Rock gneiss. Relative to the flow plane (schistosity), a clockwise acute angle between a porphyroclast long axis and the foliation is (+), and a sinistral orientation angle is (-). Representative sectional kinematic vorticity numbers are dashed lines. ***R*** is the ratio between long and short axes of porphyroclasts.

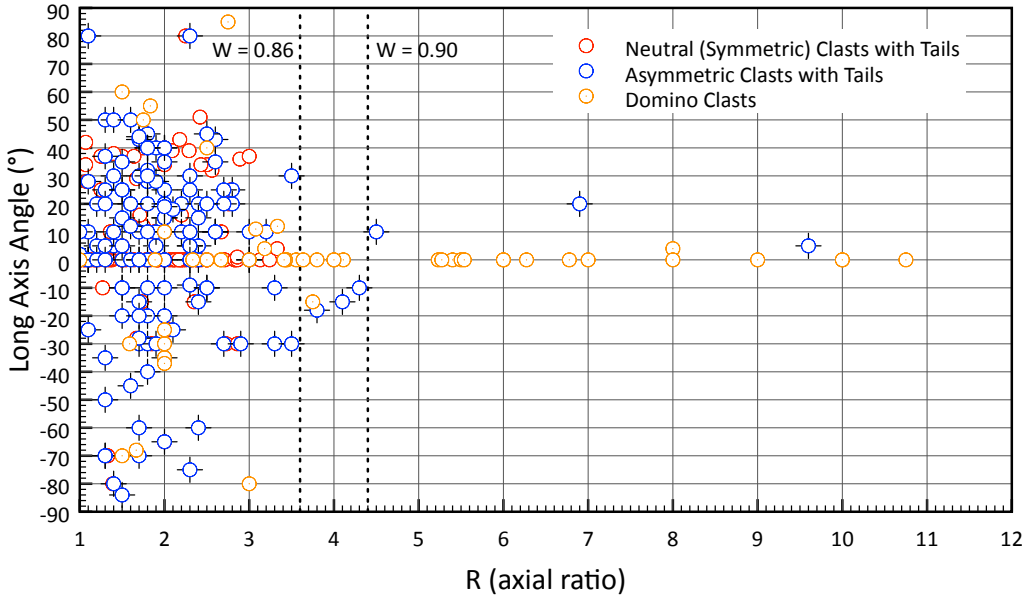

Figure 13. PAR plot of three groups of porphyroclast types. Neutral clasts have recrystallized tails symmetrically parallel to the flow plane. Asymmetric clasts are sigma porphyroclasts. Dominoes are porphyroclasts that have partly or entirely separated along mineral cleavage.

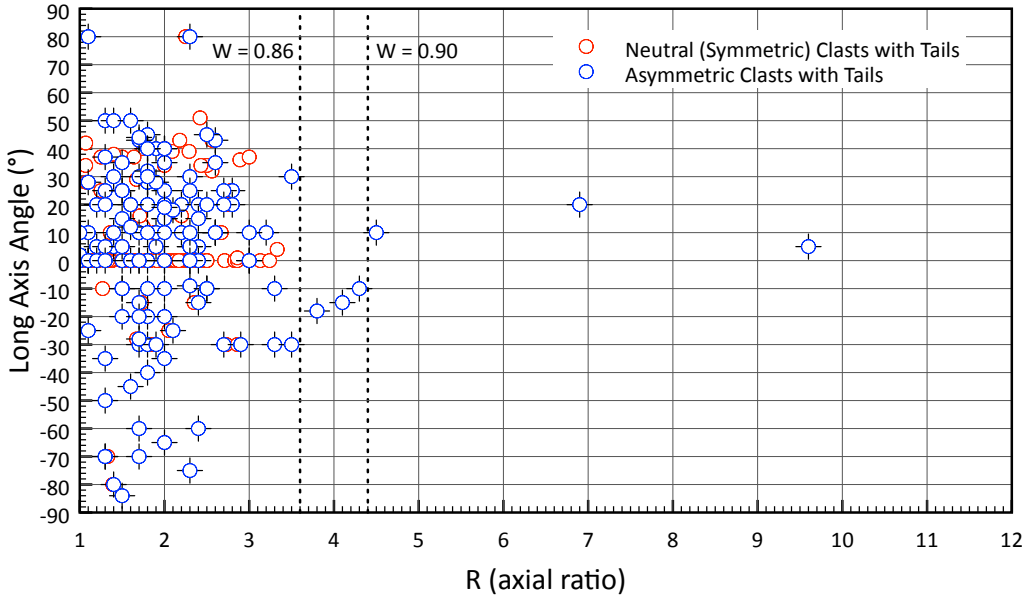

Figure 14. PAR plot without domino porphyroclasts. Strictly, domino porphyroclasts are not perfectly rigid; they have elongated by dilation. This is a plot of all measurements without dominoes. Because domino porphyroclasts typically have high ***R*** values, this plot shows that most clasts fall under ***W***= 0.86.

fragments from disarticulated dominoes. It's possible that the finite structures in these rocks reflect a progressive and evolutionary sequence of rigid rotations, syn-metamorphic intracrystalline slip of cleavage fragments in favorable oriented porphyroclasts, and rotations of these new porphyroclasts relative to the prevalent flow regime or residence in stable orientations (Bobyarchick and McDermitt, 2011). Some domino porphyroclasts appear to have been folded while they were separating because the long clast axes are bent, and quartz mineralization in pressure voids has patterns of a bent accordion (Figs. 4,5).

Feldspar porphyroclasts can be intact (euhedral crystals with minimal internal strain; minimal tail or mantle structures), mantled (sigma or delta tails; neutral or winged tails) or segmented (cleavage fragments with interstitial mineralization; domino structure). There are multiple generations of quartz-feldspar veins in the section. Most are deformed with schistosity. Some of these veins now form ghost folds (Fig. 9). These are trains of quartz-feldspar augen that align in the shape of a tight fold. Planar ghost veins are also present, similarly defined by aligned multiphase porphyroclasts.

In schistosity-parallel mylonite zones all augen types are flattened and stretched into lenticular, discontinuous felsic strips in a quartz-mica matrix (Figs. 4, 5, 8). Domino structure is still evident within porphyroclasts in the shear zones.

Vorticity from Porphyroclasts

Vorticity analyses from porphyroclast orientations and shape factors were collected in several panels across strike in the Blowing Rock gneiss at the Bailey Camp section. The strain intensity visually varies along this traverse.

For the most part, the vorticity vector is normal to cut slope outcrops on this traverse (Fig. 11). Square meter outcrop patches were measured for the following properties: porphyroclast axial ratios, long axis rotation angles relative to foliation, clast mode (sigma, delta, or neutral for clasts with tails; dominoes for fractured clasts), shear sense, and mineralogy. Clast morphologies are not simple, nor is the strain history that created them. Nonetheless, the 500 or so data collected provide considerable justification for further investigation.

Figures 12-14 are summaries of these data. Figure 12 is a simplified porphyroclast aspect ratio (PAR) plot (Passchier, 1987b; Wallis, 1995) where clast aspect ratios $\boldsymbol{R}$ are plotted against an orientation angle

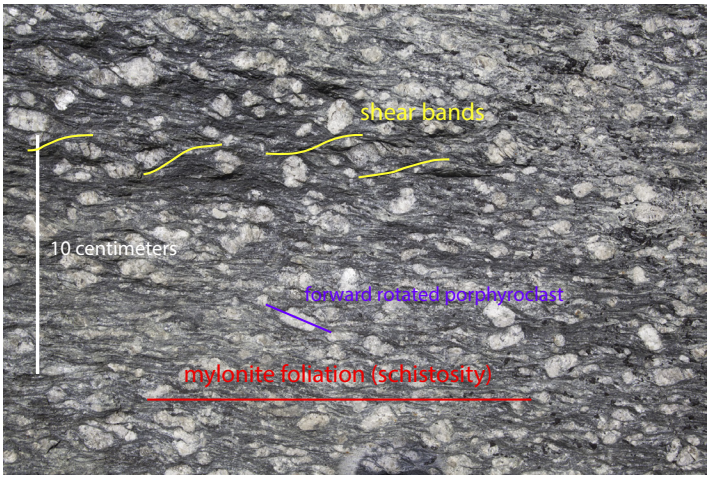

Figure 15. Porphyroclast orientations on VPP in Photo 7352. This is an image of the VPP in a moderately deformed augen gneiss. North is to left and the section is close to vertical. Uncommon shear bands indicate sinistral shear as do domino grains. This image was separately measured for particle orientations and axial ratios.

between the long clast axes and the flow plane (or the foliation reference plane containing the recrystallized tails of porphyroclasts), ostensibly a rotation angle for the clast due to vorticity. All clasts regardless of shape are included on Figure 12. Survey stations spanned a total distance of about 0.2 km across strike in the Bailey Creek section. Figure 13 groups different types of porphyroclasts by type. These are symmetrical clasts with recrystallized tails, asymmetric clasts (sigma porphyroclasts mainly, and domino clasts. Figure 14 omits the domino porphyroclasts because these grains clearly were non-rigid for some part of the deformation. This removes most points with very high $\boldsymbol{R}$-values from the data set. By inspection, a critical value of $\boldsymbol{R}$, $\boldsymbol{R_c}$ is found where the range of clast rotation angles drops into a narrow span. The mean kinematic vorticity number $\boldsymbol{W_m}$ is then calculated as:

$$W_m = (R_c^2 - 1)/(R_c^2 + 1)$$

For this graph (Fig. 14), $\boldsymbol{W_m}$ is about 0.84. In Figure 13 the value is 0.86-0.90. It's possible that differential clustering of forward (sinistral) and back (dextral) rotated porphyroclasts could be distinguished here or on a PHD plot (Simpson and DePaor, 1993), but more consistently sampled data need to be compiled first. Domino porphyroclasts very regularly show sinistral shear in the flow plane.

Measurements were collected from a photograph of a moderately deformed augen gneiss (Fig. 15) and then plotted with the entire data set (Fig. 16). The two data are roughly comparable, although the small data

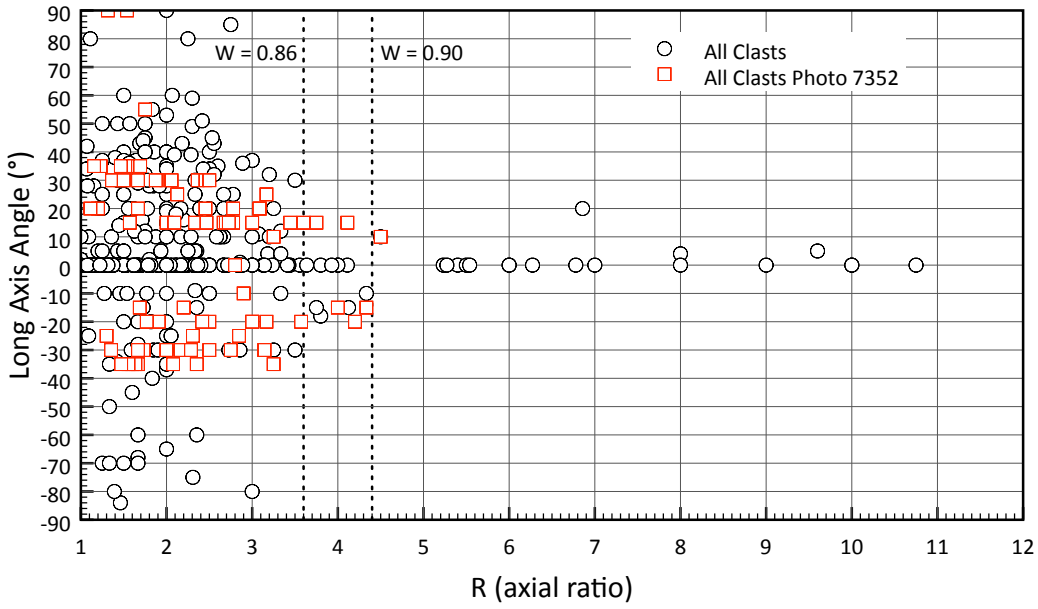

Figure 16. PAR plot comparing all data to data from Photo 7352. The small section data are squares. The small section data are conformable to the larger group but with fewer grains parallel to the foliation and R values below W = 0.90. This is caused by the general minority of domino porphyroclasts in the small section.

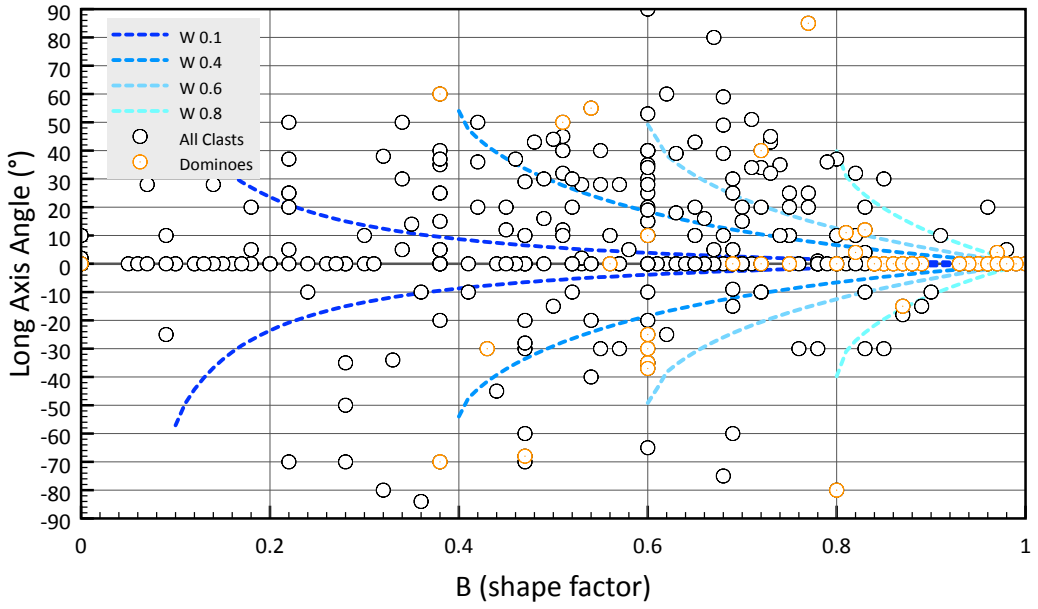

Figure 17. Shape factor vs. porphyroclast orientation plot. This plot compares particle aspect to orientation. Hyperbolic curves are for ideal vorticity states within these axial parameters. The envelope that encloses most data points is an estimate of the vorticity number for those data. The point distribution is strongly influenced by inclusion of domino porphyroclasts because many of those grains are elongated parallel to the macroscopic foliation. Omitting the most extreme dominoes with high B values, W ~ 0.86. See Jessup et al. (2007) for a discussion on different forms of vorticity analysis using rigid grains.

set has fewer very low angle porphyroclasts and few dominoes. This clusters the small section data below $W = 0.86$ (Fig. 16).

Figure 17 is a PAR plot with W_m contours superimposed on the grid. Only delta, sigma, and what were recorded as neutral tailed porphyroclasts are included on this plot. The rigid grain net (RGN) gridlines permit a rapid determination of W_m from points on the PAR axes (Jessup et al., 2007). The RGN plot suggests a W_m for the Blowing Rock gneiss data of 0.6-0.7, considerably lower than the other types of plots. All determinations, however, point to sub-simple or general shearing as the flow path for these rocks. That is consistent with a very strong foliation containing greatly elongated porphyroclasts and matrix minerals.

DISCUSSION

As a single indicator of vorticity, treating porphyroclasts in Blowing Rock gneiss is very complicated. It is likely that these rocks have experienced at least two episodes of ductile deformation. The later of the two created discrete high strain zones associated with mylonite/phyllonite formation that involved retrograde metamorphism and extensive alteration (Bryant, 1966; Hoff, 1982). Rocks in the Bailey Camp section contain unusually widespread carbonate minerals including within the matrix of augen gneiss, in deformed veins, and in later veins. Similarly sulfide minerals are very common in Blowing Rock gneiss as matrix minerals; some pyrite grains have small pressure shadows around them. It's possible that these alterations occurred while rocks in the footwall to the Linville Falls fault were farther southeast and deeper and as these

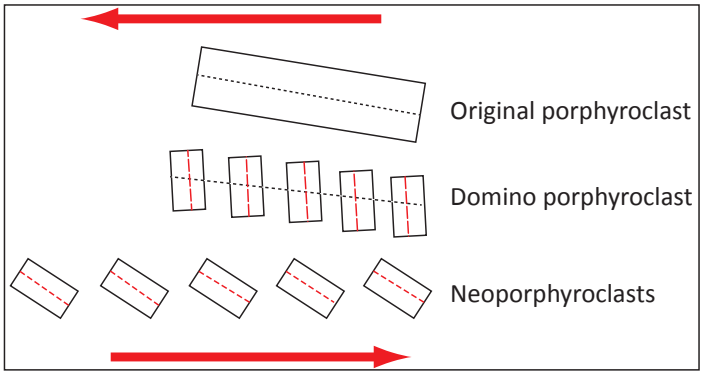

Figure 18. Neoporphyroclast formation. Domino porphyroclasts in augen gneiss separate along cleavage at some stage in their evolution. If this deconstruction occurred as older porphyroclasts approached their stabile orientations for sub-simple shearing, then the fragments may act as neoporphyroclasts. They are spawned with higher takeoff angles than the host clasts. This effect could place more data points in the lower kinematic vorticity field of a PAR plot.

crystalline rocks overrode de-watering early Paleozoic sedimentary shelf sequences. Casale et al. (2017) describe early Alleghanian amphibolite-facies metamorphism in the eastern Blue Ridge in northeast Georgia.

Nonetheless, an array of kinematic indicators in the Bailey Creek section are in agreement with sense of shear and vorticity being sinistral as viewed on the VPP with a derived movement sense to the north or northwest. Porphyroclast asymmetry, shear bands, fold vergence, foliation boudinage, layer boudinage, and stretching lineations confirm these kinematics with sparse local divergences. Ductile shear zones in the Bailey Creek section are embedded in larger deformation zones conformably but do carry substantial mineral alteration. The age of the schistosity in augen gneiss removed from those distinct high strain zones is unknown as well. Metadiabase dikes are tightly folded as are early felsic dikes and veins with this foliation axial planar. It is possible that the earlier period of prograde metamorphism and deformation was Neoacadian or Taconic or even early Alleghanian. If Blowing Rock gneiss has a Grenville deformation imprint, it is undescribed at Bailey Camp.

While far from a classic, simple case of rigid body rotation, porphyroclast kinematics here do provide some interesting challenges for using these rocks in vorticity analysis. It is clear that many of the porphyroclasts not only behaved rigidly, they also fragmented in a flowing matrix (Fig. 18). The consequence is to increase the density of points in a PAR plot at artificially lower values of kinematic vorticity.

REFERENCES CITED

Adams, M. G., 2000, The nature of the eastern-western Blue Ridge contact across the Grandfather Mountain window: Geological Society of America Abstracts with Programs, v. 32, no. 2, p. 1.

Adams, M. G., and Su, Q., 1996, The nature and timing of deformation in the Beech Mountain thrust sheet between the Grandfather Mountain and Mountain City windows in the Blue Ridge of northwestern North Carolina: Journal of Geology, v. 104, p. 197-213.

Adams, M. G., and Trupe, C. H., 2004, Extent and significance of Alleghanian faulting near the Grandfather Mountain Window, northwestern North Carolina: Geological Society of America Abstracts with Programs, v. 36, no. 2, p. 139.

Arslan, A., Passchier, C. W., and Koehn, D., 2008, Foliation boudinage: Journal of Structural Geology, v. 30, no. 3, p. 291-309.

Bartholomew, M. J., 1983, Palinspastic reconstruction of the Grenville Terrane in the Blue Ridge geologic province, southern and central Appalachians, U.S.A: Geological Journal, v. 18, no. 3, p. 241-253.

Bobyarchick, A. R., 1983, Structure of the Brevard Zone and Blue Ridge near Lenoir, North Carolina, with observations on oblique crenulation cleavage and a preliminary theory for irrotational structures in shear zones [Ph.D. dissertation) Ph.D. dissertation]: State University of New York At Albany, 360 p.

-, 1984, A late Paleozoic component of strike-slip in the Brevard Zone, Southern Appalachians: Geological Society of America Abstracts with Programs, v. 16, no. 3, p. 126.

-, 1998, Evolving concepts in tectonics and the interpretive history of the Brevard fault zone: Geological Society of America Abstracts with Programs, v. 30, no. 4, p. 4.

-, 1999, The history of investigation of the Brevard fault zone and evolving concepts in tectonics: Southeastern Geology Special Issue - Historical investigation of Appalachian geology, v. 38, no. 1, p. 223-238.

-, 2006, Foliation transposition and vorticity in a late Paleozoic orogen-parallel shear zone in the Southern Appalachian Mountains: Geological Society of America Abstracts with Programs, v. 38, no. 5, p. 78.

-, 2011, Vorticity assessment in non-uniformly deforming augen gneiss: American Geophysical Union Fall Meeting.

-, 2012, Exceptions to uniform rigid augen rotation and vorticity in a Blue Ridge crystalline massif: Geological Society of America Abstracts with Programs, v. 44, no. 4, p. 10.

-, 2013, Vorticity from kinematic indicators and exposition of regional shear in high strain zones of the central and southern Appalachian Mountains: Geological Society of America Abstracts with Programs, v. 45, no. 7, p. 741.

-, 2014a, Vorticity and strain partitioning between augen gneiss and high strain zones in the Blowing Rock Gneiss, North Carolina Blue Ridge: Geological Society of America Abstracts with Programs, v. 46, no. 3, p. 36.

-, 2014b, Vorticity, kinematics and partitioning in porphyroclastic gneiss: Geological Society of America Abstracts with Programs, v. 46, no. 6, p. 217.

Bobyarchick, A. R., and McDermitt, H., 2011, Vorticity and kinematics from feldspar porphyroclasts in the Blowing

Rock Gneiss, Grandfather Mountain Window, North Carolina: Geological Society of America Abstracts with Programs, v. 43, no. 2, p. 21-22.
Boyer, S. E., 1976, Formation of the Grandfather Mountain Window, North Carolina, by duplex thrusting: Geological Society of America Abstracts with Programs, v. 8, no. 6, p. 788-789.
-, 1978, Structure and origin of Grandfather Mountain window, North Carolina [Ph.D. dissertation]: Baltimore, The Johns Hopkins University, 306 p.
-, 1992, Sequential development of the southern Blue Ridge province of northwest North Carolina ascertained from the relationships between penetrative deformation and thrusting, in Mitra, S., and Fisher, G. W., eds., Structural geology of fold and thrust belts: Baltimore, Johns Hopkins University Press, p. 161-188.
Boyer, S. E., and Elliott, D., 1982, Thrust systems: AAPG Bulletin, v. 66, no. 9, p. 1196-1230.
Boyer, S. E., Elliott, D., Boyer, S. E., and Elliott, D., 1982, Sub-thrust geology beneath metamorphic terranes, Blue Ridge Province, North Carolina: Geological Society of America Abstracts with Programs, v. 14, no. 7, p. 450.
Bryant, B., 1963, Geology of the Blowing Rock quadrangle, North Carolina: U.S. Geological Survey, U.S. Geological Survey Geologic Map GQ-243, scale 1:62,500. https://ngmdb.usgs.gov/Prodesc/proddesc_697.htm
-, 1966, Formation of phyllonites in the Grandfather Mountain area, northwestern North Carolina, Geological Survey Research 1966, Volume 550-D: Washington, D.C., U.S. Geological Survey, p. D114-D150.
Bryant, B., and Reed, J. C., Jr, 1962, Structural and metamorphic history of the Grandfather Mountain area, North Carolina--a preliminary report: American Journal of Science, v. 260, p. 161-180.
-, 1969, Significance of lineation and minor folds near major thrust faults in the Southern Appalachians and the British and Norwegian Caledonides: Geological Magazine, v. 106, no. 5, p. 412-429. doi:10.1017/S0016756800058805
Bryant, B., and Reed, J. C., Jr., 1970, Geology of the Grandfather Mountain window and vicinity, North Carolina and Tennessee, U. S. Geological Survey Professional Paper 615, 190 p. https://ngmdb.usgs.gov/Prodesc/proddesc_4943.htm
Butler, J. R., Goldberg, S. A., and Mies, J. W., 1987, Tectonics of the Blue Ridge west of the Grandfather Window, North Carolina and Tennessee: Geological Society of America Abstracts with Programs, v. 19, no. 2, p. 77.
Butler, J. R., Trupe, C. H., Adams, M. G., Goldberg, S. A., and Mies, J. W., 1993, Kinematics and timing of Alleghanian deformation in the Southern Appalachians; a transect of the North Carolina segment: Geological Society of America Abstracts with Programs, v. 25, no. 6, p. 285.
Carrigan, C. W., Miller, C. F., Fullagar, P. D., Bream, B. R., Hatcher, R. D., Jr, and Coath, C. D., 2003, Ion microprobe age and geochemistry of Southern Appalachian basement, with implications for Proterozoic and Paleozoic reconstructions: Precambrian Research, v. 120, no. 1-2, p. 1-36.
Casale, G., Levine, J. S. F., Craig, T. D., and Stewart, C., 2017, Timing and deformation conditions of the Tallulah Falls dome, NE Georgia: Implications for the Alleghanian orogeny: Geological Society of America Bulletin, v. 129, no. 9-10, p. 1195-1208. 10.1130/B31595.1
Conley, J. F., 1978, Geology of the Piedmont of Virginia--Interpretations and problems, Contributions to Virginia geology-III, Volume 7: Charlottesville, VA, Virginia Division of Mineral Resources Publication, p. 115-149.
Cook, F. A., Albaugh, D. S., Brown, L. D., Kaufman, S., Oliver, J. E., and Hatcher, R. D., Jr, 1979, Thin-skinned tectonics in the crystalline southern Appalachians;COCORP seismic-reflection profiling of the Blue Ridge and Piedmont: Geology, v. 7, p. 563-567.
Cook, F. A., Brown, L. D., Kaufman, S., Oliver, J. E., and Petersen, T. A., 1981, COCORP seismic profiling of the Appalachian orogen beneath the Coastal Plain of Georgia: Geological Society of America Bulletin, Part I, v. 92, p. 738-748.
Corrie, S. L., and Kohn, M. J., 2007, Resolving the timing of orogenesis in the Western Blue Ridge, southern Appalachians, via in situ ID-TIMS monazite geochronology: Geology, v. 35, no. 7, p. 627-630. 10.1130/g23601a.1
Davis, G. L., Tilton, G. R., and Wetherill, G. W., 1962, Mineral ages from the Appalachian province in North Carolina and Tennessee: J. Geophy. Res., v. 67, p. 1987-1996.
Davis, T. L., Tabor, J. R., Hatcher, R. D., Jr., Dymek, R. F., and Shelton, K. L., 1989, Orogen-parallel to orogen-oblique ductile deformation and possible late Paleozoic (?) ductile deformation of the western Piedmont, Southern Appalachians, Geological Society of America Abstracts with Programs, Volume 21: Boulder, CO, Geological Society of America, p. A65.
Davis, T. L., and Yanagihara, G. M., 1993, Geology of the Columbus Promontory, western Piedmont, North Carolina, Southern Appalachians, in Hatcher, R. D., Jr, and Davis, T. L., eds., Studies of Inner Piedmont geology with a focus on the Columbus, Carolina Geological Society 1993 Field Trip Guidebook, p. 17-43.
DePaor, D. G., 1983, Orthographic analysis of geological structures - I. Deformation theory: Journal of Structural Geology, v. 5, p. 255-277.
Edelman, S. H., Liu, A., and Hatcher, R. D., Jr., 1987, The Brevard Zone in South Carolina and adjacent areas; an Alleghanian orogen-scale dextral shear zone reactivated as a thrust fault: Journal of Geology, v. 95, no. 6, p. 793-806.
Evans, C. A., and Mosher, S., 1986, Microstructures and sense of shear in the Brevard fault zone, Southern Appalachians: Geological Society of America Abstracts with Programs, v. 18, p. 596.
Fetter, A. H., and Goldberg, S. A., 1993, A Late Silurian U-Pb zircon age for Linville Metadiabase, Grandfather Mountain Window, North Carolina: Geological Society of America Abstracts with Programs, v. 25, no. 4, p. 15.
Fetter, A. H., and Goldberg, S. A., 1995, Age and geochemical characteristics of bimodal magmatism in the Neoproterozoic Grandfather Mountain rift basin: Journal of Geology, v. 103, no. 3, p. 313-326.
Forte, A. M., and Bailey, C. M., 2007, Testing the utility of the porphyroclast hyperbolic distribution method of kinematic vorticity analysis: Journal of Structural Geology, v. 29, no. 6, p. 983-1001. http://dx.doi.org/10.1016/j.jsg.2007.01.006
Fossen, H., and Cavalcante, G. C. G., 2017, Shear zones – A

review: Earth-Science Reviews, v. 171, p. 434-455. https://doi.org/10.1016/j.earscirev.2017.05.002

Fullagar, P. A., and Odom, A. L., 1973, Geochronology of Precambrian gneisses in the Blue Ridge province of northwestern North Carolina and adjacent parts of Virginia and Tennessee: Geological Society of America Bulletin, v. 84, no. 9, p. 3065-3080.

Geiser, P. A., and Engelder, T., 1983, The distribution of layer parallel shortening fabrics in the Appalachian foreland of New York and Pennsylvania; Evidence for two non-coaxial phases of the Alleghanian Orogeny, in Hatcher, R. D., Williams, H., and Zietz, I., eds., Contributions to the Tectonics and Geophysics of Mountain Chains, Volume 158: Boulder, CO, Geological Society of America, p. 161-175.

Goldberg, S. A., Butler, J. R., Trupe, C. H., and Adams, M. G., 1992, The Blue Ridge thrust complex northwest of the Grandfather Mountain Window, North Carolina and Tennessee, Chapel Hill, NC, Univ. N.C., 213-233 p.

Goldberg, S. A., and Dallmeyer, R. D., 1997, Chronology of Paleozoic metamorphism and deformation in the Blue Ridge thrust complex, North Carolina and Tennessee: American Journal of Science, v. 297, no. 5, p. 488-526.

Goldstein, A. G., Brown, L. L., Ellwood, B. B., Hrouda, F., and Wagner, J.-J., 1988, Magnetic susceptibility anisotropy of mylonites from the Brevard Zone, North Carolina, U.S.A[Monograph] Symposia on magnetic fabrics: Physics of the Earth and Planetary Interiors, v. 51, no. 4, p. 290-300.

Gomez-Rivas, E., Bons, P. D., Griera, A., Carreras, J., Druguet, E., and Evans, L., 2007, Strain and vorticity analysis using small-scale faults and associated drag folds: Journal of Structural Geology, v. 29, no. 12, p. 1882-1899. http://dx.doi.org/10.1016/j.jsg.2007.09.001

Grasemann, B., Stuewe, K., and Vannay, J.-C., 2003, Sense and non-sense of shear in flanking structures: Journal of Structural Geology, v. 25, no. 1, p. 19-34.

Hamil, A. B., Trupe, C. H., and Asher, P. M., 2009, A new look at the Bakersville Intrusive Suite; implications for delineating structural boundaries within the Blue Ridge thrust complex: Geological Society of America Abstracts with Programs, v. 41, no. 1, p. 47.

Harris, L. D., and Bayer, K. C., 1979, Sequential development of the Appalachian orogen above a master decollement - A hypothesis: Geology, v. 9, p. 568-572.

Harris, L. D., Harris, A. G., DeWitt, W., Jr, and Bayer, K. C., 1981, Evaluation of southern Eastern overthrust belt beneath Blue Ridge-Piedmont thrust: American Association of Petroleum Geologists Bulletin, v. 65, p. 2497-2505.

Harris, L. D., and Milici, R. C., 1977, Similarities between the thick-skinned Blue Ridge anticlinorium and the thin-skinned Powell Valley anticline: Geological Society of America Bulletin, v. 90, no. 6, p. 525-539. 10.1130/0016-7606(1979)90<525:sbttbr>2.0.co;2

Hatcher Jr, R. D., Merschat, A. J., and Raymond, L. A., Geotraverse: Geology of northeastern Tennessee and the Grandfather Mountain region, in Proceedings Geological Society of America 2006 Southeastern Section Meeting Field Trip Guidebook: Knoxville, University of Tennessee2006, p. 129-184.

Hatcher, R. D., Jr, and Goldberg, S. A., 1991, The Blue Ridge geologic province, in Horton, J. W., Jr, and Zullo, V. A., eds., The geology of the Carolinas: Knoxville, The University of Tennessee Press, p. 11-35.

Hatcher, R. D., Jr., 1971, Stratigraphic, petrologic, and structural evidence favoring a thrust solution to the Brevard problem: American Journal of Science, v. 270, p. 177-202.

-, 2001, Rheological partitioning during multiple reactivation of the Palaeozoic Brevard fault zone, Southern Appalachians, USA: Geological Society Special Publications, v. 186, p. 257-271. https://doi.org/10.1144/GSL.SP.2001.186.01.15

Hatcher, R. D., Jr., Hooper, R. J., McConnell, K. I., Heyn, T., and Costello, J. O., 1988, Geometric and time relationships between thrusts in the crystalline Southern Appalachians, in Mitra, G., and Wojtal, S., eds., Geometries and mechanism of thrusting, with special reference to the Appalachians: Boulder, CO, Geological Society of America Special Paper 222, p. 185-196. https://doi.org/10.1130/SPE222

Hatcher, R. D., Jr., Huebner, M. T., Rehrer, J. R., Acker, L. L., Fullagar, P. D., Liu, A., and Goad, P. L., 2017, Geologic and kinematic insights from far-traveled horses in the Brevard fault zone, southern Appalachians, in Law, R. D., Thigpen, J. R., Merschat, A. J., and Stowell, H. H., eds., Linkages and Feedbacks in Orogenic Systems, Geological Society of America. https://doi.org/10.1130/2017.1213(13)

Hoff, J. L., 1982, The petrography of the Blowing Rock Gneiss, Grandfather Mountain window, North Carolina [M.S. thesis]: Duke University, 196 p.

Holcombe, R. J., and Little, T. A., 2001, A sensitive vorticity gauge using rotated porphyroblasts, and its application to rocks adjacent to the Alpine Fault, New Zealand: Journal of Structural Geology, v. 23, no. 6-7, p. 979-989. http://dx.doi.org/10.1016/S0191-8141(00)00169-3

Horton, J. W., Jr., and Butler, J. R., 1986, The Brevard fault zone at Rosman, Transylvania County, North Carolina, in Neathery, T. L., ed., DNAG Centennial Field Guide 6 - Southeastern Section: Boulder, CO, Geological Society of America, p. 251-256.

Jessup, M. J., Law, R. D., and Frassi, C., 2007, The Rigid Grain Net (RGN): An alternative method for estimating mean kinematic vorticity number (Wm): Journal of Structural Geology, v. 29, no. 3, p. 411-421. 10.1016/j.jsg.2006.11.003

Johnson, S. E., Lenferink, H. J., Price, N. A., Marsh, J. H., Koons, P. O., West, D. P., and Beane, R. J., 2009, Clast-based kinematic vorticity gauges; the effects of slip at matrix/clast interfaces: Journal of Structural Geology, v. 31, no. 11, p. 1322-1339. http://dx.doi.org/10.1016/j.jsg.2009.07.008

Keith, A., 1903, Description of the Cranberry quadrangle, North Carolina-Tennessee, U.S. Geological Survey Geologic Atlas, Folio 90, 9 p., v. Folio 90, 9 p. https://pubs.er.usgs.gov/publication/gf90

Kunk, M. J., Southworth, S., Aleinikoff, J. N., Naeser, N. D., Naeser, C. W., Merschat, C. E., and Cattanach, B. L., 2006, Preliminary U-Pb, 40Ar/39Ar and fission-track ages support a long and complex tectonic history in the western Blue Ridge in North Carolina and Tennessee, Geological Society of America Abstracts with Programs, Volume 38, p. 66.

Lister, G. S., and Snoke, A. W., 1984, S-C mylonites: Journal of Structural Geology, v. 6, p. 617-638.

Liu, A., 1991, Structural geology and deformation history of the Brevard fault zone, Chauga Belt, and inner Piedmont, northwestern South Carolina and adjacent areas [Ph.D.

dissertation]: University of Tennessee, 200 p.
McDermitt, H., and Bobyarchick, A. R., 2011, A comparison of the structural sequences between Blowing Rock Gneiss and late Proterozoic mafic intrusions in the Grandfather Mountain Window: Geological Society of America Abstracts with Programs, v. 43, no. 2, p. 10.
McGill, K. A., Butler, J. R., and Fullagar, P. D., 1980, Tectonic history of the Brevard Zone and Blue Ridge east of Asheville, North Carolina: Geological Society of America Abstracts with Programs, v. 12, p. 480.
Means, W. D., Hobbs, B. E., Lister, G. S., and Williams, P. F., 1980, Vorticity and non-coaxiality in progressive deformations: Journal of Structural Geology, v. 2, p. 371-378.
Merschat, A. J., Bream, B. R., Huebner, M. T., Hatcher, R. D., Jr., and Miller, C. F., 2017, Temporal and spatial distribution of Paleozoic metamorphism in the southern Appalachian Blue Ridge and Inner Piedmont delimited by ion microprobe U-Pb ages of metamorphic zircon, in Law, R. D., Thigpen, J. R., Merschat, A. J., and Stowell, H. H., eds., Linkages and Feedbacks in Orogenic Systems, Geological Society of America. https://doi.org/10.1130/2017.1213(10)
Merschat, A. J., Hatcher, R. D., Jr., and Davis, T. L., 2005, The northern Inner Piedmont, Southern Appalachians, USA; kinematics of transpression and SW-directed mid-crustal flow: Journal of Structural Geology, v. 27, no. 7, p. 1252-1281.
Miller, B. V., Fetter, A. H., and Stewar, K. G., 2006, Plutonism in three orogenic pulses, Eastern Blue Ridge Province, southern Appalachians: Geological Society of America Bulletin, v. 118, no. 1-2, p. 171-184. 10.1130/B25580.1
O'Hara, K., 1990, Brittle-plastic deformation in mylonites: An example from the Meadow Fork thrust, western Blue Ridge province, southern Appalachians: Geological Society of America Bulletin, v. 102, p. 1706-1713.
Ohlschlager, J. G., McNeil, M., Thigpen, J. R., Prince, P. S., Henika, W. S., and Law, R. D., 2008, Microstructural and kinematic investigations of the Brevard fault zone near Rosman, NC; implications for material movement oblique to orogenic strike: Geological Society of America Abstracts with Programs, v. 40, no. 4, p. 10.
Passchier, C. W., 1987a, Efficient use of the velocity gradients tensor in flow modelling: Tectonophysics, v. 136, no. 1-2, p. 159-163.
-, 1987b, Stable positions of rigid objects in non-coaxial flow - a study in vorticity analysis: Journal of Structural Geology, v. 9, p. 679-690. https://doi.org/10.1016/0191-8141(87)90152-0
Passchier, C. W., and Urai, J. L., 1988, Vorticity and strain analysis using Mohr diagrams: Journal of Structural Geology, v. 10, p. 755-763.
Piazolo, S., Bons, P. D., and Passchier, C. W., 2002, The influence of matrix rheology and vorticity on fabric development of populations of rigid objects during plane strain deformation: Tectonophysics, v. 351, no. 4, p. 315-329.
Rankin, D. W., 1975, The continental margin of eastern North America in the Southern Appalachians: The opening and closing of the proto-Atlantic Ocean: American Journal of Science, v. 275-A, p. 298-336.
Rankin, D. W., Espenshade, G. H., and Newman, R. B., 1972, Geologic map of the west half of the Winston-Salem quadrangle, North Carolina, Virginia, and Tennessee:: U.S. Geological Survey Miscellaneous Investigations Map I-709-A, scale 1:250 000.
Rankin, D. W., Espenshade, G. H., and Shaw, K. W., 1973, Stratigraphy and structure of the metamorphic belt in northwestern North Carolina and southwestern Virginia: A study from the Blue Ridge across the Brevard zone to the Sauratown Mountains anticlinorium: American Journal of Science, v. 273-A, p. 1-40.
Raymond, L. A., and Abbott, R. N., 1997, Petrology and tectonic significance of ultramafic rocks near the Grandfather Mountain Window in the Blue Ridge Belt, Toe Terrane, western Piedmont Zone, North Carolina: Carolina Geological Society Field Trip and Annual Meeting, v. 1997, p. 67-85. http://www.carolinageologicalsociety.org/CGS/1990s_files/gb%201997.pdf
Raymond, L. A., and Love, A. B., 2006, Pseudobedding, primary structures and thrust faults in the Grandfather Mountain Formation, NW North Carolina, USA: Southeastern Geology, v. 44, no. 2, p. 53-71.
Raymond, L. A., Yurkovich, S. P., and McKinney, M., 1989, Block-in-matrix structures in the North Carolina Blue Ridge Belt and their significance for the tectonic history of the Southern Appalachian Orogen, in Horton, J. W. J., and Rast, N., eds., Mélanges Olistostromes of the U.S. Appalachians (Geological Society of America Special Paper), Volume 228: Boulder, CO, Geological Society of America, p. 195-215. http://dx.doi.org/10.1130/SPE228-p195
Reed, J. C., Jr., and Bryant, B., 1964, Evidence for strike-slip faulting along the Brevard Zone in North Carolina: Geological Society of America Bulletin, v. 75, no. 12, p. 1177-1196. https://doi.org/10.1130/0016-7606(1964)75[1177:EFSFAT]2.0.CO;2
Reed, J. C., Jr., Bryant, B., and Myers, W. B., 1970, The Brevard zone: a reinterpretation, in Fisher, G. W., Pettijohn, F. J., Reed, J. C., Jr, and Weaver, K. N., eds., Studies of Appalachian geology - Central and Southern: New York, Interscience Publishers, p. 261-269.
Robin, P.-Y., and Cruden, A. R., 1994, Strain and vorticity patterns in ideally ductile transpression zones: Journal of Structural Geology, v. 16, p. 447-466.
Schwab, F. L., 1977, Grandfather Mountain Formation: Depositional environment, provenance, and tectonic setting of late Precambrian alluvium in the Blue Ridge of North Carolina: Journal of Sedimentary Petrology, v. 47, no. 2, p. 800-810. http://dx.doi.org/10.1306/212F7257-2B24-11D7-8648000102C1865D
Schwerdtner, W. M., 1998, Graphic derivation of the local sense of shear strain components in stretched walls of lithotectonic boundaries: Journal of Structural Geology, v. 20, no. 7, p. 957-967. file:///Users/andybobyarchick/Documents/Sente/References/Schwerdtner/1998/Graphic%20derivation%20of%20the%20local%20sense%20of%20shear%20str/Graphic%20derivation%20of%20the%20local%20sense%20of%20shear%20str.pdf
Simpson, C., and DePaor, D. G., 1993, Strain and kinematic analysis in general shear zones: Journal of Structural Geology, v. 15, no. 1, p. 1-20. https://doi.org/10.1016/0191-8141(93)90075-L
Stahr, D. W., III, and Law, R. D., 2014, Strain memory of 2D

and 3D rigid inclusion populations in viscous flows; what is clast SPO telling us?: Journal of Structural Geology, v. 68, no. Part B, p. 347-363. http://dx.doi.org/10.1016/j.jsg.2014.05.028

Stewart, K. G., Adams, M. G., and Trupe, C. H., 1997a, Paleozoic structural evolution of the Blue Ridge thrust complex, western North Carolina, in Stewart, K. G., Adams, M. G., and Trupe, C. H., eds., Paleozoic structure, metamorphism, and tectonics of the Blue Ridge of western North Carolina (Carolina Geological Society 1997 Field Trip and Annual Meeting), Volume 1997: [location varies], Carolina Geological Society, p. 21-31. http://www.carolinageologicalsociety.org/CGS/1990s_files/gb%201997.pdf

Stewart, K. G., Adams, M. G., and Trupe, C. H., editor, 1997b, Paleozoic structure, metamorphism, and tectonics of the Blue Ridge of western North Carolina: Banner Elk, NC, Carolina Geological Society 1997 Field Trip and Annual Meeting, 101 p.

Szymanski, D. L., and Christensen, N. I., 1993, The origin of reflections beneath the Blue Ridge-Piedmont allochthon: A view through the Grandfather Mountain window: Tectonics, v. 12, no. 1, p. 265-278.

Tikoff, B., and Fossen, H., 1995, The limitations of three-dimensional kinematic vorticity analysis: Journal of Structural Geology, v. 17, no. 12, p. 1771-1784.

Trupe, C. H., 1997, Deformation and metamorphism in part of the Blue Ridge thrust complex, northwestern North Carolina [Ph.D. dissertation]: University of North Carolina at Chapel Hill, 213 p.

Trupe, C. H., Butler, J. R., Mies, J. W., Adams, M. G., and Goldberg, S. A., 1990, The Linville Falls Fault and related shear zone, western North Carolina: Geological Society of America Abstracts with Programs, v. 22, no. 4, p. 66.

Trupe, C. H., Stewart, K. G., Adams, M. G., and Foudy, J. P., 2002, An evaluation of the Paleozoic tectonic history of Blue Ridge rocks in western North Carolina and eastern Tennessee; implications for understanding the Grenville Orogeny in the Southern Appalachians: Geological Society of America Abstracts with Programs, v. 34, p. 41.

Trupe, C. H., Stewart, K. G., Adams, M. G., and Foudy, J. P., 2004, Deciphering the Grenville of the southern Appalachians through evaluation of the post-Grenville tectonic history in northwestern North Carolina: Geological Society of America Memoirs, v. 197, p. 679.

Tu, C., Hatcher, R. D., Jr., and Jessup, M. J., 2008, Kinematic vorticity of Brevard fault zone mylonite, South Carolina: Abstracts with Programs - Geological Society of America, v. 40, no. 6, p. 187-188.

Vauchez, A., 1987, Brevard fault zone, Southern Appalachians; a medium-angle, dextral, Alleghanian shear zone: Geology, v. 15, no. 7, p. 669-672.

Vauchez, A., and Brunel, M., 1988, Polygenetic evolution and longitudinal transport within the Henderson mylonitic gneiss, North Carolina (southern Appalachian Piedmont): Geology, v. 16, p. 1011-1014.

Wagener, H. D., 1979, Petrology of the Wilson Creek Gneiss, western North Carolina and its relation to the Grandfather Mountain Formation, Cranberry Gneiss, and inner Piedmont, South Portland, ME, Chiasma Consultants, Inc.

Wagener, H. D., and McHone, J. G., 1982, Uranium mineralization in the Wilson Creek and Cranberry gneisses and the Grandfather Mountain Formation, North Carolina and Tennessee.

Wallis, S., 1995, Vorticity analysis and recognition of ductile extension in the Sanbagawa Belt, SW Japan: Journal of Structural Geology, v. 17, no. 8, p. 1077-1093. https://doi.org/10.1016/0191-8141(95)00005-X

Wilson, C. G., Raymond, L. A., and Love, A. B., 2008, Structures and deformation inside the Grandfather Mountain window: the northern Goldmine Branch fault: Geological Society of America Abstracts with Programs, v. 40, no. 4, p. 11.

Xypolias, P., 2010, Vorticity analysis in shear zones: A review of methods and applications: Journal of Structural Geology, v. 32, no. 12, p. 2072-2092. 10.1016/j.jsg.2010.08.009

The Boone fault and its implications for Cenozoic topographic rejuvenation of the southern Appalachian Mountains

Jesse S. Hill
Kevin G. Stewart

Department of Geological Sciences, University of North Carolina - Chapel Hill, Chapel Hill, NC 27599

ABSTRACT

In this paper we document the first mappable fault associated with Cenozoic uplift of the southern Appalachians. Near Boone, North Carolina, at the northern edge of the Grandfather Mountain window we mapped a brittle fault zone along what was previously called the Linville Falls thrust fault. The minor faults associated with this zone, which we are calling the Boone fault, typically dip steeply and strike WNW. There are normal (north-dipping) and reverse (south-dipping) faults and both show south-side-up motion. Based on how this high-angle fault zone corresponds with a sharp topographic scarp separating the Linville Falls shear zone from the Grandfather Mountain formation, we suspect it may be younger than the Paleozoic faults bounding the rest of the window. To test if it is a late, post-orogenic structure, we performed a paleostress inversion of 165 minor faults. The inversion yields stress tensors with SSW-plunging maximum compression directions, which do not match stresses that drove Paleozoic SE-NW shortening or Mesozoic E-W rifting, but likely represent Cenozoic NNE-SSW extension associated with doming and blocky uplift of the southern Appalachians. We interpret these faults to mean the Grandfather Mountain window is not entirely framed by a Paleozoic fault, but rather is bounded in part by a high-angle Cenozoic fault zone. We mapped ~10 km of the Boone fault along the northeastern edge of the Grandfather Mountain window, but we think it could be part of the ~180 km long and 20 km wide regional-scale topographic lineament swarm spanning from the Valley and Ridge in Tennessee to the Piedmont in North Carolina.

We also present geomorphic and seismic data consistent with a landscape currently responding to uplift. We analyzed the longitudinal profiles of dozens of streams draining into the fault zone and found numerous knickpoints hundreds of meters above the valley floor. In addition to these disequilibrium profiles, some of the streams contain map-view evidence of drainage capture consistent with south-side-up motion along the Boone fault. Based on the abundance of knickpoints and the existence of perched floodplains in the headwaters, the disequilibrium streams are likely associated with the Boone fault. A cluster of shallow earthquakes occurred in 2013 and 2014 about 4 km south of the Boone fault and damaged sidewalks, roads, and building foundations in an area with abundant evidence of active slope creep. Modern earthquakes and active landslides indicate that the Boone fault is likely still jostling and is the cause of many of the unstable slopes and land-use hazards that threaten the town of Boone. Our work offers a solution to the long-standing issue of why the Appalachians are still so high and documents a seismically active fault that is accommodating uplift of the North Carolina Blue Ridge.

INTRODUCTION

The Appalachians have a well-documented tectonic history spanning the Neoproterozoic to the late Paleozoic (e.g. Hatcher et al., 2005; Hibbard et al., 2010). However, a family of well-developed topographic lineaments crossing the southern Appalachians appear to be younger than the main orogenic belt (Hack, 1982). Recent workers have shown that the southern Appalachians underwent hundreds of meters of uplift in the Neogene (Gallen et al, 2013; Miller et al., 2013; Hill and Stewart, 2018) and others have suggested that these lineaments represent fracture and fault zones that accommodated this uplift (Dennison and Stewart, 2001; Stewart and Dennison, 2006; Hill, 2013). Although there is an abundance of evidence for late Cenozoic uplift of the Appalachians, no faults in the Blue Ridge have been associated with the rejuvenation of topography.

In this study, we focus on clarifying the structural evolution of WNW-trending lineaments (Figure 1) in an area of Watauga County near Boone, North Carolina (USGS 7.5" quadrangles included: Boone, Deep Gap, Sherwood, Valle Crucis, and Zionville; all in North Carolina) where they are abundant and crosscut many Paleozoic contacts and fault zones. We mapped an 80 km^2 area, measured brittle faults for paleostress

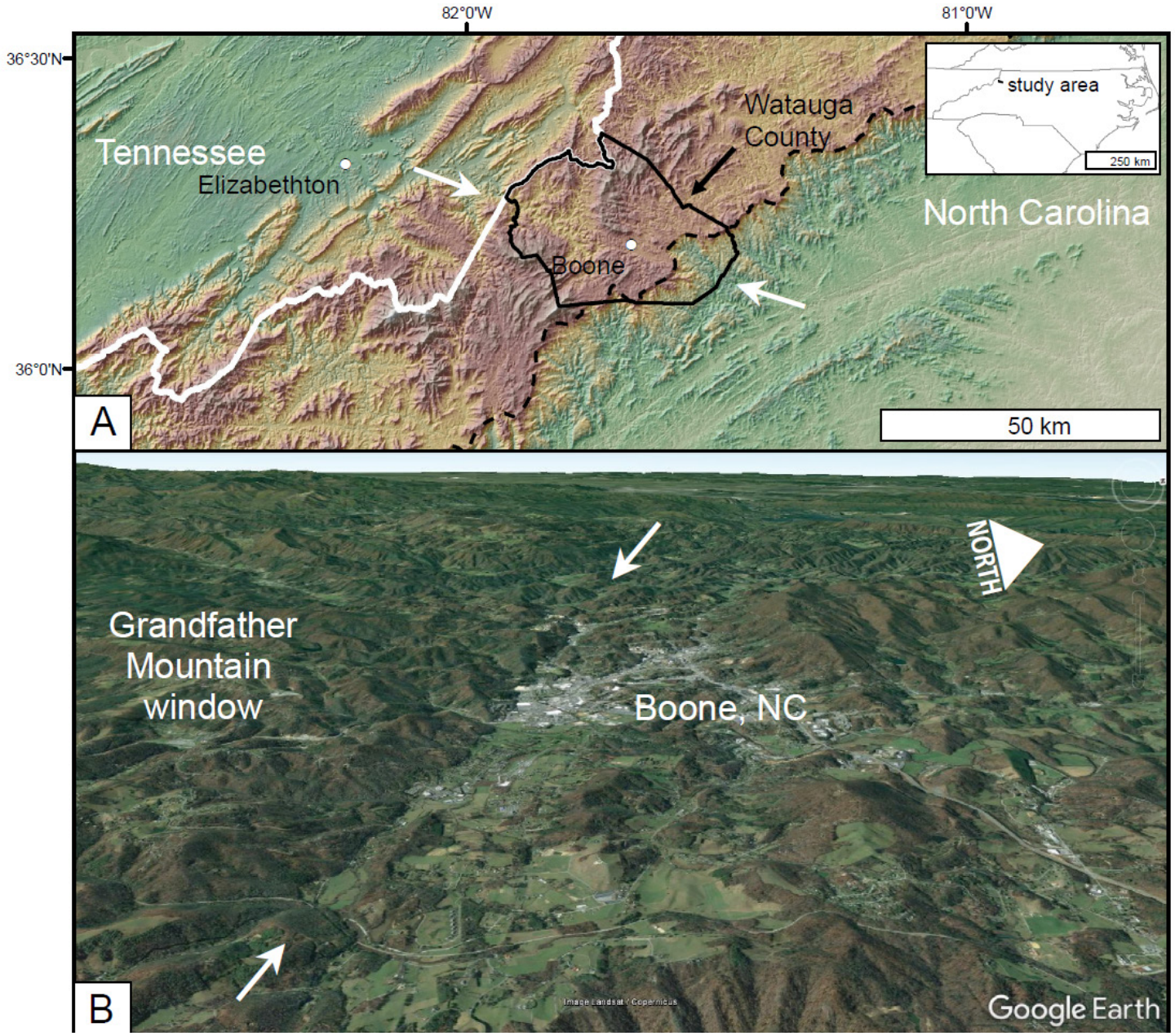

Figure 1: (A) Digital elevation model of western North Carolina and eastern Tennessee showing the Boone lineament swarm striking WNW across the NE-trending mountain belt. The dashed line is the Blue Ridge Escarpment and the white arrows correspond with those in figure part B. (B) Oblique view in Google Earth looking WNW along the topographic escarpment corresponding to the Boone fault that crosses through the town of Boone, North Carolina.

analysis, and produced a 1:12,000 scale geologic map (Figure 2). The mapping resulted in several significant changes to the existing geologic maps (Bryant and Reed, 1970; Gillon et al., 2009) and identified a previously unmapped brittle fault zone, here named the Boone fault, which post-dates the documented Paleozoic structures in the area. In addition, our study area has an exceptionally high number of modern landslides near or within the lineaments, likely because the rocks are highly fractured and faulted (Gillon et al., 2009).

To understand the driving mechanism behind the Boone fault zone, we performed a paleostress inversion of minor faults along its length. To estimate the timing and magnitude of fault motion, we used 6m horizontal, sub-meter vertical resolution LIDAR data from North Carolina's Spatial Data Download site (https://sdd.nc.gov/sdd/DataDownload.aspx) to analyze dozens of longitudinal profiles of streams draining into the fault zone. We looked for knickpoints along profiles and for map-view evidence of drainage capture to investigate whether recent vertical motion on the Boone fault was recorded as a geomorphic signature. In this paper, we highlight the importance of Cenozoic structures in understanding Appalachian landscape evolution and slope-failure related hazards

in an area classically considered to be an inactive mountain belt.

GEOLOGIC SETTING AND BACKGROUND

The rocks of the Blue Ridge geologic province of western North Carolina have a complex record of deformation, sedimentation, magmatism, and metamorphism. The oldest significant tectonic event was the Mesoproterozoic Grenville orogeny during the assembly of Rodinia (Faill, 1997, Hibbard et al., 2006; Li et al., 2008). The Grenville was followed by Neoproterozic failed rifting of Rodinia and the deposition of sedimentary rocks that would become the metasedimentary rocks of the Grandfather Mountain window, followed by opening of the Iapetus Ocean (Tull et al., 2010; Burton and Southworth, 2010). The Taconic orogeny in the Ordovician preceded an episode of localized magmatism and transpressional tectonics during the Devonian (e.g. Miller et al., 2006). The late Paleozoic Alleghanian orogeny resulted in assembly of Pangea and is generally thought to have been responsible for the mostly greenschist-grade metamorphism and mylonitic faults that are pervasive throughout the study area (e.g. Merschat et al., 2005).

The bedrock of the study area is a mix of greenschist-to-amphibolite-grade metamorphosed sedimentary and igneous rocks cut by a major Alleghanian thrust, the Linville Falls fault (Figure 2). The Linville Falls fault frames the Grandfather Mountain window and is marked by a mylonite zone locally more than a kilometer thick (Trupe et al., 2004) that separates Mesoproterozoic gneisses and Neoproterozoic metamorphosed Iapetan rift sediments in the footwall from overlying Neoproterozoic to Paleozoic schists, gneisses, and amphibolites in the hanging wall (Bryant and Reed, 1970; NCGS, 1985). The rocks are typically strongly foliated and locally lineated, especially in proximity to Paleozoic fault zones (e.g. Linville Falls fault). Alleghanian duplexing and doming of the Grandfather Mountain window tilted the foliation north of the window towards the northeast (Bryant and Reed, 1970; Boyer and Elliot, 1982). Mesozoic rifting followed the Alleghanian, and although there are no documented Mesozoic deformation structures in our field area, Spotila et al. (2004) proposed that the Blue Ridge escarpment began as a Mesozoic rift-flank uplift and has migrated westward to its present position (Figure 1).

Despite the lack of an active plate boundary in this area since the Late Triassic, there is a growing body of stratigraphic, structural, and geomorphic evidence that the southern Appalachians have undergone a period of uplift in the Neogene. Miocene conglomerates in the coastal plain of South Carolina contain large metamorphic clasts (Nystrom, 1986). Offshore sedimentation increased in the Atlantic and the Gulf of Mexico during the Middle Miocene (Poag and Savon, 1989; Galloway et al., 2011). Dennison and Stewart (2001) proposed that the sudden influx of coarse clastics into the coastal plain in the Early Neogene was a result of uplift of the southern Appalachian Blue Ridge. There are folded Paleogene rocks overlain by flat Neogene rocks along the Selma arch at the southern terminus of the Blue Ridge province (Stewart, 2015). Gallen et al. (2013) showed that knickpoints along streams in the Cullasaja basin of western North Carolina likely formed as a response to Neogene uplift. Similar knickpoints exist along the Susquehanna River in Pennsylvania, and likely were also triggered by Neogene uplift (Miller et al., 2013). The evidence for a Neogene uplift event in the Appalachians is increasing, yet there are no previously documented faults associated with this event.

In strong contrast to the Paleozoic fabrics in western North Carolina are the well-developed topographic lineaments that trend WNW-ESE, E-W, and N-S, which commonly correspond to deep linear valleys. Although some of these lineaments were recognized decades ago (Hack, 1982; Gay, 2000) many more have become apparent after the recent release of LIDAR-based digital elevation models that now cover the entire state of North Carolina (available at https://rmp.nc.gov/sdd/). The topographic lineaments cross from the Piedmont to the Valley and Ridge for over 250 km and are clearly post-Alleghanian structures (Figure 1). Hack (1982) identified and named several of the larger lineaments in the southern Appalachians and described them as trench valleys that affected the geomorphology by a combination of minor offsets and enhanced erosion due to fracturing. Stewart and Dennison (2006) speculated that the lineaments are fault or fracture zones associated with Neogene doming of the southern Appalachians. Working further south from our study area, we found that average strikes of joint surfaces and minor faults within the zone of lineaments are parallel to the lineaments while similar structures outside the lineaments are oblique to the lineament trends (Hill, 2013).

Gillon et al. (2009) identified hundreds of lineaments near Boone, NC and found that intersecting lineaments and metamorphic foliation create unstable blocks that contribute to the high concentration of

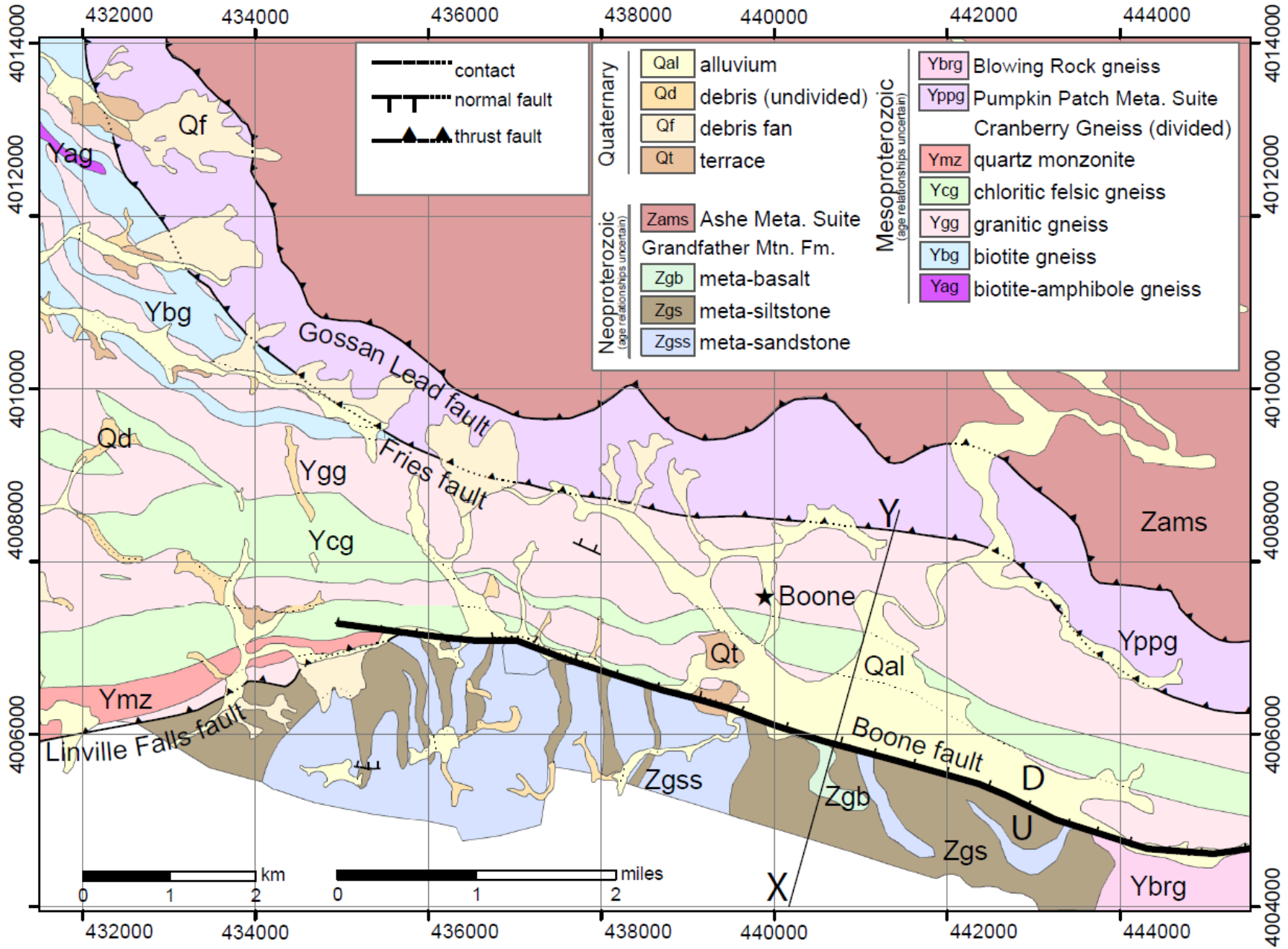

Figure 2: Simplified version of 1:12,000 scale bedrock map, centered on the town of Boone, North Carolina (modified from Hill and Stewart, 2015). The WNW-striking Boone fault separates the basement rocks of the Cranberry Gneiss from the metasedimentary rocks of the Grandfather Mountain formation along what has been previously mapped as the Linville Falls thrust fault. X and Y indicate the cross section line shown in Figure 8.

landslides in this area. In their study, they interpreted the lineaments to be part of a regional network of fractures and faults and were able to show that some had normal, dip-slip motion. They proposed a zone of existing and potential rock slope instability that corresponds strongly with what we have mapped as the Boone fault. A strong correlation between lineaments and slope movement exists at the east end of our study area where the lineaments intersect the Blue Ridge escarpment (Figure 1). The deep reentrant of the escarpment at this location is likely due to the presence of abundant fractures and faults associated with lineaments. The Blue Ridge escarpment has moved westward by stream capture of previously westward-draining headwaters (Prince et al, 2011), a process likely intensified in this area due to the intersection of the escarpment and the fracture-controlled lineaments.

GEOLOGIC BEDROCK MAPPING AND PALEOSTRESS ANALYSIS OF THE BOONE FAULT

Methods

We mapped the Boone fault at the northern edge of the Grandfather Mountain window along a section of what was previously mapped as the Linville Falls thrust fault (Figure 2). We mapped an 80 km^2 area using 560 outcrops as control points. At each location, we made detailed bedrock descriptions and measured the orientation of any metamorphic foliation, joint sets, or faults present. We divided the Cranberry Gneiss north of the window into five subunits, consisting of a quartz monzonite, chloritic felsic gneiss, a granitic gneiss, a biotite gneiss, and a biotite-amphibolite gneiss (see Appendix 2 in Hill (2018) for a detailed description of map units). We drew many of our contacts by walking parallel to the strike of foliation and were able to add detail to the existing maps that contained the Cranberry Gneiss (Bryant and Reed, 1970; Gillon et al., 2009). In the Grandfather Mountain formation, within the window, we divided the rocks into a meta-basalt, a meta-siltstone, and a meta-sandstone. We directed much of our attention to the area where the Cranberry Gneiss is in contact with the Grandfather Mountain formation along what was previously mapped as the Linville Falls thrust fault.

When a fault moves, the slip direction is assumed to be the maximum shear stress direction within the fault plane and is recorded as a fault slickenline (e.g. Twiss and Moores, 2007). One way to simplify the description of the stresses that drive faulting is with principal stress tensors, which describe only normal stresses and no shear stresses. We used a program called WinTensor (Delvaux and Sperner, 2003) to calculate the best-fit principal stress tensors using measured fault planes and slickenlines. Knowing the best-fit principal stresses that drove outcrop-scale faults lets us approximate the mechanism that caused the Boone fault to move. We performed a paleostress inversion of 165 minor brittle faults at four outcrops along its length (Figures 3 and 4) and compared the resultant stress tensors with stress directions known to have caused shortening and rifting events in the study area in an attempt to understand the timing of Boone fault motion. If it formed during NW-directed Paleozoic shortening, the expected stress tensor would show SE-NW maximum- and vertical minimum-compressional stress. Examples of NW-directed shortening structures exist throughout the orogenic belt (e.g. Hibbard et al, 2006). If the fault zone formed during Mesozoic E-W rifting, the stress tensor should have vertical maximum and horizontal E-W minimum compressional stress directions. We hypothesize that the Boone fault may be associated with a regional uplift event that drove upper crustal faulting along the lineaments. In some of our previous work on topographic lineaments cutting across the Appalachians (Hill and Stewart, 2016), we hypothesized that the lineaments accommodated Cenozoic regional doming and blocky uplift by fracturing and minor dip-slip faulting along high-angle surfaces. If the Boone fault is associated with vertical motion along the lineament that contains it, the maximum and minimum principal stresses should obliquely

Figure 3: Photo looking WNW along strike of the Boone fault, where high angle faults visibly cut metamorphic foliation associated with the Linville Falls fault (station 003 in Figure 4). These high angle faults show south-side-up motion consistent with uplift of the Grandfather Mountain window along the Boone fault.

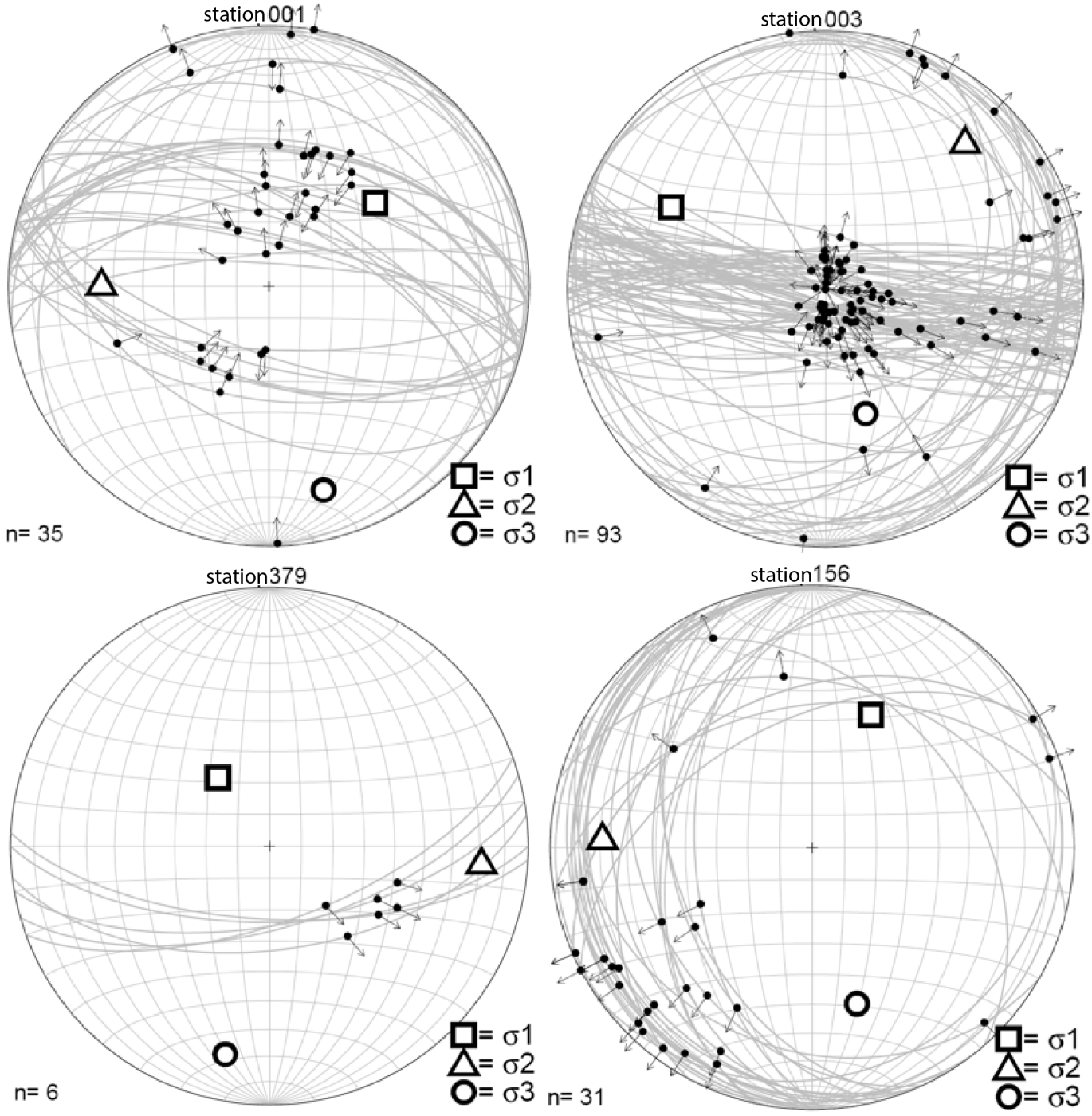

Figure 4: Equal-area, lower-hemisphere plots showing brittle faults (gray lines) with slickenlines (black dots) found along the Boone fault zone. The paleostress inversions yielded the best-fit maximum, intermediate, and minimum (circles, triangles, squares, respectively) compressive stress directions that formed the faults. Arrows on normal faults point towards center and on reverse faults they point away. We are using the engineering convention, where σ3 = maximum compression and σ1 = minimum.

plunge into the fault, and the intermediate principal stress direction should lie within the fault plane.

Results

The brittle fault zone is most evident along a ~10 km topographic scarp south of Boone, NC (Figure 1). Brittle faults within this zone typically dip steeply and strike WNW, and although most occur along the fault scarp that separates the Grandfather Mountain metasedimentary rocks in the south from the Cranberry Gneiss basement rock to the north, some exist several kilometers to the north and south of the main fault zone. There are normal (north-dipping) and reverse (south-dipping) faults and both show south-side-up motion (Figure 3). The majority of the faults we measured had slickenlines indicating dip-slip motion, although some fault surfaces show oblique or strike-

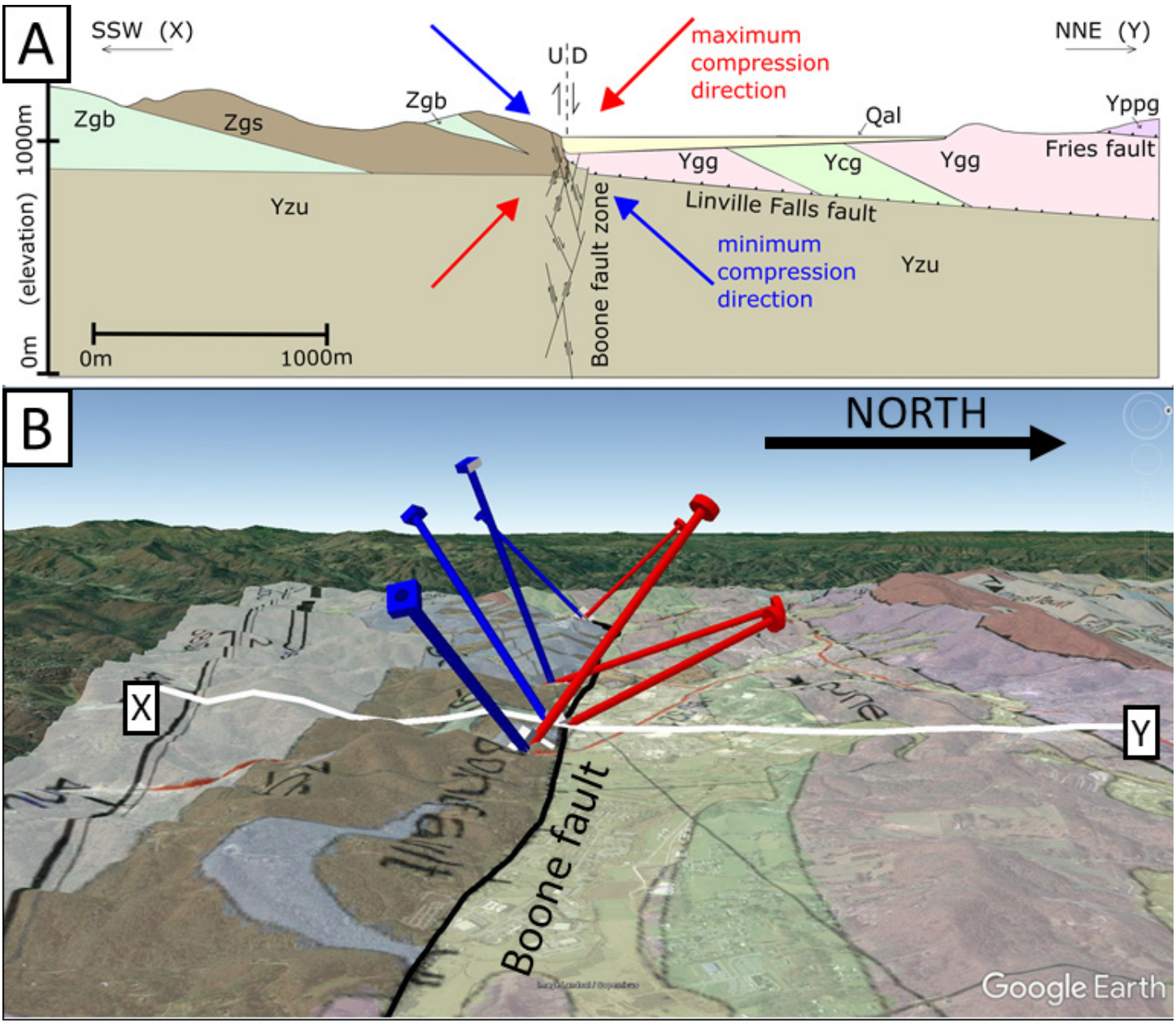

Figure 5: (A) Schematic SSW-NNE bedrock cross section showing best-fit paleostress tensors for high-angle, WNW-striking brittle faults with south-side-up motion along the Boone fault. Although there is some variation in the resultant stress directions at the four outcrops displayed in figure 2.6, the stress tensors are generally consistent with vertical motion. (B) Google Earth image looking westward along strike of the Boone fault (traced as the green line). The 3-D models show the paleostress inversion results as three orthogonal axes. The red (circles) and blue (squares) represent the maximum and minimum compressive stress directions, respectively.

slip senses of shear. Some of the high-angle faults strike N-S, but the majority are parallel to the main topographic scarp (Figure 4).

Faults typically form at ~30° to the maximum compressional direction, where the shear stress is high but the normal stress is low enough for the rocks to fail (Twiss and Moores, 2007). The inversions we performed on the Boone fault yield principal stress tensors with oblique, SSW-plunging maximum and NNE-plunging minimum compression directions. The intermediate principal stress direction is near horizontal and trends parallel to the Boone fault in 3 of the 4 outcrops at which we ran the inversion. This geometry does not fit Paleozoic SE-NW shortening or Mesozoic E-W rifting but is compatible with the south-side-up motion of the Grandfather Mountain window along high-angle, WNW-striking, normal and reverse faults (Figure 5). Based on the inversion results, we can eliminate Paleozoic or Mesozoic as the age of faulting that was recorded by the Boone fault.

Along the Boone fault, there is no mixing of the Cranberry Gneiss and Grandfather Mountain formation, which is different from the Linville Falls fault that bounds the rest of the window (Bryant and Reed,

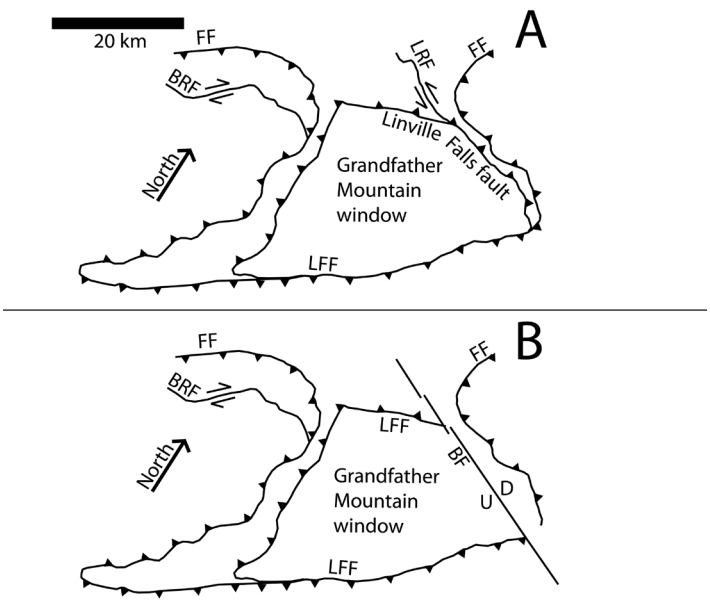

Figure 6: (A) Simplified map of the Grandfather Mountain window and surrounding faults (LFF = Linville Falls fault, FF = Fries fault, LRF = Long Ridge fault; BRF = Burnsville fault). The window was previously interpreted to be bounded on all sides by the Linville Falls fault. These contacts were modified from Hibbard et al. (2006). (B) Map of study area showing the Boone fault (BF) with south-side-up motion of along what was previously mapped as a section of the Linville Falls and the Long Ridge faults.

1970). The Boone fault and related fractures crosscut the mylonitic fabric associated with older Linville Falls fault-related foliation, which we interpret to mean the Boone fault moved along new failure surfaces rather than those of the Linville Falls fault. Adams and Su (1996) noted how the Cranberry Gneiss is separated from the Grandfather Mountain metasedimentary rocks by a structural discordance and noted the abrupt lithologic change between the two packages of rocks. Based on the brittle fault contact and the paleostress tensors that are consistent with vertical motion along WNW-striking faults, we interpret the Boone fault as a high-angle fault zone that has cut the southern edge of the Linville Falls shear zone and uplifted the northern edge of the Grandfather Mountain window.

At one outcrop along the Boone fault (Figure 4, station 156), there are abundant dip-slip brittle faults that strike predominantly N-S, but the resultant stress tensor is very similar to the best-fit tensors found at the outcrops containing WNW- and W-striking faults (Figure 4, stations 001, 003, and 379). We interpret the faults at station 156 to have formed within the same stress field as the rest of our other Boone fault sites did, and possibly pre-existing planes of weakness influenced the orientation of faulting.

We propose that the ~10 km of the Boone fault we mapped along the northeastern edge of the Grandfather Mountain window is part of the ~180 km long and 20 km wide regional-scale topographic lineament swarm spanning from the Valley and Ridge in Tennessee to the Piedmont in North Carolina (Figure 1). The topographic scarp along the Boone fault is one of many en echelon segments of the Boone lineament swarm, which may include stretches of the Long Ridge thrust fault to the west of our main study

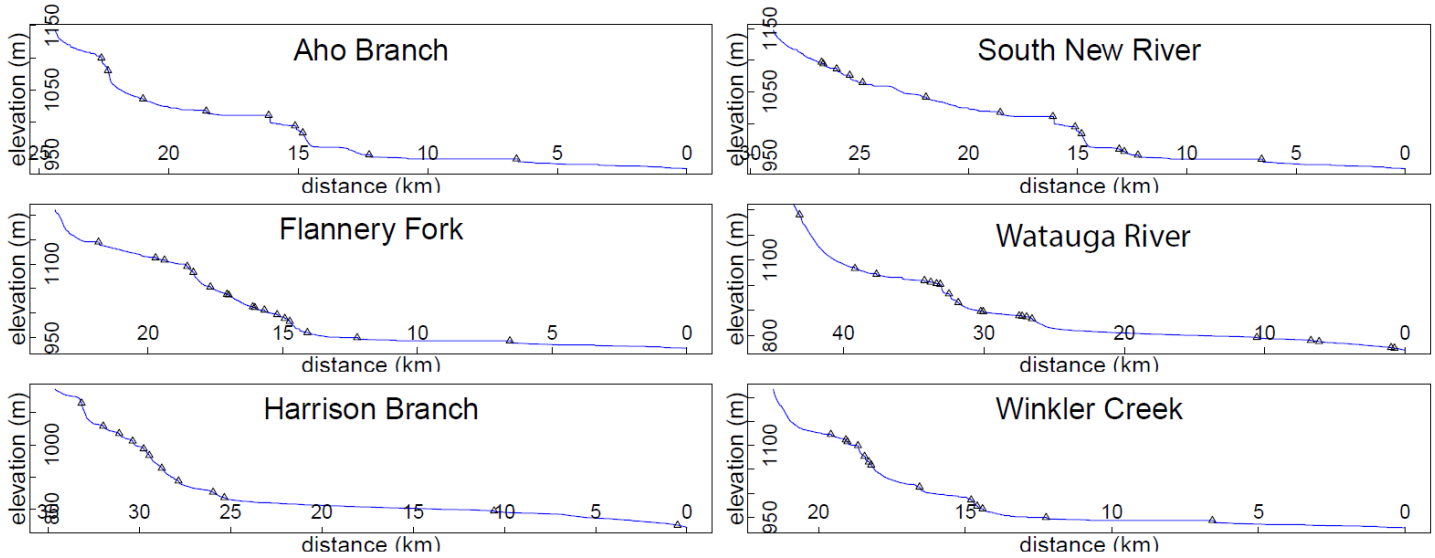

Figure 7: Six longitudinal profiles from streams that drain into the Boone fault and contain a similar pattern of knickpoints, likely from recent vertical motion on the fault. The major slope break on these profiles is between 200-400 m above the valley floor, indicating there has likely been that amount of uplift since the streams were at equilibrium. We analyzed dozens of other river profiles with similar geometries, shown on the map in Figure 8.

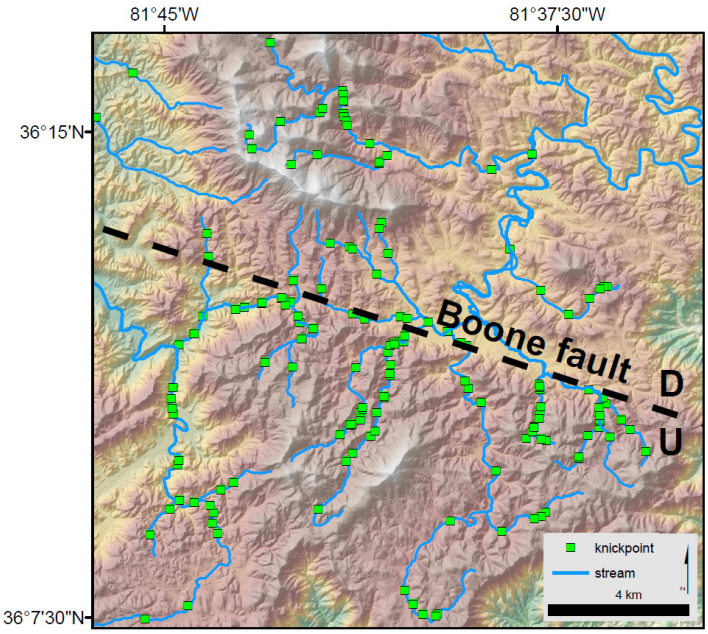

Figure 8: Digital elevation model showing streams with knickpoints that drain from the high plateau above the Boone fault. Note the hook-shaped headwaters of the streams in the southern part of the map, which we interpret as a result of stream capture related to south-side-up motion along the Boone fault.

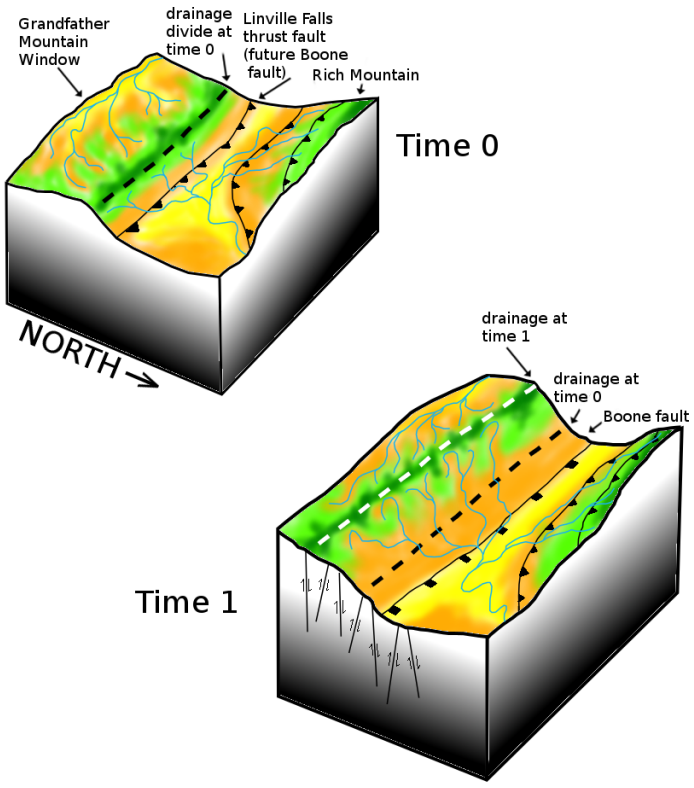

Figure 9: Block diagram illustrating how uplift on the Boone fault could have driven drainage divide migration and led to the formation of the hook-shaped drainage patterns observed in the headwaters above the fault zone.

area (Figure 6). Other WNW-trending faults and bedrock contacts are parallel and along strike of the Boone fault in many parts of the lineament swarm, such as where the Stone Mountain fault offsets the Beech Granite (Bryant and Reed, 1970). This regional fracture and fault zone likely accommodated uplift of the southern Appalachians along many vertical and near-vertical surfaces, some of which have been previously interpreted as brittle Alleghanian faults that moved during alternating ductile and brittle deformation stages during Pangean assembly (Adams and Su, 1996; Stewart et al., 1997).

GEOMORPHIC EVIDENCE FOR CENOZOIC MOTION ALONG THE BOONE FAULT

Methods

In addition to bedrock mapping, we assessed the geomorphology around the Boone fault for any evidence of recent motion. To do this, we mapped slope-movements deposits as either undivided debris flows or debris fans, as well as any alluvium and terrace deposits present (Figure 2). We also obtained LIDAR from the North Carolina Spatial Data Download (https://rmp.nc.gov/sdd/) to analyze the longitudinal profiles of dozens of streams draining into the fault zone (Figure 7). Using an automated knickpoint selection process, we searched for knickpoints along dozens of streams that drain into the Boone fault zone. We investigated the map view patterns of the streams surrounding the Boone fault for evidence of drainage capture (Figure 8). We hypothesized that the high alluvial valleys we mapped in the Grandfather Mountain window are relict landscapes that were likely part of ancient river system (Figure 9). To test this idea, we produced an elevation histogram of the streams in Watauga County (Figure 10), assuming that in mountainous terrain, flat areas such as river valleys would show a high frequency of points at the elevation of the valley.

Results

Many of the surficial deposits we mapped are consistent with a landscape responding to recent uplift. There are abundant debris deposits (Qd) throughout the study area with patches of young trees above noticeable lobes of debris toes. There are also many "pistol butt" shaped trees, an indication that the hillslopes are experiencing active creep (Ven Den Eeckhaut et al., 2009). We found numerous knickpoints (n=178) hundreds of meters above the valley floor (Figure 7), suggesting that the Boone fault ac-

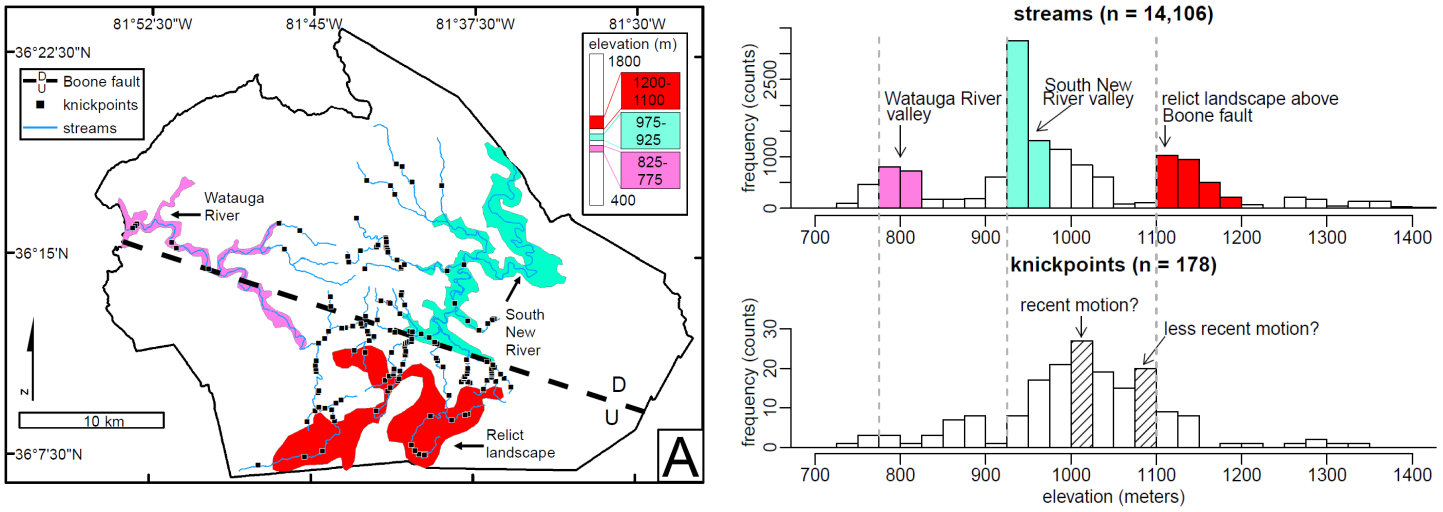

Figure 10: (A) Map of Watauga County showing three zones of flat topography: the Watauga River valley (pink), the South New River valley (cyan), and what we interpret as a relict river valley uplifted as a result of motion along the Boone fault (red). (B) Elevation histogram of the streams we analyzed, which are in three modes corresponding to the three valleys. The knickpoints are at two elevation modes between the South New River and the relict valley above the Boone fault, suggesting multiple pulses of motion on the Boone fault.

commodated ~ 200 m of uplift since the streams were in equilibrium. There is no trend between the location of the knickpoints and lithologic contacts, but they appear in two main modes of elevation. In addition to the disequilibrium longitudinal profiles, some of the headwater streams that drain into the Boone fault have hook-shaped patterns (Figure 8), indicative of drainage capture events.

There are two main river systems draining away from the Boone fault zone, the South New River to the east and the Watauga River to the west (Figure 10). These two river systems contain much of the flat topography of Watauga county and are the locations of the majority of human development around Boone. These two active rivers have flat valleys in Watauga County at ~950 m and ~800 m, accordingly, as evident in the histogram of stream elevations (Figure 10). There is a third mode of stream elevation points at ~1100 m that does not correspond with any known river valley but is immediately above the highest group of knickpoints (Figure 10).

Gillon et al. (2009) documented hundreds of slope-movement events in Watauga County, and many of these are concentrated in a zone of rock slope instability that corresponds with the Boone fault on our map. A few kilometers north of our map, Mills and Granger (2002) used cosmogenic isotopic burial age dating techniques to estimate major debris fans (Qf) on the west slopes of Rich Mountain to be as young as 1.45 Ma. The abundance of modern debris deposits suggests that the landscape is still adjusting to uplift, and the proximity to the Boone fault suggests that unstable slopes may be a result of young faulting. Terrace deposits near the Boone fault may also be remnants of floodplains abandoned due to recent uplift.

The South New River forms a large alluvial valley whose southern edge is defined by the topographic escarpment along the Boone fault, but many smaller floodplains exist to the south of the Boone fault within the Grandfather Mountain window. We interpret these to be uplifted ancient floodplains raised during the south-side-up motion of the Boone fault. There is a pattern of alternating steep-flat-steep-flat topography in the proposed uplifted landscape to the south of the Boone fault. The histogram of stream elevation has modes that correspond to the South New and Watauga Rivers, as well as a third mode that we think is related to the relict landscape above the Boone fault (Figure 10). The streams draining away from this uplifted surface are actively dissecting it by migration of the knickpoints along north-draining streams. This idea is supported by the histogram of knickpoint elevations, which shows knickpoints in two clusters between the South New River valley and the uplifted valley at 1000 m and 1100 m (Figure 10). This distribution of knickpoint elevations could represent multiple pulses of uplift along the Boone fault, where each event caused a base level change and sent a new series of knickpoints upstream. Similar stream profiles have been described in the Sierra Nevada of California, where multiple phases of uplift resulted in a relict landscape in the highest reaches of the streams and an intermediate landscape between the headwaters and the mouth (Clark et al., 2005).

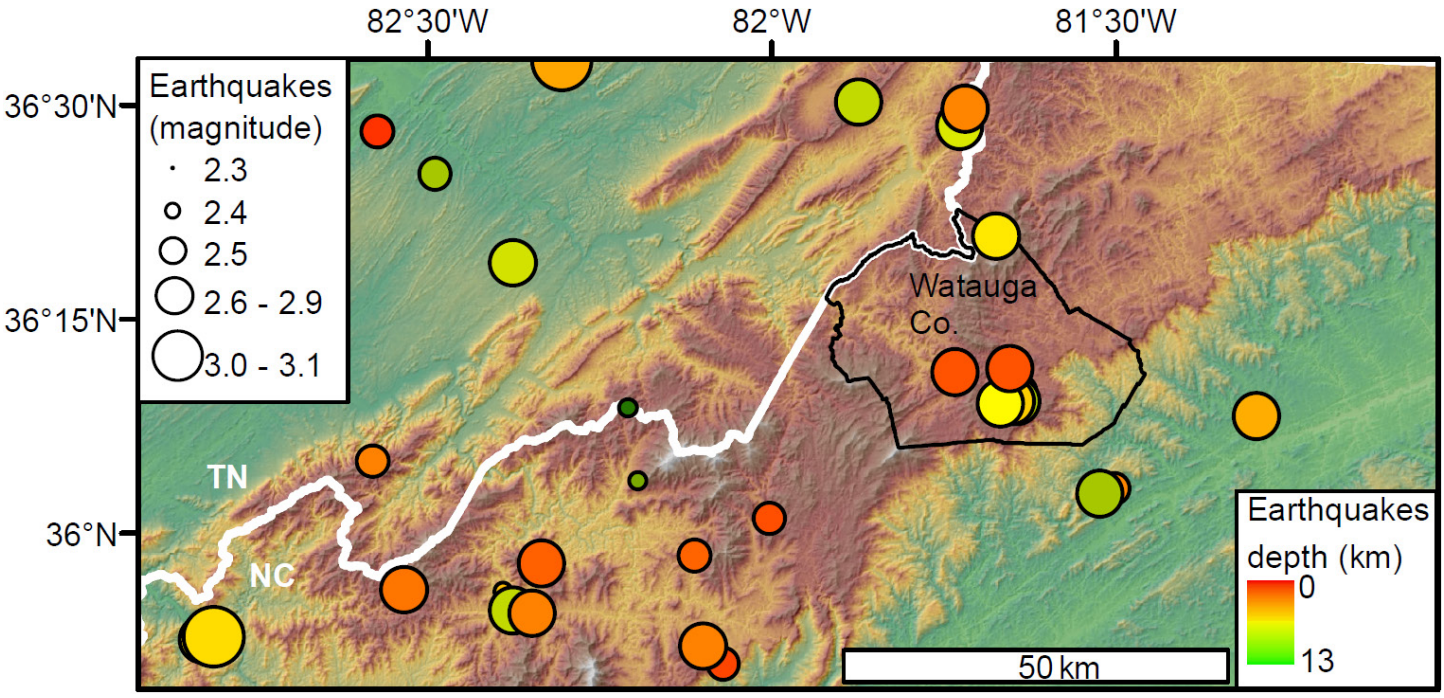

Figure 11: HydroSHEDS digital elevation model of eastern Tennessee and western North Carolina showing the WNW-trending Boone lineament that stretches over 180 km from the Valley and Ridge eastward to the Piedmont province. The circles represent earthquake epicenters (NEIC, 1973-2018), many of which are along the Boone lineament or the E-W Laurel Creek lineament in the southern part of the image.

We interpret the hook-shaped streams as evidence of drainage capture related to uplift of the landscape to the south of the fault (Figure 9). We think the hook-shaped headwaters in our study area imply that the high plateau to south of the Boone fault may still be in flux, and the presence of the hooks suggests that there may be other faults to the south that allowed the plateau to move upward. Similar hook-shaped map-view stream patterns exist where headwater streams have been captured by the migration of the eastern continental divide along the Blue Ridge Escarpment (Prince et al., 2011).

MODERN SEISMICITY AND SURFACE DEFORMATION NEAR THE BOONE FAULT

There have been minor earthquakes within and near the study area in recent years (NEIC, 2018). These events ranged from 2.3 to 3.1 in magnitude and from 1.0 to 12.7 km in depth (Figure 11). Forming a cluster near the newly mapped Boone fault, four events from 2013 and 2014 have hypocenters that align in an E-W direction, sub-parallel to the main Boone fault zone. Three of the four hypocenters lie on a plane at different depths, which is consistent with the possibility of a vertical fault plane. During the June 2014 event (M = 2.5 and depth = 6.7 km), shaking at depth led to slope movement and deformation at the surface. Although the seismicity was too small and too deep to produce a surface rupture, motion on the fault at depth triggered shaking and deformation at the surface in the form of a cracked building foundation, sidewalk, and retaining wall. At the same location, a tree was split in two, a loud sound was heard and interpreted as a truck hitting the building, a fissure formed in the hillslope, and a crack propagated across US hwy. 321 (Randy McCoy, oral communication, 2016). During the August 2014 event (M = 2.9 and depth = 9.4 km), shaking caused a foundation to crack on a house located ~8km to the WNW of the epicenter, near one of the smaller normal fault segments we mapped to the south of the main fault zone (Doug Harker, oral communication, 2017). These events mean the Boone fault is a post-orogenic fault zone that may be still active.

AGE OF THE BOONE FAULT

The high-angle Boone fault cuts the NW-dipping foliation of the Linville Falls shear zone, and the orientations of the best-fit principal stress tensors do not match the stresses that drove Paleozoic NW-directed shortening, thus the Boone fault is younger than the Linville falls shear zone. The resultant paleostress directions are also inconsistent from those that formed the generally N-S and NNE-SWW-striking Triassic normal faults or NNE-SSW-trending Jurassic diabase swarms found in the North Carolina Piedmont and

Blue Ridge, which means the Boone fault must be post-Jurassic. While the stress inversions alone are not enough to eliminate the Late Mesozoic or Early Cenozoic as possible ages of the Boone fault, our geomorphic and seismic analyses support a Late Cenozoic age.

The rivers draining into the Boone fault zone contain longitudinal profiles similar to streams Gallen et al. (2013) interpreted to have recorded 100s of meters of Neogene uplift of the North Carolina Blue Ridge. The streams analyzed by Gallen et al. (2013) drain into topographic lineaments and contain knickpoints at elevations between 900 m and 1200 m that separate active and relict landscapes hundreds of meters above the stream mouths. The similarities in the knickpoint locations and longitudinal geometries to the streams around Boone allow us to speculate that the vertical motion on the Boone fault likely began in the Neogene and has been recorded by a series of transient knickpoints currently located in the headwaters. This timing of fault initiation matches the increase in offshore sedimentation (Poag and Savon, 1989) and folding of Coastal plain sediments during the Neogene (Stewart, 2015), and we interpret the Boone fault as having helped accommodate Late Cenozoic doming and blocky uplift of the southern Appalachians.

Based on modern seismicity, the Boone fault may be active (NEIC, 1973-2018). We propose that it is the driving mechanism for the unstable landscapes around the Town of Boone. To our knowledge, the Boone fault is the first seismically active fault documented in the western North Carolina Blue Ridge.

CONCLUSIONS

In this paper, we present data consistent with a landscape responding to recent uplift, not one that has been steadily eroding since the Paleozoic. The Boone fault is a steeply dipping fault zone that accommodated south-side-up motion of the northern edge of the Grandfather Mountain window. We interpret the 10-km long Boone fault as a minor part of the ~180 km-long and ~20 km-wide Boone lineament swarm. The young faults and disequilibrium landscape suggest the Grandfather Mountain window is not entirely framed by a Paleozoic fault, but rather is bounded in part by a Neogene fault zone. There is abundant evidence that the southern Appalachians were uplifted in the Neogene, and to our knowledge, the Boone fault zone is the first mappable Blue Ridge structure attributed to late Cenozoic topographic rejuvenation. The evidence for young topography and Cenozoic tectonics related to the Boone fault we present is four-fold: (1) the WNW-brittle faults do not fit known tectonic events based on stress inversions; (2) the streams draining into the Boone fault contain abundant knickpoints and are similar to other Neogene knickpoints; (3) the hook-shaped headwaters south of the Boone fault are consistent with major drainage reorganization; and (4) the active seismicity associated with surface deformation near the fault zone implies that the Boone fault is potentially still active. We propose that the Boone lineament and other lineaments of similar size and orientation formed during blocky, Late Cenozoic uplift of the orogen associated with delamination of the lithospheric root (see Hill et al., this volume). Based on our work, the rapidly-growing mountain community of Boone should regard the Boone fault zone as potentially active when making future land use plans.

REFERENCES

Adams, M. G. and Su, Q., 1996, The nature and timing of deformation in the Beech Mountain thrust sheet between the Grandfather Mountain and Mountain City windows in the Blue Ridge of Northwestern North Carolina: Journal of Geology, v. 104, p. 197-213.

Boyer, S. E. and Elliot, D., 1982, Thrust Systems: American Association of Petroleum Geologists Bulletin, v. 66, no. 9, p. 1196-1230.

Bryant, B. and Reed, J.C., 1970, Geology of the Grandfather Mountain window and vicinity, North Carolina and Tennessee: U.S. Geological Survey, Professional Paper 615, scale 1:62,500.

Burton, W. C. and Southworth, S., 2010, A model for Iapetan rifting of Laurentia based on Neoproterozoic dikes and related rocks: Geological Society of America Memoir, v. 206, p.455- 476.

Clark, M. K., Maheo, G., Saleeby, J., and Farley, K. A., 2005, The non-equilibrium landscape of the southern Sierra Nevada, California: GSA Today, v. 15, no. 9, p. 4-10.

Delvaux, D. and Sperner, B., 2003, New aspects of tectonic stress inversion with reference to the TENSOR program, in New Insights into Structural Interpretation and Modelling (D. Nieuwland, ed.): Geological Society of London, Special Publication 212, p.75-100.

Dennison, J. M and Stewart, K. G., 2001, Regional structural and stratigraphic evidence for dating Cenozoic uplift of Southern Appalachian highlands: Geological Society of America, , Abstracts with Programs, Vol. 33, No. 6.

Gallen, S. F., Wegmann, K.W., and Bohnenstiehl, D. R., 2013, Neogene rejuvenation of topographic relief in the southern Appalachians: GSA Today, v. 23, no. 2, p. 4-10.

Galloway, W. E., Whiteaker, T. L., and Ganey-Curry, P., 2011, History of Cenozoic North American drainage basin evolution, sediment yield, and accumulation in the Gulf of Mexico basin: Geosphere, v. 7, no. 4, p. 938–973.

Gay, P. S., Jr., 2000, Unmapped topographic alignments visible on 3D stereo terrain map of a 2 degrees X 2 degrees segment of the Southern Appalachians: Geological Society of

America Abstracts with Programs, v. 32, no. 2, p.19.
Gillon, K.A., Wooten, R.M., Latham R.L, Witt A.W., Douglas, T.J., Bauer, J.B., and Fuemmeler, S.J, 2009, Integrating GIS-Based Geologic Mapping, LiDAR-Based Lineament Analysis and Site Specific Rock Slope Data to Delineate a Zone of Existing and Potential Rock Slope Instability Located Along the Grandfather Mountain Window-Linville Falls Shear Zone Contact, Southern Appalachian Mountains, Watauga County, North Carolina: American Rock Mechanics Association ARMA 09-18.
Faill, R. T., 1997, A geologic history of the north-central Appalachians. Part 1. Orogenesis from the Mesoproterozoic through the Taconic orogeny: American Journal of Science, v. 297, p. 551-619.
Hack, J. T., 1982, Physiographic divisions and differential uplift in the Piedmont and Blue Ridge: Geological Survey Professional Paper 1265, 49 p.
Hatcher, R. D. Jr., Merschat, A. J., and Thigpen, J. R., 2005, A Blue Ridge Primer, in Blue Ridge Geology Geotraverse East of the Great Smoky Mountains National Park, Western North Carolina, Hatcher, R. D., Jr., and Merschat, A. J., eds.: Carolina Geological Society Annual Field Trip Guidebook.
Hibbard, J. P., van Staal, C.R., Rankin, D.W., and Williams, H., 2006, Lithotectonic map of the Appalachian Orogen, Canada-United States of America: Geological Survey of Canada, Map 2096A, scale 1:500,000.
Hibbard, J. P., van Staal, Cees R., and Rankin, Douglas W., 2010,Comparative analysis of the geological evolution of the northern and southern Appalachian orogen: Late Ordovician-Permian: Geological Society of America Memoir, v. 206, p. 51-69.
Hill, J. S., 2013, Zoned uplift of western North Carolina bounded by topographic lineaments: M.S. Thesis, University of North Carolina at Chapel Hill, 51 p.
Hill, J.S, 2018, Post-orogenic uplift, young faults, and mantle reorganization in the Appalachians, PhD Dissertation, University of N.C. Chapel Hill, 139 p.
Hill, J. S., and Stewart, K. G., 2016, A newly discovered fault zone near Boone, North Carolina and Cenozoic topographic rejuvenation of the southern Appalachian Mountains: Geological Society of America Abstracts with Programs, v. 48, no. 7.
Hill, J. S. and Stewart, K. G., 2018, Young topography, new faults, and mantle reorganization in an ancient mountain range: A case study from the Appalachians: Geological Society of America Abstracts with Programs, v. 50, no. 3.
Li, Z.X., Bogdanova S.V., Collins A.S., Davidson A., De Waele B., Ernst R.E., Fitzsimons, Fuck, R.A., Gladkochub D.P., Jacobs J., Karlstrom K.E., Lul, S., Natapovm L.M., Pease, V., Pisarevsky S.A., Thrane K., and Vernikovsky V., 2008, Assembly, configuration, and break-up history of Rodinia: A synthesis: Precambrian Research 160, no. 1, p 179-210.
Merschat, A. J., Hatcher, R. D. Jr., and Davis, T. L., 2005, The northern Inner Piedmont, southern Appalachians, USA: kinematics of transpression and SW-directed mid-crustal flow: Journal of Structural Geology v. 27. p. 1252-1281.
Miller, B. V., Fetter, Allen H., and Stewart, Kevin G., 2006, Plutonism in three orogenic pulses, Eastern Blue Ridge Province, southern Appalachians: Geological Society of America Bulletin, v. 118, no. 1/2, p.171-184.
Miller, S. R., Sak, B., Kirby, E., and Bierman, P. R., 2013, Neogene rejuvenation of central Appalachian topography: Evidence for differential rock uplift from stream profiles and erosion rates: Earth and Planetary Science Letters, v. 369-370, p. 1-12.
Mills, H. H., and Granger, D. E., 2002, Cosmogenic isotope burial dating reveals 1.5 million-year-old fan deposit in Blue Ridge Mountains of North Carolina: Geological Society of America Abstracts with Programs, v. 34, No. 2, p. 32.
National Earthquake Information Center (2018): http://earthquake.usgs.gov/regional/neic/
Nystrom, P., 1986, Late Cretaceous-Cenozoic brittle faulting beneath the western South Carolina coastal plain; reactivation of the eastern Piedmont fault system: Geological Society of America Abstracts with Programs, v. 38, no. 3, p. 74.
North Carolina Geological Survey, 1985, Geologic Map of North Carolina, 1:500,000 scale.
Poag, W. C., and Sevon, W. D., 1989, A record of Appalachian denudation in post-rift Mesozoic and Cenozoic sedimentary deposits of the U.S. middle Atlantic continental margin: Geomorphology, v. 2, p. 119-157.
Prince, P. S., Spotila, J. A., and Henika, W. S., 2011, Stream capture as a driver of transient landscape evolution in a tectonically quiescent setting: Geology, v. 39, no. 9, p. 823-826.
Spotila, J. A., Bank, G. C., Reiners, P. W., Naeser, C. W., Naeser, N. D., and Henika, W. S., 2004, Origin of the Blue Ridge escarpment along the passive margin of Eastern North America: Basin Research, v. 16, p. 41-63.
Stewart, K. G., Adams, M. G., Trupe, C. H., 1997, Paleozoic structure, metamorphism, and tectonics of the Blue Ridge of western North Carolina: Carolina Geological Society, 1997 Field Trip Guidebook, 101 p.
Stewart, K. G., and Dennison, J. M., 2006, Tertiary-to-recent arching and the age and origin of fracture-controlled lineaments in the southern Appalachians: Geological Society of America Abstracts with Programs, v. 38. no. 3., p. 27.
Stewart, K. G., 2015, Estimates on the magnitude and timing of post-orogenic topographic rejuvenation of the southern Appalachians using isostasy and deformed Coastal Plain rocks: Geological Society of America Abstracts with Programs, v. 47, no. 2, p. 82.
Trupe, C. H., Stewart, K. G., Adams, M. G., and Foudy, J. P., 2004, Deciphering the Grenville of the southern Appalachians through evaluation of the post-Grenville tectonic history in northwestern North Carolina: Geological Society of America Memoir 197, p. 679-695.
Tull, J. F., Allison, D. T., Whiting, S. E., John, N. L., 2010, Southern Appalachian Laurentian margin initial drift-facies sequences: Implications for margin evolution: Geological Society of America Memoir 206, p. 935-956.
Twiss, R. J., and Moores, E. M., 2007, Structural Geology, 2nd Edition; W. H. Freeman and Company, New York, 736 p.
Van Den Eeckhaut, M., Muys, B., Van Loy, K., Poesen, J., and Beeckman, H., 2009, Evidence for repeated re-activation of old landslides under forest: Earth Surface Processes and Landforms, v. 34, p. 352-365.

Mantle motion and topographic rejuvenation in the Southern and Central Appalachians

Jesse S. Hill
Kevin G. Stewart
C. Berk Biryol

Department of Geological Sciences, University of North Carolina - Chapel Hill, Chapel Hill, NC 27599

INTRODUCTION

The high topography of the southern and central Appalachians does not coincide with the physiographic provinces but instead cuts across them. This band of rugged topography correlates to areas of high slope and local relief in the Appalachian Plateau of Pennsylvania, the Valley and Ridge of Virginia and West Virginia, and in the Blue Ridge of North Carolina. We present geomorphic maps to show that the surface of the Appalachians does not always match the underlying bedrock geology and believe that although currently located at a passive margin, this ancient orogen has undergone uplift likely associated with a delaminating lithosphere. To support our claim that the topography is partly controlled by rearrangement of the mantle, we compare our surface maps to tomographic maps ranging from 36 to 915 km depth. There is a reasonably good fit between the swath of high topography and a seismic anomaly that was recently interpreted as a piece of lithosphere descending into the mantle (Biryol et al., 2016). It is our interpretation that upper mantle reorganization has driven a Cenozoic rejuvenation of topography and caused many of the structures and landforms that would not exist if the ancient orogenic belt has been eroding steadily since the Paleozoic. If mantle motion is the main driver of the current landscape, it may also be responsible for the formation of the anomalous topographic lineaments that cross the mountain belt and correspond to young faults and align with clusters of earthquake epicenters. We support our claim that mantle reorganization is the cause of topographic rejuvenation by showing that removal of an eclogitic root 15-25 km thick would uplift the lithosphere between 450-750m, which is consistent with uplift estimates previously derived from geomorphic studies.

Ideas of how landscapes respond to orogenesis have evolved over time (e.g. Davis, 1899; Penck, 1953; Hack, 1975). When mountains form through the interaction of tectonic plates, they grow in elevation until they collapse due to their own weight, or are eroded away after tectonic processes cease (e.g. Teng, 1996). Burbank and Anderson (2012) described an unrelenting competition between tectonic and erosional processes that build up and break down the crust. Although much of the mountain topography forms either at the plate margins or when plates rift, intraplate relief can be generated in ways that are not fully clear. To better understand how intraplate mountains can exist long after orogenesis, we focused on the southern and central Appalachians, an ancient mountain range with a long history of both uplift and erosion.

The Appalachians have experienced multiple Wilson cycles over the past billion years and although currently located at a passive margin, this ancient orogen has rugged, high topography. While many landscape features can be attributed to the underlying local lithology, the topography and relief in each of the major physiographic provinces varies by up to a kilometer along the orogen (e.g. McKeon, et al, 2014). The Blue Ridge is much higher and has far greater relief in North Carolina than in Virginia, Maryland, or Pennsylvania (Figure 1). The Valley and Ridge is mountainous in Virginia but forms rolling hills in Tennessee and Pennsylvania. Likewise, the Appalachian Plateau in West Virginia and southern Pennsylvania is much higher than its southern counterparts. The mismatch between elevation and lithology along the mountain belt offers an excellent opportunity to improve our understanding of post-orogenic landscapes.

The main focus of this paper is to understand what mechanisms could generate the topography of the modern Appalachians. We compared maps of slope, local relief, and topography with lithologic boundaries and to test for a connection between our surficial observations and mantle dynamics, we overlaid elevation contours onto seismic tomography slices showing P-wave perturbations ranging from 36 km to 915 km depth (Biryol et al., 2016). We performed isostacy calculations to test for a causal link between mantle motion and the topography and to compare the amount of Neogene uplift estimated by Hill (2013), Gallen et al., (2013), and Miller et al., (2013) with the predicted uplift magnitude that would result from delamination of an eclogitic crustal root.

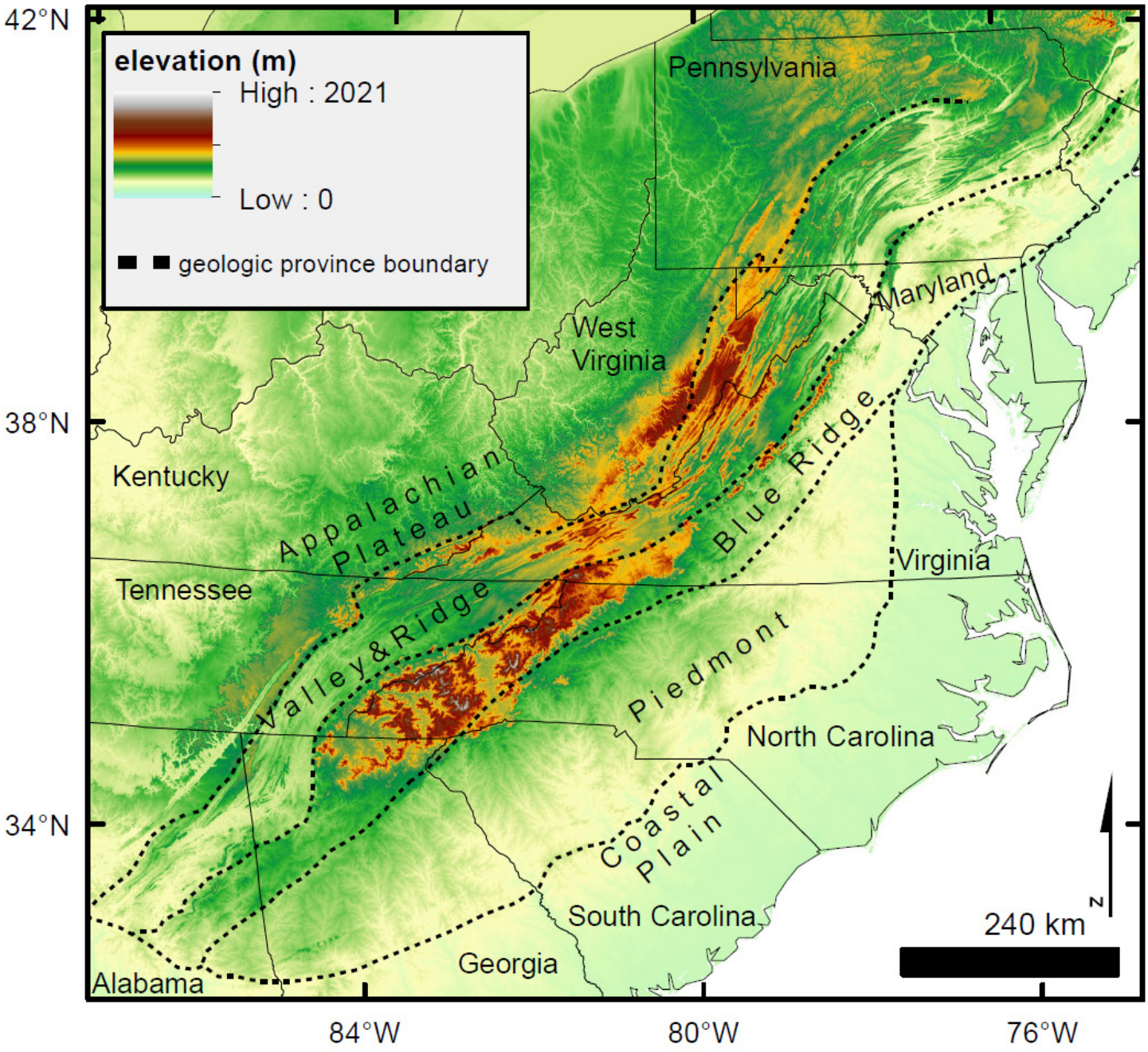

Figure 1: Digital elevation model of the southern and central Appalachians derived from HydroSHEDS data with ~90m horizontal resolution. The dashed black lines separate major geologic provinces (modified from Hibbard et al., 2006). Note the swath of high topography that starts in the Blue Ridge of North Carolina, crosses into the Valley and Ridge of Virginia, then ends in the Appalachian Plateau of West Virginia and Pennsylvania.

BACKGROUND

Sedimentological evidence for Post-Paleozoic uplift

Along the eastern seaboard of North America, there is offshore-sedimentological evidence that the mountain range has experienced multiple episodes of Mesozoic and Cenozoic topographic rejuvenation (e.g. Poag and Savon, 1989; Pazzaglia and Brandon, 1996). Although the Appalachians likely had 3.5-4.5 km of average relief by the end of the Alleghanian orogeny (Slingerland and Furlong, 1989), the post-Paleozoic story is not simply erosion wearing down the orogen to its current form. Poag and Savon (1989) showed that increased Atlantic sedimentation occurred in five pulses during the Middle Jurassic, the Early and Late Cretaceous, the Middle Miocene, and in the Quaternary. The grain sizes of sediments deposited in the Gulf of Mexico increased during the Middle Miocene (Galloway et al., 2011). Increased sedimentation and grain size in the Middle Miocene is likely the result of regional uplift that contributed material to streams

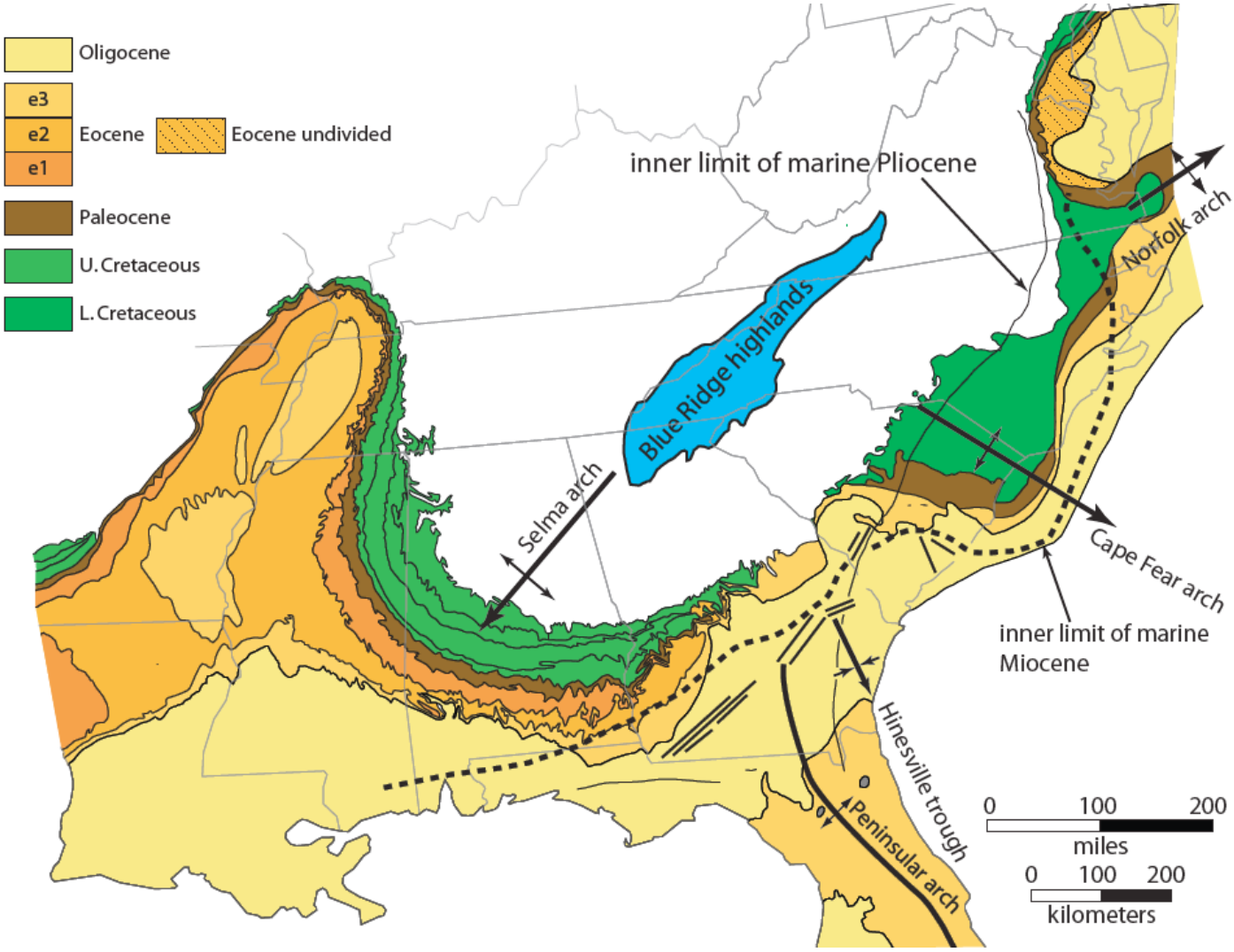

Figure 2: Map of structural arches across the southeastern US likely associated with Cenozoic uplift. Note the folded Cretaceous rocks unconformably overlain by Paleocene strata. There are also pinching out of the folded Oligocene and Eocene rocks, suggesting multiple phases of Cenozoic uplift (Stewart, 2015).

draining to both the east and west of the continental divide (Gallen et al., 2013). There is also evidence of late Cenozoic uplift of the mountain belt found in continental sedimentary records. In the Coastal Plain of South Carolina, Miocene coarse-grained conglomerates contain clasts from the Blue Ridge and Piedmont provinces (Nystrom, 1986). In southern Florida, coarse-grained Miocene rocks contain metamorphic clasts up to 5 cm that likely traveled over 700 km from their source (Missimer et al., 2014).

Stratigraphic evidence for Post-Paleozoic arching

Multiple phases of Cenozoic deformation have been recorded in the stratigraphy of the Coastal Plain. Stewart (2015) presented evidence for uplift in the Paleocene and the Miocene at the southern terminus of the mountains as the Selma arch, where Eocene rocks lie unconformably above folded Cretaceous and Paleocene units, and flat-lying Miocene rocks are above folded Oligocene sedimentary layers. In southern Florida, Maliva et al. (2006) used drill-core records to show up to 100m of arching of Middle Miocene rocks covered by Late Miocene and Early Pliocene rocks. Near the fall line of eastern North Carolina and southern Virginia, faults offset Miocene and older strata but are crossed by late Miocene rocks, indicating vertical motion around 8 Ma (Weems et al., 2009). Rowley et al. (2013) interpreted folded topographic scarps in the Coastal Plain as previously horizontal Atlantic shorelines that warped around 3.5 Ma and now have at least 60 m of elevation variation. The Cape Fear arch is a prominent feature with stratigraphic evidence of uplift ranging from the late Mesozoic through the late Cenozoic (e.g. Popenoe, 1985; Soller, 1988; Gardner, 1989; Ward et al, 1991) including into the modern day (Van de Plassche et al, 2014).

Geomorphic evidence for a landscape out of equilibrium

When a landscape is uplifted, the streams draining away from it preserve a record of base level change in the form of knickpoints, or slope breaks along the river profiles (e.g. Whipple and Tucker, 1999). These geomorphic indicators can be used to estimate the timing and magnitude of uplift. These estimates are derived from reconstructed longitudinal river profiles that contain knickpoints and separate active landscapes downstream from relict, uplifted surfaces upstream. In the southern and central Appalachians, many streams with knickpoints are actively eroding high and flat surfaces interpreted as uplifted floodplains by Hack (1982). In western North Carolina, Gallen et al. (2013) used knickpoint locations above the stream mouth and erosion rates to calculate that the knickpoints along the Cullasaja River and its tributaries initiated ~8.5 Ma in response to ~480m of base level change associated with epeirogenic uplift of the Appalachians. In our previous work (Hill, 2013), we studied the Santeetlah Creek basin, which is close to the Cullasaja River and also contains a series of knickpoints separating a high plateau upstream from steep rivers downstream. We estimated that the Santeetlah Creek knickpoints are migrating upstream in response to as much as 750 m of uplift, and based on similarities in geometry, general proximity, and a common local base level to the Cullasaja, we interpreted these knickpoints to also have initiated in the Miocene (see Ch. 1 of this dissertation for a detailed discussion of these knickpoints). In a study of the Susquehanna River in Pennsylvania, Miller et al. (2013) showed that a series of knickpoints are migrating upstream in response to ~150m of uplift that began between 3.5-15 Ma. They also used cosmogenic isotopes to calculate erosion rates upstream and downstream of knickpoints and found that erosion is much greater downstream. The fore-mentioned knickpoints in North Carolina are along streams draining to the Gulf of Mexico from high surfaces in the Blue Ridge province, while those in Pennsylvania are draining from the Appalachian Plateau towards the Atlantic Ocean, suggesting that landscapes on both sides of the continental divide are out of equilibrium.

Low-temperature geochronology can be used to estimate the timing and rates of exhumation based on (U-Th)/He ratios and annealing of fission tracks in apatite grains (e.g. Green et al., 1986; Boettcher and Milliken, 1994; Flowers et al., 2007). In a low-temperature geochronology study of the southern and central Appalachians, McKeon et al. (2014) analyzed samples from hilltops and valleys, and postulated that relief was increased during the Cretaceous, when valleys were eroded at nearly twice the rate of the surrounding hilltops. In their study, they found no record of Miocene uplift but recognized a mismatch between their results and the increase in offshore sedimentation during the Miocene (Poag and Savon, 1989). They also noted that the magnitude of Cenozoic erosion may have not been great enough to leave a cooling record in the low-temperature geochronology. Work by Naeser et al. (2004) in the Smoky Mountains used zircon and apatite fission-track thermochronology to show that denudation rates have been slow and steady since the Late Cretaceous. The lack of agreement between these low-temperature studies and the abundance of sedimentological and stratigraphic evidence for Miocene uplift may indicate the amount exhumation was less than 1 km, which is the approximate minimum required to expose the partial annealing zone and expose rocks that contain a low-temperature record (McKeon et al., 2014). However, in an earlier apatite fission track study of Pennsylvanian sandstones from the central Appalachian Valley and Ridge, Boettcher and Milliken (1994) estimated erosional unroofing of 2.3 km from 140-80 Ma, 0.4 km from 80-20 Ma, and 1.5 km from 20 Ma to the present.

Relief can be enhanced when drainage divides migrate and capture the headwaters of adjacent watersheds, which some authors have attributed as a driver of topography in the Appalachians. Previous authors proposed that the eastern continental divide has migrated westward due to capture of the previously westward-draining streams by the headwaters of those currently feeding into the Atlantic (Pazzaglia and Brandon, 1996; Spotila et al., 2004). This process may have happened as punctuated events rather than a steady retreat of the divide (Prince et al., 2010; Prince et al., 2011). Streams that once flowed to the Atlantic may also have been captured by westward-draining ones during a rearrangement of headwaters due to variability of bedrock strength, a process recently attributed the generation of up to 150 m of incision in southwestern North Carolina (Gallen, 2018). It appears that stream capture is a process that can affect river systems and landscapes on both sides of the continental divide.

Cenozoic faults and other brittle structures in the Southern and Central Appalachians

The Appalachians generally trend NE-SW, but there are topographic lineaments that cross the orogen and are clearly post-Alleghanian. These features were described by Hack (1982) as what he called 'trench valleys' with minor offsets due to faults and intense fracturing. There are three main families of lineaments that trend E-W, WNW-ESE, and N-S (Gay, 2000), and they have been interpreted to be the result of upper crustal extension due to regional doming (Dennison and Stewart, 2001; Stewart and Dennison, 2006). The orientation of fractures and minor faults is parallel to the general trend of these features, indicating that these post-Alleghanian structures are fracture controlled, and contain dip-slip faults and hot springs (Hill, 2013). There have been numerous earthquake swarms within the lineaments of North Carolina, and it appears that there may be modern motion along some of these features (see Hill and Stewart, this volume, for a more detailed discussion). In northwestern North Carolina and eastern Tennessee, there is a WNW-trending lineament that spans over 250 km. There is a WNW-striking, high-angle fault zone we are calling the Boone fault that contains minor dip-slip faults associated with south-side-up motion of the Grandfather Mountain window (see Hill and Stewart, this volume, for a detailed discussion). Based on a paleostress inversion of these faults, the shapes of streams draining into the fault zone, and modern seismicity, we interpret the Boone fault as a Cenozoic fault zone.

In the Pennsylvania Blue Ridge, there is a 120 km long E-W lineament at 40° N that contains a series of steeply-dipping, E-W normal faults in a 15 km wide zone called the Transylvania fault (Root and Hoskins, 1977). The strike of the fault zone changes from 270° to 290° as it crosses into the Valley and Ridge and into the Appalachian Plateau. Although there is no mapped surface expression in the Appalachian Plateau, the WNW lineament is evident in the topography and has been mapped in the subsurface where a vertical structural discontinuity truncates aeromagnetic signals and correlates with the boundary of oil and gas deposits (Wagner and Lytle, 1976). Some workers interpreted this feature as an Alleghanian lateral thrust ramp (Dodson and Thomas, 2008). However, Root and Hoskins (1977) noted that the Transylvanian fault offsets the bounding faults of the Triassic Gettysburg Basin, but gave no evidence for age of faulting other than post-Triassic.

Previous interpretations of a delamination underneath a passive margin

In seismic studies of the lower crust and upper mantle of the eastern United States, some workers have postulated that lithospheric delamination may have influenced the vertical position of the crust. Wagner et al. (2012) deployed seismic stations aligned in a WNW trend across the Blue Ridge and Piedmont and used receiver functions to build an image of the lithosphere underneath northwestern North Carolina. They found abrupt changes in seismic velocities at ~45 and ~60 km depth underneath the Piedmont, which they interpreted as a doubled Moho as a result of tectonic wedging underneath the Laurentian lithosphere. They proposed that the doubled Moho under the Piedmont could contribute to low topography, and the lack of this feature under the higher-elevation Blue Ridge could be evidence of delamination that drove uplift. Wagner et al. (2012) proposed that the Piedmont may being held down by a dense root and the adjacent Blue Ridge may owe its higher elevation to uplift associated with the loss of the crustal root. They also imaged a seismic discontinuity at ~100 km depth, which they interpreted as the boundary of a possible accreted fossil slab. In a more regionally extensive study, Biryol et al. (2016) used earthquake data collected by the EarthScope transportable array and the SESAME project to build a tomographic model of p-wave perturbations in the lithosphere and upper mantle ranging from 36 to 915 km depth. They showed numerous seismic anomalies in the tomographic model and found seismically fast, dense pieces of lithospheric material that appear to be foundering. As the pieces of continental lithosphere descend, they are being replaced by hot, seismically slow material. Biryol et al. (2016) proposed that delamination of the crustal root and replacement by more buoyant mantle material may be the cause of intraplate seismicity, volcanism, and uplift.

Moucha et al. (2008) produced mantle flow simulations to show that vertical movement of mantle material could have driven up to 100 m of dynamic topography in the past 30 million years and that the Coastal Plain of the eastern United States should not be considered a stable continental platform. In a different numerical uplift simulation of dynamic topography from the mid-continent to the coast, Liu (2014) presented a model based on subsidence of the Mississippi River valley and the Atlantic shelf that could have driven uplift of the mountain range. Liu speculated that subsidence-driven vertical flexure of the lithosphere caused differential erosion, which in turn

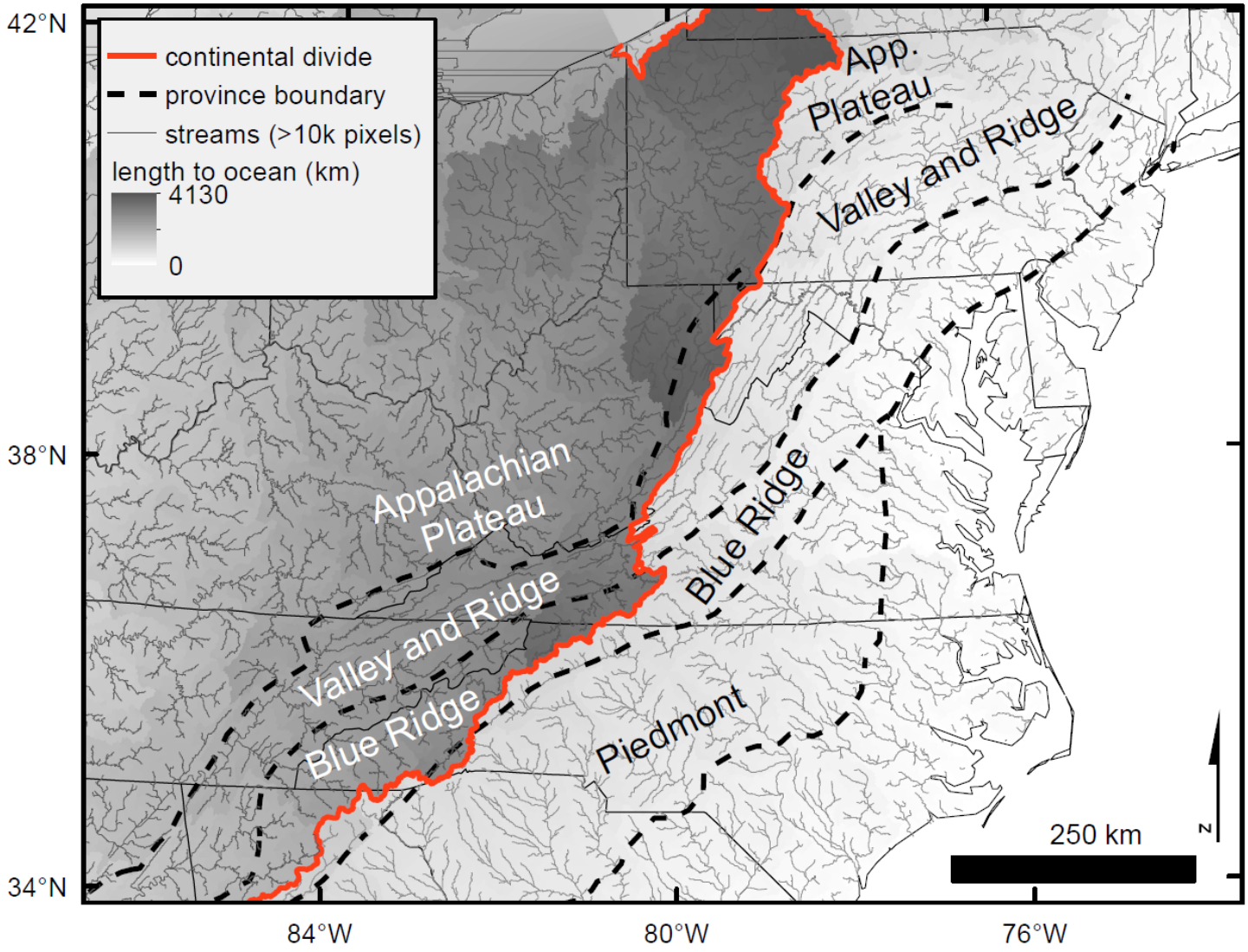

Figure 3: Stream length map showing the eastern continental divide (red line) crossing the geologic province boundaries (black dashes). The grey lines are streams with drainage areas greater than 10,000 pixels (84.6 km²).

could have generated up to 400 m of relief and 200 m of elevation change of the southern Appalachians during the Miocene.

METHODS

Topographic and geomorphic maps

To build a regional digital elevation model (DEM), we downloaded 3-arc-second HydroSHEDS (~92 m resolution) void-filled elevation data tiles (https://hydrosheds.cr.usgs.gov/dataavail.php) and merged them together in ArcMap 10.5 with the mosaic tool (Figure 3.1). We traced the boundaries between the four major geologic provinces from a regional lithotectonic map (Hibbard et al., 2006). We used this DEM and the hydrology tools in ArcMap to produce flow direction, flow accumulation, and flow length raster files. We used the hydrology raster files to determine the watersheds and to delineate the eastern continental divide (Figure 3). With the HydroSHEDS mosaic DEM, we produced geomorphic maps to compare with the major geologic provinces along the orogen, using the standard toolbox in ArcMap 10.5 and the geomorphic metrics as described at http://gis4geomorphology.com/basin-basics-i/. Before making these maps, we smoothed the DEM with the filter tool, found in the spatial analyst toolbox, using a low-pass filter, which traverses a 3x3 moving window over the DEM and reassigns the average value of the window to each center pixel. With the filtered DEM, we made a map of local relief (Figure 4), which differs from relief in that the size of the sampled area to determine the highest and lowest elevation is smaller (our sampling window was 1,390 m x 1,390 m). High local relief values can indicate areas that are responding to uplift and/or incision (Anhert, 1984), especially in a passive margin setting (Summerfield, 1991). To calculate local relief,

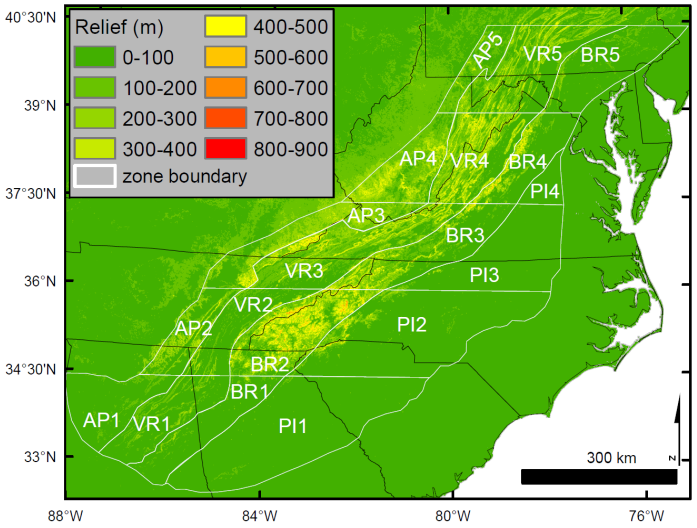

Figure 4: Local relief map calculated with a 15x15-pixel moving window (1,390 m x 1,390 m) that finds the range and reassigns the relief to each point. Note how the areas of high local relief do not match the geologic provinces but do fit reasonably well with the swath of high topography and the slow-seismic anomaly. The Appalachian Plateau of Virginia and West Virginia has high local relief that extends further west than the high topography.

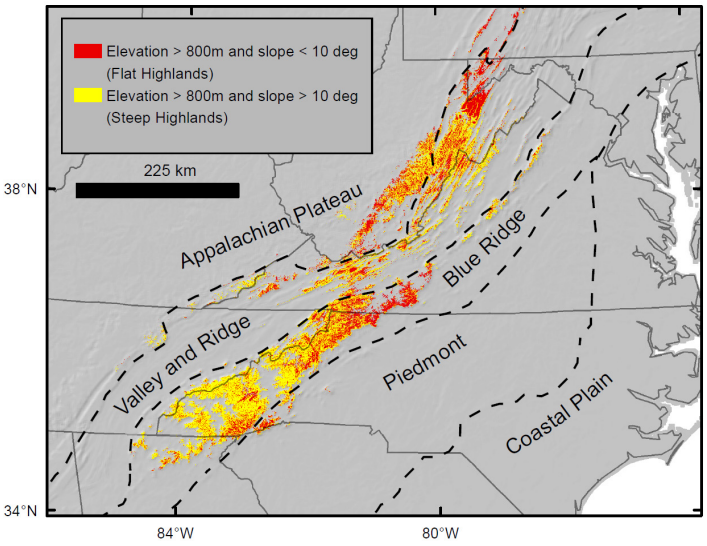

Figure 5: Binary-slope map emphasizing high peaks and high plateaus. It shows all pixels above 800 m separated by slope greater than 10° (yellow) and less than 10° (red). Note how the topographic style changes from dominantly high peaks in the south to mostly high plateaus in the north.

we used the ArcMap focal statistics tool with a 15x15 pixel rectangular window and a range operator. The local relief map allowed us to qualitatively look for patterns along strike of the major geologic provinces, and to quantify the shape of the topography with increasing latitude. To assess any changes along strike of the orogen, we separated the map into five bands of ~1.5° latitude, and then split each band by geologic province. This analysis yielded 19 zones, because the Piedmont province is not present on the continent at the highest latitudes of our study area.

There are some areas of the southern and central Appalachians that are steepest at the highest elevation, but other high-elevation areas that are relatively flat and have been interpreted as relict low-elevation landscapes that have been uplifted to their current position (Hack, 1982; Gallen et al, 2013; Hill, 2013). To distinguish between these two end-members of high topography, we produced a map that incorporates both elevation and slope into a single image and are calling it a binary-slope map (Figure 5). To construct this map, we first used the HydroSHEDS mosaic DEM to produce a slope map, in degrees. We then used the raster calculator tool to select all pixels that are above 750 m elevation and separate them into those greater than or less than 10 degrees slope. This process separated high peaks from high plateaus in order to determine the locations of any previously unrecognized relict topography.

Comparison of topography with structures in the lower crust and upper mantle

To test if the Appalachian high topography can be linked to delamination of the continental lithosphere, we compared the topographic, local relief, and binary slope-maps to results from seismic studies of the lower crust and upper mantle (Wagner et al., 2012; Biryol et al., 2016). To do this, we input the latitude, longitude, and depth values from the Biryol et al. model into ArcMap and interpolated 20 tomographic slices ranging from 36 to 915 km depth with the kriging tool in the spatial analyst toolbox. Our aim is to test whether the F5 anomaly presented in the Biryol et al. (2016) paper is spatially correlated to the swath of high topography crossing from the Blue Ridge to the Appalachian Plateau with increasing latitude. The F5 anomaly is present at 130 km depth in the North Carolina Blue Ridge, at 165km depth in the North Carolina Blue Ridge and Virginia Valley and Ridge, evident at 200 km depth under the Virginia Valley and Ridge, and fairly continuous at 240 km depth. At 280 km depth, it is present only under the Appalachian Plateau of West Virginia. The center of the fast-seismic anomaly at question is most evident at ~240 km depth, so we overlaid topographic contours corresponding with elevations higher than 750 m (at 300 m intervals) extracted from the smoothed HydroSHEDS DEM onto a tomographic slice at that depth (Figure 6A). Next, we produced a cross-section from the tomographic model along the line Y-Y'-Y", which follows the high topography and

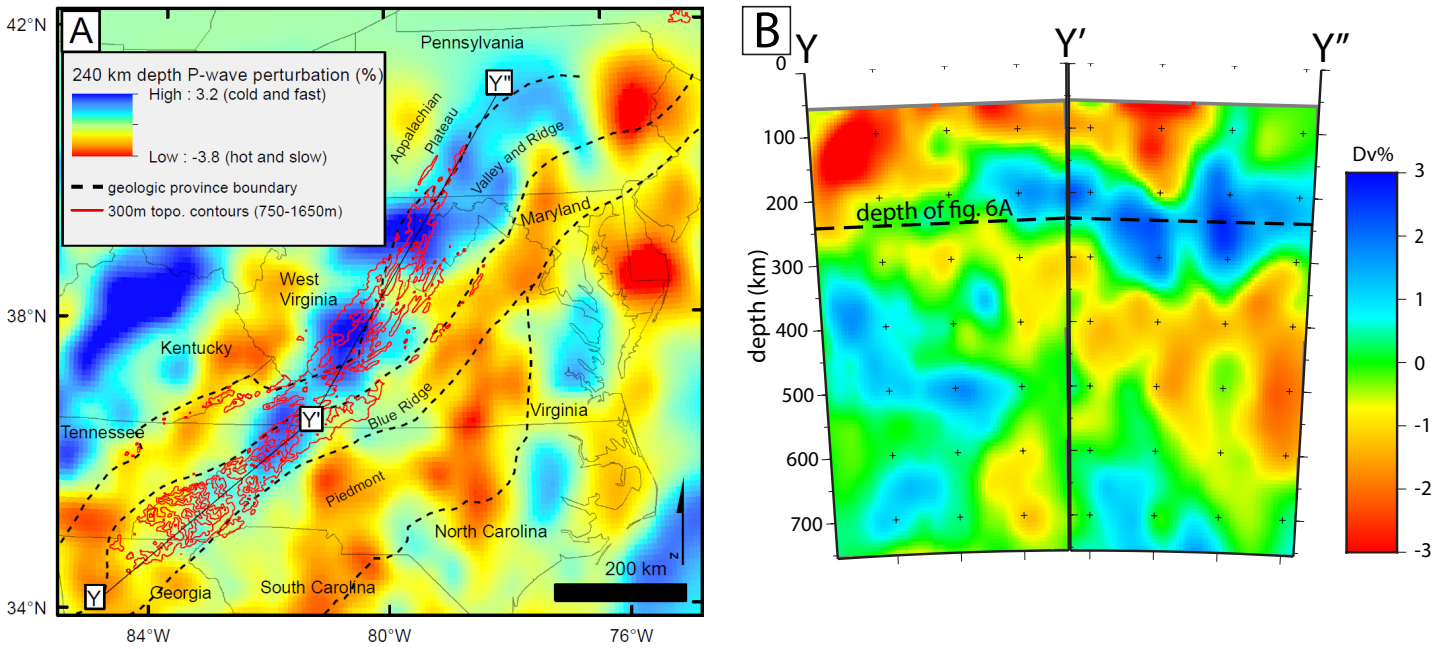

Figure 6: (A)Tomographic model showing p-wave perturbations at 240 km depth. The blue zones are cold rocks that speed up the p-waves and the red zones are hot rocks that slow down the waves. Note the large fast anomaly that matches the swath of high topography but does not fit the geologic provinces or the mountain belt as a whole, likely a drip structure associated with lithospheric delamination (Data from Biryol et al., 2016). (B) Cross section through the large fast-seismic anomaly (Y-Y'-Y"). Dashed line is the depth of the slice shown in part A.

makes a slight bend near the middle of the section line (Figure 6B).

The comparison of the topography and the tomography allowed us to test for a spatial correlation but did not allow investigation for a causal link. Wagner et al. (2012) interpreted seismic discontinuities at ~45 and 60 km depth as a doubled Moho under the Piedmont of western North Carolina and the result of underplating of a Grenville eclogitic root due to wedging of an accreted terrane during the assembly of Pangea. This piece of high-density material is present under the Piedmont but missing from the high-elevation Blue Ridge. To test the hypothesis that delamination of this ~15 km block of lithospheric root could have driven uplift we estimated the magnitude of uplift expected if it were replaced by less-dense, more buoyant mantle material. We replaced a 15 km thick block with a density of 3.4 g/cm³ (approximate density of eclogite) with material with a density of 3.3 g/cm³ (approximate estimate of upper mantle) and calculated the expected change in elevation. We estimated a 50 km thick crust with a density of 2.77 g/cm³. We then compared this change in elevation with the amounts of uplift proposed in previous geomorphic studies (~480m from Gallen et al., 2013; ~750 m from Hill, 2013) where knickpoints were used to project the relict landscapes above current river mouths as estimates of base level change.

The study by Wagner et al. (2012) was limited to one section line across high topography of western North Carolina, but we were curious how the crustal thickness compared to the topography across our entire study area. To do this, we used a crustal thickness model that was compiled from multiple seismic studies (Cook et al., 1979; Cook and Vasudevan, 2006; Hawman, 2008; French et al., 2009; Abt et al., 2010; Moidaki et al., 2010; Hawman et al., 2012; Wagner et al., 2012; and Parker et al., 2013) and presented in the supplemental material of Biryol et al. (2016). We added the latitude, longitude, and depth to Moho from this model into ArcMap and made an interpolation with the kriging tool, then added topographic contours from the HydroSHEDS DEM (Figure 7). We then split the crustal thickness map into the same 5 latitudinal zones separated by geological province from which we extracted the geomorphic data. For each zone we determined the maximum and mean crustal thickness and compared those values to the elevation for each zone (Figures 8 and 9).

Lastly, we wanted to investigate whether our study area is at isostatic equilibrium, based on the crustal thickness model and the current topography. We calculated the predicted elevation for a crust with a density of 2.77 g/cm³ and anchored our model at the thinnest crust and lowest elevation of our study area, which is at the coast where the mean crustal thickness

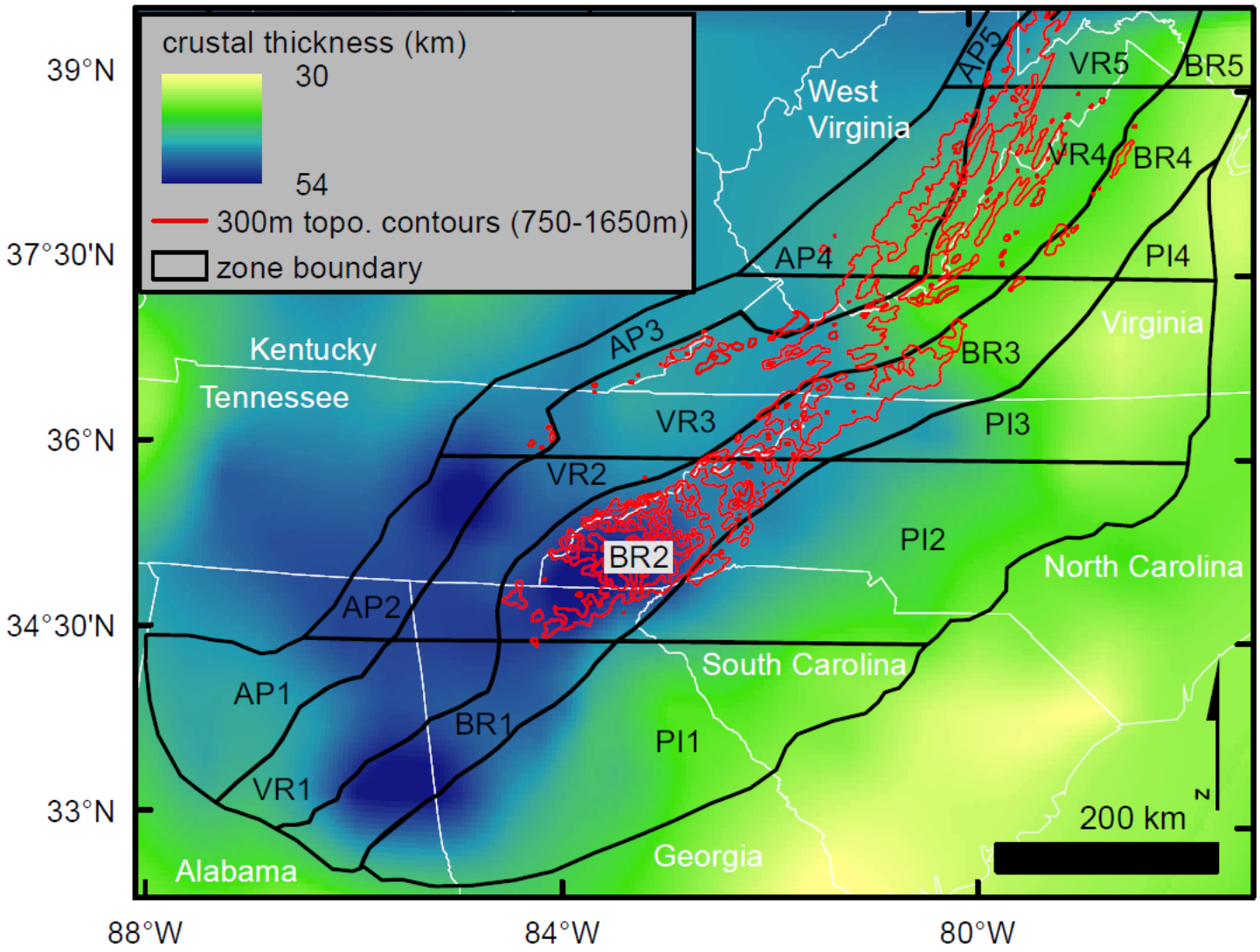

Figure 7: Map of crustal thickness with topographic contours overlain as red lines (Data from Biryol et al., 2016). There is not a strong correlation between thick crust and high elevation, except for in zone BR2. Note the thickened crust in BR1 and AP2 in the southern part of the image, where there is no topography above 750 m. The crustal thickness values were extracted from each zone and shown in Figures 8 and 9.

= ~34 km and elevation = 0 m (Figure 8). We then calculated the predicated elevation of each zone and compared these estimates to the observed data to test for isostatic equilibrium (Figure 9).

RESULTS

Topographic and geomorphic maps

The elevation, binary slope, and local relief maps we produced show a lack of consistency along the orogen in all of the major geologic provinces (Figures 1, 4, and 5). The local relief map (Figure 4) has high values in the same zones that have high elevation (Figure 1), but also shows high local relief in the Appalachian Plateau of Kentucky and West Virginia (zones AP3 & AP4) and in the Piedmont of NC (PI2). It appears that even though the streams draining from these areas have a long path to the Gulf of Mexico (Figure 3), they are experiencing incision and a roughening of the topography. The binary slope map highlights contrasting topographic styles of the high elevation areas (Figure 5). There are flat highlands in southern North Carolina where previous studies have shown flights of knickpoints separating active landscapes from relict ones upstream (Gallen et al.; Hill, 2013; Ch. 1 of this dissertation). There are steep highlands in central North Carolina that transition back to flat areas for the remainder of the Blue Ridge province along strike to the north until southwestern Virginia, where the elevation of the Blue Ridge drops quickly. As the high elevation crosses into Virginia and West Virginia, the topographic style is mixed as far as northern West Virginia, where there is a stark change to a uniformly flat highland landscape, even though the underlying

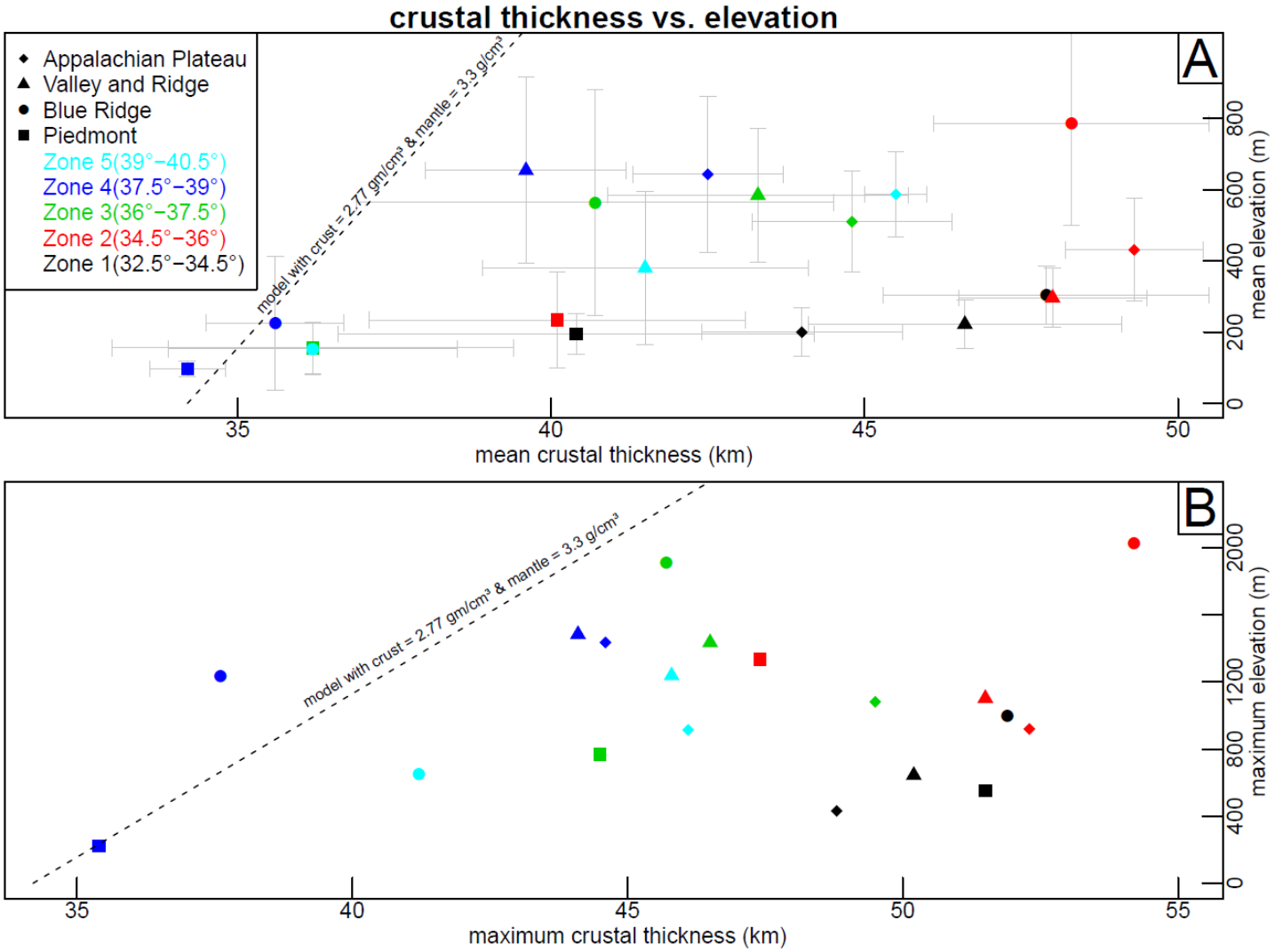

Figure 8: (A) Mean crustal thickness in km vs. mean elevation in m. The gray bars show one standard deviation from the mean. Each zone is indicated by color and each geologic province by symbol shape. The dashed line indicates the expected elevation at isostatic equilibrium, based on the thinnest crust at sea level. With the exception of the Piedmont in zone 4, all zones are overcompensated isostatically. (B) Maximum crustal thickness in km vs. maximum elevation in m for each zone. All zones except the Blue Ridge of zone 4 are overcompensated.

lithology is constant.

Seismic tomography, crustal thickness map, and isostacy calculations

The topographic contours from the HydroSHEDS DEM have a strong positive spatial correlation to the fast anomaly in the seismic tomography slice at 240 km depth (Figure 6A). Although the topography and the tomography appear to match, neither follow any of the major geologic provinces. The tomographic cross section Y-Y'-Y", which follows the high topography, shows a fast anomaly underneath a slow section of upper mantle and crust (Figure 6B). The top of the fast anomaly starts at ~100 km depth, which is consistent with the lowest seismic discontinuity imaged in the profiles of Wagner et al. (2012). Based on the distance between the doubled Moho discontinuities they presented, we calculated the expected uplift for delamination of 15 km and 25 km thick eclogitic layers, which resulted in 450 m and 750 m, accordingly.

When we combined the elevation contours with the crustal thickness map (Figure 7), only one zone of high topography overlies thick crust. With the exception of zone BR2, there are discrepancies between the amount of elevation and the thickness of crust in most of the study area. Surprisingly, the thickest crust is in the lowest latitude zone, where the topography is relatively low. As evident in Figures 8 and 9, all of the zones in our study area have lower mean elevations than expected for the amount of crustal thickness if there was isostatic equilibrium. Crustal thickness decreases from zone 2 to zone 4, then increases again

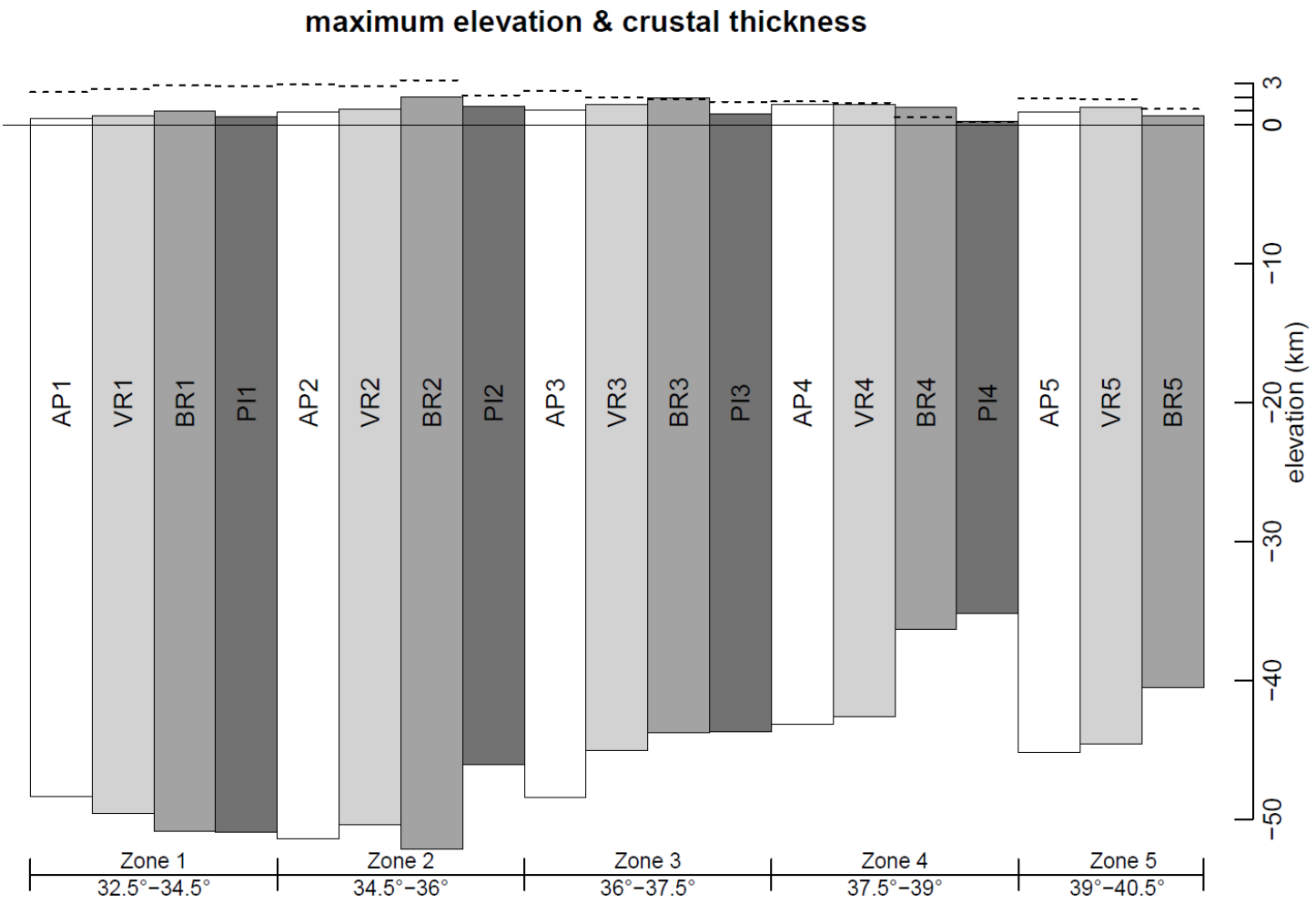

Figure 9: Model showing observed crustal thicknesses from each zone in Figure 7 with elevation data extracted from the Hydro-SHEDS DEM. The dashed lines show the expected elevation for each crustal thickness at a state of isostatic equilibrium. Note the decreasing crustal thickness from zone 2 to zone 4, then the sudden increase at zone 5. This increase coincides with the northern edge of the fast-seismic anomaly in Figure 6.

in zone 5. This increase coincides with the edge of the fast-seismic anomaly evident in the tomography cross section Y-Y'-Y" (Figure 6) and is close to the 40° N latitude Transylvania fault zone (Root and Hoskins, 1977).

DISCUSSION

It is evident that the topography of the southern and central Appalachians cannot be explained simply as a product of the underlying crustal geology, as there are major discrepancies in elevation, local relief, and type of highlands along the length of all the major geologic provinces. We have shown here that there is a much stronger spatial correlation between the high topography and the proposed delamination structure seen at 240 km depth in the seismic tomography model than between the topography and lithology. Our estimates of 450 -750m of uplift that would result from delamination of a dense lithospheric root are consistent with the amounts of uplift proposed by previous geomorphic studies by us and others (Gallen et al., 2013; Hill, 2013). Although stream capture may have contributed to some relief generation in the Appalachians, it is our interpretation that delamination and the subsequent replacement by more buoyant, less dense mantle material has driven regional-scale uplift. Rather than a broad and uniform arching along strike of the orogen, the uplift was more likely blocky and accommodated by vertical movement along the topographic lineaments. This interpretation could explain the existence of the lineaments, as well as the dip-slip, high angle fault zones we have mapped within them, and the contrasting highland topography seen in the binary-slope map. Many of the knickpoints that have been observed in the southern Appalachians are along streams that drain into lineaments, and in many places there are stark contrasts of topographic style across these linear features (Hack, 1982; Hill, 2013).

The crustal thickness compared to the topography across our study area indicates that the southern and central Appalachians are isostatically overcompensated and need to continue to move upwards to approach equilibrium (Figures 8 and 9). This observation argues against the idea that this passive margin is simply a result erosion of the mountains after the Paleozoic collisional events and supports our claim that the rejuvenation of topography is attributed to Late Cenozoic mantle dynamics. Other authors have proposed a heterogeneous crustal root with varying mechanical properties along strike of the Appalachians, which is consistent with our findings (e.g. Stewart and Watts, 1997).

Delamination of lithospheric roots has been attributed to uplift in other mountain ranges at margins that are no longer active (e.g. Ducea, 2011), such as the Sierra Nevada in California (e.g. Zandt et al., 2004), the European Alpine Belt (De Boorder et al., 1998), or the Carpathian Mountains of Romania (Girbacea and Frisch, 1998; Fillerup et al., 2010). One obvious difference between these locations and the Appalachians is the greater amount of time that has passed between when subduction was active and when the delamination occurred. To resolve this temporal issue, we propose that the delamination of the lithospheric root that we are attributing to Miocene Appalachian rejuvenation was likely not the first foundering event since the Paleozoic. It is possible that the Cretaceous uplift event that is evident in sedimentary records and low-temperature studies was also driven by delamination of the lithosphere. If the crustal root was assembled during multiple events, it is plausible that it may have fallen apart in a piecemeal fashion.

CONCLUSIONS

Although the bedrock in the Appalachians is undoubtedly very old, we propose that the topography of the mountain range is much younger. There is a clear mismatch between lithology and elevation on a regional scale, but a strong spatial correlation exists between the high elevation and the location of a foundering lithospheric root currently between 100 and 280 km depth. Our calculations of the uplift expected by removal of a 15-25 km thick, dense root are consistent with observed geomorphic estimates and support a causal link between the dynamic mantle and Cenozoic rejuvenation of topography. By comparing the thickness of crust and topography across 19 zones in our study area, we have shown that the Appalachians are overcompensated isostatically and are still responding to a vertical readjustment due to lithospheric foundering.

REFERENCES

Abt, D. L., Fischer, K. M., French, S. W., Ford, H. A., Yuan H. Y., and Romanowicz, B., 2010, North American lithospheric discontinuity structure imaged by Ps and Sp receiver functions: Journal of Geophysical Research, v. 115.

Anhert, F., 1984, Local relief and the height limit of mountain ranges: American Journal of Science, v. 284, p. 1035-1055.

Bryant, B, and Reed, J.C., 1970, Geology of the Grandfather Mountain window and vicinity, North Carolina and Tennessee: United States Geological Survey Professional Paper 615, 190 p.

Biryol, B. C., Wagner, L. S., Fischer, K. M., Hawman, R. B., 2016, Relationship between observed upper mantle structures and recent tectonic activity across the Southeastern United States: Journal of Geophysical Research Solid Earth, v. 121.

Boettcher, S. S., and Milliken, K. L., 1994, Mesozoic-Cenozoic unroofing of the southern Appalachian basin: apatite fission track evidence from Middle Pennsylvanian sandstones: The Journal of Geology, v. 102, no. 6, p. 655-668.

Burbank, D. W., and Anderson, R. S., 2012, Tectonic Geomorphology – 2nd edition: Wiley- Blackwell, West Sussex, UK, 460 p.

Cook, F. A., Albaugh, D. S., Brown, L. D., Kaufman, S., Oliver, J. E., and Hatcher, R. D., 1979, Thin-skinned tectonics in the crystalline southern Appalachians: COCORP seismic-reflection profiling of the Blue Ridge and Piedmont: Geology, v. 7, p. 563–567.

Cook, F. A., and Vasudevan, K., 2006, Reprocessing and enhanced interpretation of the initial COCORP Southern Appalachians traverse: Tectonophysics, v. 420, p. 161–174.

Davis, W. M., 1899, The geographical cycle: Geographical Journal, v. 14, no. 5, p. 481-504.

De Boorder, H., Spakman, W., White, S.H., and Wortel, M.J.R., 1998, Late Cenozoic mineralization, orogenic collapse and slab detachment in the European Alpine Belt: Earth and Planetary Science Letters, v. 164, p. 569-575.

Dennison, J. M., and K. G. Stewart, 2001, Regional structural and stratigraphic evidence for dating Cenozoic uplift of Southern Appalachian highlands: Geological Society of America, Southeastern Section Meeting, Abstracts with Programs. v. 33. no. 6.

Dodson, E. L., and Thomas, W. A., 2008, Structural geology of the Transylvania fault zone in the Appalachian thrust belt, Bedford County, Pennsylvania: Geological Society of America, Southeastern Section Meeting, Abstracts with Programs. Vol. 40. No. 2., p. 27.

Ducea, M. N., 2011, Fingerprinting orogenic delamination: Geology, v. 39, no. 2, p. 191-192.

Flowers, R. M., Schuster, D.L., Wernicke, B.P., and Farley, K.A., 2007, Radiation damage control on apatite (U-Th)/He dates from the Grand Canyon region, Colorado Plateau: Geology, v. 35, no. 5, p. 447-450.

French, S., Fischer, K., Syracuse, E., and Wysession, M., 2009, Crustal structure beneath the Florida-to-Edmonton broadband seismometer array: Geophysical Research Letters, v. 36.

Fillerup, M. A., Knapp, J. A., Knapp, C. C., and Raileanu, V., 2010, Mantle earthquakes in the absence of subduction? Continental delamination in the Romanian Carpathians: Lithosphere, v. 2, no. 5, p. 333-340.

Gallen, S. F., Wegmann, K. W., Bohnenstiehl, D. R., 2013, Miocene rejuvenation of topographic relief in the southern Appalachians: GSA Today, v. 23, no. 2, p. 4 -10.

Gallen, S. F., 2018, Lithologic controls on landscape dynamics and aquatic species evolution in post-orogenic mountains: Earth and Planetary Science Letters, v. 493, p. 150-160.

Galloway, W. E., Whiteaker, T. L., and Ganey-Curry, P., 2011, History of Cenozoic North American drainage basin evolution, sediment yield, and accumulation in the Gulf of Mexico basin: Geosphere, v. 7, no. 4, p. 938-973.

Gardner, T. W., 1989, Neotectonism along the Atlantic passive continental margin: A review: Geomorphology, v. 2, p. 71-97.

Gay, P. S., Jr., 2000, Unmapped topographic alignments visible on 3D stereo terrain map of a 2 degrees X 2 degrees segment of the Southern Appalachians: Geological Society of America Abstracts with Programs, Southeastern Section v. 32, no. 2, p. 19.

Girbacea, R., and Frisch, W., 1998, Slab in the wrong place: Lower lithospheric mantle delamination in the last stage of the Eastern Carpathian subduction retreat: Geology, v. 26, no. 7, p. 611-614.

Green, P.F., Duddy, I.R., Gleadow, A.J.W., Tingate, P.R., and Laslett, G.M., 1986, Thermal annealing of fission tracks in apatite: Chemical Geology, v. 59, p. 237-253.

Hack, J. T., 1975, Dynamic equilibrium and landscape evolution, in Melhorn, W.N, and Flemal, R.C. (eds): Theories of Landform Evolution, p. 87-102.

Hack, J. T., 1982, Physiographic divisions and differential uplift in the Piedmont and Blue Ridge: United States Geological Survey Professional Paper 1265, 49 p.

Hawman, R. B., 2008, Crustal thickness variations across the Blue Ridge Mountains, southern Appalachians: An alternative procedure for migrating wide-angle reflection data: Bulletin of the Seismological Society of America, v. 98, p. 469–475.

Hawman, R. B., Khalifa, M. O., and Baker, M. S., 2012, Isostatic compensation for a portion of the Southern Appalachians: Evidence from a reconnaissance study using wide-angle, three component seismic soundings: Geological Society of America Bulletin, v. 124, p. 291–317.

Hibbard, J. P., van Staal, C. R., Rankin, D. W., and Williams, H., 2006, Lithotectonic map of the Appalachian Orogen, Canada-United States of America: Geological Survey of Canada, Map 2096A, scale 1:500,000.

Hill, J. S., 2013, Zoned uplift of western North Carolina bounded by topographic lineaments: M.S. Thesis, University of North Carolina at Chapel Hill, 51 p.

Lehner, B., Verdin, K., and Jarvis, A., 2008, New global hydrography derived from spaceborne elevation data: Eos, Transactions, American Geophysical Union, v. 89, no. 10, p 93-94.

Liu, L., 2014, Rejuvenation of Appalachian topography caused by subsidence-induced differential erosion: Nature Geoscience, v. 7, p. 518- 523.

Maliva, R. G., Missimer, Thomas M., and Guo, Weixing, 2006, Structural deformation of the southern Florida peninsula during the Late Miocene to Early Pliocene: Geophysical log evidence: Gulf Coast Association of Geological Societies Transactions, v. 56, p. 527-538.

McKeon, R. E., Zeitler, P. K., Pazzaglia, F. J., Idleman, B. D., and Enkelmann, E., 2014, Decay of an old orogen: Inferences about Appalachian landscape evolution from low- temperature thermochronology: Geological Society of America Bulletin, v. 126, no. 1/2, p. 31- 46.

Miller, S., R., Sak, P. B., Kirby, E., and Bierman, P. R., 2013, Neogene rejuvenation of central Appalachian topography: Evidence for differential rock uplift from stream profiles and erosion rates: Earth and Planetary Science Letters, v. 369-370, p. 1-12.

Missimer, T. M., and Maliva, R. G., 2014, Miocene rejuvenation of the southern Appalachian Mountains and fluvial transport of coarse siliciclastics to southern Florida: Geological Society of America Abstracts with Programs, v. 46, no. 6, p. 379.

Moidaki, M., Gao, S. S., Liu, K. H., Abdelsalam, M. G., Hogan, J. P., and Atekwana, E., 2010, Converted P-to-S phase and Moho quality beneath the New Madrid seismic zone from receiver function studies:, Geoscience Research, v. 1 no. 1, p 7–21.

Nystrom, P., 1986, Late Cretaceous-Cenozoic brittle faulting beneath the western South Carolina coastal plain; reactivation of the eastern Piedmont fault system: Geological Society of America Abstracts with Programs, v. 38, no. 3, p. 74.

Pazzaglia, F. J., and Brandon, M. T., 1996, Macrogeomorphic evolution of the post-Triassic Appalachian Mountains determined by deconvolution of the offshore basin sedimentary record: Basin Research, v. 8, p. 255-278.

Parker, E. H., Hawman, R. B., Fischer, K. M., and Wagner, L. S., 2013, Crustal evolution across the southern Appalachians: Initial results from the SESAME broadband array: Geophysical Research Letters, v. 40, p. 3853–3857.

Penck, W, 1954, Morphological Analysis of Landforms: St. Martin's Press, New York. 80 p.

Poag, W. C., and Savon, W. D., 1989, A record of Appalachian denudation in postrift Mesozoic and Cenozoic sedimentary deposits of the U.S. middle Atlantic continental margin: Geomorphology, v. 2, p. 119-157.

Popenoe, P., 1985, Cenozoic depositional and structural history of the North Carolina margin from seismic-stratigraphic analyses, in Poag, C. W., ed., Geologic evolution of the United States, Atlantic margin: New York, Van Nostrand Reinhold, p. 125-187.

Prince, P. S., Spotila, J. A., and Henika, W. S., 2010, New physical evidence of the role of stream capture in active retreat of the Blue Ridge escarpment, southern Appalachians: Geomorphology, v. 123, p. 305-319.

Prince, P. S., Spotila, J. A., and Henika, W. S., 2011, Stream capture as driver of transient landscape evolution in a tectonically quiescent setting: Geology, v. 39, no. 9, p. 823-826.

Root, S. I., and Hoskins, D. M., 1977, Lat 40° N fault zone, Pennsylvania: A new interpretation: Geology, v. 5, p. 719-723.

Rowley, D. B., Forte, A. M., Moucha, R.t, Mitrovica, J. X.,

Simmons, N. A., and Grand, Stephen P., 2013, Dynamic topography change of the eastern United States since 3 million years ago: Science, v. 340, p. 1560-1563.
Slingerland, R., and Furlong, K. P., 1989, Geodynamic and Geomorphic Evolution of the Permo- Triassic Appalachian Mountains: Geomorphology, v. 2, p. 23-37.
Soller, D. R., 1988, Geology and tectonic history of the lower Cape Fear river valley, southeastern North Carolina: United States Geological Survey Professional Paper 1466- A, 65 p.
Spotila, J. A., Bank, G. C., Reiners, P. W., Naeser, C. W., Naeser, N. D., and Henika, W. S., 2004, Origin of the Blue Ridge escarpment along the passive margin of Eastern North America: Basin Research, v. 16, p. 41-63.
Stewart, J., and Watts, A.B., 1997, Gravity anomalies and spatial variations of flexural rigidity at mountain ranges: Journal of Geophysical Research, v. 102, no. B3, p. 5327-5352.
Stewart, K. G., Dennison, John M., 2006, Tertiary-to-recent arching and the age and origin of fracture-controlled lineaments in the southern Appalachians: Geological Society of America Abstracts with Programs, v. 38. no. 3.
Stewart, K. G., 2015, Estimates on the magnitude and timing of post-orogenic topographic rejuvenation of the southern Appalachians using isostasy and deformed Coastal Plain rocks: Geological Society of America Abstracts with Programs, v. 47., no. 2., p. 82.
Summerfield, M.A, 1991, Sub-aerial denudation of passive margins: regional elevation versus local relief models: Earth and Planetary Science Letters, v. 102, p. 460-469.
Teng, L. S., 1996, Extensional collapse of the northern Taiwan mountain belt: Geology, v. 24, no. 10, p. 949-952.
Van De Plassche, O., Wright, A. J., Horton, B. P., Engelhart, S. E., Kemp, A. C., Mallinson, D., and Kopp, R. E., 2014, Estimating tectonic uplift of the Cape Fear arch (south-eastern United States) using reconstructions of relative sea leve: Journal of Quaternary Science, v. 28, no 8, p. 749-759.
Wagner, L. S., Stewart, K., and Metcalf, K., 2012, Crustal-scale shortening structures beneath the Blue Ridge Mountains, North Carolina, USA: Lithosphere, v. 4, no. 3, p. 242-256.
Wagner, W. R., and Lytle, W. S., 1976, Greater Pittsburgh region revised surface structure and its relation to oil and gas fields: Pennsylvania Geological Survey, 4th Series, Information Circular 80, 20 p.
Ward, L. W., Bailey, R. H., and Carter, J. G., 1991, Pliocene and Early Pleistocene stratigraphy, depositional history, and molluscan paleobiogeography of the Coastal Plain, in Horton, J. Wright and Zullo, Victor A., eds., The Geology of the Carolinas, Carolina Geological Society fiftieth anniversary volume: Knoxville, The University of Tennessee Press, p. 274-289.
Weems, R. E., Lewis, W. C., and Aleman-Gonzalez, W. B., 2009, Surficial geologic map of the Roanoke rapids 30' x 60' Quadrangle, North Carolina: United States Geological Survey Open File Report 1149, scale 1:100,000.
Whipple, K. X., and Tucker, G. E., 1999, Dynamics of the stream-power river incision model: Implication for height limits of mountain ranges, response timescales, and research needs: Journal of Geophysical Research, v. 104, no. B8, p. 17,661-17,674.
Zandt, G., Gilbert, H., Owens, T. J., Ducea, M., Saleeby, J., and Jones, C. H., 2004, Active foundering of a continental arc root beneath the southern Sierra Nevada in California: Nature, v. 431, p. 41-46.

An old storm with modern consequences: The debris flow history of the August 13-14, 1940 storm event in Watauga County, North Carolina

Anne Carter Witt
Virginia Department of Mines, Minerals and Energy, Division of Geology and Mineral Resources, 900 Natural Resources Drive, Suite 500, Charlottesville, VA 22903, anne.witt@dmme.virginia.gov

Rick Wooten
North Carolina Geological Survey, Division of Energy, Mineral, and Land Resources, N.C. Department of Environment and Natural Resources, 2090 US Highway 70, Swannanoa, NC 28778, rick.wooten@ncdenr.gov

INTRODUCTION

In the southern Blue Ridge, from western North Carolina (WNC) into Virginia, storms that produce tens to hundreds of landslides occur about every 9 years while storms that produce thousands of landslides occur about every 25 years (Wooten et al, 2016). The majority of these landslides are swift-moving debris flows, slurries of mud, rock and vegetative debris that travel down steep slopes usually within natural colluvial hollows and drainages. These landslides are extremely dangerous as they often occur with little warning, strip the landscape of vegetation, and destroy objects (e.g., cars, houses) in their path. Debris flows are often triggered by high-intensity, short-duration rainfall. Major debris flow-generating storm events affecting WNC occurred in 1916, 1940, 1977, 2004, 2013 and most recently in 2018 (Witt, 2005; Wieczorek, 2009). Most of these storms were the remnants of cyclonic systems. However, localized thunderstorms and low-pressure systems can also produce numerous debris flows (Figure 1 summarizes these storm events).

Studies completed by the North Carolina Geological Survey (NCGS) have shown that certain rainfall thresholds are more likely to initiate swift-moving landslides such as debris flows. In general, debris flows are more likely to occur on natural slopes (i.e. those not modified by human disturbance) during a storm that produces 5-inches (125 mm) or more of rain in 24-hours (Eshner and Patrick, 1982; Wooten et al, 2016). High-antecedent moisture content from previous rainfall events also plays a role in destabilizing and hypersaturating the soils prior to high-intensity storms. Such paired-storm events occurred in 1916, 1940 and 2004 (Figure 1). On slopes altered by human excavation, such as steep road or house embankments, less rainfall is necessary to generate debris flows (Wooten et al, 2017).

In order to build more resilient mountain communities, geoscientists must work together with planners, local officials and citizens to communicate the potential risks of landslides. Understanding where historic storms and subsequent landslides have occurred in the past, the complexities of the underlying geology and geologic structure, and the mechanics of landslide flow and inundation is critical to protecting people and property during future heavy rainfall events. This effort is not a minor undertaking. Completing landslide inventories is a time-consuming activity and involves a mixture of the thoughtful interpretation of remotely sensed data such as LiDAR and aerial photography, and on-the-ground field verification and data collection. Geologic mapping is also time intensive, but as we will show during this field trip, metamorphic foliation, fracture/joint orientation and rock type all play crucial roles in where landslides will generate and which slopes will fail. Finally, debris flows can travel long distances from their area of origin and often inundate areas within older composite debris fans. Mapping and modeling scenarios of debris flow inundation is critical to protect lives and property where often the line between total destruction and a glancing blow is only a few feet.

THE MID-AUGUST 1940 STORM

August 1940 was a particularly bad weather month for WNC. Two record-breaking storm events occurred: the first caused by the remnants of a hurricane in mid-August that affected Watauga, Ashe, Caldwell, McDowell, and Wilkes Counties and, the second, a localized storm in late August that caused devastating flooding and landslides in Jackson and Macon Counties. These storms together caused $30 million in damages ($540 million in 2018 dollars) and killed between 30 to 40 people (U.S. Geological Survey, 1949).

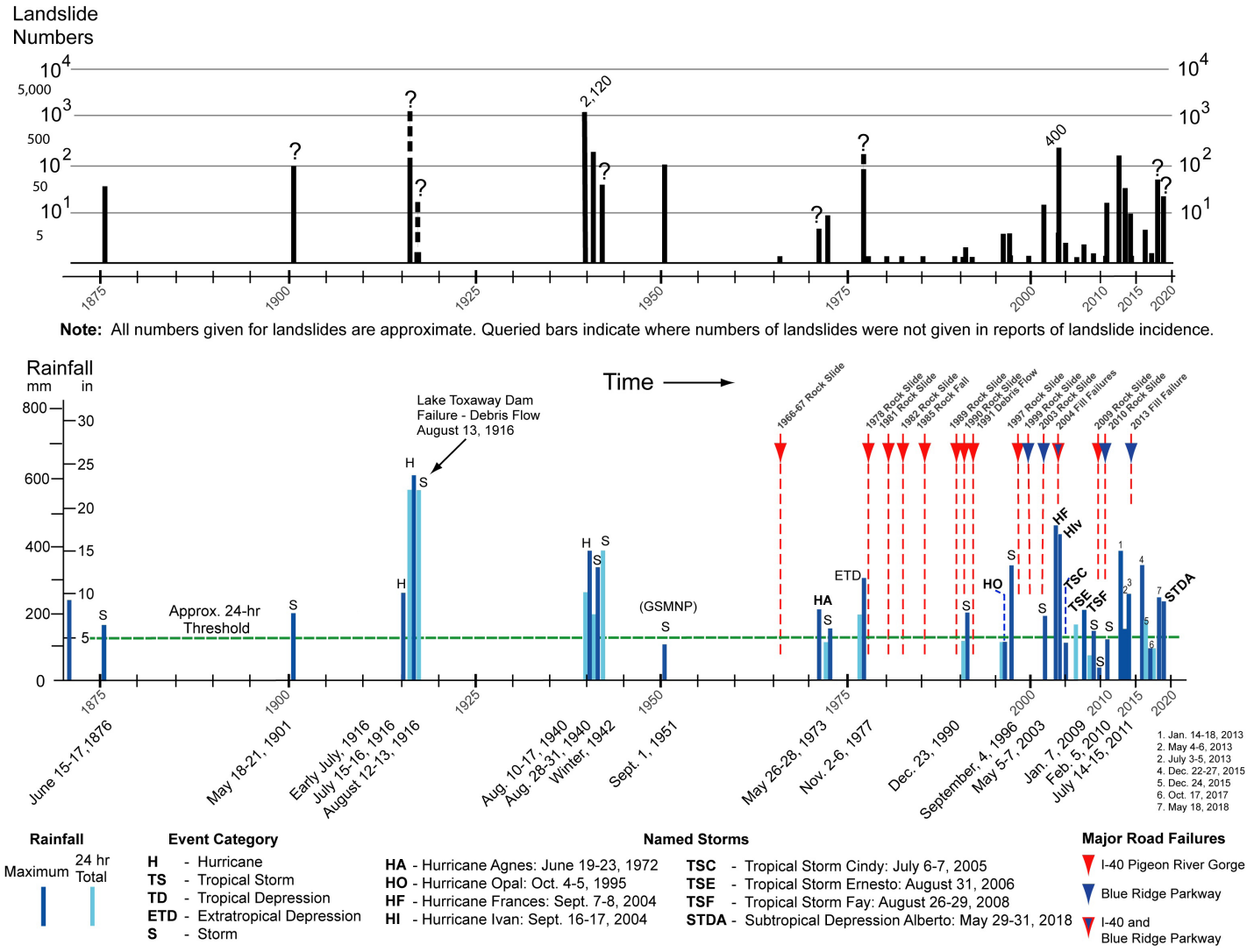

Figure 1: Chart summarizing the numbers of landslides and rainfall totals associated with major storm events in Western North Carolina.

This field trip, however, will focus on the events of August 13-14, 1940 in Watauga County. Like the July 1916 storm, considered by many to be the storm of record for WNC, there was major flooding in Boone and outlying communities. What was so unusual about this storm was the sheer number of landslides generated, over 2000 in total, in such a small area along the Blue Ridge escarpment and northern Watauga County (Wooten et al., 2008). This field trip will highlight some of the landslide scars that are still visible on the landscape in the Deep Gap region of the county. It will also discuss how these debris flows so tragically affected the community of Stony Fork and the Greene family in particular.

Like many landslide-generating storms in the southern Blue Ridge, the mid-August storm originated as a tropical cyclone. The storm first developed as a tropical depression on August 5 in the Atlantic and then into a category one hurricane on August 10. This unnamed hurricane made landfall near Beaufort, SC at about 4PM on August 11 (Figure 2). As the storm tracked inland, it turned westward and passed north of Savannah, GA between 5-6PM (Gallenne, 1940). Overall, hurricane-force winds were felt from Savannah, GA to Charleston, SC with the wind speeds reaching 73 mph in Savannah (Gallenne, 1940).

While this was only a category one hurricane, the locations affected were popular vacation destinations at the height of the summer tourist season. Hence, the coastal evacuation and the storm aftermath made the national news, pushing out the news of the war in Europe (Atlanta Constitution, 12 Aug 1940; 13 Aug 1940). There was a substantial effort by the U.S. Coast Guard to warn residents of the storm and evacuate people from the outlying barrier islands and away from beach resorts on Pawley's Island, Edisto Island

Figure 2: The storm path of the mid-August 1940 hurricane with time and day locations (blue dots) noted for the approximate center of the storm (modified from Gallenne, 1940).

and Folly Beach. Their efforts probably saved lives and property as boats and automobiles were moved inland, out of harm's way. Nevertheless, property damage for the entire coast was estimated at $3 million ($54 million in 2018 dollars) (Gallenne, 1940). Initial news reports indicated that as many as 35 were dead, but totals were revised down to 20 as missing people in the more inaccessible parts of the coastline were found safe (Gallene, 1940).

The remnants of the hurricane continued to push west and north for the next few days into WNC (Figure 2). Total precipitation for the week of August 10-17, shown on Figure 3, indicates that rain totals varied considerably in WNC, from a few inches up to 15 inches. Several centers of high precipitation were concentrated in the mountains, mainly along the Blue Ridge Escarpment, indicating that there was a significant orographic influence on rainfall distribution. The storm remnants turned east on August 14 and were headed out of the area by August 15 (Figure 2).

In Boone, Julian Yoder, future chair of the Department of Geography and Geology at Appalachian State Teachers College, recorded rainfall amounts and reported his results to the local newspaper. He describes that the rainfall became a persistent downpour on August 11 (Watauga Democrat, 15 Aug 1940), however this precipitation does not appear to be hurricane-related based on the inland storm track (Figure 2). Between 5-6PM on August 13, two inches of rain had fallen in downtown Boone, and Main Street had

Station	County	10-Aug	11-Aug	12-Aug	13-Aug	14-Aug	15-Aug	16-Aug	17-Aug	Total Precip
Laurel Springs (near)	Allegheny	0	0.3	0.35	2.97	7.33	0.87	0.34	0.02	12.18
Laurel Springs (Bluff Park)	Allegheny	0	0.3	0.5	3.38	10	0.25	0.25	0	14.68
Helton	Ashe	0	0.12	0.55	1.8	7.05	1.28	0.16	0.03	10.99
Jefferson (afternoon measure)	Ashe	0.31	0.26	1.79	4.6	5.87	0.21	0.1	0.15	13.29
Jefferson	Ashe	0	0	1.45	1.77	6.82	0	0	0	10.04
Parker	Ashe	0.12	0.39	0.71	2.42	2.77	0.27	0.19	0.08	6.95
Crossnore	Avery	0.63	0.68	4.71	8.98	0	0	0	0	15
Banner Elk	Avery	0.3	0.45	2.77	8.5	0.25	0.31	0.35	0	12.93
Plumtree	Avery	0	0.34	1.02	3.73	4.98	0.22	0	0	10.29
Smoky Gap	Avery	0	0.22	0.68	3.3	4.45	0.55	0.48	0.13	9.81
Buffalo Cove	Caldwell	0	0	0.58	2.42	8.84	0.88	0.09	0	12.81
Reese	Johnson (TN)	0	0.04	0.29	1.53	4.63	0.91	1.01	0.19	8.6
Snake Mountain	Johnson (TN)	0	0.36	0.65	1.15	4	1.56	0.57	0.11	8.4
Buck Creek	McDowell	0.4	0.8	2.5	9.6	3.05	0	0	0	16.35
Marion	McDowell	0.14	0.53	1.19	8.2	0.35	0.07		0.07	10.55
Boone	Watauga	0.59	0.2	2.51	3.63	5.1	0.65	0.02	0.15	12.85
Kilby's Gap	Wilkes	0.03	0.19	1.16	1.81	8	0.2	0.18	0	11.57
North Wilkesboro (near)	Wilkes	0.1	0.09	1.66	3.5	2.6	0.14	0	0.11	8.2
North Wilkesboro	Wilkes	0.08	0.38	1.54	2.15	4.5	0.34	0.4	0.06	9.45

Table 1: Precipitation totals for Boone, NC and nearby areas, for each day from August 10-17, 1940, in inches. Locally, rainfall totals for the week were over 10 inches in many places and up to 16 inches in McDowell County. The heaviest rain fell from August 13-14, 1940. Data modified from the U.S. Geological Survey (1949).

flooded (Watauga Democrat, 15 Aug 1940). Over the next 48 hours, 8 inches of rain was reported in Boone (U.S. Geological Survey, 1949). Nearby areas also reported their heaviest rainfall totals on August 13-14, with rainfall tapering off the remainder of the week (Table 1). For the week of August 10-17, the area around Watauga County received between 13-14 inches of rain (Figure 3).

DEBRIS FLOWS

On the night of August 13, between 8:30-9PM, the first landslides were reported in Deep Gap, to the east of Boone, along the Blue Ridge Escarpment (Watauga Democrat, 19 Sept 1940; Greene, 1941). It was initially reported that hundreds of landslides occurred in the area of Watauga, Caldwell, Avery, Ashe and Wilkes Counties (U.S. Geological Survey, 1949; Wieczorek et al, 2004). Subsequent mapping by the NCGS (Wooten et al, 2008) has shown that more than 2000 landslides, mostly debris flows and slides, occurred solely in Watauga County. Given the magnitude of the debris flow event in Watauga County, and the widespread nature of the heavy rainfall, we speculate that this storm likely triggered many more debris flows in northwestern North Carolina that have yet to be identified.

A majority (90%) of these debris flows/slides occurred on slopes greater than 20 degrees and most initiated on unmodified and unforested slopes. Landslide length varied greatly, from 30 feet to over 6800 feet, with many larger debris flows having several coalescing tracks. One unusual landslide type that was

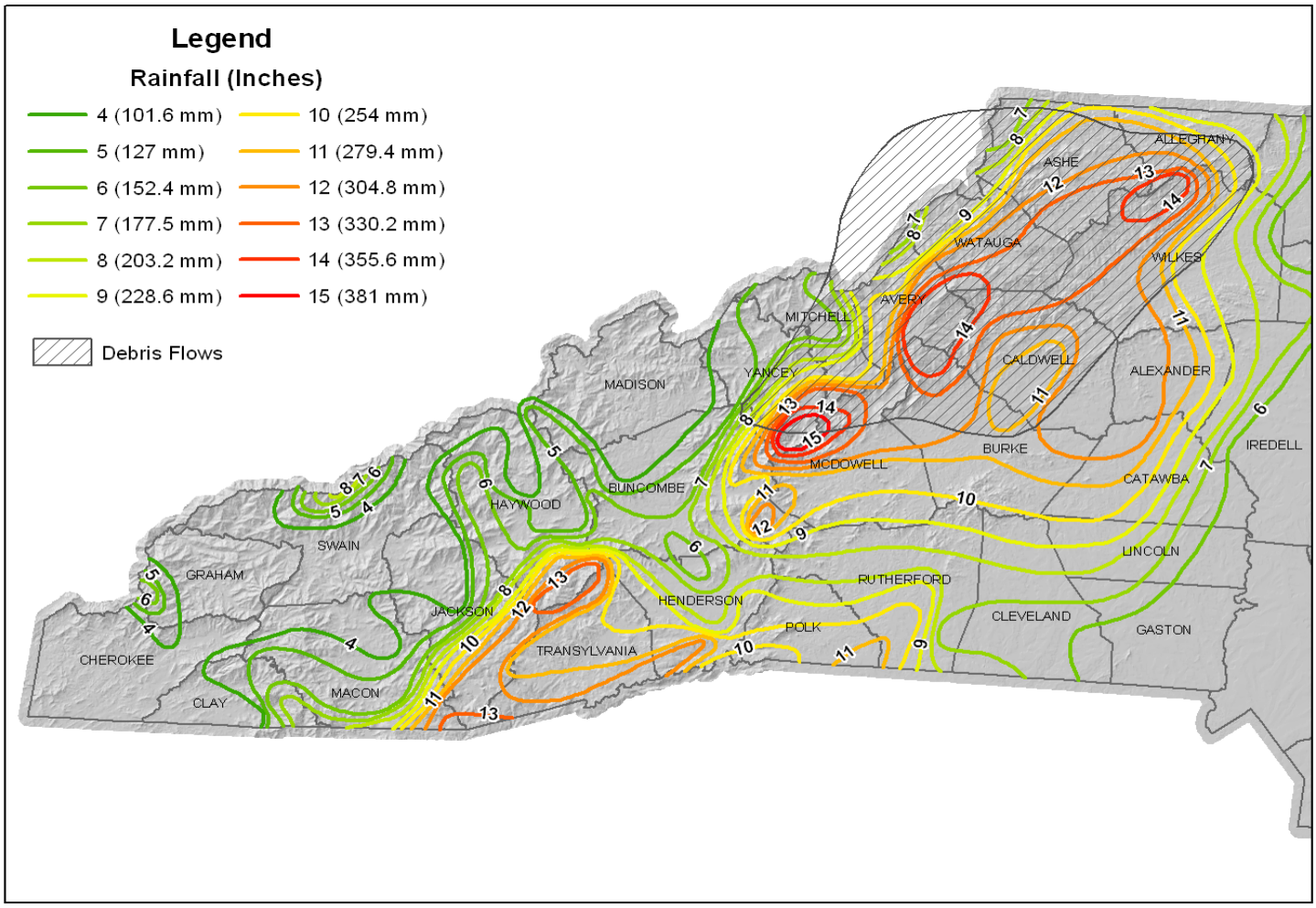

Figure 3: Isoheytal map of total rainfall from August 10-17, 1940 (modified from U.S. Geological Survey, 1949). The approximate location of known debris flow locations are shown in the hatched area.

found in Watauga as a result of the storm, were blow-outs (Wooten, et al, 2008) (Figure 4). These features are a type of slope failure where the ground bursts forth in response to excessive pore water pressure in the subsurface; however, there is insufficient water or sediment for the failure to scour a long track (Hack and Goodlett, 1960). The presence of these types of slope failures indicates that the ground in these areas was supersaturated and infiltration rates overwhelmed normal groundwater flow conditions.

There were two general concentrations of landslide occurrence: one in the Deep Gap/Elk Creek area of the county, also known as the Deep Gap reentrant (617 slides) and another in the Sherwood area (1483 slides), north and west of Boone (Figure 5). While there was a greater number of landslides in the Sherwood area, they tended to be shorter and wider than in the Deep Gap/Elk Creek region. Landslides in Deep Gap were longer, inundated a greater planimetric area, and were far more destructive than in Sherwood (Witt et al, 2008). Gryta and Bartholomew (1983) also recognized the difference in the Sherwood-type debris flow tracks when compared to those that occurred in central Virginia during Hurricane Camille in August 1969. In general, the locations of these slides in these specific areas of Watauga County probably relate to the presence of steep slopes and the location of high intensity rainfall associated with specific storm cells not visible in the 1940 isohyetal maps due to the lack of rain gauge data and radar. In addition, the geomorphology

Figure 4: A photograph taken by the NC Geological Survey in 2007 showing a 2004 blowout in Watauga County.

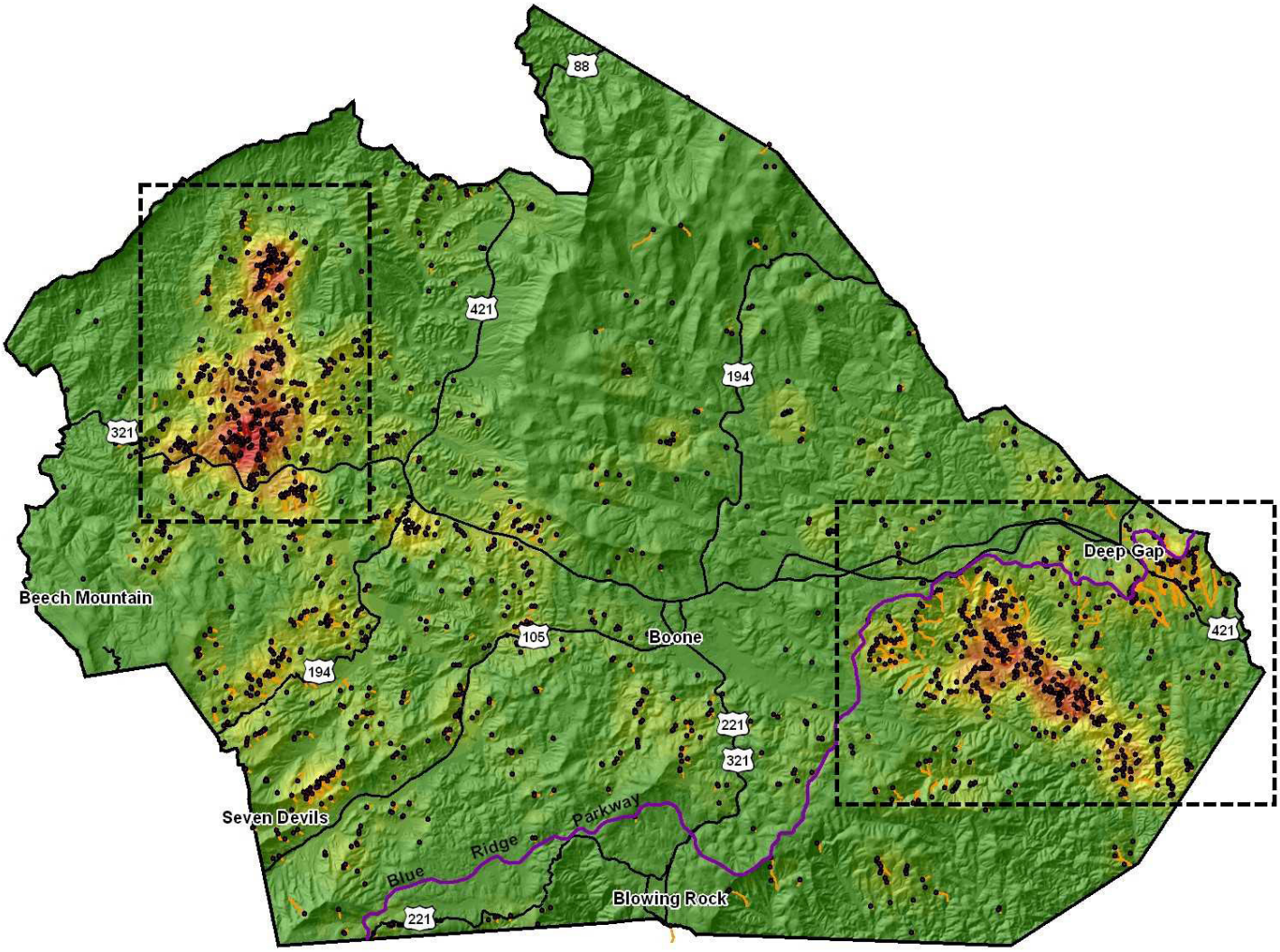

Figure 5: Map showing the concentrations of debris flows from the mid-August 1940 storm in Watauga County. Red areas indicate a greater concentration of debris flows, while green areas indicate fewer debris flows. The dashed box to the left identifies the Sherwood area where over 1600 landslides occurred, while the box to the right shows the Deep Gap/Elk Creek area.

of the Deep Gap reentrant, with narrow, nearly continuous colluvial hollows allowed first and second-order streams already at peak discharge to be conduits for excessively long debris flows that only dissipated once they reached the valley bottom.

DAMAGES AND IMPACT

The aftermath of the mid-August storm left 17 people dead in Watauga County and the surrounding area: 14 directly by landslide impact and three by drowning. Seventeen people were admitted to the Watauga Hospital with injuries related to landslides, including serious wounds with broken bones and internal injuries, and punctures and scratches from vegetative debris. The majority of those who were killed, or injured, by landslides lived in the Stony Fork area of the County. Others lived near Howard's Knob, north of Boone, or in the far western portion of the county near Banner Elk (Figure 6). Southwest of Watauga, an additional area of heavy rainfall was concentrated in northwest McDowell County, and included the North Cove reentrant into the Blue Ridge Escarpment (Figure 3). The Marion Progress (15 August 1940) reported the landslide death of John McGee and serious injuries to his wife near Ashford in North Cove. Other severe damage in the area included an 80-foot cave-in at the Swannanoa tunnel on the Old Fort railroad grade, other landslides and flooding, and destruction of farms and crops along rivers.

Overall, 32 houses were destroyed either by flooding or landslides in the storm area (Watuaga Democrat, 22 Aug 1940). In hard-hit Stony Fork, 13 houses were damaged or destroyed. The Greene family, who lived in a series of houses up the western branch of Stony Creek, by far, experienced the most destruction (Figure 7). Millard Greene, and his son Nolan, lived

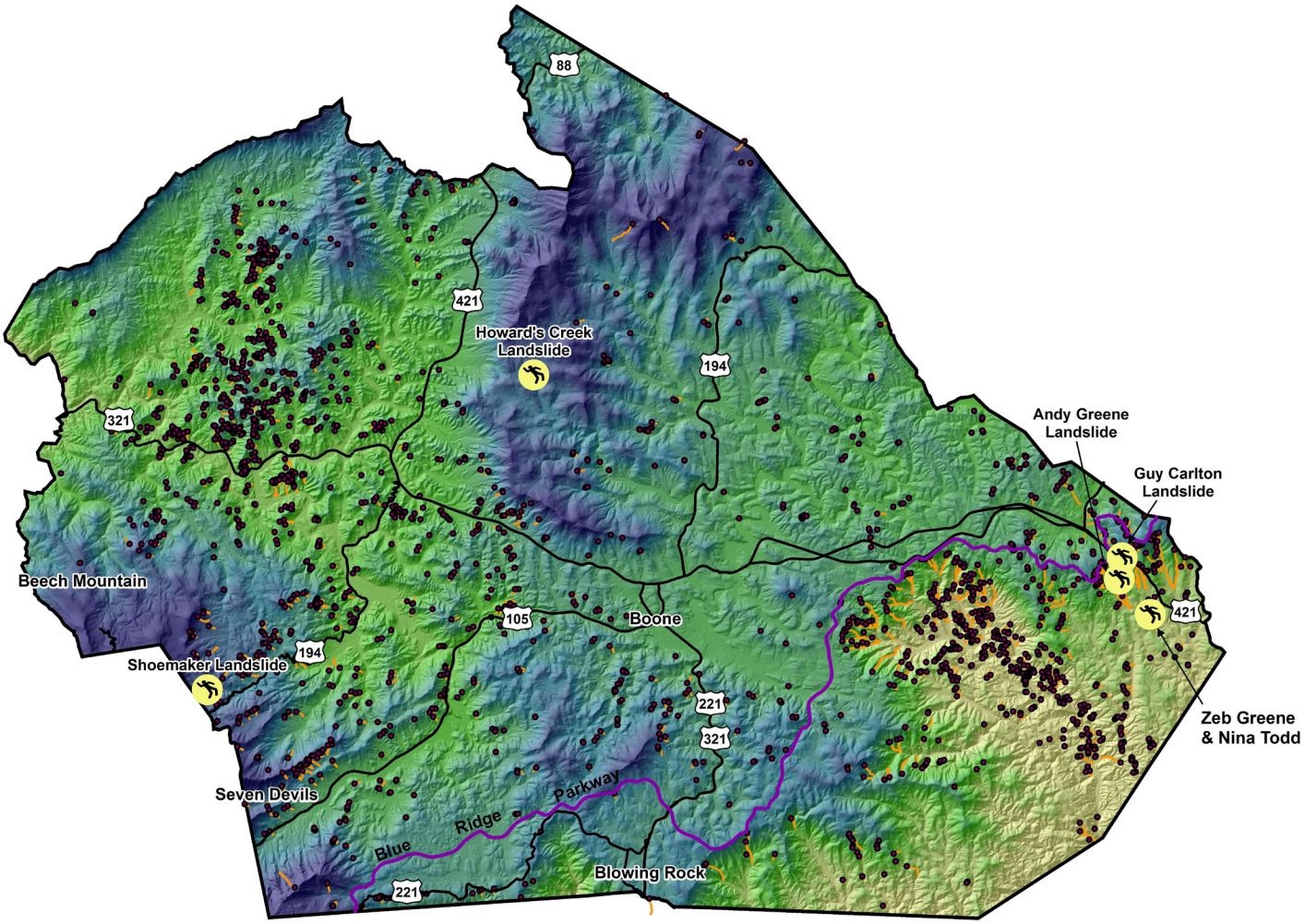

Figure 6: Map showing locations of the 2,099 landslide locations (black dots) mapped by the NCGS, and approximate locations of landslide fatalities (yellow-black symbol) that resulted from the August 13-14, 1940 storm that crossed Watauga County. Map colors indicate elevation (blue - higher elevations; tan - lower elevations) on a 6-meter LiDAR (Light Detecting and Ranging) shaded relief base map.

in two houses near the top of the Deep Gap reentrant, where both houses were destroyed by debris flows. A picture of Millard's home on the front-page of the 22 August Watauga Democrat, (incorrectly captioned as the home of Andrew Greene, see Watauga Democrat, 29 Aug 1940), shows the remnants of his kitchen wall and little else (Figure 8). Down valley, Millard's brother, Andrew Greene, and his three daughters were killed by this same debris flow. Andrew's wife Eliza and their two sons survived, but were injured and taken to the Watauga Hospital. Further downstream, the home of Bessie Greene and her five children was moved several hundred feet but managed to survive the debris flow (Figure 9). The family repaired the structure, but left it in place and it is still standing today (Optional Stop 1-7). The only home in this valley to go unscathed was that of Lawrence Greene, Andrew and Millard's brother, who lived with his parents on a slight knoll above the stream valley (Figure 7) (Greene, 1941).

Closer to Stony Fork Baptist Church (Stop 1-6), many houses and barns were flooded and damaged, but most survived. The home of Zeb Greene (no direct relation to the above Greene family) was surrounded by floodwaters and debris coming from upslope and Stony Fork (Figure 7). Worth Greene, his wife Lucy and infant daughter had been visiting Bessie Greene (Lucy's mother) but could not get home due to the flooding, so they weathered the storm at Zeb Greene's house. Unfortunately, when Zeb, Worth, and 15-year old Nina Todd, a cousin who had been attending a revival at the church with the Greene family, stepped onto the front porch, a tree in the flood swept them away. Worth managed to grab a nearby tree and survived, but Zeb and Nina's bodies were washed several miles downstream and found days later. Amazingly, the Zeb Greene house survives and is one of the oldest homes in Watauga County (Figure 10) (Watauga

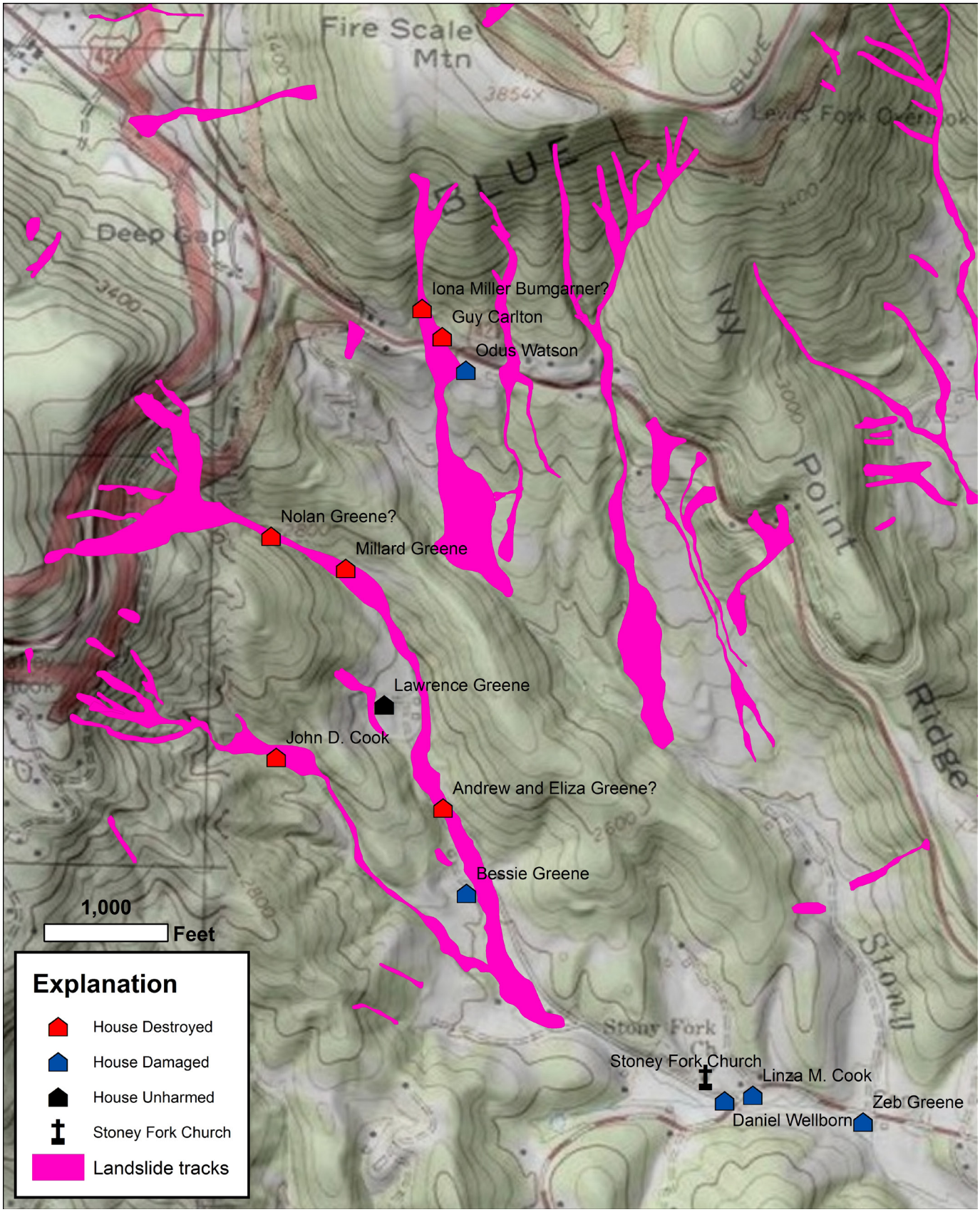

Figure 7: Map of the Deep Gap area of Watauga County showing the location of homes damaged (blue), destroyed (red) or unharmed (black) by debris flows from the mid-August 1940 storm (see text for individual narratives). The debris flow tracks are symbolized in pink, however flooding and hyperconcentrated flow continued beyond the extent of these tracks. The names of individuals indicates the homeowner, while a question mark (?) indicates that the location is approximate. The John D. Cook home was unoccupied at the time of the debris flows, but was destroyed. The Daniel Wellborn home was flooded and his family escaped to the Linza M. Cook residence and store.

Figure 8: The remains of the Millard Greene residence, destroyed by a debris flow originating upslope. (Source: Paul Weston, "Interior of Millard Greene House #3, August 1940," Digital Watauga, accessed August 16, 2018, https://digitalwatauga.org/items/show/6363).

Figure 9: The wreckage of the home owned by Bessie Greene within bouldery debris flow material. Notice the large tree, a sugar maple, at the side of the house. This tree brought the home to an abrupt stop and prevented it from continuing downstream. The Greene family repaired the home and it still stands today. (Source: Paul Weston, "Bessie Greene House, Moved Off Foundation by Flood, August 1940, #2," Digital Watauga, accessed August 16, 2018, https://digitalwatauga.org/items/show/6313).

Democrat, 15 November 2015). We will drive past the house on our way to the Stony Fork Baptist Church for Stop 1-6.

The storm also shut down transportation corridors throughout the county and washed out nearly every bridge over the Watauga River (Watauga Democrat, 22 Aug 1940). Numerous secondary gravel roads had the top layer of gravel removed and had to be repaired. Total road and bridge damage was estimated to be between $4.3-5.25 million ($77-94 million in 2018 dollars) in Watauga, Wilkes, and McDowell Counties (Watauga Democrat, 5 Sept 1940). Landslides severed U.S. 421 in several places in Deep Gap, shutting down all traffic between Boone and North Wilksboro

Figure 10: Photograph of the tombstone of Zeb Greene, killed on the night of August 13, 1940 when he was swept from the front porch of his house by landslide and flood debris. The white house in the center of the photograph is the Zeb Greene residence. The home remains in the Greene family through descendants of Zeb's brother Elster, who moved into the home after the 1940 flood. Photo by Anne Witt.

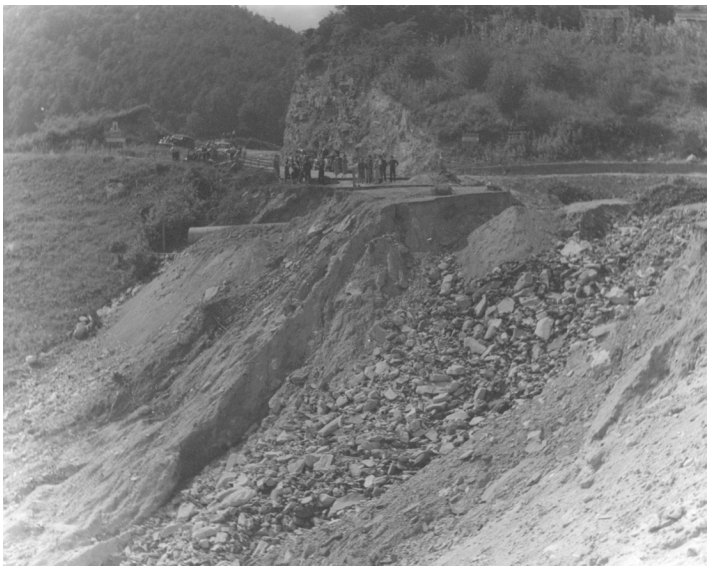

Figure 11: A 1940 photograph showing U.S. 421 after 1940 debris flows obliterated the road. Repairs took over a month to complete. This location is also where a debris flow destroyed Guy Carlton and Otus Watson's service stations. Scanned photograph by Paul Weston, courtesy of the Wilkes County Public Library, James Larkin Pearson Collection of the Wilkes Community College.

(Figure 11). The NC State Transportation Commission applied for emergency federal aid for $142,560 ($2.5 million in 2018 dollars) to repair the road and could not reopen it to traffic until 18 September (Watauga Democrat, 19 Sept 1940). In addition, the 1940 storm severely damaged the Linville River Railway, putting

Figure 12: A 1940 photograph of Otus Watson's house after a 1940 debris flow, originating from Thompkin's Knob, destroyed his filling station. Notice the gas pump near the center of the photograph. Photographer unknown. Courtesy of the Ashe County Public Library, NC Digital Collections (Available online: https://library.digitalnc.org/cdm/ref/collection/ncimages/id/3428)

an end to railroad service into Boone.

The landslides that destroyed U.S. 421 in Deep Gap also took the lives of three people and sent at least three people to the hospital. Two service stations, one owned by Guy Carlton and the other by Otus Watson, were destroyed by a debris flow that originated on Thompkin's Knob near the Blue Ridge Parkway (Figure 7). Guy Carlton took his entire family, his wife, four children, and mother-in-law, to the filing station after his house started to flood. Lula Greene Anderson, who was also there with her little brother Johnny Greene, lived above and ran the station. Together they were all washed across U.S. 421 when the station was hit by a massive debris flow. The flow also destroyed Otus Watson's station, which was directly across the street, and removed the front porch of his home next door (Figure 12). Luckily, Otus survived and helped rescue many of his neighbors, including Guys' daughter Clara who was found in an uprooted tree. Guy's mother-in-law, Martha Ann Carroll succumbed to her injuries a few days later in the hospital, but Johnny Greene was killed instantly, his body washed downstream towards Zeb Greene's house. Guy Carlton decided, though, that lightning would not strike twice and just two months later rebuilt his service station, exactly in the same place where it had been destroyed (Journal Patriot, 14 Oct 1940). The building is still there today.

THE 1940 DEBRIS FLOWS AND MODERN INFRASTRUCTURE

Since 1940, the population of Watauga County has doubled and the number of homes has increased by 80% (Witt et al, 2007). One of the concerns for the NCGS when creating landslide hazard maps for the county was just how many homes and roads had been unwittingly built near or within 1940 landslide areas. Examination of the locations of the 1940 debris flow tracks with 2005 orthophotography revealed that as of 2008, 135 modern structures (including homes and other permanent buildings) had been built within 87 of the 1940 debris flow tracks. They also found that 1940 landslides would have severed 329 modern roads (Witt et al, 2007). While this evaluation has not been replicated for this field guide, more structures and roads have been built in these areas over the past 10 years. Most recently on May 30, 2018, during rainfall from subtropical storm Alberto, a cut slope failure and subsequent gas explosion killed a couple in the Heavenly Mountain subdivision, south of Boone (Watauga Democrat, 4 June 2018). Even though the failure did not occur directly on a 1940 landslide site, the slope failed above where a 1940 landslide had been identified on 1940 black-and-white aerial photography by the NCGS. Identifying areas of past landslides will remain a crucial part of the landslide hazard mapping process.

ACKNOWLEDGEMENTS

The authors gratefully acknowledge the residents of Stony Fork and Watauga County for their willingness to provide property access, assistance, and local knowledge over the years. Much (if not all) of the landslide identification and mapping described in this article was completed between 2007-2008 by the NC Geological Survey - Landslide Hazard Mapping Team. Without the dedicated work of the additional members of "Team Slide", Jennifer Bauer, Tommy Douglas, Stephen Fuemmeler, Ken Gillon, and Rebecca Latham, this article would not have been possible.

REFERENCES

Atlanta Constitution, 13 August 1940, Many Islands still isolated: Damage Great, vol 73, no 62, p 11.

Gallenne, J.H., 1940, Monthly Weather Review: Tropical Disturbances of August 1940, vol. 68, no. 8, 217-218.

Greene, I.C., 1941, A Disastrous Flood: A True and Fascinating Story, Richmond, VA: William Byrd Press, Inc., 103 p.

Gryta, J.J., and Bartholomew, M.J., 1983, Debris-avalanche type features in Watauga County, North Carolina, in Lewis, S. E., ed., 1983, Carolina Geological Society Guidebook: North Carolina Division of Land Resources, article 5, 22p.

Hack, J.T., and Goodlett, J.C, 1960, Geomorphology and forest ecology of a mountain region in the Central Appalachians: U.S. Geological Survey Professional Paper 347, 66 p.

Journal Patriot, 14 October 1940, Rebuilds Where Slide Destroyed House, Station, vol 33, no 59, p 1.

Marion Progress, 15 August 1940, Flood Causes Heavy Losses of Property Throughout McDowell, Man Loses Life Under Landslide, vol 45, no 3, p1.

U.S. Geological Survey - Water Resources Branch, 1949, Floods of August 1940 in the Southeastern States: Geological Survey Water – Supply Paper 1006, Washington, D.C.: U.S. Government Printing Office, 554 p.

Watauga Democrat, 15 August 1940, Flood Toll Now 13, vol 53, no 6, p 8.

Watauga Democrat, 22 August 1940, Sixteen Wataugans Lose Lives As Flood Waters Sweep Over County, vol 53, no 7, p 1.

Watauga Democrat, 29 August 1940, A Correction, vol 53, no 8, p 1.

Watauga Democrat, 5 September 1940, Federal Funds Sought to Help Rebuild Roads, vol 53, no 11, p 9.

Watauga Democrat, 19 September 1940, Survivors of August Floods Describe Deep Gap Tragedy, vol 53, no 9, p 6.

Watauga Democrat, 15 November 2015, Granny Greene and the '40 Flood, Available Online: https://www.wataugademocrat.com/community/granny-greene-and-the-flood/article_61a84eac-2203-5c33-91f3-eb5c96d2a30b.html.

Watauga Democrat, 4 June 2018, Timeline of events released in Pine Ridge landslide, explosion, Available Online: https://www.wataugademocrat.com/news/timeline-of-events-released-in-pine-ridge-landslide-explosion/article_790c5fe1-a8cf-5411-a2ac-340460f73f89.html

Wieczorek G.F., Mossa G.S., Morgan B.A., 2004, Regional debris flow distribution and preliminary risk assessment from severe storm events in the Appalachian Blue Ridge Province, USA. Landslides 1:53-59.

Witt A.C., Smith M.S., Latham R.S., Douglas T.J., Gillon K.A., Fuemmeler S.J., Bauer J.B., Wooten R.M., 2007, Life, death and landslides: the August 13-14, 1940 storm event in Watauga County, North Carolina. In: Abstracts with programs, Geological Society of America Southeast Section, 39:76, Savannah, GA.

Witt, A.C., Wooten, R.M. Gillon K.A., Latham R.S., Douglas T.J., Fuemmeler S.J., Bauer J.B., 2008, Using an observational database in the preliminary statistical analysis of debris flow runout and its application to inundation modeling in Watauga County, North Carolina, USA, 33rd International Geological Congress, August 6-14, 2008, Oslo, Norway.

Wooten R.M., Witt A.C., Gillon K.A., Douglas T.J., Latham, R.S., Fuemmeler S.J., Bauer J.B., 2008, Slope movement hazard maps of Watauga County, North Carolina, N.C. Geological Survey Geologic Map Series 3, 4 sheets, scale 1:36,000.

Wooten, R.M., Witt, A.C., Miniat, C.F., Hales, T.C., Aldred, J.A., 2016, Frequency and Magnitude of Selected Historical Landslide Events in the Southern Appalachian Highlands of North Carolina and Virginia: Relationships to Rainfall, Geological and Ecohydrological Controls, and Effects, In: Natural Disturbances and Historic Range of Variation: Type, Frequency, Severity, and Post-disturbance Structure in Central Hardwood Forests USA (Greenberg, C.H. and Collins, B.S. eds), Springer, Managing Forest Ecosystems 32, p. 203-262.

Wooten, R.M., Cattanach, B.C., Bozdog, G.N., Isard, S.J., Fuemmeler, S. J., Bauer, J.B., Witt, A.C., Douglas, T.J., Gillon, K.A., Latham, R.S., 2017, The North Carolina Geological Survey's Response to Landslide Events: Methods, Findings, Lessons Learned and Challenges, In De Graff, J.V. and Shakoor, A. (eds.), Landslides: Putting Experience, Knowledge and Emerging Technologies into Practice, AEG Special Publication No. 27, p. 359-370.

Landslides and landslide hazard mapping in Watauga County, North Carolina

Rick Wooten
North Carolina Geological Survey, Division of Energy, Mineral, and Land Resources, N.C. Department of Environment and Natural Resources, 2090 US Highway 70, Swannanoa, NC 28778, rick.wooten@ncdenr.gov

Anne Carter Witt
Virginia Department of Mines, Minerals and Energy, Division of Geology and Mineral Resources, 900 Natural Resources Drive, Suite 500, Charlottesville, VA 22903, anne.witt@dmme.virginia.gov

ABSTRACT

The North Carolina Geological Survey completed landslide hazard maps for Watauga County in 2008. Ongoing mapping and other research since then reveals a regional pattern of recurring landslide events along the Blue Ridge Escarpment, and within structurally controlled topographic reentrants into it. This article summarizes the methods used to produce four GIS-based map layers for Watauga County: 1) a bedrock compilation map showing a zone of existing and potential rock slope instability; 2) an inventory map of slope movements and slope movement deposits; 3) a stability index map that shows susceptibility to landslides like debris flows and debris slides; and 4) a known and potential debris flow pathways map that shows areas that have been, or could be, inundated by debris flows. A major component of this year-long effort was to map over 2,000 landslides triggered by rainfall from a tropical cyclone that passed over northwestern North Carolina during August 13-14, 1940. Two focus areas of the Watauga County study discussed herein are the stability of rock slopes along a segment of the Linville Falls fault where it is overprinted by the younger Boone fault and, investigations into debris flow initiation zones.

INTRODUCTION

This paper will focus on landslide hazard mapping done by the North Carolina Geological Survey (NCGS) in Watauga County. Other landslide mapping and research done by the NCGS, the Virginia Division of Geology and Mineral Resources (VDGMR), and Appalachian Landslide Consultants, PLLC (ALC helps to place Watauga County in the context of the Southern Appalachians. This ongoing mapping and other research reveals a pattern of recurring landslide events along the Blue Ridge Escarpment, and within structurally controlled topographic reentrants into it. We will summarize the findings of the year-long effort to map landslide features in Watauga County, and the methods used to create the landslide hazard maps. Two focus areas of that study discussed here are the stability of rock slopes along a segment of the Linville Falls fault where it is overprinted by the Boone fault, and debris flow initiation zones. A primary research objective for the NCGS is to better understand the geologic controls on landslides. An over-arching goal of this research, however, is to protect public health and safety by reducing losses from landslides.

A key feature of the above landslide studies, has been the development of comprehensive landslide inventories in a geographic information system (GIS) environment. These inventories, developed as ArcGIS geodatabases, provide a means to geospatially document prehistoric and historic landslide occurrences and to assess the frequency and magnitude of these events. Data to develop, constrain, and calibrate predictive models like those for debris flow susceptibility and run out rely on the empirical information in the geodatabases. As we will see on this field trip, information in landslide geodatabases can help identify specific problem areas for further detailed research. Information sharing, and interdisciplinary collaboration is important to build on landslide geodatabases and further the research on landslide hazards.

From 1990 to 2018, NCGS geologists investigated over 215 landslides in response to requests for technical assistance from government agencies, the public and consultants (Wooten et al., 2017). Compilation of existing landslide information and new mapping of landslides began in 2003 in cooperation with the N.C. Division of Emergency Management (Wooten et al., 2005). From 2006 to 2011, the NCGS completed GIS-based landslide hazard maps for Macon, Watauga, Buncombe and Henderson Counties (Wooten et al., 2006, 2008b, 2009, 2011) and began work on Jackson County. The NCGS also completed a geologic inventory of the North Carolina portion of the Blue Ridge Parkway that included a landslide hazard assessment (Latham et al., 2009). In 2008, the NCGS migrated landslide data into an ArcGIS™ geodatabase to sys-

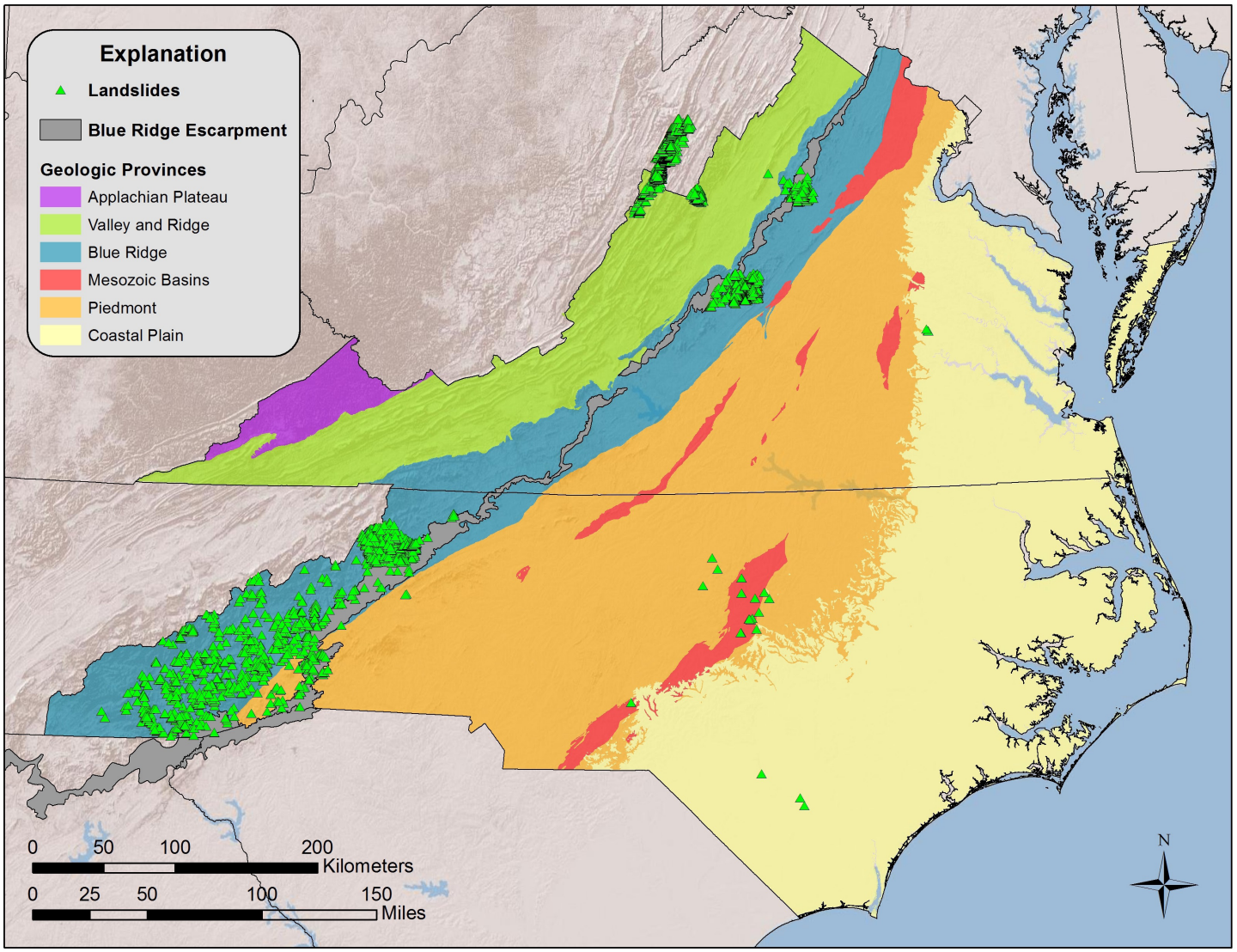

Figure 1: Geologic provinces of North Carolina and Virginia, the Blue Ridge Escarpment, and ~8,400 landslide locations in landslide geodatabases of the North Carolina Geological Survey and Virginia Department of Mines Minerals and Energy. Adapted from Witt and Wooten, 2015.

tematically document geospatial information collected at landslides sites (Witt et al., 2008; Bauer et al., 2012). Landslide geodatabases with similar attributes and fields are in use by the VDGMR (Witt and Wooten, 2015) and Appalachian Landslide Consultants (Bauer and Fuemmeler, 2017; ALC, 2018). Point locations for nearly 8,400 landslides in the NCGS and VDGMR geodatabases are shown in Figure 1.

ESCARPMENTS, REENTRANTS AND CROSS-STRUCTURES

A focus of this field trip will be the relationships between tectonic history, landscape evolution and features, and slope movement processes. To that end, a brief summary of historical landslide activity associated with the Blue Ridge Escarpment (BRE) in North Carolina and Virginia is in order. Recent work has shown that structurally controlled topographic reentrants into the BRE, such as the Deep Gap reentrant in Watauga County, are among the areas of frequent debris flow and other landslide activity in the southern Blue Ridge Mountains. Debris flow activity also can be concentrated in smaller scale landforms like the Nantahala Mountains Escarpment and the Wayah and Poplar Cove reentrants that cross it in Macon County, North Carolina.

Blue Ride Escarpment

The Blue Ridge Escarpment (BRE) that extends from northeast Georgia to Virginia is prone to historical debris flow activity (Wooten et al., 2016, and references therein). The distribution of areas affected by debris flows from the July 15–16, 1916, the August 13–14, 1940, and May 18-30, 2018 events in North

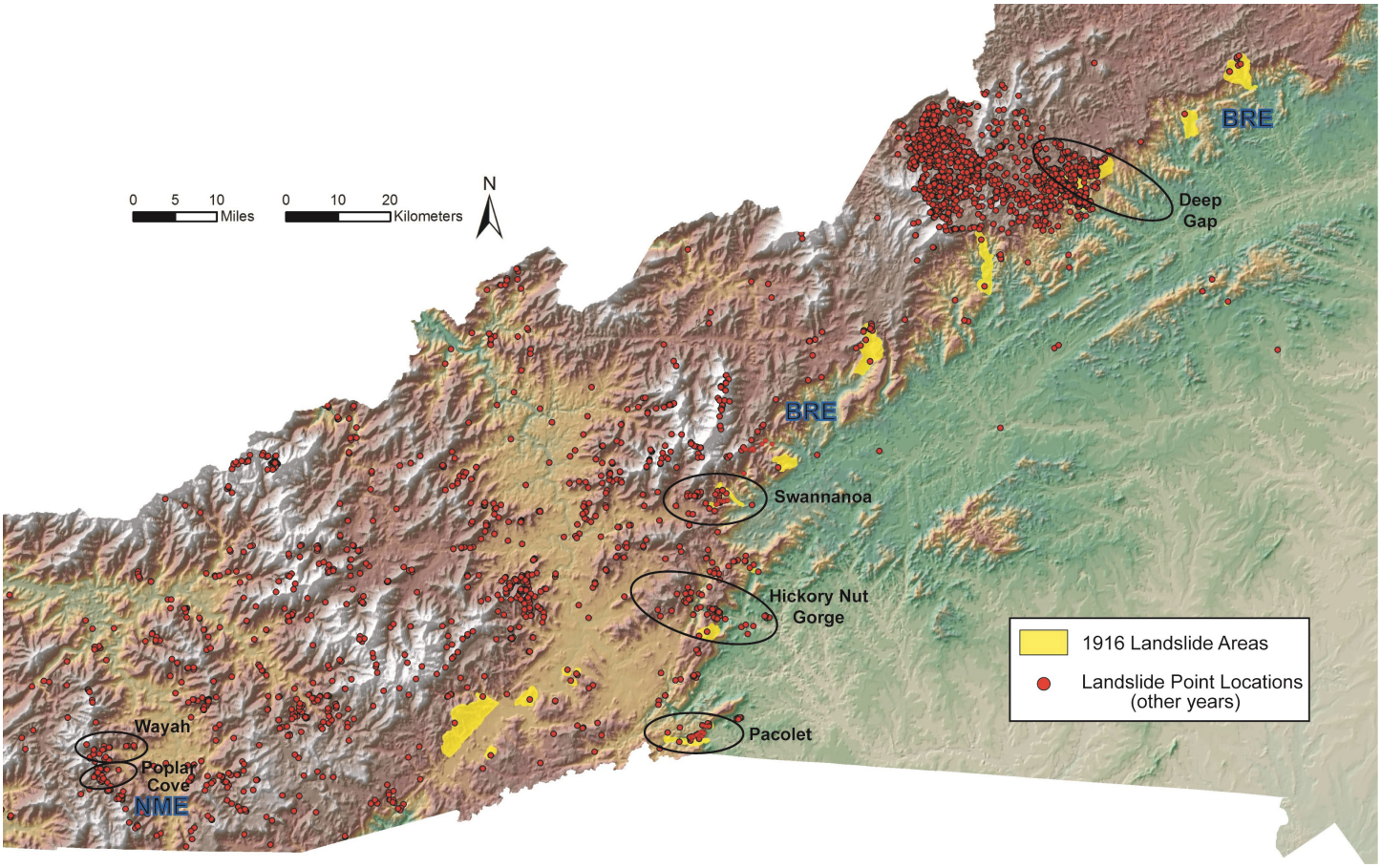

Figure 2: Map showing point locations for landslides and 1916 landslide areas in the NCGS landslide geodatabase for western North Carolina,the Blue Ridge Escarpment (BRE), and named reentrants into it. Map base is a shaded relief map and a color-coded elevation gradient derived from a 6-meter pixel resolution LiDAR DEM.

Carolina generally coincide with the BRE as do the August 19–20, 1969 (Camille) and the June 27, 1995 events in Virginia (Figure 1). High relief, steep slopes, and the dissected nature of the BRE, in combination with its orographic influence on rainfall, make it susceptible to debris flows. Orographic forcing of rainfall along the BRE is identified by greater rainfall totals as compared to the surrounding regions for the storms of July 15–6, 1916 (Scott 1972, Witt 2005), August 10–17, 1940 (US Geological Survey 1949); see Fig. 3 in Witt and Wooten, this guidebook), and June 27, 1995 (Wieczorek et al., 2004). Topographic reentrants into the BRE controlled by linear bedrock structures (e.g., fractures, faults) are also prone to debris flows and other types of landslide activity. Figure 2 shows the locations of cross structures known to be associated with recurring historical landslide activity.

Deep Gap Reentrant

A prime example of where bedrock structure can be related to recurring debris flow activity is the Deep Gap area of Watauga County where nearly 700 debris flows occurred during the August 13–14, 1940 storm (Greene, 1941; Wieczorek et al., 2004; Wooten et al., 2008b). Green (1941) also recounts debris flows in the Deep Gap reentrant triggered by heavy rainfall from the July 15-16, 1916 tropical cyclone. Here, Elk Creek and its tributaries form a highly dissected erosional reentrant within the BRE that coincides with WNW-trending ductile faults (Bryant and Reed 1970) and other WNW-trending topographic lineaments, and associated fractures and brittle faults that intersect the BRE (Gillon et al., 2009). Unstable rock slopes occur west of the Deep Gap reentrant where these WNW-trending brittle structures associated with the Boone fault (Hill, 2018; Hill and Stewart this guidebook) overprint the Linville Falls fault (Wooten et al., 2008b and Gillon et al., 2009).

Swannanoa Reentrant

The Swannanoa reentrant coincides with WSW-ENE trending Swannanoa lineament (Dennison and Stewart, 2001) where it crosses the BRE near Old Fort and Ridgecrest, North Carolina. This area of the BRE has a history of recurring landslide events, reported in 1916 (Southern Railway Company, 1917), and doc-

umented in 2004, 2013, 2015 and 2018 in the NCGS landslide geodatabase. Bedrock mapping in the Black Mountain and Montreat quadrangles (Cattanach et al., 2014; 2016) documented a dominant WNW-ESE fracture set in this area, oblique to the overall trend of the Swannanoa lineament, but parallel to the Hickory Nut Gorge lineament swarm ~6 km to the south.

Hickory Nut Gorge Reentrant

The Hickory Nut Gorge (HNG) lineament swarm transects the BRE with a WNW trend controlled by fracture orientations (Wooten et al., 2018). Where the HNG lineament swarm extends into the Mills Gap area of Buncombe County, North Carolina, detailed mapping and structural analysis identified the brittle Mills Gap fault and associated fracture sets that are subparallel to the HNG trend (Wooten et al., 2010). Within the HNG, extensive foot slope deposits of rock blocks and boulders reveal that the gorge walls have been prone to numerous Quaternary landslides. Documented historical landslide events include those in 1916, 1994, 1996, 2008 and 2014 (Soplata, 2016; Wooten et al., 2011; Wooten et al., 2017). Most recently, numerous debris flows and debris slides triggered by rainfall from subtropical storm Alberto during May 29-31, 2018 affected Chimney Rock State Park and the Town of Chimney Rock in the HNG.

The HNG reentrant and others like it may influence local weather patterns. Lee and Goodge (1984) suggest that the HNG may have provided an opening in the BRE barrier that focused low-level upslope flow into a flash flood producing thunderstorm complex in 1978. Johnstone and Burrus (1997) point to the unique terrain of the HNG as a geomorphic factor in the September 4, 1996 flash flood that produced more than 30cm of rain in 3 hours triggering debris flows and causing extensive damage in Chimney Rock, North Carolina. They concluded that the predominant mechanism responsible for the heavy rainfall was the orographic rise of moist unstable air up the east slope of the BRE, but one that could be indirectly linked to the concurrent passage of Hurricane Fran 320km to the east over the North Carolina Coastal Plain and Piedmont.

Pacolet Reentrant

The Pacolet River valley forms a sharp EW-trending reentrant into the BRE, with associated WNW-trending topographic lineaments in Polk County, North Carolina. Heavy rainfall from two successive thunderstorms the evening of May 18, 2018 triggered numerous damaging debris flows and debris slides. In the Valhalla community, two of these debris flows coalesced on the footslopes of Little Warrior Mountain destroying a house and killing an occupant. As of August 2018, ongoing mapping in the area by the NCGS and ALC has identified 11 major debris flows triggered by the May 18 storms. Structural data show a dominant EW fracture (joint) set exposed in debris flow tracks on the steep valley walls of the reentrant. Current mapping and historical accounts show that this is also an area of recurring debris flow activity. Pre-existing debris flow deposits have been identified in several of the May 18, 2018 debris flow tracks and run out zones. Landslides in this area of the BRE were reported during construction of I-26 between 1969-1975 by the N.C. Department of Transportation, on the Saluda Railroad grade during the July 15-16, 1916 storm (Southern Railway Company, 1917), and in September 2004 as recorded by the NCGS.

Middle Saluda Reentrant

About 30km southwest of the Pacolet reentrant, the Middle Saluda River follows an incised EW-trending reentrant into the BRE in Jones Gap State Park, South Carolina. Muthukrishnan (2012) documented debris slides (flows) that occurred here in 1976 and 2006 on the steep valley slopes. His studies also identified an E-W joint direction subparallel to the trend of the reentrant, and extensive boulder deposits in the valley indicating a prolonged landslide history in the area. Like other locations along the BRE, Muthukrishnan (2012) reported that the area receives precipitation >190 cm (75 in) per year, much higher than the nearby Piedmont region.

Nantahala Mountains Escarpment – Wayah and Poplar Cove Reentrants

Geologic controls on smaller scale topographic escarpments and reentrants prone to debris flows occur on the Nantahala Mountains Escarpment (NME) in Macon County, North Carolina (Figure 2). Here 25 of the 33 Macon County debris flows related to the September 2004 rainfall from the remnants of Hurricanes Frances and Ivan occurred on the steep eastern flanks of the NME (Wooten et al., 2006; 2008a). The 25 km-long NME forms an abrupt topographic rise with the headwaters of east-flowing tributaries of the Little Tennessee River. The main NW and N trends, and secondary NE trends of its different segments, parallel numerous topographic lineaments with orientations similar to measured bedrock discontinuities in

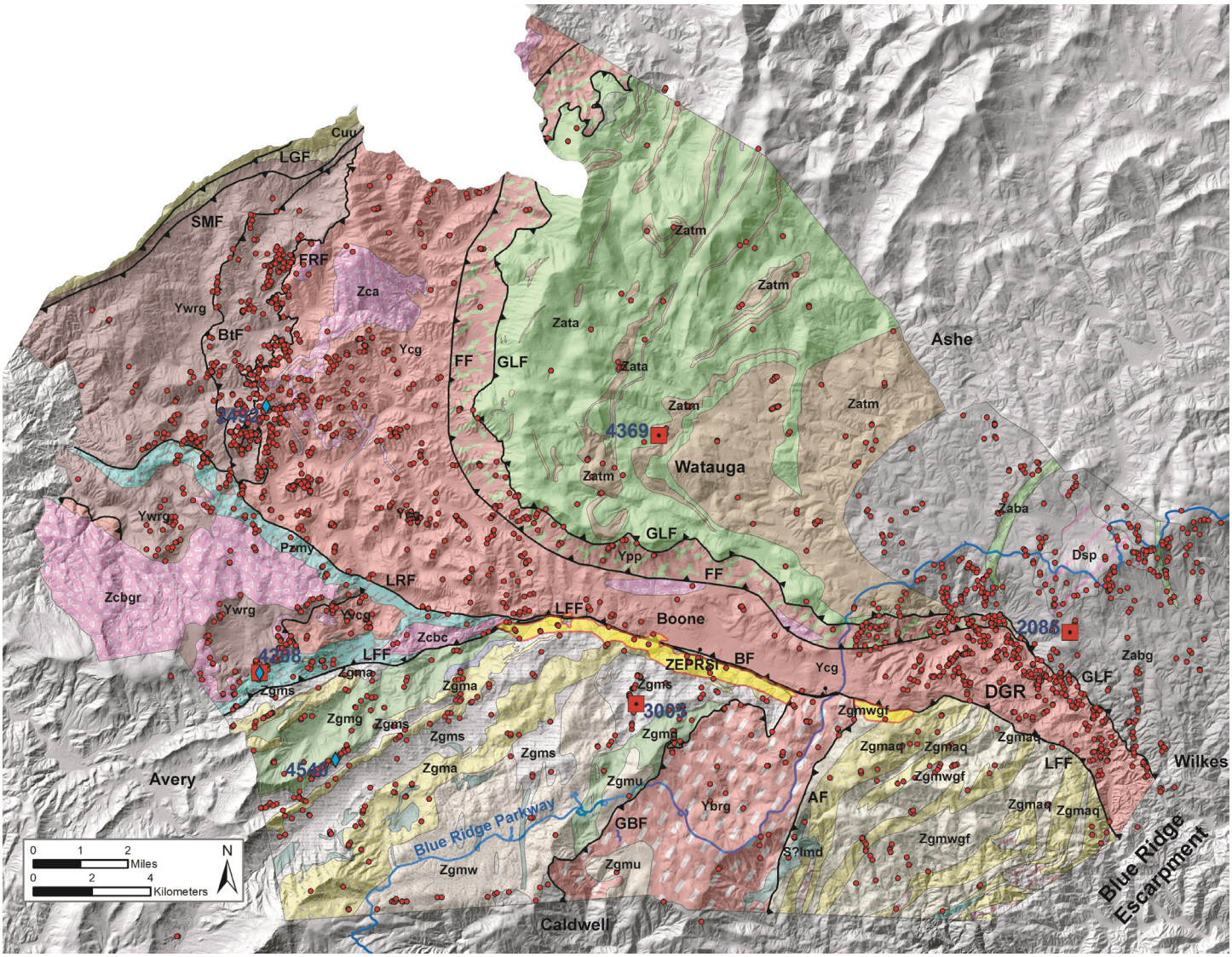

Figure 3: Compilation geologic map for Watauga County and point locations for landslides (small red dots) in the NCGS landslide geodatabase (adapted from Wooten et al., 2008b). ZEPRSI = zone of existing and potential rock slope instability. Numbered locations for detailed study sites at debris flow initiation zones: red circles-black center = residual soil sites; blue diamonds = colluvial soil sites. DGR = Deep Gap Reentrant. Bedrock map units: Late Mesoproterozoic age: Ywrg – Watauga River Gneiss; Ycg – Cranberry Gneiss; Ybrg – Blowing Rock Gneiss. Ypp – Pumpkin Patch Metamorphic Suite; Late Proterozoic: Zgm – Grandfather Mountain Formation (in Grandfather Mtn. Window); subunits a – mainly metaarkose and metasandstone; f – felsic metavolcanics; g – mainly metagraywacke, metasandstone, and metavolcanics; m – mafic metavolcanics; s – mostly metasiltstone. Zc – Crossnore Plutonic Suite; subunits a – aegirine alkalic metagranite; bc – Beech alkalic metagranite; bgr – Beech metagranite. Zat – Ashe Metamorphic Suite – Tallulah Falls Formation; subunits a – amphibolite, m – biotite gneiss, metagraywacke. Zab – Alligator Back Formation: subunits a – amphibolite; g – gneiss, conglomeratic metagraywacke, metasiltstone. Devonian age: Dsp- Spruce Pine Plutonic Suite granitic and pegmatite intrusives. Cambrian age: Ccu – Unicoi Formation mainly conglomeratic metasandstone. Faults: Thrust faults LFF – Linville Falls fault; FRF – Fork Ridge fault; FF – Fries fault; GLF – Gossan Lead fault; BtF – Bethel fault; LGF – Locust Gap fault; SMF – Stone Mtn. fault; GBF – Goldmine Branch fault; AF – Aho fault; Tear fault LRF – Long Ridge fault; Normal fault BF – Boone fault.

the area, reflecting the influence of bedrock structures on the NME. At the watershed scale, other September 2004 debris flows were concentrated within the EW-trending Wayah Creek and Poplar Cove reentrants on the NME, also controlled by orientations of bedrock foliation and fractures that intersect the NME (Wooten et al., 2008a). Orographic forcing of rainfall by the NME occurred during Hurricanes Frances and Ivan. The Mooney Gap rain gage (elevation 1,364 m) on the crest of the NME at the USDA-Forest Service Coweeta Hydrologic Laboratory received 100 mm more rainfall in each storm than did several lower ele-

vation gages in the area (Wooten et al., 2008a).

WATAUGA COUNTY LANDSLIDES AND LANDSLIDE HAZARD MAPPING

In response to the number of slope movements (landslides) and the destruction caused by the remnants of Hurricanes Frances and Ivan in western North Carolina in September 2004, the North Carolina General Assembly authorized the NCGS to produce landslide hazard maps for 19 western counties. Macon County was mapped first because of the fatalities and damage from the Peeks Creek debris flow (Wooten et al., 2006; 2008a). Watauga County was selected as the second county to be mapped because of the large number of landslides and the landslide deaths associated with the August 13-14, 1940 storm and the fast-growing population potentially at risk from other landslides. The landslide hazard maps are intended to provide the public, local government and emergency management agencies with a planning tool that identifies areas where landslides have occurred or are likely to occur and the general areas exposed to landslide hazards in order to help protect public health and safety. A key point is that the maps do not substitute for a detailed, onsite analysis by a qualified geologist or engineer, but identify areas where such investigations are warranted prior to land-disturbing activity.

Landslide hazard maps for Watauga County are in an ArcGIS™ format to facilitate use with other GIS map layers and to allow updates when new information becomes available. The four component map layers are:

1. a generalized bedrock compilation map showing a zone of existing and potential rock slope instability (ZEPRSI);
2. a slope movements and slope movement deposits map (i.e., a landslide inventory);
3. a stability index map that shows susceptibility to shallow translational slope failures like debris flows and debris slides; and,
4. a known and potential debris flow pathways map that shows areas that have been, or could be affected by debris flows (e.g., debris flow run out zones).

We made extensive use of digital elevation models (DEMs) derived from 6-meter resolution Light Detecting and Ranging (LiDAR) data, including shaded relief and slope maps, and 20-ft topographic contours. The LiDAR DEMs and various vintages of aerial imagery were used to map structural features, landslides and to target areas for field confirmation. To identify landslide features over a span of 66 years, we used scanned and georegistered 1940 aerial photography and 1993, 1998 and 2006 digital orthophotography. Figure 3 shows the compilation geologic map for Watauga County with point locations for inventoried landslides, the ZEPRSI, and locations of detailed debris flow study sites used in the stability index map modeling.

Completing a landslide inventory of an area is a first step in producing landslide hazard maps. The inventory forms the basis for determining other types of mapping, testing and modeling that is needed given the landslide types present and the landslide history of the area. Before discussing the hazard map layers and methods used to produce them, the following overview of landslide types and history is presented to summarize the inventory findings.

Landslide Types and History

A variety of landslides types occur in Watauga County (Figure 4). Of the 2,258 landslides recorded in the NCGS landslide geodatabase, debris flows (1,787) and earth flows (17) comprise the majority totaling 1,804 (80%). Next in abundance are debris blowouts (297) and earth blowouts (2), which total 299 (13%); followed by debris slides (124) and earth slides (5) which total 129 (6%). Twenty-four slides originated in weathered-rock or rock, which make up 1% of the total.

Debris-earth flows, blowouts and slides induced

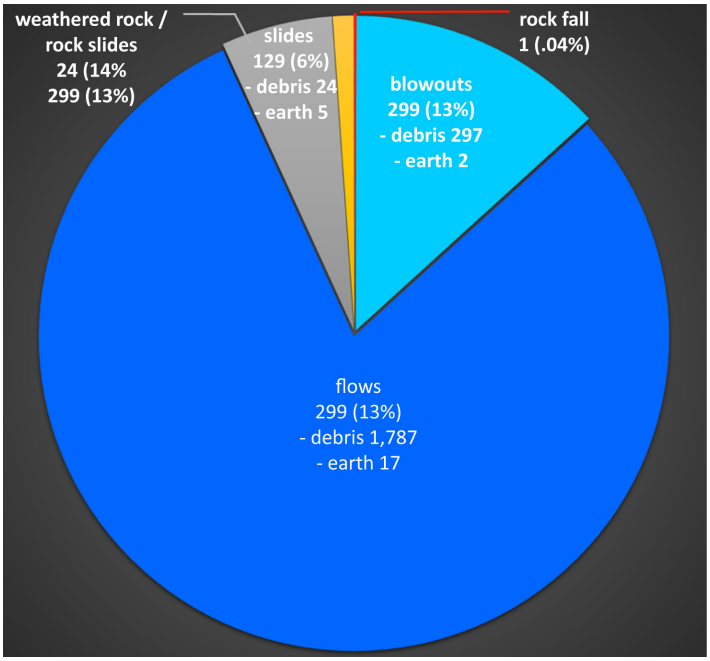

Figure 4: Pie chart showing the types of landslides for Watauga County documented in the NCGS landslide geodatabase.

Figure 5: Home in the While Laurel community destroyed by an embankment (fill) failure that mobilized into a debris flow on September 8, 2004 during rainfall from the remnants of Hurricane Frances. 2004/09/08 NCGS photo.

by heavy rainfall from tropical cyclones in 1940 and 2004 make up the vast majority of the Watauga landslides (Table 1). The 2,099 slope failures triggered by the mid-August 1940 storm make up 93% of the slope failures in the County. Twenty-one other debris flows mapped in nearby Wilkes (17), Avery (2), Ashe (2) Counties brings the mid-August 1940 storm total recorded in the geodatabase to 2,120 (Figure 3). Rainfall from the remnants of Hurricanes France and Ivan triggered 39 known slope failures during September 6-17, 2004. More recently, two landslide-related fatalities occurred in the Heavenly Mountain community on May 30, 2018 during rainfall from subtropical storm Alberto. The Watauga County Sheriff's Department reported a sequence of events in which a landslide damaged a LP gas regulator that serviced the home, causing a gas leak and subsequent explosion that destroyed the home (Watauga Democrat, 2018). Although not investigated by the NCGS at the time of this article, newspaper photographs of the scene indicate that the landslide located on the Blue Ridge

Date	Landslides	Weather Event
August 13-14, 1940	2,099	tropical cyclone
May 28, 1973	1	unknown
1983	2	unknown
1984	1	unknown
May 1987	1	unknown
June 16, 1989	1	unknown
February 1997	1	storm?
Sept. 8, 2004	6	Frances
Sept. 17, 2004	1	Ivan
Sept. 6-17, 2004	32	Frances-Ivan
January, 7-13, 2007	1	unknown
January 17, 2013	1	storm
May 24, 2017	1	storm
February 12, 2018	1	storm
May 30, 2018	1	Alberto
unknown	108	unknown
Total	2,258	

Table 1: Dates, landslide numbers, and corresponding weather events for landslides documented in the NCGS landslide geodatabase for Watauga County.

Escarpment may have been a cut slope failure. Refer to Figure 1 in Witt and Wooten, (this guidebook) for a timeline of landslide triggering storm events in the region.

Documented slope failures that are related to ground-disturbing human activity total 151 (6.7%). Broken down by category there are: 93 embankment (fill) slope failures; 49 cut slope failures and 9 unspecified road-related failures. Heavy rainfall can trigger failures in poorly constructed embankment (fill) slopes that can mobilize into debris flows and severely damage or destroy homes. Such an event occurred on September 8, 2004 during rainfall from the remnants of Hurricane Frances when an embankment failure destroyed a home in the White Laurel community (Wooten and Latham, 2004) (Figure 5). Fortunately, occupants of the house were not seriously injured. Of the 24 slides in weathered-rock or rock, only one occurs on an unmodified slope, whereas 23 of these slides involve excavated (cut) slopes. The most recent rock slide occurred on the Blue Ridge Parkway, on February 12, 2018 near Milepost 277 in gneissic metasediments of the Alligator Back Formation (Zabg). We will pass by the rock slide scar, approximately 0.27km (0.16mi) north of the Stony Fork overlook on the

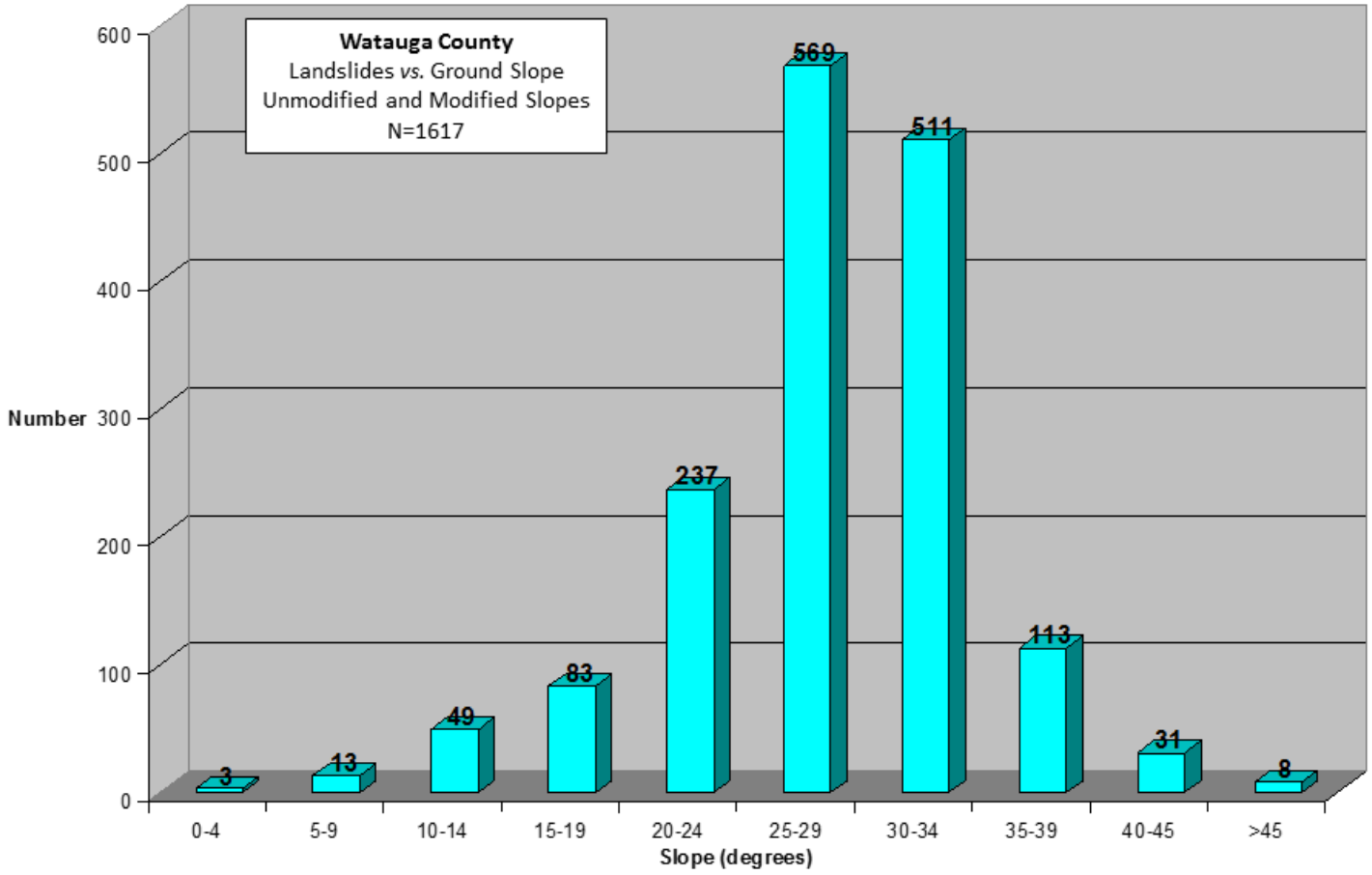

Figure 6: Histogram showing the numbers of landslides vs. ground slope in degrees for 1,167 sites in Watauga County.

way to Stop 1-5. Coincidentally, this rockslide is also within the upper portion of one of the 1940 debris flow tracks that coalesced and traveled down into the Stony Fork community where we will visit at Stops 1-6 and 1-7.

Ground slope is a primary contributing factor in most types of landslides, with the numbers of landslides increasing with steeper slopes. Figure 6 shows the distribution 1,617 Watauga failures on unmodified and modified slopes categorized by ground slope. A sharp increase in the numbers of landslides occurs on slopes in the 20°-24° degree range, a nearly 3-fold increase in landslide numbers from the 15°-19° slope range. Landslide numbers decrease abruptly on slopes greater than 40°, primarily because slopes greater than 40° are usually rock outcrop.

The NCGS identified debris deposits from past landslide activity, primarily several generations of debris flows, at 894 locations in the county. These deposits comprise a total area of ~66.4 km^2 (~25.6 mi^2), and cover roughly 8.2% of the county. Mapping revealed that modern debris flows commonly deposit sediment in areas underlain by pre-existing debris deposits. Figure 10 shows 1940 debris flow tracks that extend into pre-existing debris flow deposits in the Deep Gap area. The presence of these deposits, therefore, can indicate areas that could be affected by future debris flows.

Two of the largest debris deposits are composite debris fans on the west slopes of Snake and Rich Mountains, covering about 5.46 km^2 and 4.97 km^2 (2.1 mi^2 and 1.9 mi^2) respectively. Mills (1998) completed extensive research on the geomorphic evolution of these composite foot slope deposits that record multiple prehistoric debris flow events. Subsequent work by Mills and Grainger (2002) yielded a cosmogenic ^{26}Al/^{10}Be isotope age of 1.45±0.17 Ma, indicating that the older fan material was deposited in the early Pleistocene. We will view these debris fan complexes at Stops 2-1 and 2-2.

Because debris deposits are thick accumulations of unconsolidated, heterogenous mixtures of clay- to boulder-sized sediment (i.e., diamictons) they can be destabilized by steep, high excavations. In some cases, large, ancient(?) debris slides have developed in thicker debris deposits which can reactivate after

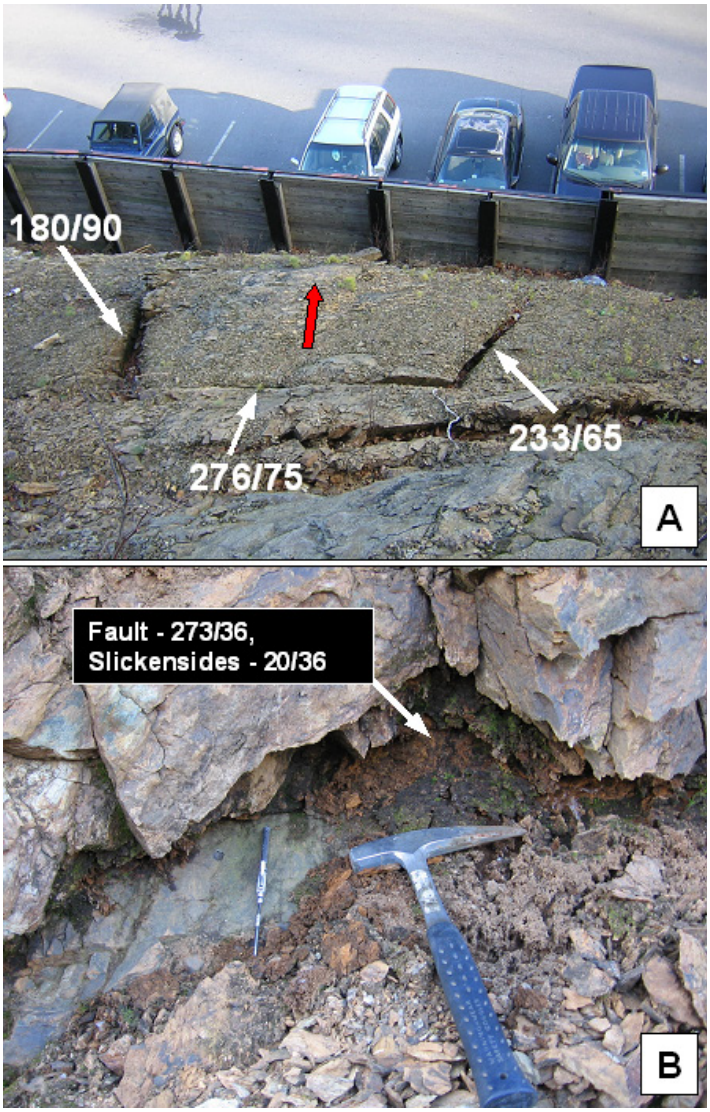

Figure 7: Rockslide block (cut slope failure) within the ZEPRSI located at Meadowview Apartments in Boone, N.C. Adapted from Gillon et al., (2009). A. Red arrow = slide movement direction. Strike azimuth and dip amount of fracture controlled back (276/75) and side release surfaces (180/90 and 233/65) are labeled. View looking north. B. Sliding surface is clayey fault gouge with slickenlines developed in mylonitic metasiltstone (?) of the Grandfather Mtn. Formation. View looking south. 2008 NCGS photo.

dormant periods (Wooten et al, 2017). Overall these slow-moving debris slides are not life threatening, but they can cause extreme hardships for property owners.

LANDSLIDE HAZARD MAP COMPONENTS AND METHODS

Generalized Bedrock Compilation Map - Zone of Existing and Potential Rock Slope Instability

The bedrock map of Watauga County, compiled in ArcGIS™, shows the general bedrock map units

Figure 8: Rockslide damage to the timber lagging of the retaining wall in Figure 7. 2015/04/28 NCGS photograph.

major thrust faults, and delineates a zone of existing and potential rock slope instability (ZEPRSI) where rock slope failures are more likely to occur on some modified slopes (Figure 3). The bedrock map units and mapped debris deposits also served as calibration regions for the debris flow susceptibility modeling (Figure A4 App. A), which is discussed in more detail in the Stability Index Map section. The map also provided the means for collecting landslide field data more accurately linked to mapped bedrock units better understanding of the structural controls on landslides especially those within the ZEPRSI.

The following published and unpublished sources were used to compile the bedrock map: Adams (1990, 1995), Acker (1983), Bartholomew and Gryta (1980), Bartholomew (1983), Bartholomew and Wilson (1984), Bryant (1963, 1965), Bryant and Reed (1970), Cattanach and others (2007), Fetter and Goldberg (1995), Hatcher et al. (2006), Keith (1903), King and Ferguson (1960), Lewis and Bartholomew (1984), NCGS (1985), Rankin (1969), Rankin et al. (1972), Raymond (1998), and Stose and Stose (1957). Discrepancies between the different authors' work

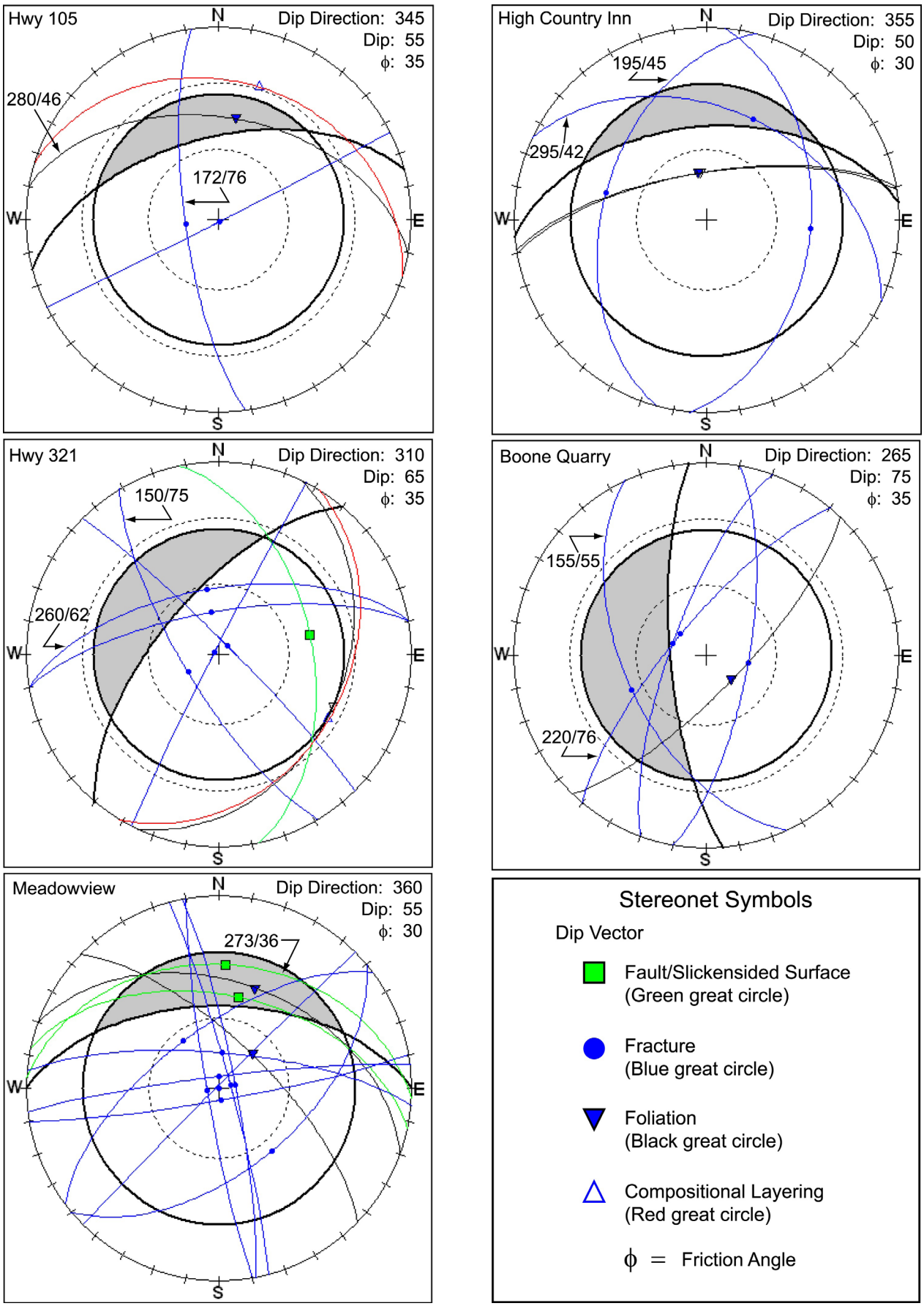

Figure 9: Markland test (stereonet) plots for rock slope failures in the ZEPRSI. Dip vectors that plot in the gray critical zone indicate the potential for planar failures; great circle intersections in the critical zone indicate the potential for wedge failures. Dip direction and dip values for the excavation face are given in the upper right of each plot. Adapted from Gillon et al. (2009).

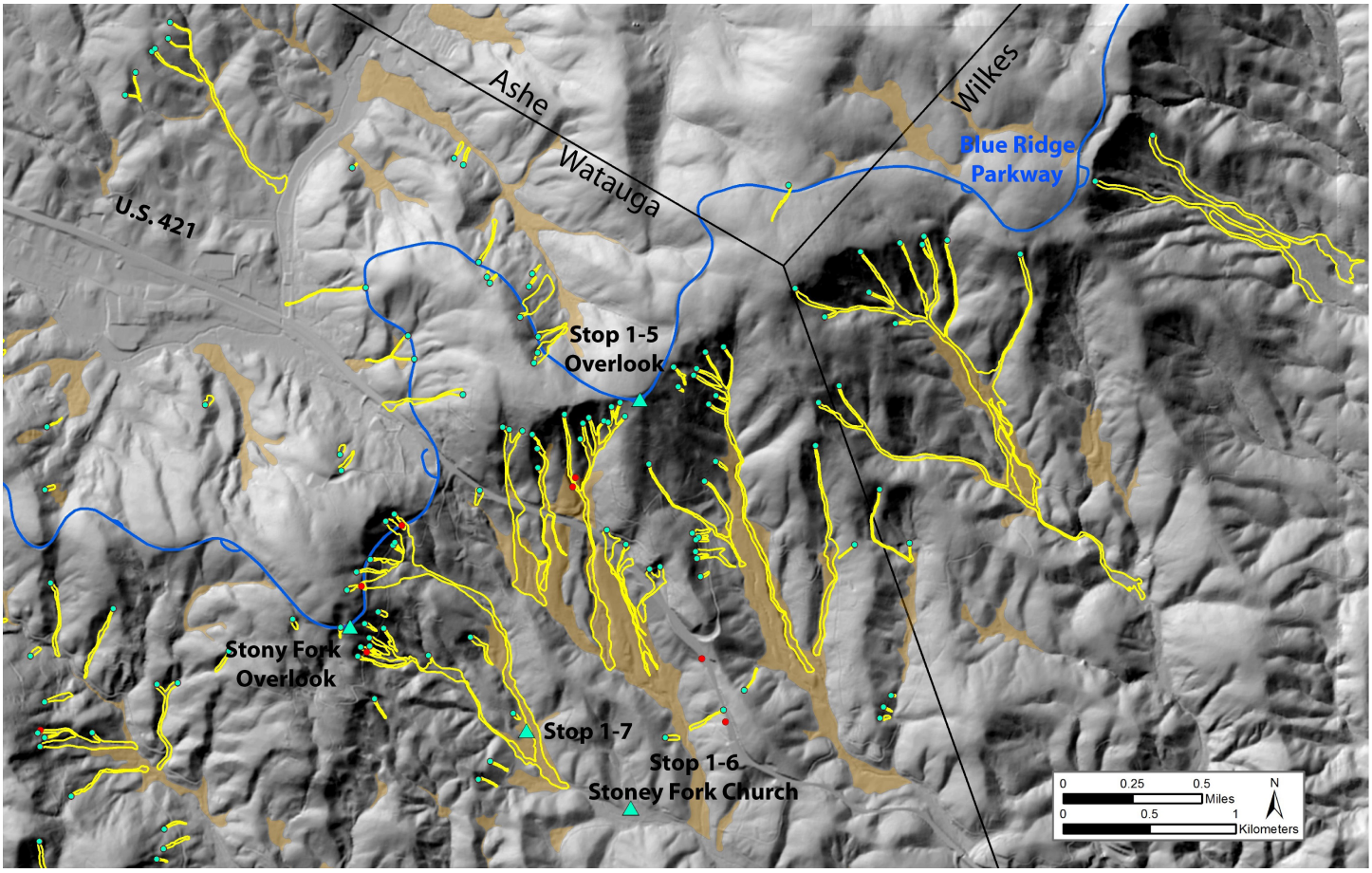

Figure 10: Excerpt of the Watauga County Slope Movement and Slope Movement Deposits Map for the Deep Gap area showing the locations of Stops 1-5, 1-6, and 1-7. Blue dots = point locations for August 13-14, 1940 landslides; red dots = point location for landslide of other dates; yellow polygons = slope movement outlines (e.g. debris flow tracks); brown polygons = slope movement deposits (e.g. debris fans). Sources: Wooten et al. (2008b); NCGS landslide geodatabase. Map base is a shaded relief map derived from a 6-meter resolution LiDAR DEM.

were addressed with limited field verification. New 12:000-scale mapping by Hill (2018) resulted in revisions in a ~75 km^2 corridor along the Linville Falls fault near Boone, which are not yet fully incorporated into the NCGS compilation map.

Reconnaissance studies of bedrock stability conditions throughout the County concentrated efforts along a segment of the Linville Falls fault and associated shear zone near the Town of Boone, where previous investigations had identified failures in rock slope excavations (Loren Raymond, personal communications, 2005; Trigon Engineering, 2006). The 14 km x 0.5 km ZEPRSI (Figure 3) encompasses WNW trending topographic ridges where 14 active and past-active rock and weathered-rock slides occur mainly in rocks of the Grandfather Mountain Formation (Figures 7, 8). The north side of this ridgeline generally coincides with Grandfather Mountain Window-Linville Falls fault (LFF) contact, and the footwall of the Boone fault identified by Hill (2018). We will visit one of the active rockslides in the ZEPRSI at Stop 1-2. Note: Rock slides also occur elsewhere in the County. The stability of rock slopes depends on site-specific conditions and slope configurations that vary throughout the County.

Integrated geologic and lineament mapping using LiDAR DEMs guided the selection of sites for detailed studies. We collected structural measurements and other bedrock data at approximately 60 locations within and outside of the ZEPRSI to assess rock types, their degree of weathering, the types and frequencies of planes of weakness (discontinuities) in the rock, and their relationships to active and past-active rock slope failures. Kinematic analyses using the Markland test function of RockPack III™ (Watts et al., 2003) were performed at 5 rock slide locations to evaluate the orientation of critical failure surfaces and to determine the likely modes of failure (Figure 9). Structural data input were field measurements (e.g., fault-slickensided surfaces, fractures, foliation, and compositional layering) along with the azimuth and slope of the cut faces. Estimated friction angles (Ø) for discontinuities

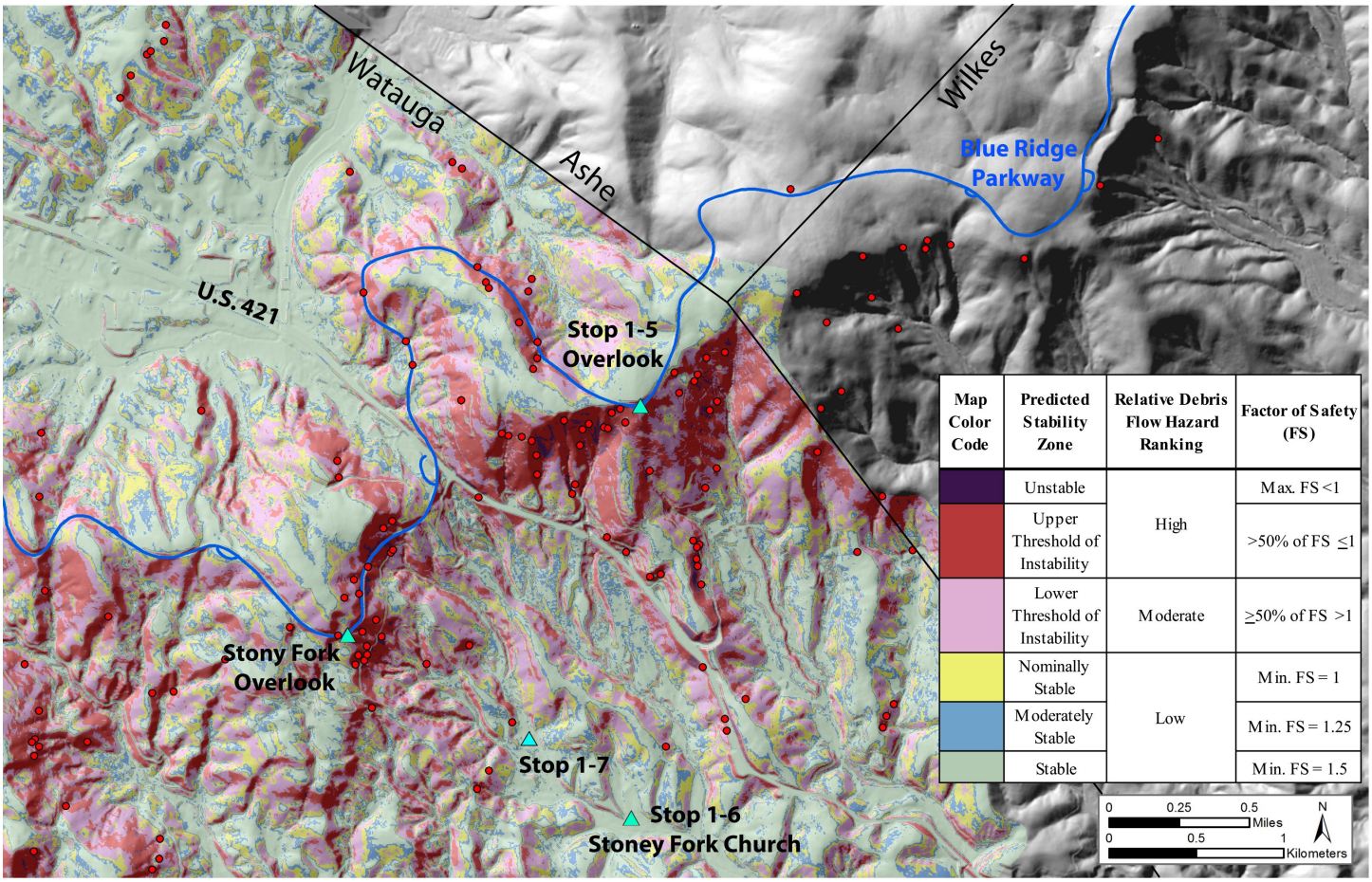

Figure 11: Excerpt of the Watauga County Slope Stability Index Map (SINMAP) for the Deep Gap area showing the locations of Stops 1-5, 1-6, and 1-7. Red dots = point location for landslides. Sources: Wooten et al., (2008b); NCGS landslide geodatabase. Map base is a shaded relief map derived from a 6-meter resolution iDAR DEM.

ranged from 30° to 35°, with 30° representing mica-rich phyllonitic rocks and 35° representing granular quartzo-feldspathic rocks with less abundant mica.

The WNW-trending lineaments associated with the ZEPRSI are expressions of a regionally extensive zone of fractures and faults. Rock slope failures within the ZEPRSI are concentrated on excavated, north-facing slopes where brittle fabrics associated with the Boone fault overprint mylonitic foliation of the LFF and other foliations. Within this zone, unstable and potentially unstable rock slopes typically occur where numerous intersecting planes of weakness coincide with zones of partially- to completely-decomposed bedrock. In general, north-dipping foliation, fault and fracture planes serve as sliding surfaces, whereas intersecting fractures create side and back release surfaces of slide blocks (Figures. 7,8) At Stop 1-2 we will examine an active slide in weathered rock within the ZEPRSI, involving mylonitic basement rocks in the hanging wall of the Boone fault.

Slope Movement and Slope Movement Deposits Map

The Slope Movement and Slope Movement Deposits (SMSMD) map layer portrays the following features related to landslides: 1) process points – point locations for landslides initiation zones (i.e., source areas); 2) slope movement outlines – polygons that show the areal extents of known landslides (e.g. debris flow tracks); 3) ground rupture lines - polylines that represent scarps and tension cracks in areas of detailed studies; and 4) deposits – polygons that show the areal extents of deposits from past landslide activity (e.g., debris fans). Landslides were classified in general accordance with Cruden and Varnes (1996). Figure 10 is an excerpt of the County SMSMD map layer for the Deep Gap area (Stops 1-5, 1-6, 1-7). Since the development of a statewide landslide geodatabase these four categories are now geospatially linked data layers that contain more recent landslide data for Watauga County than were published in 2008 (Witt et al., 2008; Bauer et al., 2012). The attribute tables for the data layers (feature classes) contain data about the landslide

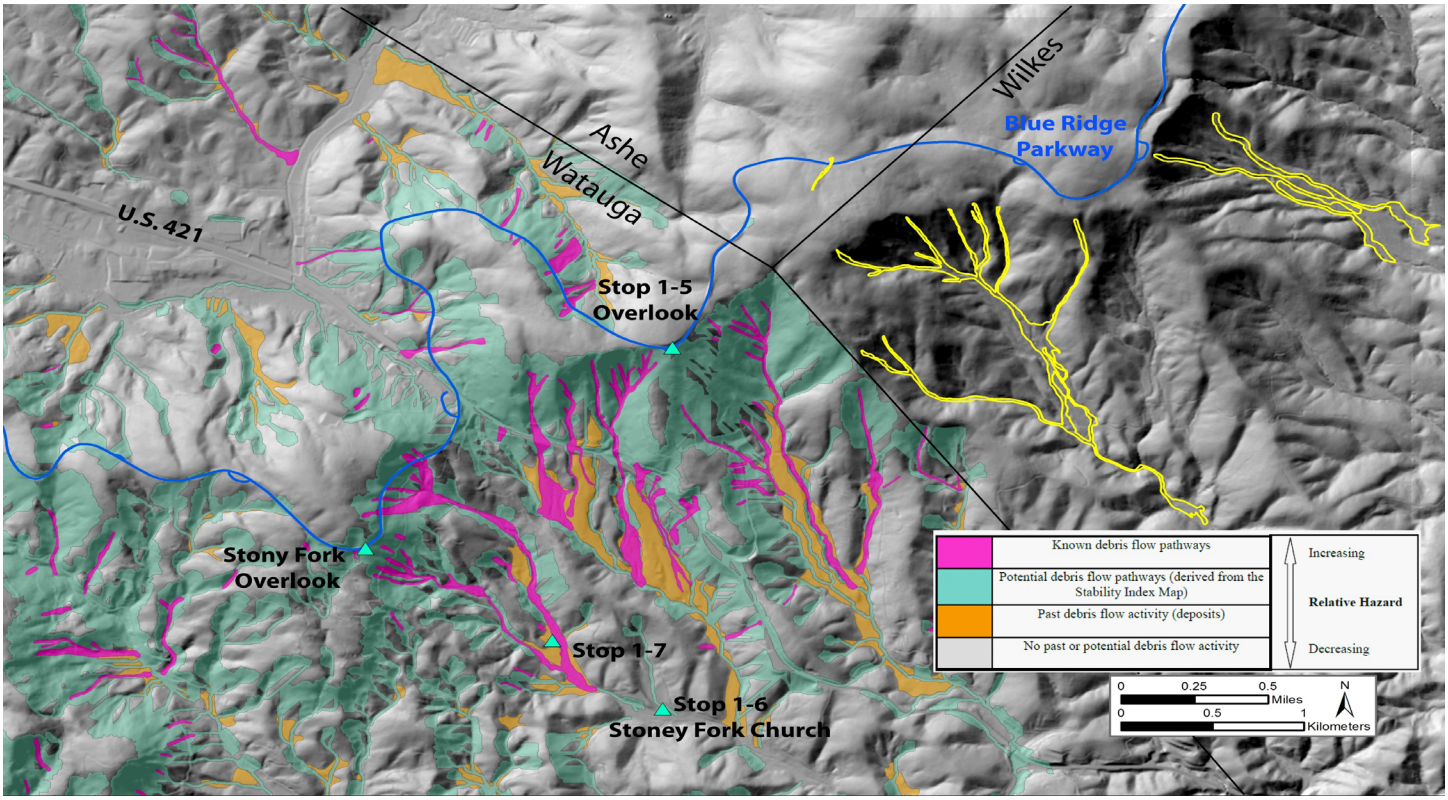

Figure 12: Excerpt of the Watauga County Debris Flow Pathways Map for the Deep Gap area showing the locations of Stops 1-5, 1-6, and 1-7. Yellow polygons = mapped debris flow tracks in Ashe and Wilkes Counties. Source: Wooten et al., (2008b). Map base is a shaded relief map derived from a 6-meter resolution LiDAR DEM.

types, dates(s) of movement, soil types, geomorphic and geologic information, slope configurations (e.g., modified or unmodified), vegetation, etc.

In addition to landslide locations identified by the NCGS, the SMSMD map for Watauga County incorporated or considered the work of Michalek (1968), Gryta and Bartholomew (1983), Mills (1998), Loren Raymond and John Callahan (personal communications, 2005) Raymond and Seramur (2006), Seramur et al. (2006), Trigon Engineering (2006), and Wieczorek et al., (2004). NCGS geohazards studies on the Blue Ridge Parkway (Latham et al., 2009) were also incorporated into the Watauga County maps. Georegistered 1940 vintage aerial photography made it possible to map the more than 2,000 slope failures from the August 13-14, 1940 storm. Orthophotography from 1993, 1998, and 2006 aided in mapping post-1940 landslides.

Stability Index Map

Debris flows and similar types of landslides make up over 90% of the landslides recorded in Watauga County (Figure 4) and have resulted in the greatest total number of landslide fatalities and damage of all the reported landslide types in North Carolina. For this reason, a debris flow susceptibility model that identifies areas where debris flows are likely to start is part of the landslide hazard map suite. After evaluating two debris flow susceptibility models (Witt et al., 2007 the NCGS chose the Stability Index Map (SINMAP) model developed by Pack et al., (1998) for use in the landslide hazard mapping effort. The Stability Index Map data layer (raster file) delineates the predicted relative hazard rankings (high, moderate, and low generalized from the six stability categories) for the initiation of naturally occurring, shallow, translational slope movements (i.e., debris/earth flows, debris/earth slides, and blowouts) in response to approximately 125 mm (5 in) or more of recharge within a 24-hour period. Figure 11 shows the excerpt of the county Stability Index Map for the Deep Gap area.

SINMAP is a stochastic, physically-based, limit equilibrium model for slope stability that uses a modified version of the infinite slope equation (Figures. A1, A2 App. A), combined with a steady-state flow accumulation function to model wetness (Figure A3 App. A). SINMAP computes a factor of safety (FS) raster using the input hydrologic, soil and topographic data derived from a 6-meter LiDAR DEM. The FS is a dimensionless number that represents the ratio of the stabilizing forces to destabilizing forces at a location with a FS>1 indicating stable conditions, and a FS<1

indicating unstable conditions given the assumptions and parameters input into the model. Model input parameters include upper and lower bounded values for recharge, soil transmissivity (hydraulic conductivity (Ksat) x soil thickness) and other soil properties (i.e., unit weight, thickness, effective friction angle (Ø eff), effective cohesion from soil (Cs) and vegetation (Cr). SINMAP randomly samples the bounded input parameter values using a uniform probability distribution to account for the variability and uncertainty inherent in natural systems (Figure A2 App. A). SINMAP then assigns a stability index based on the computed factors of safety. The six stability zones are assigned relative hazard rankings (high, moderate, and low) based on the calculated stability index ranges and known slope movement occurrences (Table A2 App. A). The infinite slope equation is highly sensitive to ground slope (Hammond et al., 1992); therefore, SINMAP output strongly correlates with ground slope. Refer to Appendix A for more detail on the SINMAP model.

The 125 mm (5 in) steady state recharge value used in the SINMAP analysis approximates an equivalent amount of rainfall within a 24-hour period. Historical evidence (Eschner and Patric, 1982; Neary and Swift, 1987; and Witt, 2005) and recent examples in North Carolina (Wooten et al., 2017) indicate that 125 mm (5 in) of rainfall within a 24-hour period is an approximate threshold for triggering debris/earth flows and slides. Watershed studies at the USDA- Forest Service Coweeta Hydrologic Laboratory in Macon County, however, show that 3-19% of rainfall from storms can be direct runoff (storm flow) rather than recharge (Hewlett et al., 1984). This being the case, then as much as 154 mm (6 in) or more of rainfall could be required to produce the 125 mm of recharge used in the SINMAP analysis.

Map Production and Calibration

SINMAP calibration regions were based on the bedrock compilation map and mapped debris deposits (Figure A4, Table A1 App. A.) because a modern soil survey was not available at the time the Watauga County maps were being prepared. Detailed geologic studies and soil testing (e.g., triaxial shear strength and hydraulic conductivity) were conducted at six debris flow initiation zones (see Detailed Study Sites – Debris Flow Initiation Zones section). These data, along with literature values for soil properties given in Hammond et al. (1992) were used to constrain reasonable ranges of soil input parameters for the stability index modeling. The stabilizing effect of vegetation is accounted for as root cohesion in the dimensionless cohesion parameter. Input values for root cohesion were constrained using the results of research at the U.S. Forest Service Coweeta Hydrologic Laboratory (Hales et al., 2007; see also Wooten et al., 2016).

The model calibration (i.e., the parameter adjustment process) was performed as recommended by the SINMAP developers (Pack et al., 1998). Parameter values (primarily dimensionless cohesion, soil thickness, internal angle of friction, and hydraulic conductivity) were adjusted within reasonable ranges so that the majority of the slope movement locations used for calibration were captured in the high hazard (upper threshold and unstable) zones. Table A1 (App. A) shows the final values used for the model calibration after 28 calibration model runs. Figure A5 (App. A). shows the landslide frequency (landslides/unit area) for each stability class.

Potential Debris Flow Pathways Map

This map portrays areas that could potentially be inundated by debris flows or other shallow, translational slope movements such as debris/earth slides/flows. Designated units on this map are known debris flow pathways, predicted debris flow pathways, areas of past debris flow activity, and areas of no known or predicted debris flow activity (Figure 12). The Stability Index Map shows areas where shallow translational slope movements are more likely to originate in response to a 125 mm (5 in) or greater recharge event within a 24-hour period. The Map of Potential Debris Flow Pathways delineates areas likely to be in the paths of these slope movements should they occur, including areas significantly further downslope from where the slope movements originate. In these locations, further slope stability analysis, including field verification, is recommended prior to citing facilities or undertaking ground disturbing activities.

Map Production

The Map of Known and Potential Debris Flow Pathways is derived from two sources: 1) outlines of debris flow tracks and slope movement deposits from the Slope Movements and Slope Movement Deposit Locations Map and 2) high hazard areas of the Stability Index Map. The following sequential steps outline the method used to produce the areas of predicted debris flow pathways using a 6 m (20 ft) resolution LiDAR DEM.

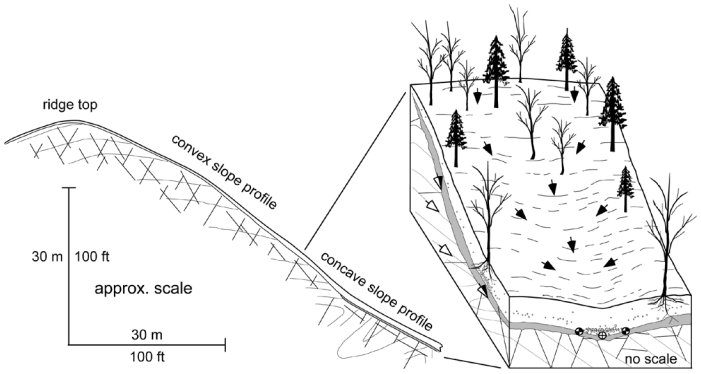

Figure 13: Generalized cross section and conceptual model for debris flow initiation zones in colluvial hollows. Arrows depict converging flow lines for surface water and shallow ground water in the hollow.

Figure 14: NCGS field crew investigating an August 13-14, 1940 debris flow initiation at detailed study site ID 4208 (location on Fig. 3) within a colluvial hollow. Concave topography in the fore- and middle-ground of the photo is the debris flow source area. 2007/05/01 NCGS photo.

1. High hazard areas from the Stability Index Map greater than 0.25 acres (10,893 ft2 or 1,012 m2) were designated as the most likely source areas for debris flows.
2. Hydrologic flow paths, based on topographic gradients and streams mapped by the North Carolina Stream Mapping Project, were then created in ArcGISTM from starting points derived from the high hazard areas on the Stability Index Map.
3. Flow paths were terminated once they encountered slope gradients less than three degrees for contiguous areas > 0.25 acres (10,893 ft2 or 1,012 m2). Three degrees was selected as a nominal gradient consistent with the lowermost downslope extent of most slope movement deposits and tracks delineated in the accompanying Slope Movements and Slope Movement Deposits Map.
4. These flow paths were then buffered to 10 m (33 ft) on all sides to delineate potential debris flow pathways. This buffer approximates the average track width of mapped debris flows in Watauga County. Note: In some cases the automated 33-ft (10-m) buffering routine may extend the predicted debris flow pathways slightly upslope and over ridge tops above debris flow source areas.

Significant manual editing of the digital map was required to adjust the downstream extents of the predicted debris flow pathways in order to terminate unrealistic flow paths where warranted. These adjustment procedures are outlined as follows: 1) flow paths that originated on man-made cut slopes were terminated near the base of the cut; 2) flow paths were terminated before flowing over dams; and, 3) flow paths were removed that originated from features where the LiDAR data did not represent "bare-earth" topography.

DETAILED STUDY SITES – DEBRIS FLOW INITIATION ZONES

Debris/earth flows and debris/earth slides typically originate where thin (usually less than 2 m or 6 ft thick) soil overlies relatively low permeability layers such as bedrock or weathered bedrock on steep slopes, typically those greater than 20 degrees. From 2004 to 2011, the NCGS completed detailed studies at 23 locations in Macon, Watauga, Buncombe, Henderson and Transylvania counties to develop conceptual models for known and potential debris flow initiation zones, and to obtain parameters used to constrain county-wide debris flow susceptibility models (Wooten et al., 2012). Each of the six Watauga County sites studied in detail is in a separate calibration region used for the SINMAP debris flow susceptibility modeling (Figure 3).

Study methods included field-developed geologic cross sections, soil sampling for gradation and Atterberg limits testing, and in situ testing of saturated soil hydraulic conductivity (Ksat), and Shelby tube sampling for consolidated undrained triaxial shear strength tests. Data for the six sites are summarized in Table 2. Shelby tube samples and Ksat test locations are biased toward the finer-grained components of soil profiles (i.e., fewer rock clasts) where sample tubes and hand auger borings could be advanced. See Stop 1-4 (Sky Valley) for the geologic cross section and discussion of the detailed investigation at site 3005. A challenge in reconstructing conditions at debris flow initiation

						Soil Depth		Soil Gradation					Atterberg Limits										Hydraulic Conductivity		
Site ID	Test	Lat.	Long.	Soil Origin	Slope (deg.)	Rupt. Zone (ft)	Total (ft)	Gravel Ret #4 (%)	P #10 (%)	P #40 (%)	Silt & Clay P#200 (%)	Clay < 0.005 mm (%)	LL	PL	PI	ASTM Class	Specific Gravity	Dry Density Avg (lb/ft^3)	Sat. Density Avg (lb/ft3)	Void Ratio Avg	C_{eff} (lb/ft^2) Avg	Φ_{eff} (deg) Avg	Ksat cm/sec	Bedrock Map Unit	Lithology
2085	Triaxial Ksat	36.2062	-81.5183	residuum	32	4.0	6.3	1	95	76	35	16.2	34		NP	SM	2.66	95.0	121.6	0.75	124	31	4.09E-03	Zabg	migmatitic granitic gneiss
2492	Quality	36.2689	-81.8248	colluvium	25	3.5	7.0	3.0	80	70	54	16.0	32		NP	ML								pCc	biotite schist; mylontitic biotite feldspar gneiss
2492	Ksat	36.2689	-81.8248	colluvium				0.0	92	83	66	18.0	30	24	6	ML							3.93E-04	"	"
2492	Triaxial	36.2689	-81.8248	colluvium				2.0	95	87	68	30.5	27	23	4	ML	2.76	86.8	118.0	0.98	0	34		"	"
3005	Ksat	36.1807	-81.6816	residuum	35	4.4	5.4	0.0	98	95	67	8.0	37		NP	ML							1.45E-04	Zgms	mylonitic calcareous phyllite
3005	Quality	36.1807	-81.6816	colluvium				13.0	67	57	45	20.0	34	25	9	SM								"	"
3005	Triaxial	36.1807	-81.6816	residuum				0.0	99	89	62	22.2	29		NP	ML	2.72	89.1	118.7	0.91	284	29		"	"
4208	Ksat	36.1871	-81.8244	colluvium	35	3.2	7.0	0.0	100	76	50	18.0	32	27	5	ML							7.06E-04	Ybgg	biotite granodioritic gneiss
4208	Quality	36.1871	-81.8244	residuum				0.0	87	76	48	8.0	33	25	8	SM								"	"
4208	Triaxial	36.1871	-81.8244	colluvium				2.0	96	78	54	26.3	34	25	9	ML	2.73	87.7	117.5	0.96	0	39		"	"
4369	Triaxial Ksat	36.2632	-81.6757	residuum	22	7.2	7.2	7.0	89	72	28	12.2	42		NP	SM	2.76	83.4	114.5	1.11	58	29	2.09E-03	Zata	biotite muscovite garnet schist; metagraywacke; metasiltstone
4540	Ksat	36.1611	-81.7947	colluvium	34	4.6	4.6	10.0	76	68	60	49.0	48	36	12	ML							7.38E-05	Zgmg	feldspathic chlorite phyllite (metavolcanic)
4540	Triaxial	36.1611	-81.7947	colluvium				9.0	88	82	72	58.9	47	31	16	ML	2.84	78.9	113.5	1.25	0	34		"	"
4540	Quality	36.1611	-81.7947	colluvium				6.0	77	62	51	38.2	59	30	29	CH								"	"

Table 2: Locations and test result from detailed studies of debris flow initiation sites in Watauga County. ASTM soil classification abbreviations: C = clay, M= silt; S = sand; L = low plasticity, H = high plasticity.

sites is to sample and test in situ properties of the missing soil!

Geomorphic and Geologic Settings

All Watauga County detailed study sites are in the initiation zones (source areas) of August 13-14, 1940 debris flows. Interestingly, site 2492 is also an initiation zone for a debris flow that occurred during either Hurricane Frances or Ivan during September 6-17, 2004, indicating a relatively short debris flow recurrence interval for this drainage. All sites are within concave hollows at the heads of first-order drainages on steep, topographically convergent slopes, characteristic of many debris flow initiation zones in the North Carolina Blue Ridge (Wooten et al., 2016) (Figures. 13, 14). Inferred rupture surfaces are within colluvium at three sites and involve residuum at three other sites. Ground slope ranges from 22° to 35° at residual sites, which overlaps the 25° to 35° range at colluvial sites. The Watauga slope values are within the 22° to 40° range of slope angles at debris flow initiation sites in the multi-county study.

Of the six Watauga County study sites, two are on the dip slope of foliation. Four sites are on slopes oblique to the foliation, i.e., those where the angle between the strike of foliation and the cross section bearing is within 35°. Two of the sites on slopes oblique to foliation, however, are on the dip slope of fractures (joints). Four of the six sites, therefore, are on the dip slope of bedrock discontinuities.

Soil Characteristics

Like most debris flow initiation zones elsewhere in North Carolina, Watauga County soil depths are relatively shallow, about 7 ft (~2.1 m) or less. Total soil depths for colluvial sites range from 4.6 ft to 7.0 ft (1.4 m to 2.1 m), comparable with the 5.4 ft to 7.0 ft (1.6 m to 2.1 m) range for residual sites. Inferred rupture depths for colluvial sites range from 3.2 ft to 4.6 ft (1.0 m to 1.4 m), generally less than those for residual sites that range from 4.0 ft to 7.2 ft (1.2 m to 2.2 m). Contacts between colluvium and the underlying residuum or partly decomposed rock are relatively sharp, whereas gradational contacts characterize the transition from residuum (completely decomposed bedrock) to partly decomposed and stained state bedrock.

Soil matrix (P40) fractions for colluvium classify as ML to CH and residuum as ML to SM, with both categories clustering in the ML field (Figure 15, Table 2). An exception is the higher plasticity colluvium at site 4540 that plots on the A-line between the CH and MH fields. Liquid limit values for colluvium range from 27 to 59 and overlap the 29 to 42 range for residuum. Plastic indices for residuum (nonplastic to 8) fall within the range for colluvium (nonplastic to 29). In general, soil tested at the Watauga sites has low plasticity and liquid limit values, not unlike those in the broader study area.

An Amoozemeter™ constant head permeameter was used for in situ measurements of saturated hydraulic conductivity (Ksat). The values for Ksat in colluvium range from 7.38E-05 to 3.94E-04 cm/sec, which overlap the lower end of the range in residuum from 1.45E-04 to 4.09E-03 cm/sec. A broad trend is

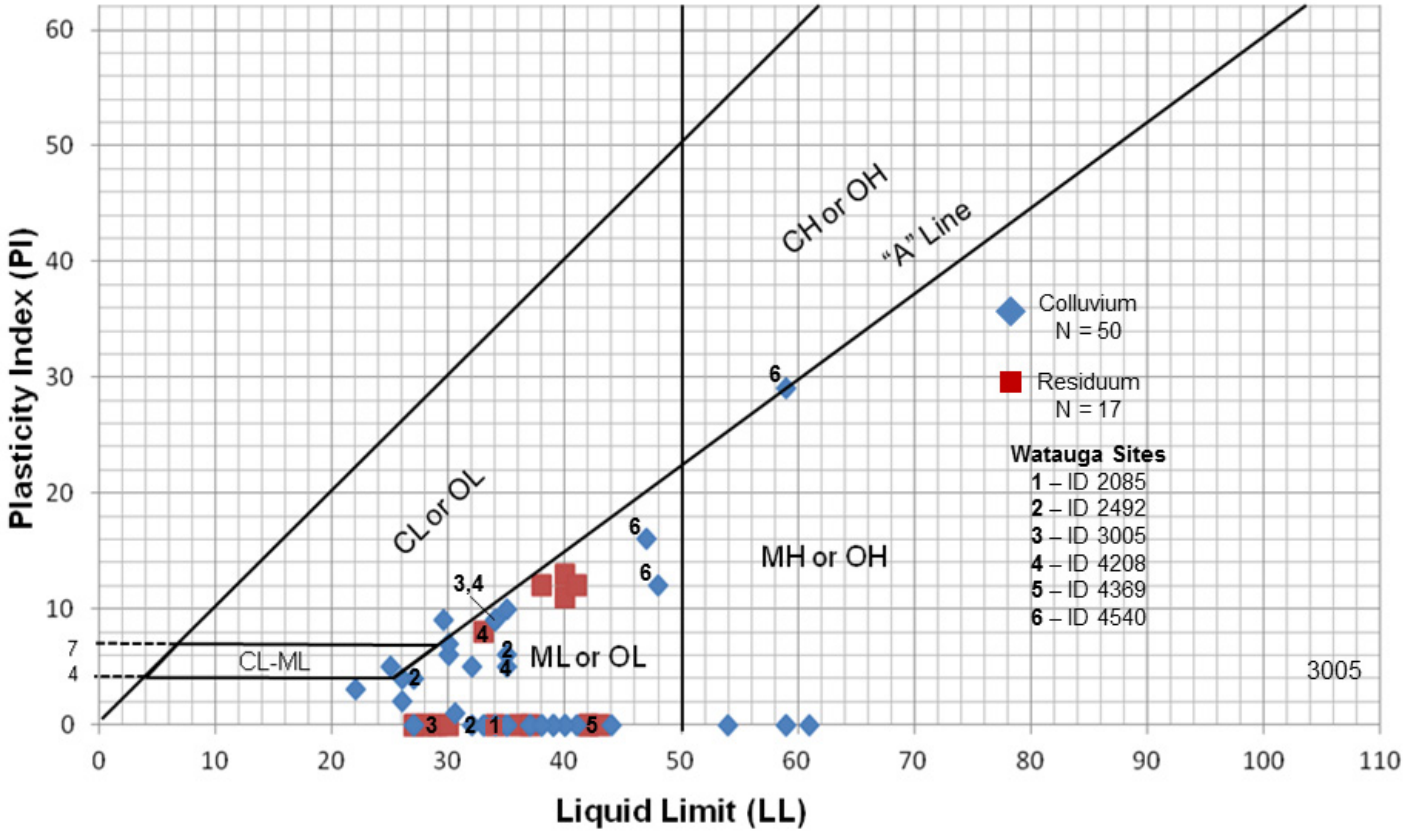

Figure 15: Chart showing plastic index vs. liquid limit values for the soil matrix or P40 fractions (% passing the #40 sieve) at 67 debris flow initiation sites studied in western North Carolina. Numbered labels indicate the Watauga County sites. ASTM soil classification abbreviations: C = clay, M= silt, O = organic; L = low plasticity, H = high plasticity.

indicated as a decrease in Ksat as the silt and clay fraction (P200) of soil increases (Figure 16).

The results of the consolidated undrained (CU) triaxial shear strength testing at the Watauga sites in comparison with those in the broader study is shown in Figure 17. Effective soil friction angles ($Ø_{eff}$) for colluvial soil at the Watauga sites range from 34° to 39°, and for residual soil from 29 to 31°. Effective cohesion (Cs_{eff}) values for residual soil range from 58 to 284 lb/ft2 (2.8-13.6 kPa); whereas colluvial soil is cohesionless (Cs_{eff} = 0). The higher cohesion in residual soil likely results from mineral grain bonding inherited from the parent bedrock. To account for the bias toward finer-grained soil sampled with Shelby tubes, a $Ø_{eff}$ of 42° was used as an upper bound to represent clast-supported soil types in the SINMAP modeling,

Note that the upper bound for Cs_{eff} of 51 lb/ft2 (2.45 kPa) used in the SINMAP modeling is less than those measured for residual soil at the Watauga sites (Figure 17). At sites 2085 and 3005 we sampled in residuum below the inferred rupture zone, (i.e., a higher strength zone not within displaced mass of the debris flow) yielding 124 lb/ft^2 (5.9 kPa) and 284 lb/ft^2 (13.6 kPa) respectively. A Cs_{eff} of 58 lb/ft^2 (2.8 kPa) measured for residuum at site 4369, however, is marginally higher than the upper bounding value used in the SINMAP modeling. At site 4639 the sampled interval was within the depth range of the residuum inferred to have been involved in the rupture zone immediately down slope, and may, therefore, more closely approximate of the shear strength of residual soil involved in the rupture zones of debris flow initiation sites.

Detailed Study Sites Summary

In this limited study, test values do not show distinctive differences between the geotechnical properties of colluvial soil types vs. residual soil types except for generally higher values of Cseff for residuum than for colluvium. Overall test results do however, show considerable variation in parameters (e.g., shear strength and Ksat, supporting the concept that county-wide modeling should reflect this variability, but also pointing to inherent difficulties in scaling up such models from site data. Probabilistic models, such as SINMAP, can incorporate variability in parameter values. One limitation of SINMAP is that it uses only a uniform probability distribution function from which to sample values (Figure A2, App. A) based on the in-

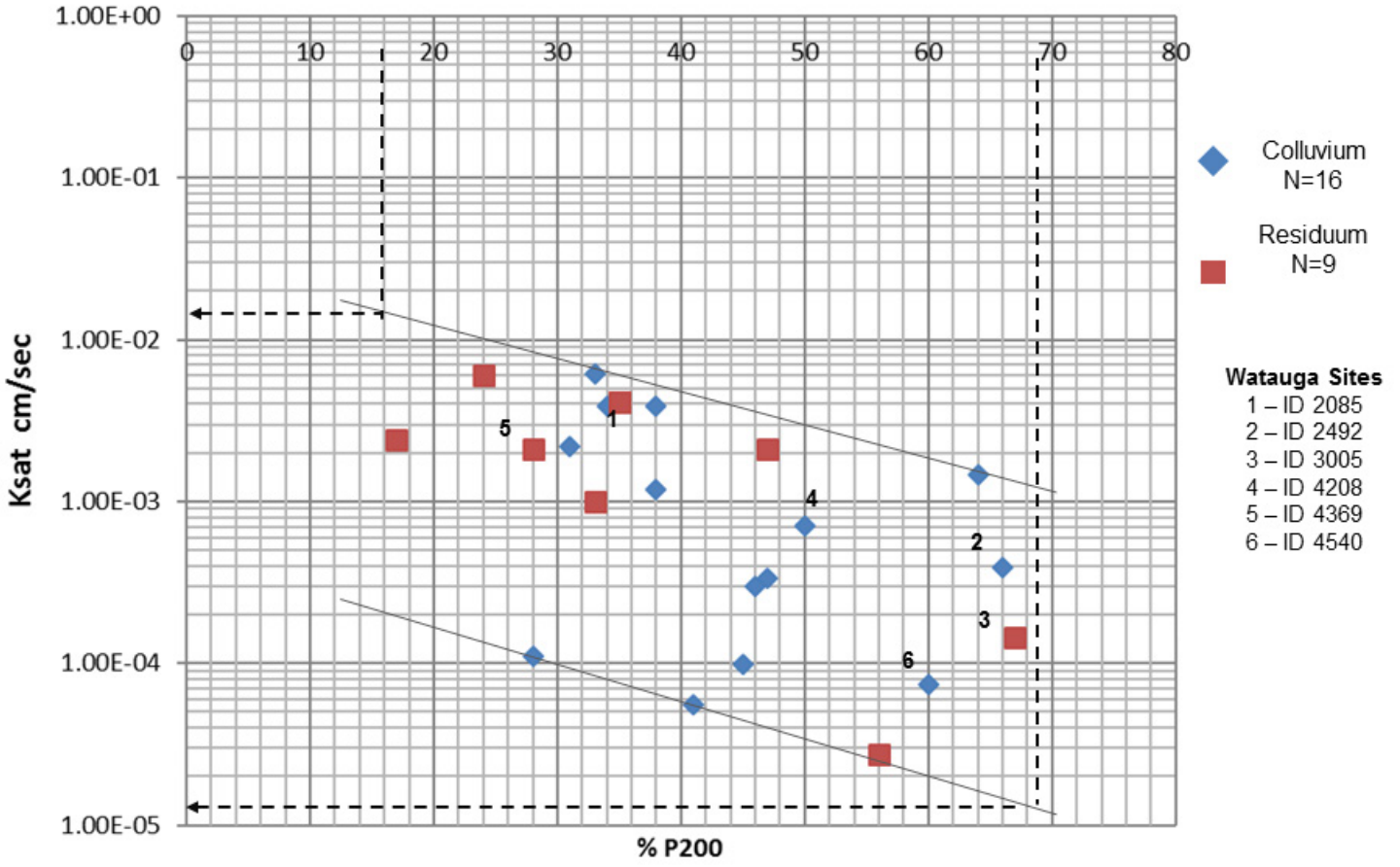

Figure 16: Chart showing values for in situ saturated hydraulic conductivity (Ksat) vs. the P200 fraction (% passing the #200 sieve) of corresponding soil samples for 23 debris flow initiation sites studied in western North Carolina. Numbered labels indicate the Watauga County sites. Dashed lines indicate a general range in the orders of magnitude of Ksat values that could be expected given the overall pattern of a decrease in Ksat with an increase in the P200 fraction.

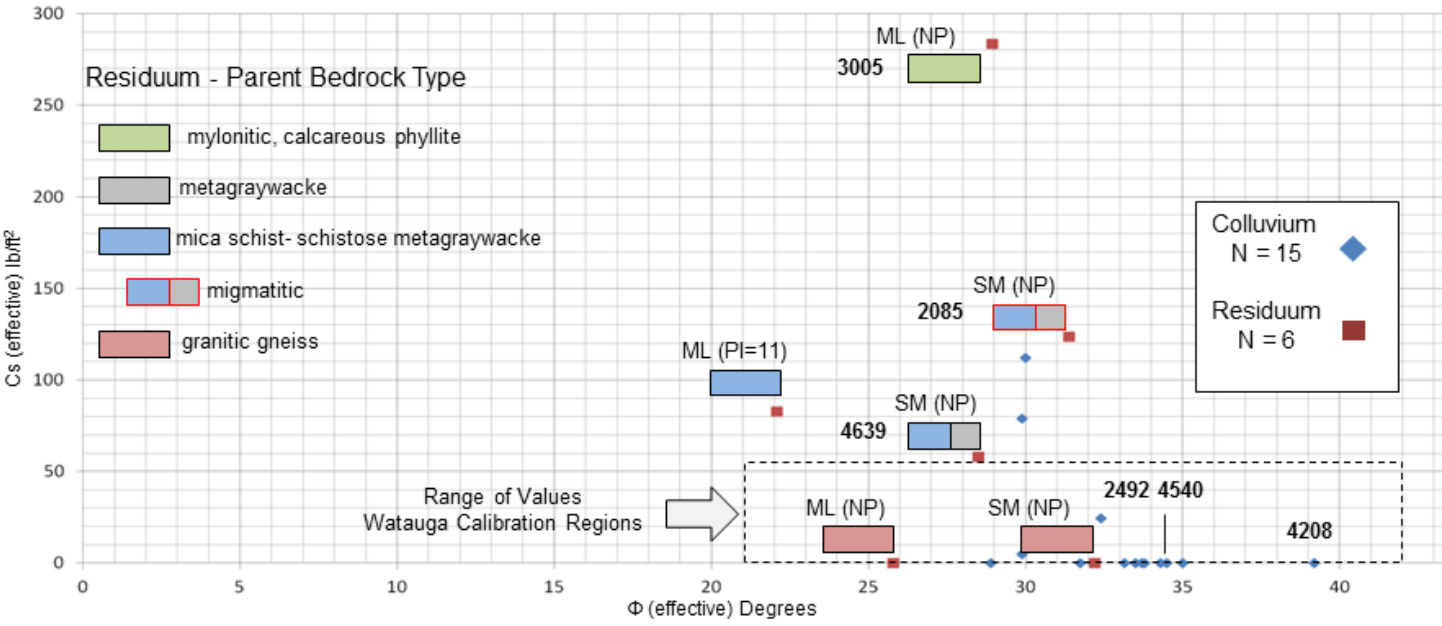

Figure 17: Chart showing effective cohesion (Cseff) vs. effective friction angle (from CU triaxial shear strength tests of Shelby tube samples taken in colluvial and residual soils at 21 debris flow initiation sites studied in western North Carolina. Color bars indicate the bedrock classifications of the parent rock type of residual soils tested. Dashed box = range of Cseff and Øeff values used in the stability index (SINMAP) modeling of Watauga County.

put of minimum and maximum values. In our experience, if the range of upper and lower bounding values specified in the model calibration process is too wide, then SINMAP over-samples the low and high ends of the range, thereby giving unsatisfactory results. Completing detailed studies at more debris flow initiation zones should improve our understanding of the probability distribution functions of these parameters and site characteristics.

CONCLUSIONS AND KEY POINTS

Basic geologic mapping is a necessary foundation for landslide hazard maps. Landslide geodatabases are important tools to document prehistoric and historic landslide events and to assess their frequency and magnitude. As sources of information that show where landslides have happened, or are happening, geodatabases are essential components of landslide hazard maps. Data to develop, constrain, and calibrate predictive models like those for debris flow susceptibility and run out rely on the empirical information in geodatabases. Information sharing and interdisciplinary collaboration is important to build on landslide geodatabases and further the research on landslide hazards.

Landslide hazard maps are useful planning tools, but they do not substitute for detailed, onsite analyses by qualified geologists and engineers. The maps do show areas where such detailed investigations are warranted prior to land-disturbing activity. Importantly, these maps provide context for site-specific studies that might otherwise miss the bigger picture. Like floodplain maps, landslide hazard maps should be periodically updated as new information, techniques, and improved modeling approaches become available.

Much of the past geologic research in the North Carolina Blue Ridge has focused on the Paleozoic ductile structures and their relationships to tectonic history. Much more work is needed on younger brittle structures and related fractures that have direct applications to the kinematic and hydrogeologic aspects of slope stability at the site, mountainside and larger scales. Likewise, much more research is needed on debris deposits (i.e., footslope and piedmont cove deposits, debris field, and debris fans). These deposits hold answers to questions on the spatial and temporal aspects of uplift and erosion, linkages between climate change and the recurrence intervals of catastrophic storms, and what areas could be affected by future debris flow events. As we have seen on this field trip, these deposits are also important in understanding hillslope hydrogeology.

ACKNOWLEDGEMENTS

Many people and agencies have contributed to this effort, but the dedicated work of Jennifer Bauer, Tommy Douglas, Stephen Fuemmeler, Ken Gillon, Rebecca Latham, and Anne Witt of the NCGS landslide mapping team from 2005 to 2011 made it possible. The NCDOT Materials and Test Unit graciously provided soil testing. Special thanks go to the residents of Watauga County for their willingness to provide information and property access during the mapping effort. Reviews and comments on the maps and in the field by Louis Acker, Bart Cattanach, Jack Callahan, Carl Merschat, Hugh Mills, Katherine Scharer, Jim Simons, and Kenneth Taylor greatly improved the Watauga landslide hazard maps. NCGS geologists Bart Cattanach, Nick Bozdog and Sierra Isard have provided invaluable support in landslide responses and in GIS.

REFERENCES

Acker, L.B., 1983, Draft geologic map of portions of the Deep Gap, Buffalo Cove, Maple Springs, Grandin, Globe, and Boone, NC 7.5' quadrangles: NCGS unpublished, open-file map, scales 1:24,000 and locally 1:12,000.

Adams, M.G., 1990, The geology of the Valle Crucis area, northwestern North Carolina [M.S. thesis]: University of North Carolina at Chapel Hill, 95 p.

Adams, M.G., 1995, The tectonothermal evolution of part of the Blue Ridge thrust complex, northwestern North Carolina [Ph.D. dissertation]: University of North Carolina at Chapel Hill, 193 p.

Appalachian Landslide Consultants, 2018, Landslide maps of western North Carolina; https://applandslide.maps.arcgis.com/apps/MapTools/index.html?appid=db6c795b22a14a6e8df71f4ec2912798. Accessed 2018/09/04.

Bartholomew, M.J., and Gryta, J.J., 1980, Geologic map of the Sherwood Quadrangle, North Carolina-Tennessee: North Carolina Geological Survey Map GM 214-SE, scale 1:24,000.

Bartholomew, M.J., 1983, Geologic map and mineral resources summary of the Baldwin Gap quadrangle, North Carolina-Tennessee: North Carolina Geological Survey Map GM 220-NW, scale 1:24,000.

Bartholomew, M.J., and Wilson, J.R., 1984, Geologic map of the Zionville quadrangle, North Carolina-Tennessee: North Carolina Geological Survey Map 220-SW (Unpublished), scale 1:24,000.

Bauer, J.B., Fuemmeler, S.F., Wooten, R.M., Witt, A.C., Gillon, K.A., and Douglas, T.J, 2012, Landslide hazard mapping in North Carolina – overview and improvements to the program, In Eberhardt, E., Froese, C., Turner, S., Leroueil, S., (Editors), Landslides and Engineered Slopes: Protecting Society through Improved Understanding, 11th International,

and 2nd North American Symposium on Landslides, Banff, AB, pp. 257-263.
Bauer, J.B. and Fuemmeler, S.J., 2017, The science and stories of landslide inventory and susceptibility mapping in Haywood and Jackson Counties, North Carolina, USA, In De Graff, J.V. and Shakoor, A. (eds.), Landslides: Putting Experience, Knowledge and Emerging Technologies into Practice, AEG Special Publication No. 27, pp. 675-686.
Bryant, B., 1963, Geology of the Blowing Rock quadrangle, North Carolina: U.S. Geological Survey Geologic Quadrangle Map 243, scale 1:62,500.
Bryant, B., 1965, Geology of the Linville quadrangle, North Carolina-Tennessee: U.S. Geological Survey Geologic Quadrangle Map 364, scale 1:62,500.
Bryant, B., and Reed, J.C., Jr., 1970, Geology of the Grandfather Mountain window and vicinity, North Carolina and Tennessee: U.S. Geological Survey Professional Paper 615, 190 p.
Cattanach, B.L., Merschat, C.E., Bozdog, G.N., Latham, R.L., and Wooten, R.M., 2007, A new digital geologic map of the Blue Ridge Parkway in North Carolina: Geological Society of America Abstracts with Programs, v. 39, no. 2, p. 99.
Cattanach, B.L., Bozdog, G.N., and Wooten, R.M., 2014, Bedrock geologic map of the Black Mountain 7.5-minute quadrangle, North Carolina, North Carolina Geological Survey Open-file Map 2014-3, 1:24,000 scale.
Cattanach, B.L., Bozdog, G.N., Isard, S.J., and Wooten, R.M., 2016, Bedrock geologic map of the Montreat 7.5-minute quadrangle, Buncombe, McDowell, and Yancey Counties, North Carolina, North Carolina Geological Survey Open-file Map 2014-3, 1:24,000 scale.
Cruden, D.M., and Varnes, D.J., 1996, Landslide types and processes, in Turner, A.K., and Schuster, R.L., eds., Landslides: Investigation and Mitigation: Transportation Research Board Special Report No. 247, National Research Council, National Academy Press, Washington, D.C., pp. 36-75.
Dennison, J.M. and Stewart, K.G., 2001, Regional structural and stratigraphic evidence for dating Cenozoic uplift of Southern Appalachian highlands, [abstr]: Geol. Soc. of Amer.,Southeastern Section Abstracts with Programs, vol. 33, no. 6.
Eschner, A.R., and Patric, J.H., 1982, Debris avalanches in eastern upland forests: Journal of Forestry, v. 80, pp. 343-347.
Fetter, A.H. and Goldberg, S.A., 1995, Age and geochemical characteristics of bimodal volcanism in the Neoproterozoic Grandfather Mountain rift basin: Journal of Geology, v. 103, pp. 313-326.
Gillon, K.A., Wooten, R.M., Latham, R.L., Witt, A.W., Douglas, T.J., Bauer, J.B., and Fuemmeler, S.J., 2009, Integrating GIS-based geologic mapping, LiDAR-based lineament analysis and site specific rock slope data to delineate a zone of existing and potential rock slope instability located along the Grandfather Mountain Window-Linville Falls shear zone contact, Southern Appalachian Mountains, Watauga County, North Carolina, In: Proceedings of the 43rd US Rock Mechanics Symposium and 4th U.S.-Canada Rock Mechanics Symposium, Asheville, North Carolina, June 28th – July 1,2009; American Rock Mechanics Association ARMA 09-181, 13 p.
Greene, I.C., 1941, A Disastrous Flood: A True and Fascinating Story, Richmond, VA: William Byrd Press, Inc., 103 p.
Gryta, J.J., and Bartholomew, M.J., 1983, Debris-avalanche type features in Watauga County, North Carolina, in Lewis, S.E., (ed.), Geologic investigations in the Blue Ridge of Northwestern North Carolina: Carolina Geological Society Field Trip and Annual Meeting, 22 p.
Hales, T.C., Hwang, T., Band, L., Ford, C., and Vose, J.M., 2007, Long term adjustment of canopy root depth and strength: implications for catchment hydrology and slope stability, [abstr:] EOS Transactions, American. Geophysical. Union, 88 (52), Fall Meeting Supplement, Abstract H31G-0741.
Hammond, C., Hall, D., Milller, S., and Swetik, P., 1992, Level I stability analysis (LISA) documentation for Version 2.0: General Technical Report INT-285, U. S. Department of Agriculture, Forest Service, Intermountain Research Station, 190 p.
Hatcher, R.D. Jr., Merschat, A.E., and Raymond, L.A., 2006, Geotraverse: Geology of northeastern Tennessee and the Grandfather Mountain region, in Labotka, T.C., and Hatcher, R.D., Jr., eds., Geological Society of America 2006 Southeastern Section Meeting Field Trip 6, pp. 129-184.
Hewlett, J.D., Fortson, J.C., and Cunningham, G.B., 1984, Additional tests on the effect of rainfall intensity on storm flow and peak flow from wild-land basins: Water Resources Research, v.20, n.7, pp. 985-989.
Hill, J.S, 2018, Post-orogenic uplift, young faults, and mantle reorganization in the Appalachians, PhD Dissertation, University of N.C. Chapel Hill, 139 p.
Johnstone, T.P. and Burrus, S.A., 1998, An analysis of the 4 September 1996 Hickory Nut Gorge flash flood in western North Carolina, 16th Conf. on Weather Analysis and Forecasting, American Meteorological Society, Phoenix, AZ, pp. 275 -277.
Keith, A., 1903, Description of the Cranberry quadrangle (North Carolina-Tennessee): U.S. Geological Survey Geologic Atlas, Folio 90, 9 p.
King, P.B., and Ferguson, H.W., 1960, Geology of Northeasternmost Tennessee: U.S. Geological Survey Professional Paper 311, 136 p.
Latham, R.S., Wooten, R.M., Cattanach, B.L., Merschat, C.E., and Bozdog, G.N., 2009, Rock slope stability analysis along the North Carolina section of the Blue Ridge Parkway: using a geographic information system (GIS) to integrate site data and digital geologic maps, In: Proceedings of the 43rd US Rock Mechanics Symposium and 4th U.S.-Canada Rock Mechanics Symposium, Asheville, North Carolina, June 28th – July 1,2009, American Rock Mechanics Association ARMA 09-171, 12 p.
Lee, L.G. and Goodge, G.W., 1984, Meteorological analysis of an intense “east-slope” rainstorm in the southern Appalachians, 10th Conf. on Weather Forecasting and Analysis, Clearwater Beach, FL, American Meteorological Society, pp. 30-37.
Lewis, S.E. and Bartholomew, M.E., 1984, Geologic map of the Elk Park quadrangle, North Carolina-Tennessee: North Carolina Geological Survey Map 215-NW (Unpublished), scale 1:24,000.
Michalek, D.D., 1968, Fanlike features and related periglacial phenomena of the southern Blue Ridge [Ph.D. dissertation]:

University of North Carolina at Chapel Hill, 198 p.
Mills, H.H., 1998, Surficial deposits and landforms on the west piedmont slopes of Rich and Snake Mountains between Silverstone, North Carolina and Trade, Tennessee: A field guide, in Deposits and landforms on the piedmont slopes of Roan, Rich, and Snake Mountains, Northwestern North Carolina and Northeastern Tennessee: Southeastern Friends of the Pleistocene 1998 Field Trip Guidebook, pp. 50-82.
Mills, H.H. and Grainger D.E., 2002 Cosmogenic isotope burial dating reveals 1.5 million-year-old fan deposit in Blue Ridge Mountains of North Carolina [abstr]: Geological Society of America Southeastern Section Abstracts with Programs, 34, A-32.
Muthukrishnan, S., 2012, Road log for Sunday, October 14, 2012 Jones Gap State Park, in Garihan, J.M., and Ranson, W.A., eds, Geologic studies in the inner Piedmont, Brevard zone, and Blue Ridge, South Carolina and North Carolina, Guidebook for the seventy-fifth anniversary of the Carolina Geological Society, 73rd annual meeting, Oct. 12-14, Greenville S.C., pp. 124-132.
Neary, D.G., and Swift, L.W., Jr., 1987, Rainfall thresholds for triggering a debris avalanching event in the southern Appalachian Mountains: In: Costa, J.E., and Wieczorek, G.F., eds., Debris flows/avalanches; Process, recognition and mitigation: Geological Society of America, Reviews in engineering geology, v. VII, pp. 81-92.
North Carolina Geological Survey, 1985, Geologic map of North Carolina: North Carolina Geological Survey, scale 1:500,000. Out of print. Available online: http://gis.enr.state.nc.us/sid/bin/index.plx?client=zGeologic_Maps&site=9AM
Pack, R. T., Tarboton, D. G., and Goodwin, C. N., 1998, Terrain stability mapping with SINMAP, technical description and users guide for version 1.00: Terratech Consulting Ltd., Salmon Arm, B. C., Canada, Report Number 4114-0, 68 p.
Rankin, D.W., 1969, The Fries Fault: a major thrust in the Blue Ridge of southwestern Virginia: Geological Society of America Abstracts with Programs, v. 4, p. 66.
Rankin, D.W., Espenshade, G.H., and Neuman, R.B., 1972, Geologic map of the west half of the Winston-Salem quadrangle, North Carolina, Virginia, and Tennessee: U.S. Geological Survey Miscellaneous Investigations Map I-709-A, scale 1:250,000.
Raymond, L.A., 1998, Geology of the Blue Ridge belt of northwestern North Carolina: in Mills, H.H., Cowan, E.A., Seramur, K.C., Raymond, L.A., Allison, J.B., and Acker, L.L., leaders: Deposits and landforms on the Piedmont slopes of Roan, Rich, and Snake Mountains, northwestern North Carolina and northeastern Tennessee: Southeastern Friends of the Pleistocene 1998 Field Trip Guidebook, p. 1-8.
Raymond, L.A. and Seramur, K.C., 2006, Geologic hazard map for the Town of Seven Devils, Watauga County, NC, scale 1:7,200.
Scott, R.C., Jr., 1972, Geomorphic significance of debris avalanching in the Appalachian Blue Ridge Mountains: Ph.D. dissertation, Univ. of Georgia, Athens, GA., 184p.
Seramur, K.C., Raymond, L.A., and Neel, E., 2006, Slope hazard map for the Town of Banner Elk, Avery County, North Carolina, scale 1:6,000.
Soplata, C.A., 2016, Case study of historically destructive landslides in Hickory Nut Gorge near Chimney Rock North Carolina, Unpublished M.S. Thesis, University of Memphis, 77 p.
Southern Railway Company, 1917, The Floods of July 1916, How the Southern Railway Organization Met an Emergency, Southern Railway Company, 130 p.
Stose, A.J. and Stose, G.W., 1957, Geology and mineral resources of the Gossan Lead district and adjacent areas in Virginia: Virginia Division of Mineral Resources, Bulletin 72, 291 p.
Trigon Engineering, 2006, Town of Boone Hazard Map (Working Copy, Dated July 14, 2006, scale 1:30,000.
U.S. Geological Survey - Water Resources Branch, 1949, Floods of August 1940 in the Southeastern States: Geological Survey Water – Supply Paper 1006, Washington, D.C.: U.S. Government Printing Office, 554 p.
Watts, C.F., D.R. Gillam, M.D. Hrovatic, and H. Hong. 2003. User's Manual Rockpack III for Windows (ROCK Slope Stability Computerized Analysis PACKage). C.F. Watts and Associates.
Watauga Democrat, 4 June 2018, Timeline of events released in Pine Ridge landslide, explosion, Available Online: https://www.wataugademocrat.com/news/timeline-of-events-released-in-pine-ridge-landslide-explosion/article_790c5fe1-a8cf-5411-a2ac-340460f73f89.htm
Wieczorek G.F., Mossa G.S., and Morgan B.A., 2004, Regional debris flow distribution and preliminary risk assessment from severe storm events in the Appalachian Blue Ridge Province, USA. Landslides 1: pp. 53-59.
Witt. A.C., 2005, A brief history of debris flow occurrence in the French Broad River Watershed, western North Carolina, The NC Geographer 13: pp. 58-82.
Witt, A.C., Wooten R.M, Latham R.S., Fuemmeler, S.F, Gillon, K.A., Douglas, T.J., and Bauer, J.B. 2007, A comparative study of two GIS slope stability models for use in the N. C. landslide hazard mapping program: In: Schaefer, V.R., Schuster, R.L., and Turner, A.K., (eds.), Conference presentations 1st North American landslide conference, Vail Colorado, AEG Special Publication 23, pp. 387-400.
Witt, A.C., Wooten, R.M., Latham, R.S., Gillon, K.A., Douglas, T.J., Fuemmeler, S.J., and Bauer, J.B., 2008, Migration to a Geospatial Database to Improve Data Management in the N.C. Geological Survey's Landslide Hazard Mapping Program, [abstr]: Geological Society America. Abstracts with programs, Vol. 40, No. 6.
Witt, A.C. and Wooten, R.M., 2015, The laws of physics don't stop at state boundaries: challenges and accomplishments in documenting landslide activity in the Central and Southern Appalachian, (abstract, poster) AEG Professional Forum, Time to Face the Landslide Dilemma: Bridging Science, Policy, Public Safety, and Potential Loss, Seattle, WA., p. 104.
Wooten, R.M. and Latham, R.S., 2004, Preliminary Report on Slope Movements at the White Laurel Community, Watauga County, North Carolina, to Watauga County Emergency Management, 7 p.
Wooten R.M., Reid, J.C., Latham, R.S., Medina, M.A., Bechtel, R., and Clark, T.W., 2005, An overview of the North Carolina Geological Survey's geologic hazards program – phase I: In: Proceedings of the 56th Highway Geol Symposium, Wilmington, NC, May 4-6, 2005.
Wooten R.M., Latham R.S., Witt A.C., Fuemmeler S.J., Gillon

K.A., Douglas T.J., and Bauer J.B., 2006, Slope movement hazard maps of Macon County, North Carolina: North Carolina Geological Survey Geologic Hazards Map Series 1, 3 sheets, scale 1:48,000, and Digital Data Series GHMS-1 (DDS-GHMS-1).

Wooten, R.M., Gillon, K.A., Witt, A.C., Latham, R.S., Douglas, T.J., Bauer, J.B., Fuemmeler, S.J., and Lee, L.G., 2008a, Geologic, geomorphic, and meteorological aspects of debris flows triggered by Hurricanes Frances and Ivan during September 2004 in the Southern Appalachian Mountains of Macon County, North Carolina (southeastern USA): Landslides v. 5 n. 1, pp. 31-44.

Wooten R.M., Witt A.C., Gillon K.A., Douglas T.J., Latham R.S., Fuemmeler S.J., and Bauer J.B., 2008b, Slope movement hazard maps of Watauga County, North Carolina: North Carolina Geological Survey Geologic Hazards Map Series 3, 4 sheets, scale 1:36,000, and Digital Data Series GHMS-3 (DDS-GHMS-3).

Wooten R.M., Witt A.C., Gillon K.A., Douglas T.J., Fuemmeler S.J., Bauer J.B., and Latham R.S., 2009, Slope movement hazard maps of Buncombe County, North Carolina: North Carolina Geological Survey Geologic Hazards Map Series 4, 3 sheets, scale 1:52,000, and Digital Data Series GHMS-4 (DDS-GHMS-4).

Wooten, R.M., Witt, A.C., Douglas, T.J., Fuemmeler S.J., Bauer, J.B., Gillon, K.A., and Latham, R.S., 2011, Digital data and maps of the slope movement hazards for Henderson County, North Carolina: North Carolina Geological Survey Digital Data Series GHMS-5 (DDS-GHMS-5).

Wooten, R.M., Cattanach, B.L., Gillon, K.A., and Bozdog, G.N., 2010, Geology of the Mills Gap area, Buncombe County, North Carolina: North Carolina Geological Survey Report of Special Investigation 2010-09-30, Technical Memorandum to the U.S. Environmental Protection Agency, U.S. Geological Survey, and the North Carolina Department of Environment and Natural Resources, Division of Waste Management, 19 p., 2 Plates, map scale 1:12,000.

Wooten R.M., Witt A.C., Douglas T.J., Fuemmeler S.J., Bauer J.B., Gillon K.A., and Latham R.S., 2011, Slope movement hazard maps of Henderson County, North Carolina: N.C. Geological Survey Geologic Digital Data Series DDS-5.

Wooten, R.M., Douglas, T.J., Bauer, J.B., Fuemmeler, S.J., Gillon, K.G., Witt, A.C., and Latham, R.S., 2012, Geologic, Geomorphic and Geotechnical Aspects of Debris Flow Initiation Sites in the Blue Ridge Mountains of Western North Carolina at Study Locations in Buncombe, Haywood, Henderson, Jackson, Macon, Transylvania and Watauga Counties [abstr]: Geological Society of America Abstracts with Programs, p. 147.

Wooten, R.M., Witt, A.C., Miniat, C.F., Hales, T.C., and Aldred, J.A., 2016, Frequency and Magnitude of Selected Historical Landslide Events in the Southern Appalachian Highlands of North Carolina and Virginia: Relationships to Rainfall, Geological and Ecohydrological Controls, and Effects, In: Natural Disturbances and Historic Range of Variation: Type, Frequency, Severity, and Post-disturbance Structure in Central Hardwood Forests USA (Greenberg, C.H. and Collins, B.S. eds), Springer, Managing Forest Ecosystems 32, pp. 203-262.

Wooten, R.M., Cattanach, B.C., Bozdog, G.N., Isard, S.J., Fuemmeler, S. J., Bauer, J.B., Witt, A.C., Douglas, T.J., Gillon, K.A., and Latham, R.S., 2017, The North Carolina Geological Survey's Response to Landslide Events: Methods, Findings, Lessons Learned and Challenges, In De Graff, J.V. and Shakoor, A. (eds.), Landslides: Putting Experience, Knowledge and Emerging Technologies into Practice, AEG Special Publication No. 27, pp. 359-370.

Wooten, R.M., Cattanach, B.L., Isard, S.J., and Bozdog, G.N., 2018, Bedrock controls on quaternary debris deposit morphology, composition and processes: Swannanoa Mountains, Oteen and Black Mountain quadrangles, Buncombe County, North Carolina; [abstr]: Geological Society of America Southeastern Section Abstracts with Programs, p 28

Appendix A - Stability Index Map (SINMAP) Infinite Slope Equation, Calibration Regions and Parameters, and Calibration Results for Watauga County

Infinite Slope Equation - SINMAP

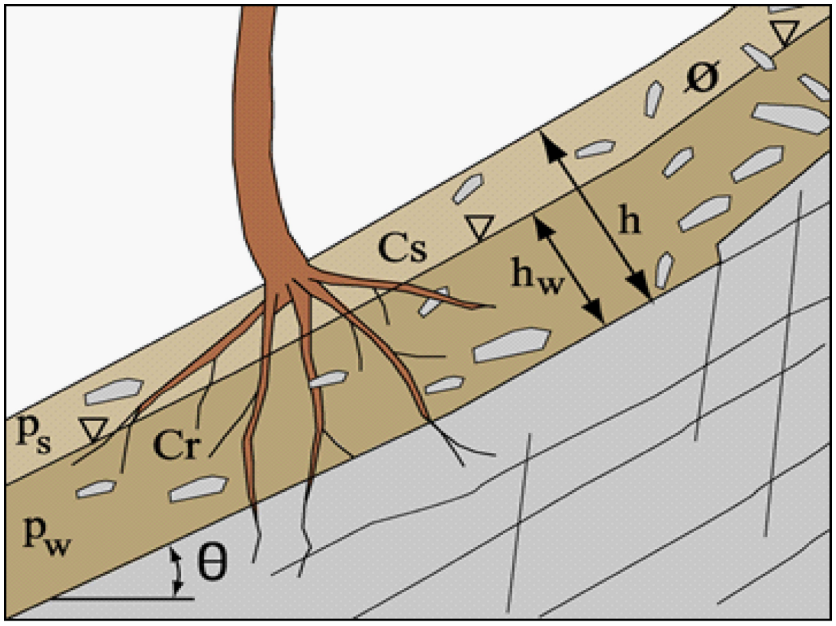

$$FS = \frac{C + \cos\theta\left[1 - \min\left(\frac{R\,a}{T\sin\theta}, 1\right) r\right]\tan\phi}{\sin\theta}$$

Figure A1: Schematic showing the modified version of the infinite slope equation and a cross section of hillslope conditions used to compute factors of safety in SINMAP (adapted from Pack and others, 1998).

FS = Factor of Safety: Ratio of forces resisting slope failure to the forces driving slope failure. A FS >1 indicates stable conditions whereas a FS<1 indicates unstable conditions. SINMAP computes a factor of safety at each point on the 20-foot (6-meter) LiDAR DEM grid to derive the stability index.

a = Topographic catchment area (see diagram below)

C = Dimensionless cohesion = (Cr +Cs)/ (hp_sg); where Cr = root cohesion; Cs = soil cohesion; h = soil thickness; p_s = soil density; g = gravity constant

$\mathbf{h_w}$ = height of water measured normal to slope

R = Recharge (5 inches/24 hours assumed)

r = water density (p_w) to soil density ($p_{s)}$ ratio

T = Soil transmissivity = soil hydraulic conductivity (Ksat) x soil thickness

Ø = Soil internal angle of friction

θ = Slope

$\mathbf{h_w/h}$ = Relative wetness = $\min\left(R\,a / T\sin\theta\right), 1$

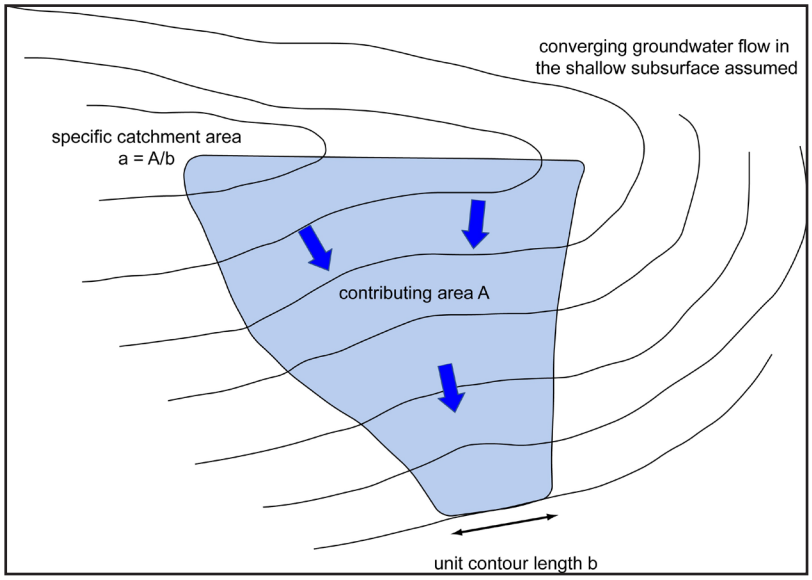

Figure A2: Schematic diagram of a topographic catchment derived from a LiDAR DEM used by SINMAP to model relative soil wetness. Shallow groundwater flow lines are assumed to converge in areas of concave topography.

Constant and User-Defined Values

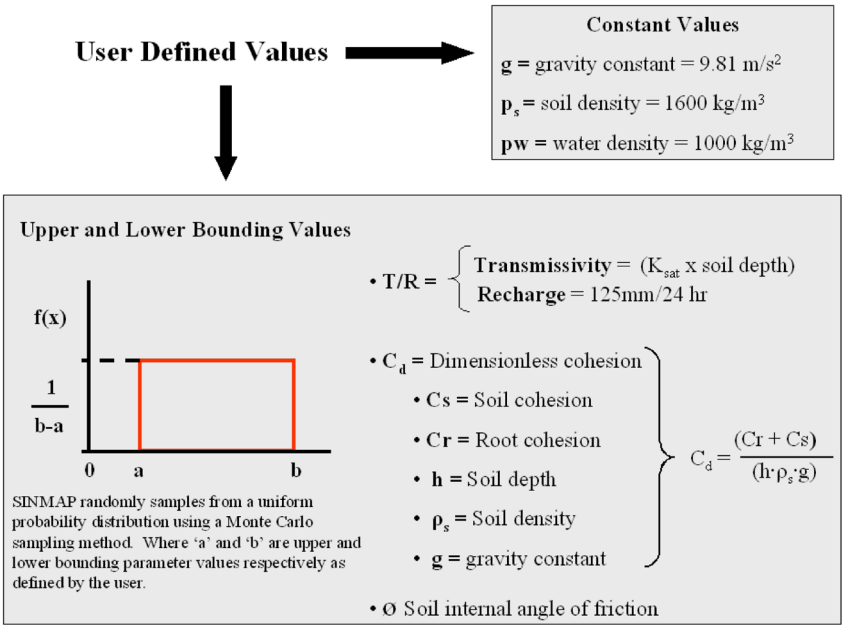

Figure A3: For each calibration region SINMAP allows the user to define constant values, and upper and lower bounding values for certain parameters. SINMAP uses the upper and lower bounding values to define uniform probability distributions for T/R (transmissivity to recharge ratio), C_d (dimensionless cohesion), and Ø (soil internal angle of friction). SINMAP then uses the constant values and values randomly sampled from the uniform probability distributions for input into the modified infinite slope equation to compute factors of safety and derive the stability indices.

SINMAP Calibration Regions

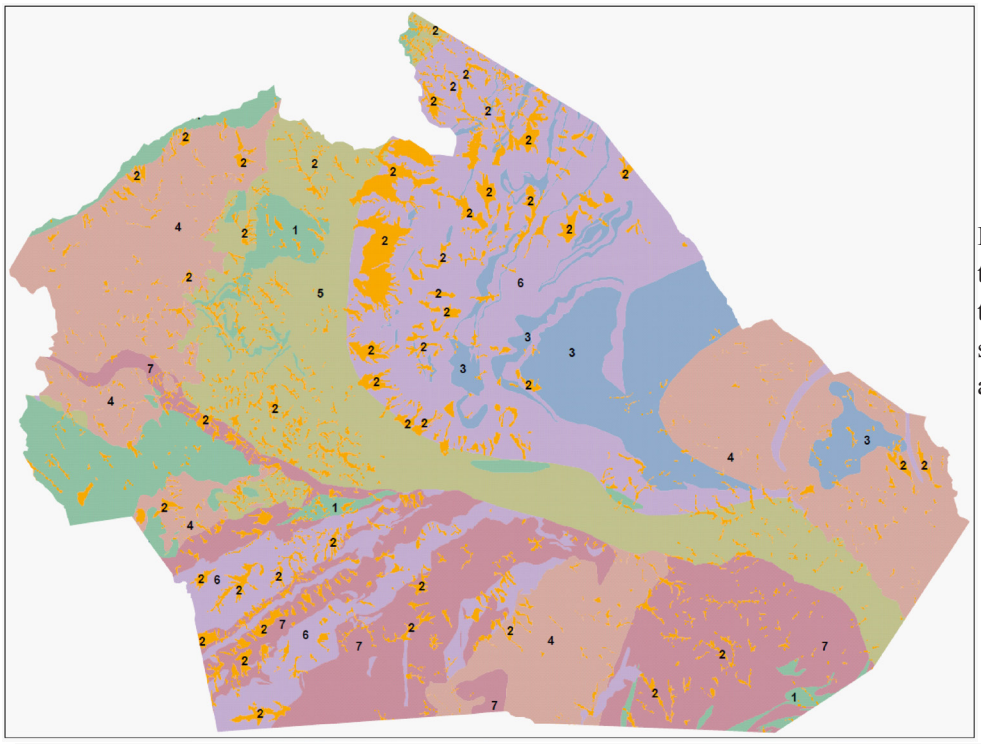

Figure A4: Calibration regions for the SINMAP analysis derived from the compilation geologic map and slope movement deposits (Wooten et al., 2008b).

CALIBRATION REGIONS AND PARAMETER VALUES USED TO GENERATE THE STABILITY INDEX MAP

Region[1]	Calibration Unit[2]	T/R (m) Low[3]	T/R (m) High[3]	Dimensionless Cohesion Low[4]	Dimensionless Cohesion High[4]	Friction Angle (degrees) Low[5]	Friction Angle (degrees) High[5]
1	Cul, Cuu, Pzgp, PzZmgb, Zca, Zcbc, Zcbgr, Zcco, Zcw, ZYgg	0.80	46.15	0.25	0.34	24	42
2	slope movement deposits	3.72	172.44	0.10	0.19	21	35
3	Dsp, Zatcs, Zatm, Zats, Zatu	6.64	469.51	0.17	0.19	21	42
4	Ybrg, Ywrg, Zabg	0.94	208.67	0.21	0.26	21	42
5	Ycg, Yvcg	0.35	38.45	0.23	0.28	21	42
6	S?lmd, Ypp, Zaba, Zata, Zatmgb, Zcbg, Zgma, Zgmg	0.65	64.01	0.22	0.25	21	42
7	Pzmy, Pztbsv, Zgmaq, Zgmf, Zgms, Zgmu, Zgmw, Zgmwgf	0.50	52.21	0.21	0.25	21	42

Table A1: Summary table of values used for each calibration regions in the Watauga SINMAP model. (Wooten et al., 2008b).

Explanatory notes for Table A1

[1]**Region**. A numbered area used in the SINMAP modeling process with assumed similar soil, geologic, and hydrologic properties derived from the compilation geologic map and slope movement (debris) deposits. Individual upper and lower bounded value estimates for T/R, (ratio of soil transmissivity to recharge) dimensionless cohesion, and soil friction angle were derived for each region.

[2]**Calibration Unit**. Abbreviations for calibration units from the compilation geologic map of Watauga County and mapped slope movement (debris) deposits.

[3]**T/R (m) Low/High.** The upper and lower bounding values for the ratio of soil transmissivity (T) to the rate of recharge (R). Transmissivity was calculated by multiplying the hydraulic conductivity (permeability) of the soil by the thickness of the soil. Values for soil thickness were derived primarily from field data. The recharge rate was modeled as 5 inches (125 mm) per day, the minimum threshold rate for debris flows to initiate in the Southern Appalachians (Eschner and Patric, 1982). The value for T/R represents length of hillslope, in meters, required to develop soil saturation during the 24-hour recharge period considered.

[4]**Dimensionless Cohesion Low/High.** The upper and lower bounding values for dimensionless cohesion. These calculated estimates were derived using the ratio of the combined values for effective soil (Cseff) and root cohesion (Cr) relative to the soil density and thickness, as shown in Pack and others (1998).

[5]**Friction Angle (degrees) Low/High.** The upper and lower bounding values for the effective internal soil friction angle (Øeff). Internal friction is the friction between individual grains within a mass of material.

Map Color Code	Predicted Stability Zone	Relative Debris/Earth Flow/Slide Hazard Ranking [1]	Stability Index Range [2]	Factor of Safety (FS) [3]	Probability of Instability [4]	Predicted Stability With Parameter Ranges Used in Analysis	Possible Influence of Stabilizing or Destabilizing Factors [5]
	Unstable	High	0	Maximum FS <1	100%	Range cannot model stability	Stabilizing factors required for stability
	Upper Threshold of Instability		0 - 0.5	>50% of FS ≤1	>50%	Optimistic half of range required for stability	Stabilizing factors may be responsible for stability
	Lower Threshold of Instability	Moderate	0.5 - 1	≥50% of FS >1	<50%	Pessimistic half of range required for instability	Destabilizing factors are not required for instability
	Nominally Stable	Low	1 - 1.25	Minimum FS = 1	___	Cannot model instability with most conservative parameters specified	Minor destabilizing factors could lead to instability
	Moderately Stable		1.25 - 1.5	Minimum FS = 1.25	___	Cannot model instability with most conservative parameters specified	Moderate destabilizing factors are required for instability
	Stable		>1.5	Minimum FS = 1.5	___	Cannot model instability with most conservative parameters specified	Significant destabilizing factors are required for instability

Table A2: Stability class definitions for stability index map units delineated using SINMAP. Modified from Pack and others (1998, Table 1).

Explanatory notes for Table 2:

[1] **Relative Debris/Earth Flow/Slide Hazard Ranking.** This column designates the relative hazard ranking for the initiation of shallow translational landslides on unmodified (i.e., natural or undisturbed) slopes.

[2] **Stability Index.** The stability index is a numerical representation of the relative hazard for shallow translational slope movement initiation based on the factors of safety computed at each point on a 20 foot (6 meter) digital elevation model grid derived from Li-DAR elevation data. The stability index is a dimensionless number based on factors of safety generated by SINMAP that indicates the probability that a location is stable considering the most and least favorable parameters for stability input into the model. The breaks in the ranges of values for the stability index categories are the default values recommended by the program developers.

[3] **Factor of Safety (FS).** The factor of safety is a dimensionless number computed by SINMAP using a modified version of the infinite slope equation, as used in Pack and others (1998), that represents the ratio of the stabilizing forces that resist slope movement to destabilizing forces that drive slope movement. A FS >1 indicates a stable slope, a FS <1 indicates an unstable slope, and a FS =1 indicates the marginally stable situation where the resisting forces and driving forces are in balance.

[4] **Probability of Instability.** This column shows the likelihood that the factor of safety computed within this map unit is less than one (FS <1, i.e., unstable) given the range of parameters used in the analysis. For example, a <50% probability of instability means that a location is more likely to be stable than unstable given the range of parameters used in the analysis.

[5] **Possible Influence of Stabilizing or Destabilizing Factors.** Stabilizing factors include increased soil strength, root strength, or improved drainage. Destabilizing factors include increased wetness or loading, or loss of root strength.

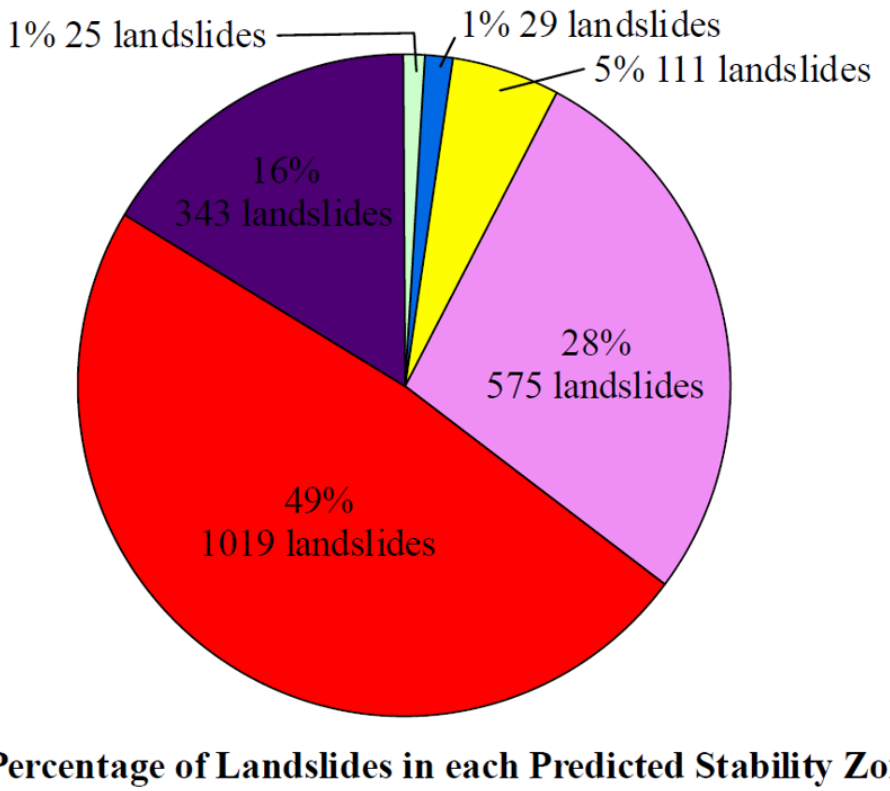

Figure A5: Pie chart showing the numbers of calibration landslide points for each stability class in the SINMAP model for Watauga County (Wooten et al, 2008b).

Map Color Code							
Predicted Stability Zone	**Stable**	**Modearately Stable**	**Nominaly Stable**	**Lower Threshold**	**Upper Threshold**	**Unstable**	**Total**
Area (km2)	237	77	127	191	132	24	787
% of Region	30%	10%	16%	24%	17%	3%	100%
# Landslides	25	29	111	575	1019	343	2102
% of Slides	1%	1%	5%	27%	48%	16%	100%
Frequency/Unit Area	0.1	0.4	0.9	3.0	7.7	14.4	2.7

Table A3: Statistical summary for each stability class in Watauga County

Compilation geologic map for Watauga County showing field trip stop locations. Bedrock map units: Late Mesoproterozoic age: Ywrg – Watauga River Gneiss; Ycg – Cranberry Gneiss; Ybrg – Blowing Rock Gneiss. Ypp – Pumpkin Patch Metamorphic Suite; Late Proterozoic: Zgm – Grandfather Mountain Formation (in Grandfather Mtn. Window); subunits a – mainly metaarkose and metasandstone; f – felsic metavolcanics; g – mainly metagraywacke, metasandstone, and metavolcanics; m – mafic metavolcanics; s – mostly metasiltstone. Zc – Crossnore Plutonic Suite; subunits a – aegirine alkalic metagranite; bc – Beech alkalic metagranite; bgr – Beech metagranite. Zat – Ashe Metamorphic Suite – Tallulah Falls Formation; subunits a – amphibolite, m – biotite gneiss, metagraywacke. Zab – Alligator Back Formation: subunits a – amphibolite; g – gneiss, conglomeratic metagraywacke, metasiltstone. Devonian age: Dsp- Spruce Pine Plutonic Suite granitic and pegmatite intrusives. Cambrian age: Ccu – Unicoi Formation mainly conglomeratic metasandstone. Faults: Thrust faults LFF – Linville Falls fault; FRF – Fork Ridge fault; FF – Fries fault; GLF – Gossan Lead fault; BtF – Bethel fault; LGF – Locust Gap fault; SMF – Stone Mtn. fault; GBF – Goldmine Branch fault; AF – Aho fault; Tear fault LRF – Long Ridge fault; Normal fault BF – Boone fault; GMW – Grandfather Mountain window.